Characterization of ACC oxidase during leaf ontogeny in white clover (*Trifolium repens* L.) and *Trifolium occidentale*

Zhen-Ning Du

2004

Massey University
COLLEGE OF SCIENCES

INSTITUTE OF MOLECULAR BIOSCIENCES
Te Kura Pūtaiao Koiora-ā-Ngota
Private Bag 11 222
Palmerston North
New Zealand
T 64 6 356 9099
F 64 6 350 5688
IMBS@massey.ac.nz
http://imbs.massey.ac.nz

CERTIFICATE OF REGULATORY COMPLIANCE

This is to certify that the research carried out in the Doctoral Thesis entitled "Characterization of ACC oxidase during leaf ontogeny in white clover (*Trifolium repens* L.) and *Trifolium occidentale*" in the Institute of Molecular BioSciences at Massey University, New Zealand:

(a) is the original work of the candidate, except as indicated by appropriate attribution in the text and/or in the acknowledgements;

(b) that the text, excluding appendices/annexes, does not exceed 100,000 words;

(c) all the ethical requirements applicable to this study have been complied with as required by Massey University, other organizations and/or committees which had a particular association with this study, and relevant legislation.

Please insert Ethical Authorisation code(s) here (if applicable):
Genetic Technology Committee GMO 02/MU/05
Massey University Animal Ethics Committee 97/5

Candidate's Name: Zhenjing Du
Signature:
Date: 18/08/04

Supervisor's Name:
Signature: M.T. McManus
Date: 18/08/04

Massey University
COLLEGE OF SCIENCES

INSTITUTE OF MOLECULAR BIOSCIENCES
Te Kura Pūtaiao Koiora-ā-Ngota
Private Bag 11 222
Palmerston North
New Zealand
T 64 6 356 9099
F 64 6 350 5688
IMBS@massey.ac.nz
http://imbs.massey.ac.nz

SUPERVISOR'S DECLARATION

This is to certify that the research carried out for the PhD thesis entitled "Characterization of ACC oxidase during leaf ontogeny in white clover (*Trifolium repens* L.) and *Trifolium occidentale*" was done by Zhen-Ning Du in the Institute of Molecular BioSciences at Massey University, Palmerston North, New Zealand. This thesis material has not been used in part or in whole for any other qualification, and I confirm that the candidate has pursued the course of study in accordance with the requirements of the Massey University regulations.

M.T. McMANUS

Supervisor' s name

Signature

18/08/04

Date

Massey University
COLLEGE OF SCIENCES

INSTITUTE OF MOLECULAR BIOSCIENCES
Te Kura Pūtaiao Koiora-ā-Ngota
Private Bag 11 222
Palmerston North
New Zealand
T 64 6 356 9099
F 64 6 350 5688
IMBS@massey.ac.nz
http://imbs.massey.ac.nz

CANDIDATE'S DECLARATION

This is to certify that the research carried out for my PhD thesis entitled "Characterization of ACC oxidase during leaf ontogeny in white clover (*Trifolium repens* L.) and *Trifolium occidentale* " in the Institute of Molecular BioSciences at Massey University, Palmerston North, New Zealand is all my own work and that the thesis material has not been used in part or in whole for any other qualification.

Zhenning Pu

Candidate's Name

Signature

18/08/04

Date

Characterization of ACC oxidase during leaf ontogeny in white clover (*Trifolium repens* L.) and *Trifolium occidentale*

A thesis presented in partial fulfillment of the requirements
for the degree of

Doctor of Philosophy
in
Plant Biochemistry and Molecular Biology

at Massey University, Palmerston North
New Zealand

Zhen-Ning Du

2004

ABSTRACT

To produce plant material for this thesis, *Trifolium repens* (white clover) (genotype 10F) and *Trifolium occidentale* (genotype 18Z) were propagated to produce individual stolons trained over a plastic matrix to inhibit nodal root formation. These stolons comprised leaf tissue representative of all developmental stages, from leaf initiation, maturation through to senescence. The developmental pattern for both species in terms of leaf ontogeny was generally reproducible between vegetatively propagated clones.

Three distinct 1-aminocyclopropane-1-carboxylate (ACC) oxidase genes expressed during leaf ontogeny in white clover (*Trifolium repens* L.) have been identified (Hunter *et al.,* 1999). Of the three ACC oxidase genes identified, one designated *TR-ACO2* is expressed in newly initiated and mature green leaves while *TR-ACO3* is expressed predominantly in the senescent leaf tissue. In order to further characterize the protein products of these genes, a series of FPLC columns was used to partially purify isoforms of ACC oxidase from leaf tissue of white clover at different developmental stages, followed by 2D gel electrophoresis to obtain further purification. Two distinct isoforms of ACC oxidase were identified and partially purified from newly initiated green (designated the NIGI isoform) and senescent (designated the SEI isoform) leaf tissue. Both purified NIGI and SEI proteins were recognized by western analysis using an anti-(*Trifolium repens*) TR-ACO2 antibody after SDS-PAGE or 2D gel electrophoresis. To determine whether NIGI is coded for by *TR-ACO2* and SEI is coded for by gene *TR-ACO3*, protein spots (after 2D gel electrophoresis) were digested with trypsin and the masses of the peptide determined by matrix-assisted laser desorption ionization-time of flight (MALDI-TOF) mass spectrometric analysis. For NIGI, the coverage of the putative protein sequence (TR-ACO2) by tryptic digestion ranged from 24.5% to 37.6%, while the observed pI (5.1) and molecular mass (37 kDa) were close to the theoretical pI (5.3) and computed mass (35.7 kDa). For SEI, the percentage coverage of the putative protein sequence (TR-ACO3) from the peptides identified ranged from 13.4% to 18.0%, while the observed pI (5.2) and molecular masses (35.0-35.5 kDa) were also close to the theoretical pI (5.5) and computed mass (35.2 kDa). These data suggest that the NIGI isoform is encoded by *TR-ACO2*, while the SEI isoform is encoded by *TR-ACO3*.

ACC oxidase activity *in vitro* and ACC oxidase protein accumulation over 24 h in mature green leaf tissue extracts during both short and long days has been shown to be under circadian control. There are two ACC oxidase activity peaks observed, in which the pattern of fluctuation in ACC oxidase activity resulted in a high level of enzyme activity at 12:00 am (0.18-0.27 nmol ethylene/h/mg), and maximum activity at 12:00 pm (0.24-0.31 nmol ethylene/h/mg). Lowest activity was observed in both long and short days at 9:00 pm (0.09-0.10 nmol ethylene/h/mg). In addition, northern analysis indicated that the *TR-ACO2* mRNA level also displayed a circadian pattern of expression.

Investigation of the effect of protein phosphorylation and dephosphorylation on ACC oxidase activity indicated that ACC oxidase activity *in vitro* during the periods of maximum activity increased 36% (at 12:00 am) and 56% (at 12:00 pm) after dephosphorylation, respectively. However, there was only 21% increase in enzyme activity at the time point with lowest activity (9:00 pm) in the dephosphorylated extracts. SDS-PAGE using a mini-protein gel system or a gradient gel system showed that the molecular mass of ACC oxidase decreased after dephosphorylation when compared with phosphorylation of the enzyme. These results suggest that the phosphorylation and dephosphorylation of the ACC oxidase proteins occurs *in vitro* and the state does affect enzyme activity.

In the second part of this thesis, the coding regions of putative ACC oxidase gene transcripts were generated from leaf tissue of genotype 18Z of *T. occidentale* using RT-PCR. Sequence alignments indicated that the sequences could be grouped into two distinct classes, and these coding regions were designated *TO-ACO2* (*Trifolium occidentale* ACC oxidase 2) and *TO-ACO3* (*Trifolium occidentale* ACC oxidase 3). *TO-ACO2* and *TO-ACO3* share 82% similarity in nucleotide sequence and 84% similarity in amino acid sequence. The *TO-ACO2* and *TO-ACO3* sequences were validated as encoding ACC oxidases by comparison with other ACC oxidases in the GenBank database and both TO-ACO2 and TO-ACO3 deduced amino acid sequences contain all the residues hitherto shown to be important for maximal activity of the enzyme. Further, *TO-ACO2* had 97% identity with *TR-ACO2* at the nucleotide level, and 98% identity at the amino acid level. *TO-ACO3* had 97% identity with *TR-ACO3* at the nucleotide level, and 96% identity at the amino acid level. Genomic Southern

analysis, using 3'-UTRs of *TR-ACO2* and *TR-ACO3* as probes, could not confirm that *TO-ACO2* and *TO-ACO3* are encoded for by distinct genes.

Expression studies of *TO-ACO2* and *TO-ACO3* genes during leaf maturation and senescence of *T. occidentale* were examined using northern analysis. *TO-ACO2* is expressed predominantly in newly initiated and at the onset of the mature-green leaf stage, while *TO-ACO3* shows maximal expression in senescent leaf tissue. The changes of ACC oxidase activity during leaf ontogeny of *T. occidentale* coincided with the pattern observed for ACC oxidase protein accumulation using western analysis and image analysis.

ACKNOWLEDGEMENTS

I would like to first express sincere appreciation and gratitude to my supervisor, **Associate Professor Michael T. McManus** (Institute of Molecular BioSciences, Massey University), for excellent guidance and encouragement throughout the course of my PhD project. Without his persistent support in both my research project and my personal life, it would have been impossible for me complete my research work. Thank you Michael for always being available no matter how busy you were and for being such an enthusiastic and unbounded patient supervisor.

I am very grateful to **Professor Paula E. Jameson** (Institute of Molecular BioSciences, Massey University), and **Dr. Mike Hay** (Grasslands, AgResearch) for their support, guidance, and helpful comments.

I gratefully acknowledge **Dr. Deming Gong** and **Dr. Richard Scott** for generous help and suggestion in my project. Thanks to **Mr. Dick Poll** (Institute of Fundamental Sciences, Massey University) for his kindness whenever I came to him with questions about FPLC, **Associate Professor Peter Lockhart** for phylogenetic analysis, and **Mrs. Sue Nicholson** (Institute of Food, Nutrition and Human Health, Massey University) for helping me use the GC.

I would like to thank all those people in the Institute of Molecular BioSciences, especially Dr. Shuguang Zhang, Trish McLenachan, Ningxin Zhang, Zhuojian Liu, and Jason Song.

I would like to thank my great lab mates, Susanna, Rachael, Balance, Mathew, Vikki, Simone, Greg, Jan, and Anya for their cooperation and help in the lab. Thank you all!

I wish to express my appreciation to the New Zealand Foundation for Research Science & Technology and New Zealand Pastoral Agriculture Research Institute Ltd. for providing a **"Bright Future Scholarship"**

Finally, a special thanks you to my wife Ningxia and my daughter Jiaqi for their love and excellent support.

TABLE OF CONTENTS

LIST OF FIGURES

LIST OF TABLES

LIST OF ABBREVIATIONS

$A_{595\ nm}$	absorbance at 595 nm
ACC	1-aminocyclopropane-1-carboxylic acid
ACO	ACC oxidase
ACS	ACC synthase
AdoMet	*S*-adenosyl-$_L$-methionine
Amp^{100}	ampicillin (100 mg/ml)
AOA	aminoethoxyacetic acid
APS	ammonium persulphate
AU	absorbance unit
AVG	aminoethoxyvinylglycine
BCIP	5-bromo-4-chloro-3-indolyl phosphate
BSA	bovine serum albumin
°C	degree celsius
ca.	*circa* (approximately)
CBB	coomassie brilliant blue
DMF	*N, N*-dimethyl formamide
DMSO	dimethyl sulphoxide
DNA	deoxyribonucleic acid
DTT	dithiothreitol
E. coli	*Escherichia coli*
EIN	ethylene insensitive
EDTA	ethylenediamine tetra-acetic acid
EFE	ethylene forming enzyme
FPLC	fast protein liquid chromatography
FW	fresh weight
GACC	1-(gamma-$_L$-glutamylamino) cyclopropane-1-carboxylic acid
g	gram
g	acceleration due to gravity (9.8 m/s^2)
GC	gas chromatography
GUS	β-glucuronidase
h	hour
HEPES	*N*-2-hydroxyethylpiperazine-*N'*-ethanesulphonic acid

HIC	hydrophobic interaction chromatography
HPLC	high performance liquid chromatography
IAA	indole-3-acetic acid
IPG-IEF	immobilized pH gradient- isoelectric focusing
IPTG	isopropyl-β-$_D$-thiogalactopyranoside
kb	kilobase-pairs
kDa	kilodaltons
K_m	substrate concentration at half maximum reaction rate
L	litre
LB	luria-Bertani (media or broth)
Log	logarithm
MACC	1-(malonylamino) cyclopropane-1-carboxylic acid
M	Molar, moles per litre
mg	milligram
µg	microgram
µl	microlitre
MilliQ water	water purified by a MilliQ ion exchange column
min	minute
ml	millilitre
MOPS	sodium [3-(*N*-morpholiono)] propanesulphonic acid
Mr	relative molecular mass (g mol^{-1})
NBT	*p*-nitro blue tetrazolium chloride
ng	nanogram
2-ODD	2-oxoacid dependent dioxygenase
OKA	okadaic acid
PA	1, 10-phenanthroline
PAGE	polyacrylamide gel electrophoresis
PBSalt	50 mM sodium phosphate, pH 7.4, containing 250 mM NaCl
PCR	polymerase chain reaction
Pers. comm.	personal communication
pH	- log [H^+]
pI	isoelectric point
PLP	pyridoxal-5'-phosphate

ppm	part per million
PVDF	polyvinylidene difluoride
PVPP	polyvinyl polypyrrolidone
3'-RACE	3'-rapid amplification of cDNA ends
RNase	ribonuclease
RO	reverse osmosis
RT-PCR	reverse transcriptase-dependent polymerase chain reaction
s	second
SAM	*S*-adenosyl-$_L$-methionine
SDS	sodium dodecyl sulphate
SE	standard error of mean
TEMED	*N,N,N',N'*-tetramethylethylenediamine
Tris	tris (hydroxymethy) aminomethane
Triton X-100	octylphenoxy polyethoxyethanol
Tween-20	polyoxyethylenesorbitan monolaurate
UTR	untranslated region
UV	ultra violet light
V_{max}	maximum rate of reaction
v/v	volume per volume
w/v	weight per volume
w/w	weight per weight

ABBREVIATIONS FOR AMINO ACIDS

Amino acid	Three-letter abbreviation	One-letter symbol
Alanine	Ala	A
Arginine	Arg	R
Asparagine	Asn	N
Aspartic acid	Asp	D
Cysteine	Cys	C
Glutamine	Gln	Q
Glutamic acid	Glu	E
Glycine	Gly	G
Histidine	His	H
Isoleucine	Ile	I
Leucine	Leu	L
Lysine	Lys	K
Methionine	Met	M
Phenylalanine	Phe	F
Proline	Pro	P
Serine	Ser	S
Threonine	Thr	T
Tryptophan	Trp	W
Tyrosine	Tyr	Y
Valine	Val	V

1. Chapter One: Introduction

1.1 Overview

Ethylene (C_2H_4) is a gaseous plant hormone, that regulates many aspects of plant growth, development, and senescence (Yang and Hoffman, 1984; Kende, 1993). In higher plants, the complete ethylene biosynthetic pathway has been elucidated and, as a simplified sequence comprises: methionine→ *S*-adenosylmethionine (SAM)→ 1-aminocyclopropane-1-carboxylic acid (ACC)→ ACC → C_2H_4 (Adams and Yang, 1979; Yang and Hoffman, 1984; Abeles *et al.,* 1992). There are two crucial enzymes associated with this pathway: ACC synthase (EC 4.4.1.14) and ACC oxidase (EC 1.4.3). While ACC synthase has long been considered the rate-determining step in the pathway, more recent evidence suggests that regulation of ACC oxidase also constitutes an extra tier of control. In particular, ACC oxidase has been shown to be a small multi-gene family in plants (typically 3 to 4 members), including white clover, and expression studies have revealed that expression of these genes is developmentally- and environmentally-regulated (Hunter *et al.,* 1999). In contrast, there are fewer studies in which regulation of ACC oxidase enzyme activity in different tissues has been examined (Gong and McManus, 2000).

Using leaf ontogeny of white clover (*Trifolium repens* L.) as a model system, leaf senescence-associated ethylene biosynthesis has been characterized at the physiological, biochemical and molecular levels (Butcher, 1997; Hunter *et al.,* 1999; Gong and McManus, 2000). Thus far, previous work has identified three ACC oxidase genes that are differently expressed during leaf ontogeny (Hunter *et al.,* 1999). Of the three ACC oxidase genes identified, one designated as *TR-ACO2* (*Trifolium repens* ACC oxidase gene 2), is expressed in newly initiated and mature green leaves, and *TR-ACO3* is expressed predominantly in the senescent leaf tissue. Concurrently, two isoforms have been purified to homogeneity: one purified from mature green leaves (designated MGI), and a second isoform purified from senescent leaves (designated SEII). However, a second distinct isoform (designated SEI) was also identified (but not purified) from senescent leaf tissue of white clover (Gong and McManus, 2000).

In the first section of this thesis, the study by Gong (1999) is extended where two white clover ACC oxidase isoforms have been partially purified to determine which isoform *TR-ACO2* or *TR-ACO3* code for. Further, more information about the role of ethylene in regulating leaf senescence of white clover is obtained through the investigation of the possibility that *TR-ACO2* gene expression and TR-ACO2 protein accumulation exhibits a circadian rhythm. In the second section, the transcription and translation of ACC oxidase genes during leaf maturation and senescence in the diploid clover species, *Trifolium occidentale* has been characterized and compared with white clover. To do this, genes encoding the ACC oxidase have been cloned and their expression patterns studied in mature-green and senescent leaf tissues. The aim of this section is to seek evidence for differential transcription and translation of the ACC oxidase gene family in the related species during these developmental processes.

1.2 Ethylene in Plant Development

Ethylene, the simplest unsaturated hydrocarbon, regulates many diverse physiological processes during plant growth and development. However, human civilization has unknowingly used the plant hormone ethylene to manipulate plant development for hundreds, perhaps thousands of years. For example, in China, people used burning incense to ripen their fruits (Yang and Dong, 1993), and Puerto Rican pineapple growers and Philippine mango growers used bonfires around their crops to help initiate and synchronise flowering (Salisbury and Ross, 1985). Although it was clear in the mid-nineteenth century that the presence of gaseous materials in the air could modify the growth of plants, it was not until the Russian plant physiologist Neljubov (1879-1926) (cited in Abeles *et al.*, 1992) observed that etiolated pea seedlings grew horizontally in his laboratory but upright in outside air. He showed that this abnormal growth habit was caused by contaminating illuminating gas, and proved subsequently that the active principle in illuminating gas was ethylene in 1901. Chemical proof that plants produce ethylene was provided by Gane (1934), who analyzed the gases released by ripening apples. Since then it has been shown that ethylene is produced from essentially all parts of higher plants and plays an important role in regulating many plant processes. These processes range from seed germination, including breaking seed dormancy, and seedling emergence (Harpham *et al.*, 1991; Bewley and Black, 1994; Matilla, 2000); shoot elongation and the regulation of epinastic growth responses

(Sanders *et al.,* 1990; Woeste *et al.,* 1999); root production and growth, and root growth initiation (Sarquis *et al.,* 1992; Zacarias and Reid, 1992; Dolan, 1997); fruit ripening (Lelievre *et al.,* 1997); leaf senescence (Grbic and Bleecker, 1995) and abscission (Osborne, 1989). The production of this gaseous hormone in plant tissue is usually low, but is greatly induced at certain stages of plant development, and in response to a wide range of environmental stresses and stimuli (Abeles *et al.,* 1992; Mattoo and Suttle, 1991; Imaseki, 1999). As a gas, ethylene moves from its site of synthesis by diffusion. Therefore, ethylene synthesized in one part of the plant can affect other tissues as well (Tieman and Klee, 1999). With various stresses in plants, the increase in ethylene synthesis serves as a common step in the chain of events leading to a variety of responses. Even the emission of ethylene by a plant is strictly regulated, varying from one organ to another and among different species. The inability of a stressed plant to initiate ethylene-related responses decreases its chance for survival (see review by Grichko and Glick, 2001).

All these roles for ethylene during plant growth and development underline how complex the mechanisms must be which regulate ethylene biosynthesis and its signal transduction pathway in higher plants (Johnson and Ecker, 1998).

1.3 Ethylene Perception and Signal Transduction

The range of physiological responses regulated by ethylene is surprisingly wide and has been described by Abeles *et al.* (1992) and Mattoo and Suttle (1991). The ability of ethylene as a signal molecule to influence such a diverse array of plant responses begs the question as to how a single hormone is able to achieve this. Currently, it is widely accepted that ethylene perception rather than metabolism is responsible for the mediation of ethylene responses, as these responses are not provoked by the intermediates of ethylene metabolism, but can be elicited by some ethylene-like hydrocarbons (McKeon *et al.*, 1995; Bleecker and Kende, 2000).

Ethylene is presumed to act by binding to ethylene receptors and then to elicit subsequent signal transduction and translation (Abdi *et al.*, 1998; Golding *et al.*, 1998; Jiang *et al.*, 1999). The ethylene receptor complex alters the activity of signal transduction reactions, leading to the transcription of specific genes and the synthesis and /or activation of enzymes responsible for the physiological effects (Woltering and

De Vrije, 1995). Attempts to isolate and purify ethylene receptors or ethylene binding proteins using biochemical methods alone have so far failed (Jiang and Fu, 2000). However, in recent years, there has been significant progress in elucidating the ethylene perception and signal transduction pathway through the analysis of *Arabidopsis* and tomato mutants defective in ethylene-dependent responses (see review by Bleecker and Kende, 2000; Stepanova and Ecker, 2000; Ciardi and Klee, 2001; Alexander and Grierson, 2002). Thus far, two categories of these mutants have been defined. For the first category, dark grown seedlings do not exhibit the "triple response" in the presence of ethylene. These are known as the ethylene insensitive (EIN) mutants as they show reduced or no response to exogenously applied ethylene. This class of mutations includes *etr1* (for ethylene triple response), *etr2*, *ein2* to *ein7* (for ethylene insensitive), and *ain1* (for ACC insensitive) (Bleecker *et al.*, 1988; Johnson and Ecker, 1998; Hua *et al.*, 1998). The second category of ethylene perception mutants, the constitutive ethylene response (CER) mutants, demonstrates the triple response phenotype even in the absence of ethylene (Ecker, 1995). This mutant family can be further divided into two sub-classes based on their sensitivity to ethylene inhibitors (Johnson and Ecker, 1998). In the first sub-class, the constitutive triple response appears to be caused by the overproduction of endogenous ethylene. These mutants, whose phenotypes are suppressed by ethylene synthesis inhibitors, are designated ethylene overproduce (*eto*) mutants, and include *eto1* to *eto4* (Vogel *et al.*, 1998). The second class of CER mutants display the triple response regardless of the presence of ethylene or inhibitors of ethylene synthesis, and are designated the constitutive triple response (*ctr*) mutants (Johnson and Ecker, 1998).

In *Arabidopsis*, analysis of mutants that display either etiolated growth in the presence of ethylene in the dark or show a constitutive triple response in the absence of the hormone, have led to the identification of multiple ethylene receptor genes involved in ethylene signal transduction, which include *CTR1* (Kieber *et al.*, 1993), *EIN2* (Alonso *et al.*, 1999), *EIN3* (Chao *et al.*, 1997), *ERF1* (Solano *et al.*, 1998), and *ETR1* (Chang *et al.*, 1993).

The cloning and characterization of several of the genes disrupted in such mutants has led to the identification of proteins involved in ethylene biosynthesis, perception and signal transduction. The *ETR1* gene was the first member of the receptor family to be

cloned from *Araibdopsis thaliana*, which lack the ethylene triple response of dark grown seedlings (Bleeker *et al.*, 1988; Chang *et al.*, 1993). The ETR1 protein is homologous to the prokaryotic family of signal transduction known as two-component regulators in bacteria (Wurgler-Murphy and Saito, 1997). Two component regulators are typically composed of a sensor protein with an input domain that receives signals and a catalytic transmitter domain that autophosphorylates on an internal histidine residue. The second component, a response regulator protein, is composed of a receiver domain that receives phosphate from the transmitter on an aspartate residue and an output domain that mediates response depending on the phosphorylation state of the receiver (Chang and Meyerowitz, 1995; Stock *et al.*, 2000). Several mutant alleles of *ETR1* have been identified, all of which confer dominant ethylene insensitivity (Bleecker *et al.*, 1988; Guzman and Ecker, 1990). One of these mutant alleles, *etr1-1*, exhibits a complete lack of measurable ethylene response (Bleecker *et al.*, 1988).

In addition to ETR1, four ethylene receptors exist in *Arabidopsis*: ETR2, ERS1, ERS2 and EIN4 (Hua *et al.*, 1995; Sakai *et al.*, 1998). The receptor family can be further divided into two subfamilies based on structural similarities. The ETR1-like subfamily, consisting of ETR1 and ERS1, features three hydrophobic subdomains at the N terminus, where ethylene binding occurs, and a well-conserved histidine kinase domain at the C-terminal part of the protein (Schaller and Bleecker, 1995; Hall *et al.*, 2000). The ETR2-like subfamily, which includes ETR2, ERS2 and EIN4, have an additional hydrophobic extension at the N terminus and possess degenerate histidine kinase domains that lack one or more elements considered necessary for catalytic activity (see review by Wang *et al.*, 2002). In a screen for *Arabidopsis* mutants that display the constitutive triple response phenotype, only one complementation group, *ctr1*, proved to be unaffected by ethylene synthesis inhibitors or ethylene antagonists, which indicate that the *CTR1* gene product acts as a negative regulator of response pathways (Kieber *et al.*, 1993). Recessive mutations in several additional loci result in complete or partial insensitivity to ethylene in *Arabidopsis*. Of particular significance are the *EIN2* and *EIN3* loci (Roman *et al.*, 1995). Loss-of-function mutations in *EIN2* render plants completely insensitive to ethylene. Mutations in *EIN2* are epistatic to mutations in *CTR1* because the double mutant shows no response phenotype. Mutations at the *EIN3* locus exhibit reduced sensitivity to ethylene, but in no case is complete insensitivity observed. Overexpression of *EIN3* results in plants displaying a

constitutive ethylene response phenotype (Chao *et al.*, 1997). Genetic evidence has shown that *EIN2* acts downstream of *CTR1* and upstream of *EIN3* (Wang *et al.*, 2002).

In tomato, a family of at least six ethylene receptor genes has been identified. For consistency in nomenclature, these have been named *LeETR1-6* in the order of their cloning. However, for historical reasons, *LeETR3* is denoted as *NR* (Payton *et al.*, 1996; Zhou *et al.*, 1996; Tieman and Klee, 1999; Ciardi and Klee, 2001). Moreover, two *CTR1* homologues, *TCTR2* (Lin *et al.*, 1998) and *ER50* (Zegzouti *et al.*, 1999), have been identified. Each tomato gene has a distinct pattern of expression through development and in response to external stimuli (Lashbrook *et al.*, 1998; Tieman and Klee, 1999). *LeETR1* and *LeETR2* are expressed constitutively in all tissues throughout development, *NR* is up-regulated at anthesis and both *NR* and *LeETR4* are up-regulated during ripening, senescence, abscission (Payton *et al.*, 1996; Tieman *et al.*, 2000) and pathogen infection (Ciardi *et al.*, 2000). *LeETR5* is also expressed in fruit, flowers and during pathogen infection (Tieman and Klee, 1999).

Added ethylene has been found to induce a rapid and transient phosphorylation of several proteins in tobacco, which supports the idea that a protein kinase cascade is involved in the ethylene signal transduction pathway (Raz and Fluhr, 1993). The identification of the gene products *ETR1* and *CTR1*, a negative regulator of the ethylene response pathway in *Arabidopsis* encoding a member of the Raf-like family of protein kinases (Kieber, *et al.*, 1993), suggests that the activity of phosphatase plays an important role in ethylene response. The phosphatase activity could down-regulate the basal level of a yet to be identified mitogen-activated protein (MAP) kinase cascade (Fluhr and Mattoo, 1996). The use of inhibitors has established a role for phosphorylation in the regulation of both ethylene biosynthesis and action. Direct involvement of phosphorylation events in ethylene action was demonstrated when specific polypeptides were shown to undergo transient phosphorylation in the presence of ethylene (Raz and Fluhr, 1993). The transient phosphorylation was abrogated in the presence of kinase inhibitors. Thus, the gene products are involved in the signal transduction pathway through phosphorylation (Jing and Fu, 2000).

1.4 Ethylene Biosynthesis in Higher Plants

Ethylene synthesis is tightly regulated during plant development with the rate of biosynthesis frequently changing depending on the developmental stage and the hormonal status of tissues, and in response to environmental stresses and stimuli (Nakagawa *et al.*, 1991). Several excellent reviews concerning the biochemical aspects of ethylene biosynthesis have been published (Kende, 1993; Zarembinski and Theologis, 1994; Ecker, 1995; Fluhr and Mattoo, 1996; Imaseki. 1999; Jiang and Fu, 2000).

The biosynthetic pathway of ethylene in higher plants has been studied in detail, and it is now well established that ethylene is formed predominantly *via* the ACC-mediated biosynthetic pathway (Yang and Hoffman, 1984). The enzymes involved in this ACC-dependent pathway comprise AdoMet (SAM) synthetase (EC 2.5.1.6), ACC synthase and ACC oxidase (Figure 1.1). Typically, the biosynthetic pathway in higher plants is considered to have two committed steps. The first committed and the key regulatory step is the conversion of *S*-adenosyl-$_L$-methionine (AdoMet) to 1-aminocyclopropane-1-carboxylic acid (ACC) catalyzed by ACC synthase. This has long been considered the rate-determining step in the pathway, with many inducers of ethylene biosynthesis acting through stimulation of this enzyme (Kende, 1993; Theologis, 1992; Yang and Hoffman, 1984). By contrast, the second enzyme step, in which ACC is converted to ethylene by ACC oxidase, was originally considered not to be a major control point in the regulation of ethylene biosynthesis (Yang and Hoffman, 1984). However, more recent evidence suggests that regulation of ACC oxidase also constitutes an extra tier of control. In particular, ACC oxidase has been shown to comprise a small multi-gene family in many plant species, and this has led to the now widely accepted view of this enzyme as a further regulation point in the pathway (Imaseki, 1999). In addition to being converted to ethylene, ACC can also be irreversibly conjugated to form 1-(malonylamino) cyclopropane-1-carboxylic acid (MACC) or 1-(gamma-$_L$-glutamylamino) cyclopropane-1-carboxylic acid (GACC). In this pathway, it is well known that biosynthesis is subject to both positive and negative feedback regulation (Kende, 1993; Alexander and Grierson, 2002). Furthermore, the expression of ACC synthase and ACC oxidase is differentially regulated by various developmental, environmental and hormonal signals (Barry *et al.*, 2000)

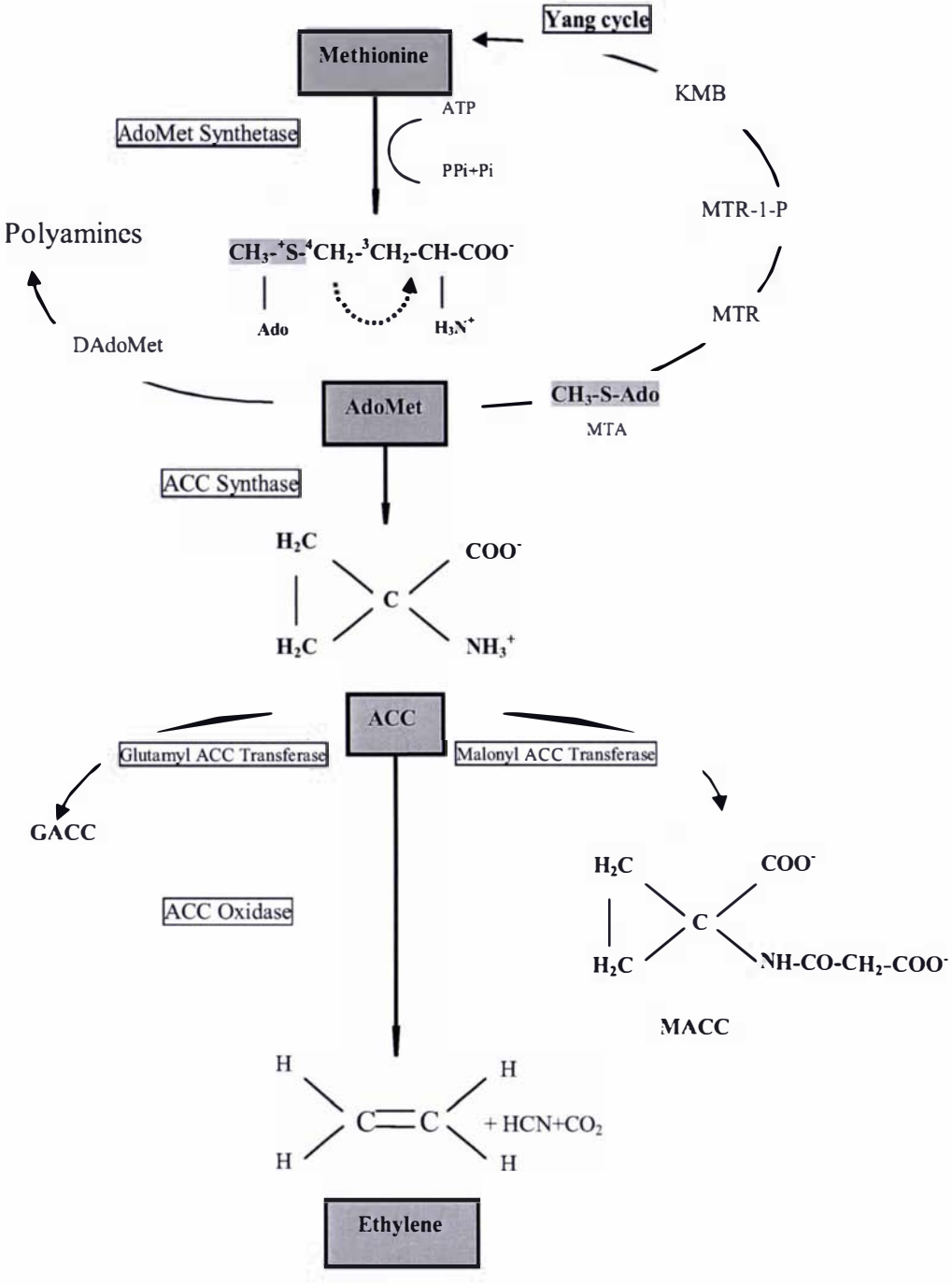

Figure 1.1 Ethylene biosynthetic pathway in higher plants

AdoMet, *S*-adenosylmethionine; **DAdoMet,** decarboxylated AdoMet;
MTA, 5'-methylthioadenosine; **MTR,** 5'-methylthioribose;
MTR-1-P, 5'-methylthioribose-1-phosphate; **KMB,** 2-keto-4-methylthiobutyrate;
GACC, 1-(gammal-$_L$-glutamylamino) cyclopropane-1-carboxylic acid;
MACC, 1-(malonylamino) cyclopropane-1-carboxylic acid.

1.4.1 SAM Synthetase

SAM synthetase is the enzyme catalyzing the synthesis of SAM from methionine and ATP. It is a ubiquitous enzyme found in both prokaryotic and eukaryotic organisms (Tabor and Tabor, 1984). SAM synthetase is classified as a housekeeping enzyme due to its pivotal role in cellular biochemistry (Fluhr and Mattoo, 1996). In plants, SAM (AdoMet) is the precursor in ethylene biosynthesis (Yang and Hoffman, 1984; Kende, 1993). However, SAM also participates in an array of biochemical reactions, including the biosynthesis of polyamines and transmethylation of nucleic acids, proteins, fatty acids and polysaccharides (Tabor and Tabor, 1984). The link between ethylene biosynthesis and polyamine production is of particular interest as application of polyamines has been shown to inhibit ethylene production in some plant tissues (Pandey *et al.*, 2000). In carnation flowers, for example, the application of spermine delayed flower senescence, reduced ethylene production, ACC content, and activity and transcript levels of both ACC synthase and ACC oxidase (Lee *et al.*, 1997). Due to the fact that SAM is a universal methyl donor participating in a range of reactions, SAM synthetase has not been considered to catalyze a committed step in the biosynthesis of ethylene pathway in higher plants. Further, only a minor portion of cellular SAM is utilized for ACC production in higher plants (Yu and Yang, 1979).

However, SAM synthetase is present in multiple forms and is encoded by a small multigene family in plants with different family members under developmental and environmental control (Peleman *et al.,* 1989; Schroder *et al.,* 1997). The gene family members have been shown to be expressed differentially during senescence in carnation flowers (Woodson *et al.,* 1992), in response to treatment of pea ovaries with indole-3-acetic acid (IAA) (Gomez-Gomez and Carrasco, 1998), and during ethylene dependent ripening of kiwifruit (*Actinidia chinesis*) (Whittaker *et al.,* 1997). Further, the enzyme has been suggested to play an important role in replenishing the level of SAM, particularly during periods of high ethylene production, such as during the ethylene climacteric in fruit tissues (Whittaker *et al.,* 1997). With further biochemical and molecular characterization, it may be that this enzyme-catalyzed step in the pathway can be included as a committed part of the pathway in the future.

1.4.2 ACC Synthase

ACC synthase (AdoMet methylthioadenosine-lyase) is a pyridoxal-5'-phosphate-requiring enzyme, which is present in cytosolic fractions and converts the substrate SAM into ACC (Adams and Yang, 1979). Like other enzymes that require pyridoxal-5'-phosphate, ACC synthase is competitively inhibited by aminoethoxyvinylglycine (AVG) and aminoethoxyacetic acid (AOA) (Imaseki, 1999). ACC synthase is widely regarded as the major rate-determining enzyme because of its low abundance, instability, rapid induction, and because the rate of ethylene production appears to correlate well with its activity in the ethylene biosynthetic pathway (Kende, 1993; Yang and Dong, 1993). This proposal was initially suggested by the observation that ethylene production increased in plant organs after application of ACC (Hoffman and Yang, 1980). The level of endogenous ACC was highest in tissue that produced high amounts of ethylene at certain developmental stages, such as in fruit ripening, flower senescence, and in response to stress (Yang and Hoffman, 1984). ACC synthase was the first enzyme identified as a rate-limiting enzyme in the biosynthesis of a plant hormone. Therefore, early attempts were focused on the purification of the enzyme for further characterization. However, low abundance and instability of the enzyme greatly hampered its purification (Yang and Oetiker, 1998).

ACC synthase protein was first purified from ripened tomato pericarp after a wounding pretreatment (Bleecker *et al.,* 1986). Subsequently it has been completely purified from wounded mesocarp of winter squash (*Cucurbita maxima*) fruits by a series of chromatographic steps, and polyclonal antibodies were raised against the preparation (Nakajima and Imaseki, 1986; Nakajima *et al.,* 1988). In addition, it has been partially purified and characterized from hypocotyls of mungbean (Tsai *et al.,* 1988), or fruits of tomato (Van Der Straeten *et al.,* 1989), zucchini (Sato *et al.,* 1991), and apple fruit (Yip *et al.,* 1991).

Native ACC synthases have been found to be active as monomers in fruits, such as wound-induced tomato (Bleecker *et al.,* 1986) and apple (Yip *et al.,* 1991) or as a homodimer in zucchini fruit (Sato *et al.,* 1991). Molecular masses have been reported to range from 48 kDa in apple fruit (Yip *et al.,* 1991), 53 kDa from zucchini fruit (Sato *et al.,* 1991), 56 kDa from tomato (Van Der Straeten *et al.*, 1990), and 58 kDa from squash fruit (Fluhr and Mattoo, 1996). In many plants, ACC synthase exists in

several isoforms (Imaseki, 1999). The amino acid sequence identities of the different ACC synthase vary from 48% to 97% (Spanu *et al.*, 1994). Wounded tomato fruit tissue contains at least three isoenzymes, with pI values of 5.3, 7 and 9 (Mehta *et al.*, 1988), while the partially purified enzyme from zucchini fruit had a pI value of 5.0 (Sato *et al.*, 1991).

ACC synthase shows high substrate specificity for AdoMet, and affinity to the substrate is high with apparent K_m ranging from 12 μM for an apple ACC synthase expressed in *E. coli* (White *et al.*, 1994) to 60 μM for a partially purified enzyme from zucchini fruit (Nakajima and Imaseki, 1986). ACC synthases have pH optimum in the alkaline region, with an optimum of pH 8.0 for an enzyme partially purified from mungbean fruit (Tsai *et al.*, 1988; 1991) and pH 9.5 for an enzyme from zucchini fruit (Sato *et al.*, 1991). Low abundance and lability of the enzyme are characteristics of ACC synthase, with the lability of the enzyme considered to be due to the catalytic-based inactivation where a covalent linkage is formed at the active site between its substrate AdoMet and ACC synthase (Satoh and Esashi, 1986; Satoh and Yang, 1988; Casas *et al.*, 1993). In terms of abundance, the level of ACC synthase protein was calculated to be as less than 0.0001% of total soluble protein in the pericarp of ripening tomato fruit (Bleecker *et al.*, 1986).

A multi-gene family encodes ACC synthase in many plant species, and these genes are developmentally regulated or differentially expressed in response to various internal and external inducers (Lanahan *et al.*, 1994; Theologis, 1992; Yi *et al.*, 1999; Bekman *et al.*, 2000). Because of their central role in ethylene biosynthesis, the regulation of ACC synthases has been an intensively studied. The first ACC synthase cDNA clone was isolated from a tomato fruit cDNA library by Van Der Straeten *et al.* (1990). Subsequently, Olson *et al.* (1991) reported differential expression of two ACC synthase genes in ripening and wound-induced tomato pericarp tissues. To date, genes for about fifty ACC synthases have been cloned from a variety of plant species (see review by Grichko and Glick, 2001). For example, there are nine ACC synthase genes that have been identified in tomato, and the final number may be even higher (Zarembinski and Theologis, 1994; Oetiker *et al.*, 1997; Shiu *et al.*, 1998). At least three genes are expressed in tomato fruit, with the most abundant mRNA species corresponding to the *LE-ACS2* gene and to a lesser extent *LE-ACS4* (Lincoln *et al.*,

1993; Olson *et al.,* 1991; Rottmann *et al.,* 1991; Yip *et al.,* 1992; Barry *et al.*, 2000). Highly divergent ACC synthase gene families and their differential expression patterns have now been identified including *Arabidopsis thaliana* (twelve; Liang *et al.,* 1992; Van Der Straeten *et al.,* 1992; Arteca and Arteca, 1999; Chae, *et al.*, 2003; Wang *et al.*, 2004a), mungbean (seven; Yu *et al.,* 1998), potato (three; Destefano-Beltran *et al.,* 1995), cucumber (three; Mathooko *et al.*, 1998; Shiomi *et al.,* 1998), pea (two; Peck and Kende, 1995), and carnation (three; Park *et al.,* 1992; Jones and Woodson, 1999). However, the role that ACC synthase plays in ripening has been most widely studied in tomato. ACC synthase shows homology to pyridoxal-5'-phosphate (PLP)-dependent aminotransferases and mutant complementation studies have shown that the enzyme can act as a dimer (Tarun *et al.,* 1998). More recent studies of the ACC synthase crystal structure (Capitani *et al.*, 1999) and with the PLP cofactor binding (Huai *et al.*, 2001) have confirmed similarity between the ACC synthase catalytic binding site and those of other PLP-dependent aminotransferases. Recent work has also confirmed the presence of *LE-ACS1A* and *LE-ACS6* in tomato fruit before the onset of ripening and shown that each ACC synthase in fruit has a different expression pattern (Barry *et al.*, 2000).

The presence of several genes and proteins for ACC synthase raises questions about their functional significance. It is evident that most of these genes are induced in a regulated manner, each gene differentially regulated by a similar group of inducers. Whether cell types with different lineages are expressed different ACC synthase genes and regulated differentially remains to be determined (Fluhr and Mattoo, 1996; Jiang and Fu, 2000).

Protein phosphorylation and dephosphorylation is important for the induction of ACC synthase (Mattoo *et al.*, 1992). Regulatory phosphorylation was observed in tomato cell cultures, where ACC synthase activity was stimulated by phosphatase inhibitors and suppressed by kinase inhibitors (Spanu *et al.*, 1994). A recent study has shown that LE-ACS2 is phosphorylated in wounded tomato fruit and is not truncated (Tatsuki and Mori, 2001). A sequence analysis has identified a conserved domain that is considered to be the phosphorylation site (F/L)RLS(F/L). Recombinant LE-ACS3 and LE-ACS2 containing this domain were phosphorylated *in vitro* whereas LE-ACS4 was not phosphorylated and does not contain this site (Tatsuki and Mori, 2001). It seems that the role of ACC synthase phosphorylation is not to regulate specific activity, but to

control the rate of enzyme turnover (Spanu *et al.*, 1994). The possibility that phosphorylation of ACC synthase regulates ethylene production is supported by the finding that alteration of the C-terminal region of *Arabidopsis* ACS5 induces the *eto2-1* mutant to overproduce ethylene (Vogel *et al.*, 1998). More recently, Ecker's group reported that the lesion in another ethylene-overproducer mutation, *eto1*, is in a gene that negatively regulates ACC synthase activity and ethylene production. ETO1 protein directly interacts with and inhibits the enzyme activity of ACS5 and targets it for protein degradation (Wang *et al.*, 2004a). The hypothesis then is that phosphorylated ACC synthase would be protected from the degradation system, which in turn could cause ACC synthase to accumulate and ACC synthase activity to increase, accounting for the burst of ethylene produced by ripening fruit (Tatsuki and Mori, 2001).

1.4.3 ACC Conjugation

Not all of the ACC that is synthesized by plants is converted to ethylene. ACC can be conjugated into either 1-(malonylamino) cyclopropane-1-carboxylic acid (MACC) by *N*-malonyltransferase (Amrhein *et al.*, 1981; Hoffman *et al.*, 1982) or 1-(gammal-$_L$-glutamylamino) cyclopropane-1-carboxylic acid (GACC) by glutamyl ACC transferase (Martin *et al.*, 1995; Fluhr and Mattoo, 1996). MACC is found throughout the plant including vegetative tissue, seeds and ripening fruit (Amrhein *et al.*, 1981; Satoh and Esashi, 1984; Yang and Dong, 1993). *N*-malonyltransferase has now been partially purified from etiolated hypocotyls of mung bean (Guo *et al.*, 1992; Benichou *et al.*, 1995) and tomato fruit (Martin and Saftner, 1995). Two isoenzymes have been identified in mung bean that have different molecular masses and kinetic parameters (Benichou *et al.*, 1995).

The physiological significance of ACC conjugation for controlling ethylene production is still unclear. However, MACC is considered to be an inactive form of ACC, and cannot be hydrolyzed to release free ACC or oxidized to ethylene (Hoffman *et al.*, 1983). In tomato, *N*-malonyltransferase activity was found to be enhanced by exposure to ethylene in immature green and mature green, but not ripening tomato fruit (Martin and Saftner, 1995). This ethylene-induced activation of *N*-malonyltransferase activity has led to the proposition that the enzyme might act as a negative regulatory component in ethylene production in fruit tissues. Therefore, MACC appears not to be source of ACC, *in vivo*, but may be important in controlling the rate of ethylene production since

the formation of the conjugate causes depletion of ACC levels and so reduces ethylene production (Reid, 1995). During ripening of tomato fruits, the activity of *N*-malonyltransferase increases just after a period of ethylene production (the ethylene climacteric) (Yang and Hoffmen, 1984).

In contrast, GACC appears only when sufficient GSH tripeptide (the substrate of gamma-glutamyl-transpeptidase) is available. GACC transferase activity has been detected in ripening tomato fruit, but not in any other plant organs producing high levels of ethylene production. This implies that GACC is not a universal conjugation form with ACC, but might act as a tissue-specific regulatory component to ripening tomato fruit (Peiser and Yang, 1998). Also, Peiser and Yang (1998) pointed out that the biological function of glutamyl ACC transferase is as a hydrolase rather than a peptide-transferase. Taken together, these undermine the significance of GACC conjugation as a method of sequestering ACC *in vivo.*

1.5 ACC Oxidase

The enzyme ACC oxidase, previously referred to as the "ethylene-forming enzyme", catalyzes the final step of ethylene biosynthesis, the conversion of ACC to ethylene. Initially it was thought that ACC synthase was the key step in controlling the production of ethylene and that ACC oxidase was considered to be expressed in a constitutive manner in many plant tissues. This was interpreted originally as evidence that regulation of ACC oxidase was not a major control point of ethylene biosynthesis (Yang and Hoffmann, 1984; Theologis *et al.*, 1993). However, the role that ACC oxidase activity plays in the regulation of ethylene biosynthesis has become apparent in recent years, which suggest that ACC oxidase expression also increases when ethylene production is maximized, such as during fruit ripening (Kende, 1993), and the evidence is accumulating that ACC oxidase also constitutes an extra tier of control for ethylene biosynthesis in higher plants.

1.5.1 Identification of EFE as ACC Oxidase

Characterization of ACC oxidase (previously the ethylene-forming-enzyme, EFE) has lagged behind ACC synthase because the enzyme was thought to be unstable and difficult to purify by conventional techniques. However, EFE could be readily assayed

in vivo by administration of its substrate, ACC, to a wide variety of tissues (Cameron *et al.,* 1979). Some direct evidence for the conversion of ACC to ethylene *in vivo* came from ACC-feeding experiments. Cameron *et al.* (1979) and Lurssen *et al.* (1979) reported that a significant increase in ethylene production was observed when labeled ACC was fed to plant organs, except preclimateric fruits and flowers. Many candidates were initially suggested for the EFE. These included a peroxidase, an IAA-oxidase, a carnation microsomal enzyme, a pea microsomal enzyme, and an enzyme from a pea seedling extract that could convert ACC to ethylene in the presence of various cofactors. However, activity of the enzyme *in vitro* did not resemble those *in vivo* (Yang and Hoffmann, 1984). The dependence of ethylene production *in vivo* on ACC concentration has been studied in detail in some plant tissues. For example, the reported apparent K_m for the conversion of internal ACC to ethylene from pea epicotyls was determined to be 66 μM (McKeon and Yang, 1984) indicating the high affinity for ACC of the ethylene production system *in vivo.*

Slater *et al.* (1985) and Smith *et al.* (1986) first identified the EFE protein as the translation product of an mRNA isolated from tomato fruits. They identified nineteen non-homologous groups of tomato ripening-related clones. One of these clones, designated pTOM13 (now *LE-ACO1*) was shown to be homologous to an mRNA, which accumulated prior to the wounding-induced ethylene peak in unripe fruit and leaf tissue of tomato (Smith *et al.,* 1986). It was suggested that the pTOM13 transcript might either be involved in ethylene production, or be a transcript that was rapidly induced by ethylene. Subsequently, pTOM13 was shown to be induced by ethylene in mature green tomato fruit (Maunders *et al.,* 1987).

From the observation of greatly reduced ethylene production by tomato plants transformed with an antisense construct of a ripening-related cDNA (pTOM13), Hamilton *et al.* (1990) suggested that the gene encoded an enzyme involved in ethylene biosynthesis. It appeared that from a comparison of the molecular mass of partially purified ACC synthase from zucchini fruit (53 kDa; Sato *et al.,* 1991) with the translation product of pTOM13 (35 kDa; Smith *et al.,* 1986), the coded protein was too small to be an ACC synthase (Hamilton *et al.,* 1990). To further confirm whether pTOM13 could encode EFE, an activity assay *in vivo* was performed on leaf discs from both wild type and plants transformed with pTOM13 in the antisense orientation, and it

was shown that the ethylene-forming ability was reduced in the antisense plants in a gene dosage-dependent manner (Hamilton *et al.*, 1990). In addition, Hamilton *et al.* (1991) then reported that a full-length clone of pTOM13 (pRC13) was found to confer EFE activity when the cDNA was expressed heterologously in yeast.

The DNA sequence of pTOM13 and related cDNA showed a comparatively high homology to flavonone-3-hydroxylase genes (Hamilton *et al.*, 1990). As these enzymes had been known to require ascorbate and iron (Fe^{2+}) as cofactors when the same conditions were used to assay EFE, complete recovery of the activity from the soluble fraction of melon fruit was observed (Ververidis and John, 1991). These cofactors, therefore, were found to be essential for the assay of ACC oxidase activity *in vitro*, and the failure of previous attempts to assay enzyme activity was now attributed to the loss of these cofactors during protein extraction from plant tissue.

Confirmation for both EFE activities *in vitro* and *in vivo* was achieved by finding a parallel increase in preclimateric apple fruits treated with ethylene (Fernández-Maculet and Yang, 1992), indicating that the activity *in vitro* was representative of the activity *in vivo*. By analyzing the stereospecificity of the reaction (Ververidis and John, 1991; Kuai and Dilley, 1992; Fernández-Macule and Yang, 1992), the stoichiometry of the EFE catalyzed reaction was determined (Dong *et al.*, 1992) (Fig.1.2) and as a consequence of this, EFE was renamed ACC oxidase.

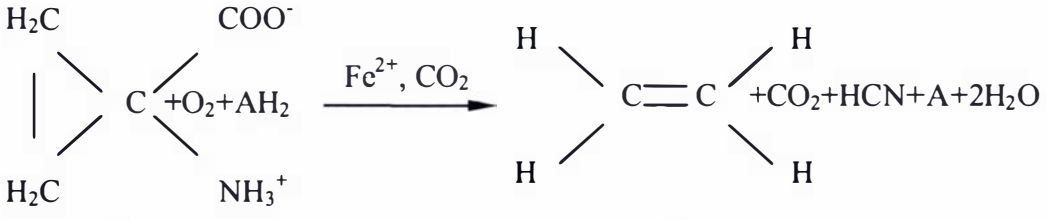

(ACC) **(Ethylene)**

Figure 1.2 Stoichiometry of reaction catalyzed by ACC oxidase

AH_2 and A stand for ascorbate and dehydroascorbate respectively.

1.5.2 Biochemical Studies of ACC Oxidase

1.5.2.1 Purification and Characterization of ACC Oxidase

Once ACC oxidase activity, *in vitro*, was fully recovered from crude protein extracts using appropriate cofactors (ascorbate and Fe^{2+}), purification and characterization of the enzyme from many plant species has progressed very quickly. Since the first successful extraction from melon fruit (Ververidis and John, 1991), ACC oxidase protein has now been identified and partially purified from apple fruit (Dong *et al.,* 1992; Kuai and Dilley, 1992; Dupille *et al.,* 1993; Pirrung *et al.*, 1993), avocado (McGarvey and Christoffersen, 1992), kiwifruit (MacDiarmid and Gardner, 1993), tomato (English *et al.,* 1995), banana fruit (Moya-Leon and John, 1995), cherimoya (Escribano *et al.,* 1996), citrus peel (Dupille and Zacarias, 1996), papaya fruit (Dunkley and Golden, 1998), pear (Vioque and Castellano, 1994; Kato and Hyodo, 1999), and breadfruit (Williams and Golden, 2002). In addition, enzyme activity *in vitro* has also been found in senescing carnation floral tissue (Kosugi *et al.*, 1997), leaf tissues of both white clover (Butcher, 1997; Hunter *et al.*, 1999) and barley (Kruzmane and Ievinsh, 1999) and in pine needles (Kruzmane and Ievinsh, 1999). Moreover, ACC oxidase protein has been purified to near homogeneity or homogeneity from fruit of apple (Dong *et al.,* 1992; Dupille *et al.,* 1993; Pirrung *et al.*, 1993), banana (Moya-Leon and John, 1995), papaya (Dunkley and Golden, 1998), pear (Kato and Hyodo, 1999), and breadfruit (Williams and Golden, 2002). Fewer ACC oxidases have been partially or purified to homogeneity from vegetative plant tissue (Gong and McManus, 2000).

ACC oxidase is now classed as an 2-oxoacid dependent dioxygenase (2-ODD) (Prescott and John, 1996). As soluble enzymes, 2-ODDs require Fe^{2+} and ascorbate for optimal substrate conversion *in vitro.* Most 2-ODDs have an absolute requirement for 2-oxoglutarate, but ACC oxidase appears to be unique in this family in that is uses ascorbate not 2-oxoglutarate as a cosubstrate (Prescott and John, 1996). For example, when 2-oxoglutarate instead of ascorbate was added to the assay mixture extracted from pear fruits, most of the enzyme activity *in vitro* was lost (Vioque and Castellano, 1994). The activating effect of CO_2 for ACC oxidase activity has also been reported from protein extracts of many plant species (John, 1997). It has been proposed that ACC oxidase originated by an alteration in the substrate specificity of the closely related 2-oxoacid dependent dioxygenase (John, 1997).

The molecular masses of ACC oxidase have now been determined from several plant species by gel filtration chromatography and SDS-PAGE analysis, respectively. The native molecular mass of the partially purified enzyme from banana fruit was determined to be 35 kDa (Moya-Leon and John, 1995), smaller than the enzyme from melon (41 kDa, Smith *et al.,* 1992) and breadfruit (42.3 kDa, Williams and Golden, 2002), but equal to the enzyme both from tomato (35 kDa) encoded by pTOM13 (Hamilton *et al.*, 1990) and apple (35 kDa, Dong *et al.*, 1992). Recently, the native molecular mass of the purified isoforms MGI and SEII from the leaf tissues of white clover was determined to be 37.5 kDa by size exclusion chromatography and molecular masses of MGI and SEII were observed to be 37 kDa and 35 kDa, respectively by SDS-PAGE analysis (Gong and McManus, 2000).

The optimal pH for ACC oxidase activity *in vitro* has been shown to vary from as low as pH 6.8 in apple fruit (Ponelcit and Dilley, 1993) and sunflower seedlings (Finlayson *et al.,* 1997) to pH 7.5-8.0 for avocado fruit (McGarvey and Christoffersen, 1992). However, the optimal pHs for isoforms MGI and SEII from leaf of white clover was 7.5 and 8.5, respectively (Gong and McManus, 2000). Recently, Williams and Golden (2002) reported that optimum activity of ACC oxidase from breadfruit was obtained at a pH of 7.2 at 28°C. ACC oxidase has been shown to be an acidic protein in some fruits. The partially purified enzyme from cherimoya fruits has an isoelectric point (pI) at pH 4.35 (Escribano *et al.,* 1996), and pH 4.9 for that of banana fruit (Moya-Leon and John, 1995) determined by chromatofocusing on a Mono P column. Bidonde *et al.* (1998) reported that one of the three isoforms of tomato ACC oxidase expressed in yeast, *LE-ACO2*, had a pI of 6.8 while both *LE-ACO1* and *LE-ACO3* had the same pI of 6.2 using denaturing isoelectric focusing (IEF).

All ACC oxidases characterized from plant tissues have been determined to display Michaelis-Menten kinetics for the substrate ACC. K_m values for ACC oxidase have been reported to range from 6.4 μM for the partially purified enzyme from apple (Kuai and Dilley, 1992) in the absence of carbon dioxide, and 20 μM in the presence of a saturating carbon dioxide level (20%) (Ponelcit and Dilley, 1993), 39.7 μM and 110 μM for the purified isoforms MGI and SEII from leaf of white clover (Gong and McManus, 2000), to 425 μM for the enzyme in the crude homogenate of carnation petals (Nijenhuis-De Vries *et al.,* 1994). These results indicate that the enzyme has a

high affinity for ACC. However, in determinations for the same plant species and tissue, the enzyme in a crude extract had a higher K_m for ACC when compared with the purified and partially purified enzyme. For example, the K_m for ACC of the partially purified enzyme from carnation flowers (Kosugi *et al.*, 1997) ranged from 111 μM to 125 μM when compared with 425 μM determined for the crude enzyme (Nijenhuis-De Vries *et al.*, 1994). In addition, the value of the K_m is dependent upon the concentration of carbon dioxide/bicarbonate in the assay mixture. For example, when 30 mM sodium bicarbonate is omitted from the reaction mix in the carnation petal extract, the K_m for the enzyme is reduced from 425 μM to 30 μM (Nijenhuis-De Vries *et al.*, 1994).

There have also been some studies on the inhibition of ACC oxidase activity *in vitro*. Nijenhuis-De Vries *et al.* (1994) reported that the enzyme from senescing carnation flowers had a K_i of 5 mM for α-aminoisobutyrate (AIB, an analog of ACC), which was 10-fold higher than the apparent K_m for ACC (425 μM). A cyclobutane ACC analog, 1-aminocyclobutane-1-carboxylate (ACBC), strongly inhibited the activity *in vitro* of the partially purified enzyme from senescing carnation flowers (Kosugi *et al.*, 1997). It appears as a strong competitive inhibitor with the K_i of 20 to 31 μM, which was only about 20% of the K_m value (125 μM) for ACC. It was suggested that ACBC could bind to the active site of the enzyme (Kosugi *et al.*, 1997). In addition, Co^{2+} was reported to be 50% inhibitory at a concentration of 25 μM to the enzyme partially purified from melon fruit (Ververidis and John, 1991), and 46% inhibitory for the enzyme partially purified from apple fruit at 10 μM (Kuai and Dilley, 1992). Pirrung *et al.* (1995) examined the inhibition of a purified ACC oxidase from apple fruit with different amino acid hydroxmates and suggested that they acted through both chelating and hydrophobic interactions at the active site. The most potent inhibitor, ACC-hydroxmate, had a K_i similar to the K_m for the substrate ACC. Chelating agents, such as tropolones, were also found to inhibit ACC oxidase activity *in vitro* which was recovered by the addition of Fe^{2+} in the assay mixture (Mizutani *et al.*, 1995). Therefore, the inhibition of ACC oxidase activity and ethylene production was attributed to the Fe^{2+} chelating ability of these tropolones. Recently, Williams and Golden (2002) reported that the purified ACC oxidase from breadfruit showed marked inhibition by cobalt sulphate, sodium metabisulphite, sodium dithionite, zinc sulphate and hydrogen peroxide.

In terms of amino acid sequencing from purified ACC oxidase by the Edman method, no sequence was obtained from the purified apple protein (Dong *et al.*, 1992). Attempts to determine the N-terminal sequence of the purified ACC oxidase from apple fruit were unsuccessful (Dupille *et al.*, 1993). These results suggest that its N-terminus is blocked. Electrospray mass spectrometry showed that the molecular mass (35,332 ± 5 amu) was ~ 50 amu higher than that predicted from the cDNA sequence, and the blocking group at the N-terminus of a purified apple ACC oxidase was identified as an *N*-acetyl group (Pirrung *et al.*, 1993).

It has been suggested that ACC oxidase contains some conserved amino acid residues and requires some crucial amino acid residues for maximal activity of the enzyme (Kadyrzhanova *et al.*, 1997; 1999; Dilley *et al.*, 2003). Inactivation experiments using diethylpyrocarbonate (DEPC) (Zhang *et al.*, 1995) presented evidence for the presence of His residues at the active site of an ACC oxidase from tomato fruit expressed in *E. coli*. This core structure of ACC oxidase is thought to be similar to that of isopenicillin N synthase (IPNS): His^{177}, Asp^{179} and His^{234} in ACC oxidase are likely ligands for Fe^{2+} based on similarly placed His and Asp residues in IPNS (Kadyrzhanova *et al.*, 1997).

Site-directed mutagenesis of ACC oxidase has been used to determine the nature and role of conserved amino acid residues in the mechanism by which CO_2 activates the enzyme. Dilley *et al.* (2003) concluded that Arg^{244}, Ser^{246} and Thr^{157} were binding sites for the ACC carboxyl group based on steady-state kinetics of the mutants Arg^{244}Lys, Ser^{246}Ala and Thr^{157}Ala as single, double and triple mutants of the three residues. The ACC K_m of the triple mutant (Arg^{244}Lys/ Ser^{246}Ala/Thr^{157}Ala) was increased while the V_{max} was decreased. This is consistent with the ACC carboxyl group interacting with the Arg^{244} guanidinium group and the hydroxyl group of Ser^{246} and Thr^{157}. In addition, a consensus sequence search of 38 known or putative ACC oxidase revealed 8 completely conserved lysine residues (K^{72}, K^{144}, K^{158}, K^{172}, K^{199}, K^{230}, K^{292}, and K^{296}). All of the lysine mutant forms were typically activated by CO_2 indicating that none of them is essential for CO_2 activation by a carbamylation mechanism. However, because ascorbic acid binds to proteins *via* salt bridges and H-bonding (Li *et al.*, 2001), it also forms a Schiff base with the Lys E-amino group. Lys^{158}, Lys^{230} and Lys^{292} appear to be most critical for ascorbate activation (Dilley *et al.*, 2003).

Some of the residues in the C-terminal region are critically important for enzyme activity. This portion of the protein is predicted to be in close proximity to the catalytic site (Roach *et al.*, 1997). Of the conserved residues, K^{292}, E^{297}, R^{299} and E^{301} are important while Q^{294} and K^{296} are not (Kadyrzhanova *et al.*, 1999). More recently, it has been found that $Arg^{175}Lys$ is able to directly interact with HCO_3^- (not CO_2). In this way, HCO_3^- serves to position Fe^{2+} into its binding site (His^{177}, Asp^{179} and His^{234}) (Dilley *et al.*, 2003).

1.5.2.2 Localization of ACC Oxidase

Whether the ACC oxidase is localized to the cytosol or cell wall has been debated for many years. Before 1990, due to the difficulty in recovering the authentic enzyme activity from extracts of broken cells, it was thought that ACC oxidase was membrane-bound (Yang and Hoffman, 1984). Mayne and Kende (1986) have shown that the enzyme was a membrane protein and was located in the vacuole, and proposed that membrane integrity was required for the enzyme activity. Since 1990, some new techniques have been used to re-examine this issue. These include antibodies raised against ACC oxidase produced in *E. coli*, and also methods to recover the enzyme activity in different compartments of the plant cell. A cytosolic location was initially suggested because of recovery of ACC oxidase in the soluble fraction of melon (Ververidis and John, 1991), avocado (McGarvey and Christoffersen, 1992) and mandarin fruits (Dupille and Zacarias, 1996). Dupille and Zacarias (1996) found that addition of Triton X-100 (a detergent which aids solubilization of enzymes from membranes) did not increase recovery of the enzyme from the peel of mandarin. Reinhardt *et al.* (1994) have pointed out that the enzyme in tomato suspension cells is localized in the cytoplasm. However, immunocytolocalization experiments performed by Rombaldi *et al.* (1994) indicated that ACC oxidase is located at the cell wall in the pericarp of ripening tomato and climacteric apple. Ramassamy *et al.* (1998) combined cell fractionation and immunocytological methods and found that ACC oxidase is mainly located at and associated with the external face of the plasma membrane. Due to the lack of a typical signal peptide in the amino acid sequence of ACC oxidase known (Yang and Dong, 1993), it was proposed that ACC oxidase is not secreted *via* the endoplasmic reticulum (ER) pathway (Rombaldi *et al.*, 1994).

It is known that not all plasma membrane or secretory proteins contain an N-terminal consensus sequence that is cleaved following translocation across the ER membrane. Conserved hydrophobic regions in the amino acid sequence of ACC oxidase have been suggested to play a possible role in interactions of ACC oxidase with membranes (Balagué *et al.*, 1993; Kende, 1993). Recently, Chung *et al.* (2002) re-examined the subcellular localization of ACC oxidase in apple fruit by immunogold labeling with a highly specific antibody raised against the recombinant apple enzyme. It was demonstrated that apple ACC oxidase was located mainly, if not solely, in the cytosol of apple fruit mesocarp cells.

1.5.2.3 Evidence for the Occurrence of ACC Oxidase Isoforms in Plants

The biochemical characterization of ACC oxidase protein extracted from many plant species now suggests that the enzyme, which was supported by the evidence from multigene families, exists as more than one isoform in plants (McGarvey and Christoffersen, 1992; Vioque and Castellano, 1994; Dupille and Zacarias, 1996; Finlayson *et al.*, 1997)

Two ACC oxidase activities, designated as EFE1 and EFE2, were first found after differential ammonium sulphate precipitation of a crude extract of avocado fruit (McGarvey and Christoffersen, 1992). The demonstration of typical stereo-substrate specifically, and the inhibitory effect of 2-aminoisobutyric acid (2-AIB) confirmed that both EFE1 and EFE2 were authentic ACC oxidase proteins. Furthermore, the analysis of EFE1 showed a relatively low K_m (32 μM) for ACC with a pH optimum of 7.5 to 8.0 and optimal temperature at 25°C to 30°C. In later studies, two optimal temperatures at 28°C and 38°C were observed in the enzyme extracts from pear fruits (Vioque and Castellano, 1994), 27.5°C and 35°C in chickpea seeds (Munoz De Rueda *et al.*, 1995), and 35°C and 45°C in citrus peel (Dupille and Zacarias, 1996). These results implied that there might be more than one isoform of ACC oxidase in these plant tissues.

Further evidence for the occurrence of ACC oxidase isoforms has been found from studies with leaf and root tissues of corn (*Zea mays*) and sunflower (*Halianthus annus*) (Finlayson *et al.*, 1997). Both corn and sunflower seedlings have been shown to possess organ-specific ACC oxidase activities, which demonstrate a distinct pH dependence and K_m for ACC, dioxygen, ascorbate and carbon dioxide. These results suggest that

the different ACC oxidase protein isoforms have evolved to adapt to the environment to which each organ of the plant is exposed. Three isoforms of tomato ACC oxidase expressed in yeast were reported to demonstrate differences in the apparent K_m for ACC, pI and specific activity (Bidonde *et al.,* 1998). Gong and McManus (2000) purified two isoforms of ACC oxidase to homogeneity during leaf ontogeny from white clover. One isoform, designated MGI, was purified from mature green leaf tissues, while SEII was one of two isoforms identified in senescent leaf tissues. In addition to molecular mass, differences between the two isoforms were observed in terms of pH optima, isoelectric point (pI), K_m for ACC, optimal requirements for the co-substrate ascorbate, and $NaHCO_3$ and Fe^{2+} as co-factors, which demonstrate that these two isoforms are distinct ACC oxidases from the same tissue at different developmental stages. The significance of the determination of isoforms in these tissues is that it supports the observation of ACC oxidase gene families.

1.5.3 Molecular Studies of ACC Oxidase

1.5.3.1 Identification and Characterization of ACC oxidase Genes in Plant Species

The identification of ACC oxidase by molecular cloning is an instructive case of 'reverse' biochemistry. Due to the difficulties of measuring ACC oxidase activity in a cell-free system in earlier studies, this enzyme was first identified at the cDNA level by differential screening. Since the first ACC oxidase cDNA, pTOM13 was identified in tomato (Hamilton *et al.,* 1990), numerous ACC oxidase cDNA clones have been isolated from a variety of plant species and the enzyme is encoded by small multi-gene families (Kende, 1993; Barry *et al.*, 1996; Fluhr and Mattoo, 1996; Imaseki, 1999). Multiple gene members of ACC oxidase have been identified in plants by screening genomic libraries, including four members in the tomato ACC oxidize gene family, designated *LE-ACO1, LE-ACO2, LE-ACO3* and *LE-ACO4* (Bouzayen *et al.,* 1993; Barry *et al.*, 1996; Nakatsuka *et al.*, 1998), four members in Petunia flowers (*Petunia hybrida*; Tang *et al.*, 1993), three members in cantaloupe melon (Lasserre *et al.,* 1996), three members in tobacco (Kim *et al.,* 1998), two members in peach (Ruperti *et al.*, 2001), and two members in papaya (Chen *et al.*, 2003; Lopez-Gomez *et al.*, 2004). By screening cDNA libraries, two members in mung bean (Kim and Yang, 1994; Jin *et al.,*

1999), three members in sunflower seedlings (Liu *et al.,* 1997), two in banana fruit (Huang and Do, 1998), two members in broccoli floral tissue (Pogson *et al.,* 1995), one in apricot fruit (Mbeguie-A-Mbeguie *et al.,* 1999), and one in potato (Zanetti *et al.*, 2002) have been isolated and characterized. Shiomi *et al.* (1998) cloned two ACC oxidase homologs from cucumber fruit using the reverse transcriptase-polymerase chain reaction (RT-PCR) and both 5'-and 3'-rapid amplification of cDNA ends (RACE) PCR. Hunter *et al.* (1999) reported that three ACC oxidase genes, designated *TR-ACO1*, *TR-ACO2* and *TR-ACO3*, have been isolated and characterized during leaf ontogeny in white clover using a combination of RT-PCR and 3'-RACE. The ACC oxidase proteins encoded by these genes are highly identity, while ACC oxidase genes share identical numbers and positions of introns.

Sequence comparison from more than thirty ACC oxidase genes indicates a high nucleotide sequence identity (70-80%) both within the same family and between families from different plant species (Lasserre *et al.,* 1996). The gene families of tomato and petunia are particularly similar with the three genes of tomato showing 88 to 94% similarity to each other, and just as high similarity to the three genes of petunia (88 to 95%) when deduced amino acid sequences were compared (Lasserre *et al.,* 1996). In contrast, in petunia flowers, the four ACC oxidase cDNAs displayed only 42 % to 43% identity in their 5'-untranslated regions (UTRs) and 50% to 57% identity in their 3'-UTRs (Tang *et al.,* 1994). The three isoforms of ACC oxidase from tomato show 58% to 60% homology in their 5'-UTRs and 44% to 52% identity in their 3'-UTRs (Barry *et al.,* 1996). Two ACC oxidase genes, *CP-ACO1* and *CP-ACO2*, were identified from papaya. The deduced amino acid sequences share 77% identity with each other (Chen *et al.*, 2003). Two ACC oxidase genes from peach, *PP-ACO1* and *PP-ACO2*, displayed 78% identify in the deduced amino acid sequences (Ruperti *et al.*, 2001). *PP-ACO1* and *PP-ACO2* show highest degree of similarity with petunia (*PH-ACO3*; 84%) and apple (85%) ACC oxidase genes, respectively. Three genes, designated as *CM-ACO1*, *CM-ACO2* and *CM-ACO3*, were identified from melon (Lasserre *et al.,* 1996). The *CM-ACO1* gene has three introns, whereas *CM-ACO2* and *CM-ACO3* have two introns. The DNA sequence of *CM-ACO1* show 59% and 75% identity with those of *CM-ACO2* and *CM-ACO3*, respectively, while *CM-ACO2* and *CM-ACO3* show 59% identity. All these genes displayed considerable divergence in their 5'- and 3'-untranslated regions. Two ACC oxidase cDNA clones from cucumber

fruit, *CS-ACO1* and *CS-ACO2*, were 73% identical to each other at the amino acid level and 66% homologous at the nucleotide level (Shiomi *et al.*, 1998). Furthermore, *CS-ACO1* was highly identiy to *CM-ACO1* isolated by Lasserre *et al.* (1996) with a identity of 96% at the nucleotide and 97% identity at the amino acid levels, respectively, while *CS-ACO2* was 74% similar to other ACC oxidases at both levels (Shiomi *et al.*, 1998). Similarly, in the leaves of white clover (*Trifolium repens* L.), the three distinct ACC oxidase genes exhibit a high degree of identity in their coding regions that ranges from 75% to 84%, but show a much greater level of sequence divergence within their 3'-untranslated regions from 55% to 61% (Hunter *et al.*, 1999). Unlike ACC synthase, ACC oxidase is encoded by a small multigene family. However, specific expression of these genes is important for the regulation of ethylene biosynthesis, not only in ripening fruits and flower tissues but also in vegetative tissues. In concert with these reports, more and more studies now reveal that ACC oxidase genes are differentially expressed during plant development and in response to various stimuli.

1.5.3.2 Expression and Regulation of ACC Oxidase Genes during Plant Development

The expression of ACC oxidase activity was generally believed to be constitutive in plant tissues (Yang and Hoffman, 1984). However, with the identification of ACC oxidase as the product of an mRNA (pTOM13), subsequent gene expression studies have indicated that the constitutive expression of ACC oxidase in plant tissue is not due to a single gene. Differential expression of a small multigene family in a temporal and a spatial manner has been observed in orchid flowers (Nadeau *et al.,* 1993), mungbean epicotyls (Kim and Yang, 1994), petunia floral tissues (Tang *et al.* 1993; Tang and Woodson, 1996), broccoli floral tissue (Pogson *et al.,* 1995), tomato (Barry *et al.,* 1996; Blume and Grierson, 1997) and melon leaf tissue (Lasserre *et al.,* 1996, 1997), carnation floral tissues (Ten Have and Woltering, 1997), sunflower seedling tissue (Liu *et al.,* 1997), leaf tissue of *Nicotiana glutinosa* (Kim *et al.,* 1998), rice (Chae *et al.*, 2000) peach (Ruperti *et al.*, 2001), and papaya (Chen *et al.*, 2003; Lopez-Gomez *et al.*, 2004).

In tomato, the most widely studied fruit model, the developmental expression of the ACC oxidase multigene family was examined using a combination of northern analysis,

ribonuclease protection assays, and promoter-β-glucuronidase (GUS) fusions (Barry *et al.,* 1996; Blume and Grierson, 1997). *LE-ACO1* and *LE-ACO3* are expressed during the senescence of leaves, fruit and flowers. *LE-ACO1* transcripts continue to accumulate throughout ripening, whereas *LE-ACO3* transcript accumulation increases transiently at the breaker stage and then declines very quickly. No *LE-ACO2* expression is observed in the fruit at any developmental stage (Barry *et al.,* 1996). A fourth tomato ACC oxidase gene, *LE-ACO4*, with low sequence similarity when compared with the other three ACC oxidase genes (Barry *et al.*, 1996), has recently been observed to be expressed upon commencement of ripening (Nakatsuka *et al.,* 1998).

In cantaloupe melon, the expression of ACC oxidase is also under spatial and temporal regulation (Lasserre *et al.*, 1996). The *CM-ACO1* isoform is expressed predominantly in leaves, flowers, roots, and etiolated hypocotyls. In contrast, expression of *CM-ACO2* is limited to etiolated hypocotyls, while *CM-ACO3* is the predominant isoform in flowers with very little transcript present in leaves and etiolated hypocotyls. Similarly, Barry *et al.* (1996) found that *LE-ACO1* is expressed predominantly in the petals and stigma and style of tomato, whereas *LE-ACO2* is expressed only in tissues associated with the anther cone. However, *LE-ACO3* is expressed in all floral parts examined except for the sepals. In papaya, northern analysis revealed that *CP-ACO2* was induced only at the late stage of fruit ripening and leaf senescence, while *CP-ACO1* was induced before the color break (mature) stage. These results suggest that *CP-ACO2* is a late-stage-associated ACC oxidase occurring during organ senescence, such as fruit ripening and leaf senescence, while *CP-ACO1* is maturation-associated (Chen *et al.*, 2003).

Two members of the ACC oxidase gene family of peach are also expressed in a differential manner in flowers, fruit and leaves (Ruperti *et al.*, 2001). *PP-ACO1* expression is upregulated in fruitlet abscission, in ripe mesocarp, in response to ethylene, and in senescent leaves, whereas *PP-ACO2* expression is confined to the early development of fruit and is not induced by ethylene. A similar behavior in relation to ethylene treatment has been observed in rice, where two ACC oxidase cDNAs (*OS-ACO2* and *OS-ACO3*) have been isolated (Chae *et al.*, 2000). In etiolated seedlings, exogenous ethylene induced an accumulation of *OS-ACO3* mRNA, while it partially inhibited *OS-ACO2* expression.

In *Nicotiana glutinosa*, it appears that the ACC oxidase isogene *pNG-ACO2* is required for the basal production of ethylene in leaves, whereas the expression of the *pNG-ACO1* and *pNG-ACO3* isogenes occurs in response to stresses such as wounding and viral infection (Kim *et al.,* 1998). Accumulation of the isogenes also varies markedly between roots and stems, where *pNG-ACO1* and *pNG-ACO3* are predominantly expressed in the roots, while *pNG-ACO2* is expressed in stems.

Taken together, these studies suggest that various developmental and tissue-specific ACC oxidase isogenes exist in higher plants and their expression is highly regulated by developmental and environmental stimuli. The differential expression of these multigene families provides evidence that ACC oxidase does confer a degree of control on ethylene biosynthesis.

1.5.4 Post-Transcriptional and Translational Regulation of ACC Oxidase

Changes in ACC oxidase activity, both induced by plant developmental signals or by various external stimuli does not always follow changes in transcript abundance in plants (Kim and Yang, 1994; Liu *et al.*, 1997; Jin *et al.*, 1999). For example, in mungbean hypocotyls, *VR-ACO1* gene expression, ACC oxidase activity, and ACC oxidase protein accumulation increased in parallel over 2 hs after ethylene treatment. However, the rate of increase in ACC oxidase activity, and ACC oxidase accumulation was much slower than the increase of *VR-ACO1* transcripts, which suggests that the ethylene-responsive increase of ACC oxidase activity in mungbean hypocotyls is regulated at both the transcriptional and post-transcriptional levels (Kim and Yang, 1994; Jin *et al.*, 1999).

Liu *et al.* (1997) reported that there are discrepancies between ACC oxidase transcript accumulation and ACC oxidase protein accumulation in sunflowers. When wounding and treatment with silver ions induced ACC oxidase transcripts and ACC oxidase activity, ACC oxidase protein accumulation did not correlate with this increase. In addition, Hunter (1998) reported that wounding mature green leaves of white clover increased *TR-ACO3* gene expression, but it was not correlated with increased protein accumulation or ACC oxidase enzyme activity. However, initial evidence demonstrated by Gong (1999) from biochemical studies in the leaf tissue of white clover showed that there is an induced ACC oxidase activity peak that could be the wound response-related

isoform of ACC oxidase encoded by the *TR-ACO3*. These results support that the notion that ACC oxidase activity is controlled at a post-transcriptional level.

Post-translation modifications are now known to play a fundamental role in regulating the activity, location and function of a wide range of proteins. In plant cells, work on different types of post-translational modification has progressed largely along independent lines (Battey *et al.*, 1993). Protein phosphorylation is one of the most widely used post-translation modifications of proteins in living cells. Reversible protein phosphorylation is a fundamental post-translational regulatory mechanism, and is involved in controlling a vast array of cellular events and processes in plants. A significant number of genes of the sequenced *Arabidopsis* genome encode for protein kinases and protein phosphatases that catalyze reversible phosphorylation. For optimal regulation, kinases and phosphatases must strike a balance in any given cell. Only a very small fraction of the thousands of protein kinases and phosphatases in plants has been studied experimentally. Nevertheless, the available results have demonstrated critical functions for these enzymes in plant growth and development, such as hormonal, pathogen, or environmental stress responses (Luan, 2003; Mumbly and Walter, 1993; Smith and Walker, 1993; Garbers *et al.,* 1996; Janssens and Goris, 2001). While serine/threonine phosphorylation is widely accepted as a predominant modification of plant proteins, the function of tyrosine phosphorylation, despite its overwhelming importance in animal systems, had been largely neglected until recently when tyrosine phosphatases (PTPs) were characterized from plants. The genetic, biochemical and molecular analyses of plant growth and development have yielded a lengthy and rapidly growing list of phenomena controlled by protein phosphorylation, and have revealed some surprises, such as the importance of histidine-aspartate phosphorelay systems in plant signal transduction (Hardie, 1999; Thomason and Kay, 2000; DeLong *et al.*, 2002). For example, in higher plants, nitrate reductase (NR) is rapidly inactivated/activated by phosphorylation/dephosphorylation in response to environmental stimuli and various treatments (Lillo *et al.*, 2004). The adjustment of NR activity by a post-translational mechanism takes place in only 5-20 min, depending on the species.

1.5.4.1 Circadian Regulation of Physiological Processes

During the past decade, there has been a tremendous increase in our understanding of the molecular bases of the biological clocks in a wide range of organisms. In higher plants, diurnal and circadian regulation of gene expression is very common and is necessary for the efficient temporal regulation of many physiological processes. These range from opening of the stomatal aperture, leaf movement, growth processes, ion uptake, nitrogen assimilation, carbon metabolism and fragrance emission, through to photosynthesis (McClung, 2001; Harmer *et al.*, 2000; Schaffer *et al.*, 2001). For example, circadian rhythms are a conspicuous feature of NR regulation and have been observed in many but not all plant species. For example, *Arabidopsis*, barley, *Chenopodium rubrum*, maize, tobacco, and tomato display strong circadian NR activity rhythms (see review by Tucker *et al.*, 2004).

In particular, one of the fundamental circadian-regulated events is control of the flowering time through the photoperiodic long-day pathway (Kreps and Kay, 1997; Somers 1999; Barak *et al.*, 2000; McClung, 2000, 2001; Simpson and Dean, 2002). The list of genes under the control of the circadian clock is constantly growing (Kreps and Kay, 1997; Fejes and Nagy, 1998). Although the circadian rhythms that are observed originate from the circadian regulation of gene expression, the molecular mechanisms that effect clock control are many, and common control points, like transcription and protein phosphorylation, are used to effect this regulation (Strayer and Kay, 1999).

There are examples of circadian regulation of gene expression in higher plants at each step: transcription (Millar and Kay, 1991; Liu *et al.*, 1996), transcript abundance (Fujiwara *et al.*, 1996; Zheng *et al.*, 1998), translation (Mittag *et al.*, 1994), and post-translational processing (Nimmo, 1998).

Conceptually, the circadian rhythm system comprises three basic components: the input pathways, the oscillator and the output pathways. The environmental cues that set the phase of the clock are usually light and temperature, and the signal transduction pathways that reset the clock in response to these signals are known as input pathways. Circadian time keeping is mediated by a central oscillator, which is thought to consist of a biochemical feedback loop. To be useful as a clock, this oscillator has to be set to local time. Downstream of the oscillator, other signal transduction pathways, known as output pathways, mediate the control of overt rhythms. The persistence of circadian

rhythms even in the absence of environmental timing cues indicates that they are driven by a self-sustaining oscillator. Integral to the oscillator are clock proteins that oscillate with a 24-hs rhythm: clock genes are rhythmically transcribed and after a certain delay clock proteins feed back to inhibit transcriptional activity of their own genes (Dunlap, 1999; Young and Kay, 2001). Moreover, post-transcriptional regulation of the clock transcripts as well as post-translational modifications of the clock proteins contributes to the maintenance of the 24-h periodicity (Edery, 1999; Allada *et al.*, 2001). The rhythmically produced clock proteins in turn translate temporal information into rhythmic physiology *via* output-signal trasduction chain (Brown and Schibler, 1999). Thus the phases of clock gene mRNA and clock protein oscillations are indicators of internal time.

To our knowledge, there have been no reports that demonstrate protein phosphorylation and dephosphorylation of ACC oxidase in higher plants. However, in tomato, a recent study clearly showed that protein phosphorylation of ACC synthase occurs *in vivo* (Tatsuki and Mori, 2001). In addition, sequence analysis of TR-ACO2 and TR-ACO3 indicates possible phosphorylation sites, which means there is at least the theoretical possibility for protein phosphorylation of these ACC oxidases. Furthermore, previous preliminary observations have suggested that *TR-ACO2* may be under circadian control (Hunter, 1998). Therefore, post-translational regulation of ACC oxidase from white clover merits for further investigation.

1.6 ACC Oxidase during Leaf Maturation and Senescence

Leaf senescence is a developmentally programmed degeneration process that constitutes the final step of leaf development and is controlled by multiple developmental and environmental cues (Lim *et al.*, 2003; Yoshida, 2003). To date, changes in ACC oxidase gene expression during leaf maturation and senescence has now been observed from several plant species, which includes tomato (Barry *et al.*, 1996; Blume and Grierson, 1997), melon (Lasserre *et al.*, 1996), tobacco (Lasserre *et al.*, 1997; Kim *et al.*, 1998), white clover (Hunter *et al.*, 1999), and papaya (Chen *et al.*, 2003).

In tomato (Barry *et al.*, 1996), leaf senescence (as judged by chlorosis) was accompanied by a dramatic increase in the abundance of the *LE-ACO1* transcript (up to

27-fold) at the onset of leaf senescence before declining slightly at the most advanced stage. The expression of *LE-ACO3* also increased, but it was only about 50% of the level of the *LE-ACO1* gene, while no *LE-ACO2* gene expression was detected in leaves at any developmental stage. In contrast, in tobacco, all three ACC oxidase genes are up-regulated in senescent leaves when compared with younger leaf tissue (Kim *et al.*, 1998). Two tobacco full length ACC oxidase clones, *pNG-ACO1* and *pNG-ACO3*, have been observed to accumulate during leaf senescence while *pNG-ACO2* was constitutively present in leaf tissue. In leaf tissue of melon, quantitative RT-PCR has shown that expression of the two ACC oxidase isoforms is differentially regulated during leaf development and senescence (Lasserre *et al.*, 1996). Of these, *CM-ACO1* expression was lowest in young green leaves before increasing to the highest level at the onset of senescence followed by a decline during the later stages of senescence, while expression of *CM-ACO3* was found to be highest in young green leaves before declining to its lowest level in the most senescent stage.

Studies of ACC oxidase gene expression during leaf maturation and senescence have been extended through the use of GUS-promoter fusion analysis. The promoter of the ageing-related ACC oxidase gene (*LE-ACO1*) from tomato was used to direct expression of GUS in both tomato and tobacco (Blume and Grierson, 1997). The GUS activity in senescent leaf tissue was 150 to 300-fold higher when compared with young leaf tissue. These results confirm that it is the promoter driving the increased accumulation of ACC oxidase gene transcript during leaf senescence, and also that it can retain this ability even in a heterologous system (Blume and Grierson, 1997). In addition, the ACC promoters from the ACC oxidase genes, *CM-ACO1* and *CM-ACO3* (from melon) have been used to direct the expression of GUS in tobacco (Lasserre *et al.*, 1997). Expression of GUS activity broadly matched the accumulation of the two transcripts as measured by RT-PCR, therefore further confirming the importance of the promoters for directing expression of the transcripts during maturation and senescence.

Taken together, these studies have provided molecular evidence for the regulation of ACC oxidase gene expression during leaf maturation and senescence in plants. As yet, no complementary biochemical studies on ACC oxidase activity during leaf maturation and senescence have been undertaken in these species.

1.7 Ethylene Biosynthesis during Leaf Maturation and Senescence in White Clover

The model plant used in the first part of this study is the perennial forage legume white clover (*Trifolum repens* L.). White clover is the most agronomically important member of the 200 to 300 species comprising the genus *Trifolium*, and is considered the most important pasture legume in many temperate climates throughout the world (Baker and Williams, 1987). In New Zealand, it is grown in combination with rye grass to provide nitrogen to the pasture ecosystem, and high quality feed for livestock (Brougham *et al.,* 1978).

Associate professor Michael McManus's laboratory has been studying the role of ethylene in regulating leaf development of white clover with Dr. Mike Hay and colleagues at AgResearch Grasslands. The aim is to improve the persistence of this important forage legume in pastures.

In pasture, white clover has a typical stoloniferous growth habit (Thomas, 1987). The basic structure of the stolon consists of internodes separated by nodes. Each node bears a trifoliate leaf with an erect petiole, two root primordia, which may or may not develop, and an axillary bud. The growth of white clover in the model system used is maintained by the regular excision of axillary buds, and root development is prevented by growing stolons over a plastic matrix. Finally, a single stolon develops from a single major root system with leaves, which show the whole range of developmental stages from initiation at the apex, through mature green to senescence, and then necrosis (Figure 1.3; from Hunter, *et al.,* 1999).

The sequential nature of white clover leaf senescence has been utilized by Butcher (1997) and Hunter *et al.* (1999) for studying ethylene evolution during leaf maturation and senescence.

Figure 1.3 Stages of leaf development using the stolon growth model system of white clover

Using this system, it has been demonstrated that leaf senescence of white clover (as judged by chlorophyll decrease; leaf number 10-16) is accompanied by an increase in ethylene evolution levels by the tissue, and that this increase is most probably by reason of the increased activity of the ACC-mediated biosynthetic pathway (Figure 1.4; from Hunter *et al.*, 1999). Further, endogenous levels of ACC have also been observed to increase and precede that of ethylene evolution (Butcher *et al.*, 1996; Butcher, 1997; Hunter *et al.*, 1999).

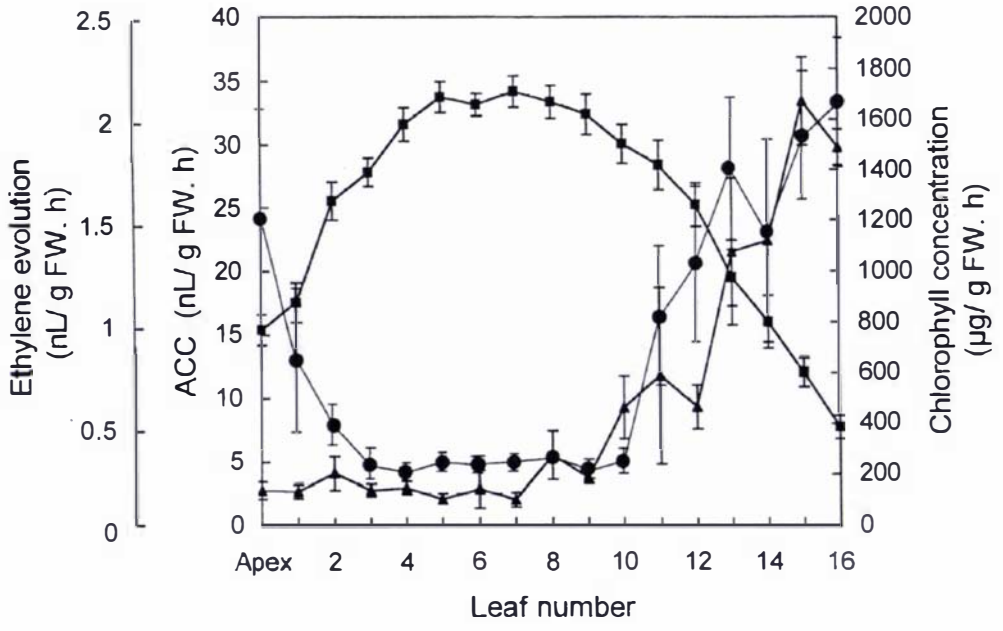

Figure 1.4 Ethylene evolution and chlorophyll content during leaf development in white clover

● Ethylene evolution ▲ ACC content ■ Total chlorophyll

Hunter *et al.* (1999) have identified three distinct DNA sequences designated *TR-ACO1, TR-ACO2,* and *TR-ACO3* respectively, and characterized these in terms of gene expression and protein accumulation during leaf maturation and senescence in white clover. Southern analysis confirmed that these sequences represent three distinct ACC oxidase genes. Northern analysis revealed that *TR-ACO1* is expressed almost exclusively in the apical structure, and *TR-ACO2* is expressed in the apex, in newly initiated leaves, and in mature green leaves, with maximum expression in newly initiated leaf tissue. The third gene, *TR-ACO3*, is expressed predominantly in senescent leaf tissue. Comparison of the reading frames of each gene revealed that identities ranged over 75% (*TR-ACO3* against *TR-ACO1*), 77% (*TR-ACO1* against *TR-ACO2*) to 84% (*TR-ACO3* against *TR-ACO2*). In contrast, comparison of 3'-UTR regions of each gene ranged from 55% (*TR-ACO3* against *TR-ACO1*), 59% (*TR-ACO2* against *TR-ACO3*) to 61% (*TR-ACO1* against *TR-ACO2*) identity.

Polyclonal antibodies have been raised to the translation products of *TR-ACO1*, *TR-ACO2* and *TR-ACO3* expressed in *E. coli,* and western analysis has shown that the *TR-ACO1* antibody recognizes a high molecular mass (*ca.* 205 kDa) protein complex with highest accumulation in the apical tissue. The anti-TR-ACO2 antibody recognizes a protein of approximately 36.4 kDa in newly initiated leaves and mature green leaves, as well as in petioles and roots (Hunter, 1998; Yoo, 1999; Hunter *et al.,* 1999). Currently, this antibody recognition data agrees with the ACC oxidase activity *in vitro*, as well as *TR-ACO2* gene expression in the tissue (Hunter *et al.,* 1999). No protein recognition by an antibody raised to TR-ACO3 could be detected in senescent tissue or at any other stage of leaf development.

At the biochemical level, ACC oxidase isoforms have been purified from leaf tissues at different stages of development and the regulation of the enzyme *in vivo* examined. Three isoforms of ACC oxidase, one from mature green leaves, designated MGI and two from senescent leaves, designated SEI and SEII, have been identified by Gong and McManus (2000). Two of the three isoforms (MGI and SEII) were purified to homogeneity as judged by sodium dodecyl sulphate-polyacrylamide gel electrophoresis (SDS-PAGE) analysis with Coomassie Brilliant Blue staining and western analysis. Some kinetic properties of MGI and SEII have been studied. However, Gong (1999) did not obtain any amino acid sequence from MGI and SEII and so it is as yet unclear whether these proteins are the products of *TR-ACO2* (MGI) and *TR-ACO3* (SEI or SEII)? Therefore, the focus of one aim of this thesis is to confirm the identity of their encoding genes.

1.8 *Trifolium occidentale*

Trifolium occidentale (*T. occidentale*) is a stoloniferous perennial clover indigenous to England, France and Channel Islands where it grows in relatively dry coastal habitats, on shallow pockets of soil, and in maritime sand dunes, always near the sea (Coombe, 1961; Coombe and Morisset, 1967). This species resembles *T. repens* in morphology, although it is cytologically, ecologically, and geographically distinct and lacks vegetative vigour. Its relatively short stems and very small leaves render it morphologically suited to dry, windy, coastal habitats (Figure 1.5). It is also probably resistant to salty soils.

Figure 1.5 Stages of leaf development using the stolon growth model system of *T. occidentale*

It has been suggested that *T. occidentale* is a naturally occurring diploid form and it is not a highly variable species and, being a self-compatible and self-fertilizing species, is probably highly homozygous (Coombe, 1961). As a diploid species of clover, *T. occidentale* has the chromosome number, 2n =16 whereas the vast majority of natural and cultivated forms of *T. repens* are tetraploid 2n = 4x =32 (Badr *et al.*, 2002). Since *T. repens* has been regarded as allotetraploid in origin with two ancestral genomes (Williams, 1987), a number of studies have addressed the ancestors of *T. repens*. Based on its ability to cross with some closely related species, Gibson and Beinhart (1969) proposed that the diploid *Trifolium nigrescens* (2n =16) is one of the ancestors of *T. repens*, and that the other ancestor may be *T. occidentale*. Chen and Gibson (1971) indicated a close karyological and phylogenetic relationship between *T. repens*, *T. nigrescens* and *T. occidentale*, in addition to the tetraploid *Trifolium uniflorum* (2n =32). Chen and Gibson (1972) suggested that these species might share a common genome indicated by their ability to make successful crosses and the occurrence of chromosome pairing in their hybrids.

However, recently Kakes and Chardonnens (2000) found that the distribution of cyanotypes in *T. repens* and *T. occidentale* are dissimilar, and are regulated by different mechanisms. These findings lend support to the view of Kakes and Hakvoort (1994) that *T. occidentale* did not donate active *Li* alleles to *T. repens*. The gene *Li* regulates the presence/absence of a specific β-glucosidase, linamarase, which hydrolyses linamarin and lotaustralin producing HCN. More recently, Badr *et al.* (2002) revealed that an ancestral form of *T. uniflorum* and *T. nigrescens* are the likely donors of the two genomes of *T. repens*. However, the high values of genetic identity and the low values of genetic distance between *T. occidentale* and each of *T. uniflorum* and *T. nigrescens* may be indicative of introgression of genes from the former species into the genomes of the latter two species. Some of these genes may have been subsequently introduced into the genome of *T. repens* (Badr *et al.*, 2002).

However, as described above, *T. occidentale*, as a diploid species of clover with a smaller genome compared with *T. repens*, may also be a better model to study the role of the ACC oxidase multiple gene family in detail, and this is another aim of this thesis.

1.9 Aims of the Thesis

- To further purify the two white clover ACC oxidase isoforms MGI and SEII (Gong, 1999) and obtain sequence information using MALDI-TOF mass spectrometry to determine which isoform *TR-ACO2* or *TR-ACO3* code for.

- To investigate the rhythmicity of ACC oxidase activity and protein accumulation in leaf tissue of white clover.

- To explore whether the phosphorylation and dephosphorlation status of ACC oxidase protein from white clover alters its activity or its properties.

- To isolate gene sequences encoding ACC oxidases from *Trifolium occidentale* and examine changes in gene expression during leaf maturation and senescence in this diploid clover species.

2. Chapter Two: Materials and Methods

2.1 Propagation and Harvesting Methods

2.1.1 Plant Material

White clover (*Trifolium repens* L., Figure 2.1) cultivar Grasslands Challenge, genotype 10F (AgResearch Grasslands, Palmerston North, New Zealand) and *Trifolium occidentale*, genotype 18Z (AgResearch Grasslands, Palmerston North, New Zealand) were used in this thesis.

Both *T. repens* and *T. occidentale* consist of a prostrate primary stolon axis with leaves, and occasional adventitious roots and lateral branches at the nodes. Each has a sequential growth pattern, with new nodes forming at the apex, whilst basal nodes senesce and die (Hay *et al.*, 1991). In pasture, clover is vegetatively propagated and spreads clonally (Brock *et al.*, 1988, Hay *et al.*, 1989, 1991). Nodes must be rooted or have a root basipetal to them on the stolon, as mineral nutrients are only transported acropetally (Sackville-Hamilton and Harper, 1989). Thus nodes unsupported by a root die. However, as sections of the primary axis senesce, rooted lateral branches are released to form new plants, that are genetically identical to the parent (Hay *et al.*, 1991).

2.1.2 Plant Growth Conditions

Plants were grown in a temperature-controlled greenhouse in horticultural grade bark/peat/pumice (Dalton Nursery Mix, Tauranga, New Zealand) mixed in a ratio of 50:30:20 supplemented with nutrients (Table 2.1) at the Plant Growth Unit, Massey University, Palmerston North, New Zealand. The greenhouse was maintained at a minimum temperature of 12°C (night time) and 18°C (day time), and vented at 25°C. Automated irrigation occurred at 10 am and 5 pm each day for a 5 min period using a time-controlled mist watering system (Automation Services Ltd., Auckland, New Zealand). The insect pests aphids, whitefly and mite were controlled by spray application of the insecticide Attack® (Crop Care Holdings Ltd., Richmond, Nelson,

New Zealand). Blackspot was controlled by the application of Benlate (Du Pont de Nemours and Co., In., Wilmington, Delaware, USA).

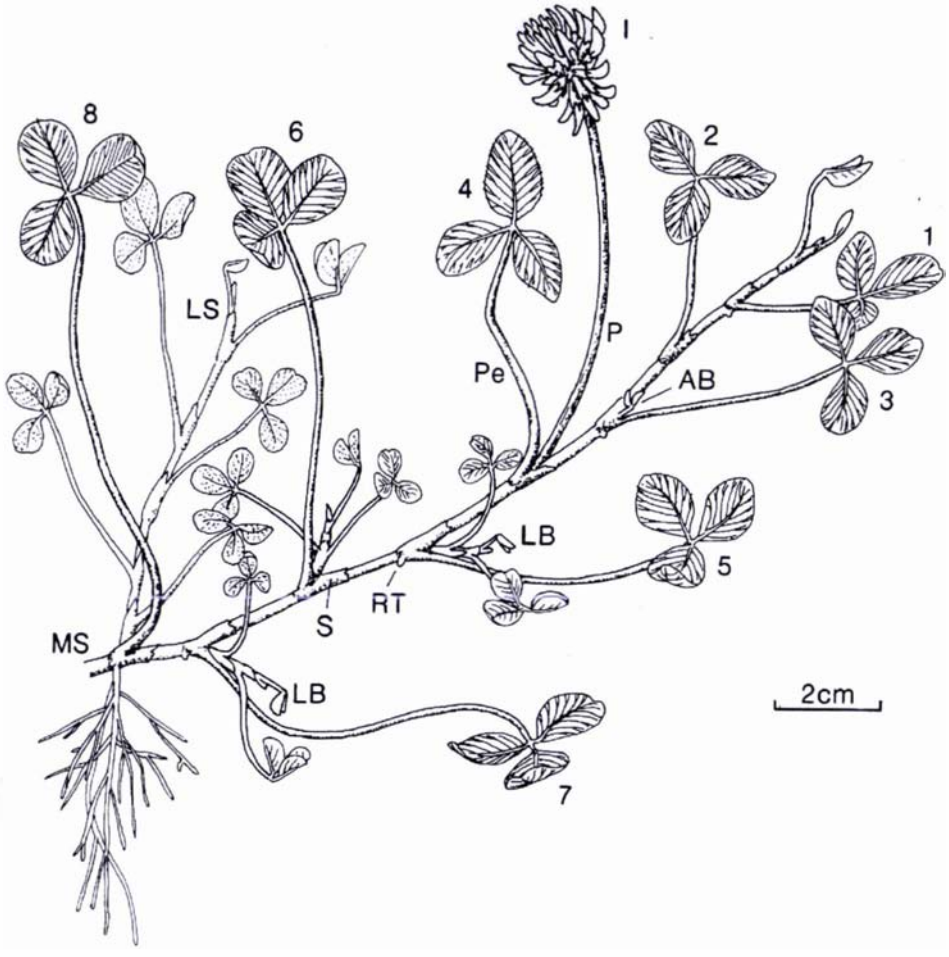

Figure 2.1 A typical mature stolon of white clover plant

A mature stolon of white clover (from Thomas, 1987). Nodes, and emerged leaves arising from these nodes are numbered 1 to 8.

AB = axillary bud; I = inflorescence; LB = lateral branches; LS = lateral stolon; MS = main stolon; P = peduncle; Pe = petiole; RT = nodal root primordium.

Table 2.1 Composition of long term fertilizer added to the horticultural grade bark base

Ingredient	Rate (g/L)	Supplier
Dolomite	3.0	Daltons, Matamata, NZ
Agricultural lime	3.0	Daltons, Matamata, NZ
Iron sulphate	0.5	Hodder Tolcy, Palmerston North, NZ
Osmocote	50	Carran Agencies, Hamilton, NZ

2.1.3 Propagation of Stock Plants and Initiation of the Plant Growth Model System

To maintain stock plants, apical cuttings containing two or three leaves were placed in trays filled with the nutrient-horticultural bark and grown under greenhouse conditions until required. During the course of experiments, approximately five trays (50 cm × 30 cm) of stock plants were maintained in this way, with new cuttings routinely taken to obtain fresh plant material.

To initiate single stolons, apical cuttings comprising the apex and two or three nodes were excised from the stock plants (Butcher, 1997; Hunter, 1998). All the leaves except those ensheathing the terminal bud and the first leaf were removed by excision at the junction of the petiole and stolon, and the cuttings placed in bark/nutrient potting mix in the greenhouse. After establishment of root growth (usually four weeks), the most homogeneous cuttings were transferred into trays containing fresh bark/nutrient mix with six plants per tray. Single stolons were trained out of the tray over a dry polythene surface to ensure that nodal roots did not develop. All axillary shoots and buds, flowers and unhealthy leaves were removed routinely (at ten days intervals) to maintain single stolons attached to a basal root (Figure 2.2). Stolons were allowed to grow until they provided a consistent pattern of leaf developmental stages, ranging from initiation through to senescence (usually at least three months).

A

B

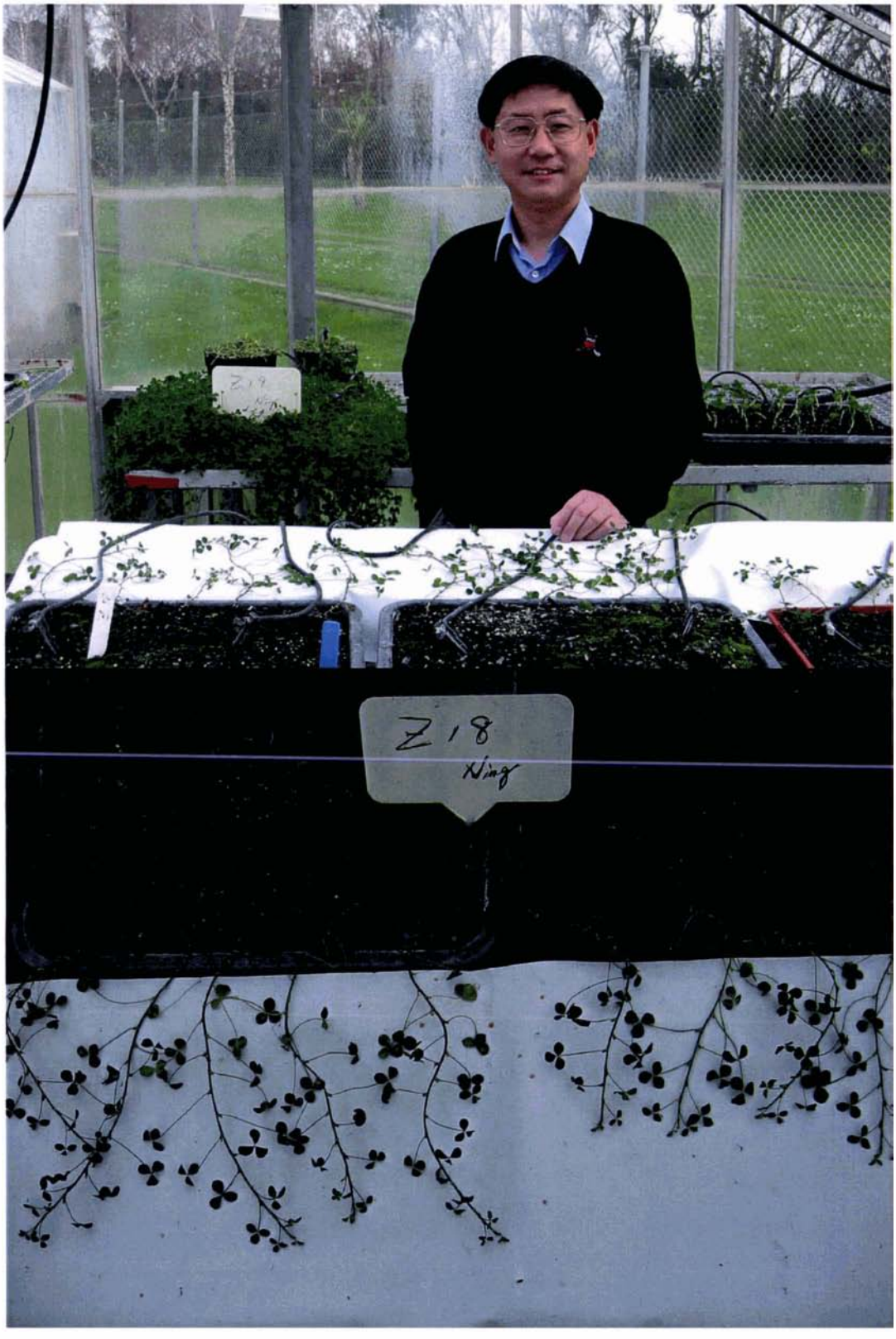

Figure 2.2 The single stolons of *T. occidentale* (Z 18)

A. The author amongst stolons of *T. occidentale* growing in one of the greenhouses of the Plant Growth Unit, Massey University, Palmerston North, New Zealand.

B. Stolons of *T. occidentale* with leaves ready for harvesting.

2.1.4 Harvesting of Plant Material

Plants were harvested when the leaves nearest the roots were completely senescent. At this stage, stolons of both white clover and *T. occidentale* comprised between 14 and 20 fully expanded leaves. At least three days prior to harvesting leaf tissue, all axillary bud and flowers were removed, and the plants were then left without any further manipulation until harvesting. Leaves were excised with sharp scissors from a single stolon at the junction of the lamina and petiole, weighed, placed either individually into labeled microfuge tubes or as pooled leaves into 50 ml Nunc™ centrifuge tubes (Nalge Nunc International, Naperville, USA), snap frozen immediately in liquid nitrogen and were either used immediately after harvesting or stored at -80°C until use. When pooled leaf tissue was to be used in multiple analyses or isolation and purification, the tissue was removed from -80°C, powdered and apportioned into separate prechilled microfuge tubes or 50 ml Nunc™ centrifuge tubes.

2.2 Physiological Methods

2.2.1 Growth Measurement during Leaf Ontogeny

Leaf fresh weight and leaf area at each node were determined using an AG204 balance (Mettler Toledo, Switzerland) and a leaf area meter (LI-COR, Model 3100 Areameter Square Centimeters, Industrial & Electronic Equipment, USA), respectively.

2.2.2 Chlorophyll Quantitation

Chlorophyll measurement was performed using the method as described by Moran and Porath (1980). Typically, leaf tissue was powdered under liquid nitrogen with a mortar and pestle, and 50-200 mg of the ground material was extracted with 1 ml of chilled *N,N*-dimethyl formamide (DMF) for 16 hs at 4°C in the dark. Prior to chlorophyll determination, samples were vigorously mixed by vortexing, and the cellular debris pelleted by centrifugation at 20 800 × *g* for 5 min at room temperature. A 200 µl aliquot of the supernatant was added to 2 ml of DMF in a glass cuvette and the absorbance read at both 647 nm and 665 nm in an LKB Novaspec® II spectrophotometer (Pharmacia LKB, Biochrom Ltd., Cambridge, England) in the fumehood. The spectrophotometer was blanked only at 647 nm with DMF. All the

samples measured at 665 nm had 0.007 absorbance units added to their values as this was the difference in the blank at 647 nm when compared with 665 nm.

Chlorophyll concentrations were calculated on the basis of the formula of Inskeep and Bloom (1985).

Chlorophyll A = $12.7A_{664.5} - 2.79A_{647}$ (mg/ml)

Chlorophyll B = $20.7A_{647} - 4.62A_{664.5}$ (mg/ml)

Total Chlorophyll = $17.9A_{647} + 8.08A_{664.5}$ (mg/ml)

2.2.3 Ethylene Analysis

2.2.3.1 Measurement of Ethylene by Gas Chromatography

The concentration of ethylene in gas samples produced by ACC oxidase was analyzed using a Shimadzu Model GC-8A Gas Chromatograph (Shimadzu Corporation, Kyoto, Japan) equipped with a flame ionization detector. The 2.5 m × 3 mm I.D. glass column prepacked with Porapak-Q with a mesh size of 80/100 (Alltech Associates Inc., Deerfield, II. USA) was used for the ethylene analysis. The carrier gas used was nitrogen with a column flow rate of 50 ml/min and the flame of the detector was generated by hydrogen and air at 60 kPa and 50 kPa respectively. At least 1 h before use, the column was incubated at 200°C with a nitrogen carrier gas at 150 kPa. For measurement of samples, the oven and the injector/detector temperatures were set at 85°C and 150°C, respectively.

One ml of sample gas was injected onto the column and the peak retention time for ethylene was observed to be between 1.2 and 1.3 min. A standard calibration gas of 0.101ppm ethylene in nitrogen (BOC Gased (NZ) Ltd., Palmerston North, New Zealand) was used for ethylene quantification.

2.2.3.2 Ethylene Calculations

The concentration of ethylene from the headspace of the reaction containers was measured in ppm by comparison to the peak height obtained from 1 ml of standard

ethylene gas. The equation was used to calculate the number of moles produced by the reaction as following:

$n\ (mol) = PV/RT \times ppm \times 10^{-6}$ (Hunter, 1998)

Where: n = total number of moles

P = pressure (101325 Pa)

V = volume of headspace

R = universal gas constant (8.314)

T = temperature (298 K)

In this study, the unit of ACC oxidase activity is expressed as nmol ethylene/h/mg protein.

2.2.4 Nitrogen Analysis

Initiated newly green, mature green and senescent leaves were collected from node 1 to 15 for both *T. repens* and *T. occidentale*. Leaves were then dried at 60°C *ca.* 12 h, weighed and ground to a fine powder. The total nitrogen concentration was assayed by Mr. John Menneer (AgResearch, Hamilton, New Zealand)

2.3 Biochemical Methods

2.3.1 Chemicals

Unless otherwise stated, all general chemical reagents were analytical grade and sourced either from BDH Laboratory Supplies (Dorset, England), or Sigma Chemical Company (St. Louis, MO, USA). Water for making solutions was produced by reverse-osmosis (RO) followed by a microfiltration system containing ion exchange, solvent exchange, organic and inorganic removal cartridges (Milli-Q, Millipore Corp., Bedford, MA, USA). All solutions were prepared with this Milli-Q water. The Eppendorf centrifuge 5417C (Pierce LabSupply) and the Sorvall® RC-5B refrigerated superspeed centrifuge (DuPont Instruments, USA) were used for centrifugation of all samples. Solution pH was measured using a digital pH meter (Radiometer Copenhagen, France). All solutions were stored at 4°C or room temperature unless specified.

2.3.2 Extraction of ACC Oxidase

Reagents:

- Extraction buffer: (100 mM Tris-HCl, pH 7.5, 10% (v/v) glycerol, 30 mM sodium ascorbate, 2 mM DTT and 10 μM PA)

ACC oxidase was extracted from white clover leaf tissues by a procedure modified from McGarvey and Christoffersen (1992) and Kuai and Dilley (1992).

Frozen leaf tissue (previously weighed) was ground with liquid nitrogen in a pre-cooled mortar and pestle. Extraction buffer was added in a 3:1 (v/w) ratio to the ground frozen powder, incubated on ice with gentle stirring for 45 min, and then filtered through double layers of Miracloth (Calbiochem-Novabiochem Corporation, La Jolla, CA, USA). After centrifugation at 26,000 × *g* for 20 min at 4°C, the resulting supernatant (crude extract) was used for further purification.

2.3.3 Protein Precipitation Using Ammonium Sulphate

Ammonium sulphate precipitation of proteins is dependent on the hydrophobic nature of the surface of the protein (Harris, 1989). It is the most commonly used method for reducing the volume of the crude extract and aiding protein purification. In this study,

the protein extraction was fractionated with 40% - 80% (w/v) saturated ammonium sulphate.

Reagents:

- Ammonium sulphate
- Resuspension buffer: (50 mM Tris-HCl, pH 7.5, 10% (v/v) glycerol, 30 mM sodium ascorbate, 2 mM DTT and 10 μM PA)

The supernatant volume (section 2.3.2) was measured, and then adjusted to 40% (w/v) saturated (226 g/L at 0°C) ammonium sulphate. The mixture was incubated on ice with stirring for 40 min and then centrifuged at 26,000 × *g* for 20 min at 4°C. The supernatant was transferred to a fresh pre-cooled beaker and adjusted to 80% (w/v) saturated (by adding a further 258 g/L at 0°C) ammonium sulphate. After 1 h incubation on ice with stirring, the protein was pelleted by centrifugation at 26,000 × *g* for 30 min at 4°C. The supernatant was discarded and the protein pellet redissolved in a minimal volume of pre-cooled resuspension buffer.

2.3.4 Sephadex G–25 Gel Filtration Chromatography

Sephadex G-25 was used to remove ammonium sulphate (desalting) and also any putative small molecular mass inhibitors from the protein extract. This method is modified from that described by Neal and Florini (1973).

Reagents:

- Sephadex G-25 resin (Pharmacia Biotech, Uppsala, Sweden)
- Resuspension buffer: (50 mM Tris-HCl, pH 7.5, 10% (v/v) glycerol, 30 mM sodium ascorbate, 2 mM DTT and 10 μM PA)

To prepare the column, a 50 ml syringe barrel (Becton-Dickensen, USA) was plugged with glass fibre discs (Whatman International Ltd., Maidstone, England) in the bottom of the barrel, and Sephadex G-25 resin pre-equilibrated with resuspension buffer was poured and allowed to settle. The protein suspension from section 2.3.3 was carefully loaded onto the column, pre-equilibrated with the resuspension buffer. Proteins were chromatographed through the Sephadex G-25 column at a flow rate of 2.0 ml/min, and the eluted protein collected as 2 ml fractions. Fractions containing protein were pooled and concentrated using Amicon Centriprep-10 centrifugal concentrators (10 kDa cut-

off, NANOSEP™) at 3,000 × *g* for several h at 4°C. The concentrated protein samples were either used immediately for further purification, or stored at -20°C until use.

At the conclusion of chromatography, the Sephadex G-25 resin was immediately placed into a clean beaker, 0.2 M NaOH solution was added and the slurry incubated at room temperature with gentle stirring for 20 min. The gel was allowed to settle, the supernatant removed and gel washed with Milli-Q water several times, until the supernatant was pH 7.0, and then stored at 4°C until use.

In order to retain the ACC oxidase activity, the protein extraction, ammonium sulphate precipitation, Sephadex G-25 gel filtration chromatography and concentration of the protein preparation were carried out within the same day and the concentrate stored at -20°C overnight for further purification next day.

2.3.5 Fast Protein Liquid Chromatography (FPLC)

Chromatography is the separation of solutes according to their different distributions between two phases, usually a solid matrix as the stationary phase and a liquid as the mobile phase. Separation is achieved through the partitioning of the analyte between these two phases. Proteins adsorb to a variety of solid phases in a selective manner and using a series of different chromatographic matrices, a protein can be purified from a complex biological mixture. The ACC oxidase protein purification in this study used the fast protein liquid chromatography (FPLC) system with several purpose-made prepacked columns. All buffer solutions for FPLC were filtered through a 0.22 μM hydrophilic polypropylene membrane filter (GelmanSciences, Ann Arbor, Michigan, USA) immediately before use. Protein samples were either filtered through an Acrodisc® Syringe Filter 0.2 μM Supor® Membrane (Gelman Laboratory, Ann Arbor, Michigan, USA) or centrifuged at 10,000 × *g* for 20 min at 4°C immediately prior to being loaded onto each column. All FPLC steps were carried out at 4°C.

2.3.5.1 Hydrophobic Interaction Chromatography

Hydrophobic interaction chromatography (HIC) separates proteins by exploiting the variability of exposed hydrophobic amino acid residues on different proteins on the basis of their different surface hydrophobic interactions with the aliphatic or aromatic

ligands of the resin matrix (Roe, 1989). This interaction can be controlled through the appropriate choice of both the ligand and the mobile phase. Van der Waals interactions between non-polar amino acid side chains play a role in both protein folding (Privalov, 1992) and HIC (Ståhlberg *et al.*, 1992). In HIC, the ligands are sparsely distributed on the surface so that proteins will not experience steric interactions with one another. The spacer arms used to link the functional groups to the matrix are longer and it is possible for the solute to reach the surface of the gel. The charged surface of the protein thus rests against the polar surface of the gel while the hydrophobic chains are able reach into hydrophobic grooves in the protein (Scopes, 1994). The Hydrophobic matrices of the column usually contain alkyl, aryl or phenyl functional groups covalently linked to an inert matrix such as Superose or Sepharose. The binding of protein molecules to these groups is promoted by the presence of high concentrations of salts in the mobile phase. The concentration and type of salt modify these interactions where they are strengthened by high concentrations of lyotropic salts such as ammonium sulphate and weakened by high concentrations of chaotropic salts such as sodium chloride. Protein samples are loaded in high salt solutions and eluted in decreasing salt gradients.

HIC as the first FPLC step was used for ACC oxidase purification in this study. The column used was Phenyl Sepharose, connected to a Pharmacia FPLC system equipped with a single path UV-1 monitor, chart recorder and fraction collector (Pharmacia Biotech)

Reagents:

- Phenyl Sepharose High Performance HiLoad 26/10 prepacked column (Pharmacia Biotech)
- Buffer A: 50 mM Tris-HCl, pH 7.5, containing 5.0%(v/v) glycerol, 30 mM sodium ascorbate, 2 mM DTT, 10 μM PA and 2.0 M ammonium sulphate (FPLC grade)
- Buffer B: Buffer A without ammonium sulphate

A Phenyl Sepharose HiLoad 26/10 column was equilibrated with Buffer A (kept chilled on ice). Approximately 400-600 mg of total protein extract was adjusted to 1.0 M ammonium sulphate by dissolving the appropriate amount of ammonium sulphate in the protein extract and then loaded onto the column. About 8-10 ml of the protein solution was injected three times onto the column with a 3 ml loop, allowing the column to equilibrate between each injection. After loading was completed, the bound

proteins were eluted in a decreasing gradient from 100% Buffer A (2.0 M ammonium sulphate): 0% Buffer B (Buffer A without ammonium sulphate) to 0% Buffer A (0.0 M ammonium sulphate): 100% Buffer B at a flow rate of 5.0 ml/min. Fractions (16 ml for each fraction) were collected using an automatic fraction collector, and each fraction was assayed for protein content using the Bradford method (section 2.3.7.1). ACC oxidase purity was assessed by SDS-PAGE and western analysis using the anti-TR-ACO2 antibody (section 2.3.9). Active fractions were pooled and concentrated using a Centriprep-10 centrifugal concentrator (10 kDa cut-off, NANOSEP™, Pall Filtron Corporation) to 2% original volume (~2 ml).

Once used, the Phenyl Sepharose HiLoad 26/10 column was cleaned by passing at least four column volumes of 1 M NaOH through the column at a flow rate of 2 ml/min to remove most proteins non-specifically adsorbed to the gel, and at least four column volumes of 30% (v/v) acetonitrile to remove hydrophobic proteins, lipoproteins and lipids. After cleaning, the column was immediately equilibrated with two column volumes of filtered water and two column volumes of 20% (v/v) acetonitrile at a flow rate of 4 ml/min before storage.

2.3.5.2 Anion Exchange Chromatography

Ion exchange chromatography separates proteins based on their different net charges at a given pH. The side chains of surface amino acids may be protonated or deprotonated depending on the pH of the environment, so that their surface distribution and overall net charge dictate the unique behavior of a protein in an ion exchange environment. The functional groups on the matrix carry either positive or negative charges that can interact with proteins primarily through ion pairing. These interactions depend not only on the net charge of the protein but also on the ionic strength and pH of the buffer ions, the nature of these ions, and properties of the functional ligands. Stationary phase matrices carrying charged groups that retain their charge over a narrow pH range are regarded as weak ion exchangers whereas those stable over a wide pH range are considered strong exchangers. Separation of proteins is achieved by their difference in equilibrium distribution between a buffered mobile phase and a stationary phase consisting of a matrix to which charged (Roe, 1989). The proteins that bind to ion exchange chromatography columns are generally eluted by increasing the ionic strength of elution buffer.

Reagents:

- Buffer A: 50 mM Tris-HCl, pH 7.5, containing 5.0% (v/v) glycerol, 30 mM sodium ascorbate, 2 mM DTT and 10 μM PA
- Buffer B: Buffer A, pH 7.5, with 1.0 M NaCl (FPLC grade)

The Mono Q prepacked HR 5/5 strong anion exchange column (Pharmacia Biotech) was pre-equilibrated with Buffer A (kept chilled on ice). Protein samples were loaded at 0.5 ml/min onto the column to allow time for interactions to occur and bound proteins were eluted using a linear increasing gradient of sodium chloride concentration from 0 to 0.8 M at a flow rate of 0.5 ml/min. Fractions (1.2 ml) were automatically collected in 1.5 ml Eppendorf tubes placed on ice, assayed for protein content using the Bradford method (section 2.3.7.1). ACC oxidase purity was assessed by SDS-PAGE and western analysis using the anti-TR-ACO2 antibody (section 2.3.9). Active fractions were pooled, concentrated and used for further purification.

Once used, the Mono Q column was cleaned by carrying out the following steps in sequence with a reversed flow rate of 0.25 ml/min: (1) 0.5 ml of 2 M NaCl solution injected and then rinsed with filtered Milli-Q water, (2) 0.5 ml of 2 M NaOH solution injected and then rinsed with water, and (3) 0.5 ml of 75% (v/v) acetic acid injected and then rinsed with water. After cleaning, the column was equilibrated with at least 10 column volumes of 20% (v/v) acetonitrile before storage.

2.3.5.3 Gel Filtration Chromatography

Gel filtration or gel permeation chromatography separates proteins on basis of their size (Preneta, 1989). The matrix used is commonly a hydrated agarose or dextran gel and consists of an open, cross-linked, three-dimensional molecular network with pores between 40-120 μM in diameter (Scopes, 1994). The pores within the beads act like a molecular sieve that completely exclude large proteins while proteins small enough to penetrate the pores are retained to differing extents depending on their size. Consequently, large protein molecules that are completely excluded from the pores are eluted first from the column, while other protein molecules are eluted from the column in order of decreasing molecular mass. The buffer usually contains a low concentration of salt to minimize interaction between the matrix and protein. The sample volume of the protein should be within 0.5% of the bed volume of the column and smaller than the

separation volume between peaks. Thus column dimensions where a long column with a small diameter operating at a low flow rate gives much better resolution than a short with a big diameter column.

Reagents:

- Buffer A: 50 mM Tris-HCl, pH 7.5, containing 5.0% (v/v) glycerol, 30 mM sodium ascorbate, 2 mM DTT 10 μM PA and 150 mM NaCl (FPLC grade)

A pre-packed Superose 12 HR 10/30 column (Pharmacia Biotech) was pre-equilibrated with at least 50 ml of Buffer A (kept on ice) at a flow rate of 0.3 ml/min. The concentrated protein preparation (220 μl to 240 μl) was loaded onto the column, and protein was eluted using the same buffer (kept on ice) at a flow rate of 0.3 ml/min and fractions (0.66 ml) were collected in 1.5 ml Eppendorf tubes placed on ice. Each fraction was assayed for protein content using the Bradford method (section 2.3.7.1). ACC oxidase purity was assessed by SDS-PAGE and western analysis using the anti-TR-ACO2 antibody (section 2.3.9). The best fractions were stored at -20°C until use.

After use, the column was washed in the following sequence (one column volume of each solution) at a low flow rate of 0.1 ml/min: (1) 50% (v/v) acetic acid and then rinsed with filtered Milli-Q water, (2) 20% (v/v) ethanol, and (3) 0.1 M NaOH solution followed with filtered Milli-Q water, and then 3 × 200 μl 50% (v/v) acetic acid injected. After cleaning, the column was equilibrated with at least 10 column volumes of 20% (v/v) acetonitrile before storage.

2.3.6 Analysis of ACC Oxidase Activity *in vitro*

The measurement of ACC oxidase activity *in vitro* was performed using a method modified from that described by Hunter (1998). A standard reaction cocktail was made for 20 samples, and the composition of reaction mixture is shown in Table 2.2.

Reagents:

- Buffer A (2 × stock): 100 mM Tris-HCl, pH 7.5, containing 20% (v/v) glycerol
- 1 mM $FeSO_4.7\ H_2O$ (made fresh)
- 1 M $NaHCO_3$ (made fresh)
- 1 M DTT (stored frozen)

- 40 mM ACC (stored frozen)
- 1 M sodium ascorbate (made fresh)

After all components were mixed, the substrate ACC was added to the reaction cocktail just prior to assay, and then the pH of the mixture was re-adjusted to 7.5 with HCl. To perform each assay, triplicate 0.8 ml aliquots of the reaction cocktail were pippeted into 4.5 ml Vacutainer tubes and then put into a heating block at 30°C with shaking at 180 rpm for 7 min. Triplicate 0.2 ml enzyme samples were aliquotted into Eppendorf tubes and equilibrated in another heating block for 1 min at 30°C. To start the reaction, 0.2 ml of the enzyme samples were mixed with 0.8 ml of the reaction cocktail. The Vacutainer tubes were sealed immediately, and then incubated with shaking at 200 rpm for 20 min at 30°C, after which 1 ml gas sample was withdrawn from the head space of the reaction tube and stored with the needle tip embedded in rubber. Ethylene content determined using a Shimadzu gas chromatograph (section 2.2.3.1).

Table 2.2 Formulation of standard reaction mixture for ACC oxidase activity assay *in vitro*

Component	Final Concentration (mM)	Amount for 20 Samples (ml)
Buffer A (2 ×)	-	10
Tris-HCl	50	-
Glycerol	10% (v/v)	-
1 M DTT	2	0.04
40 mM ACC	1	0.5
1 mM $FeSO_4 \cdot 7\ H_2O$	0.02	0.4
1 M sodium ascorbate	30	0.6
1 M $NaHCO_3$	30	0.6
H_2O	-	3.86

2.3.7 Protein Quantification

2.3.7.1 Bradford Method

Reagents:

- Protein assay reagent (Bio-Rad, Richmond, CA, USA)

- BSA (1 mg/10 ml stock, stored at -20°C)

The protein concentration of samples was estimated by a microassay version of Bradford method described by Bradford (1976) and Zor and Selinger (1996) with BSA as a protein standard. Typically, samples were diluted to the appropriate concentration with water before protein measurement. Aliquots (2 or 4 µl) of the diluted sample were pipetted into wells of a microtitre plate, in triplicate, and made up to 160 µl with water. After which, 40 µl of the protein assay reagent was added and mixed gently by pipetting up and down. After standing for 5 min, the protein concentration was determined at 595 nm using an AnthosHT II plate reader (Anthos Labtech Instruments, Salzburg, Austria) by comparison to a protein standard curve prepared from the BSA concentration used (Figure 2.3). Only absorbances within the linear region of the standard curve were used to calculate the protein concentration.

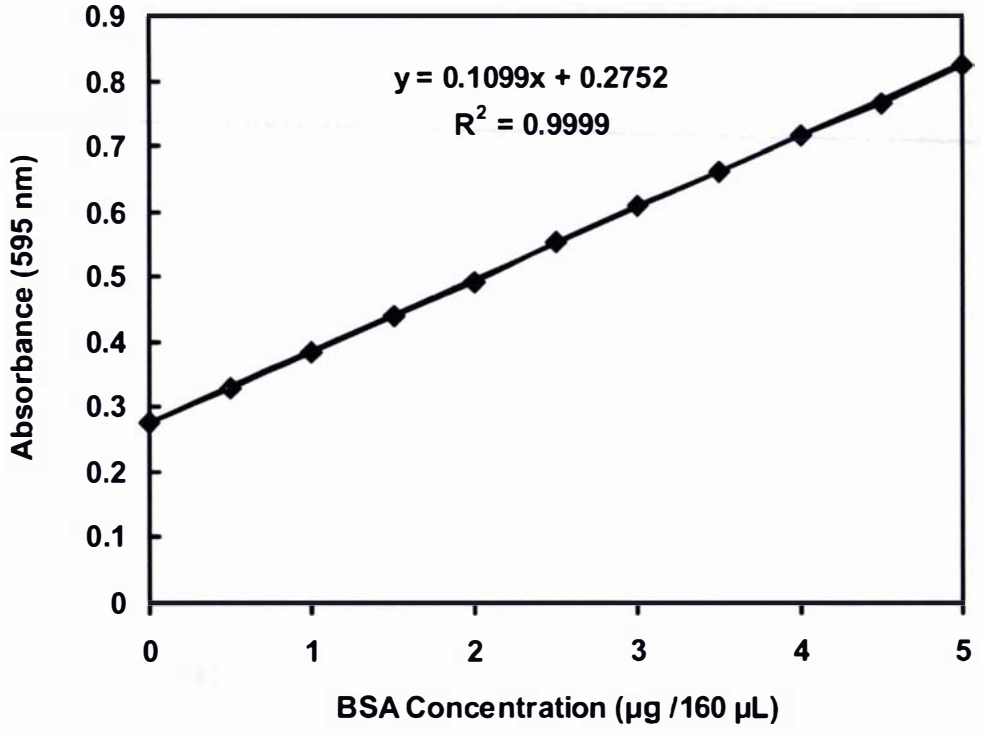

Figure 2.3 A typical protein standard curve for the Bio-Rad protein microassay procedure

2.3.7.2 Coomassie Blue Method

Reagents:

- Coomassie Blue Reagent (Bio-Rad)
- BSA (1 mg/ml stock, standard grade, stored at -20°C)
- Rehydration Buffer: (8 M Urea, 2% (w/v) Chaps)

Protein in samples used for 2D-electrophoresis was estimated using a modified version of the Bradford method. A range of standards containing from 0 to 6 µg/ml of BSA was prepared. After the protein sample was pelleted with ice-cold acetone (section 2.3.10.1), the protein pellet was resuspended with rehydration buffer and diluted to the appropriate concentration using same buffer. Five µl of protein sample was added to 1 ml of Coomassie Blue Reagent and absorbance read at 595 nm after 2 min and before 1 h. Protein content of the samples was estimated by reference to the BSA standard curve (Figure 2.4).

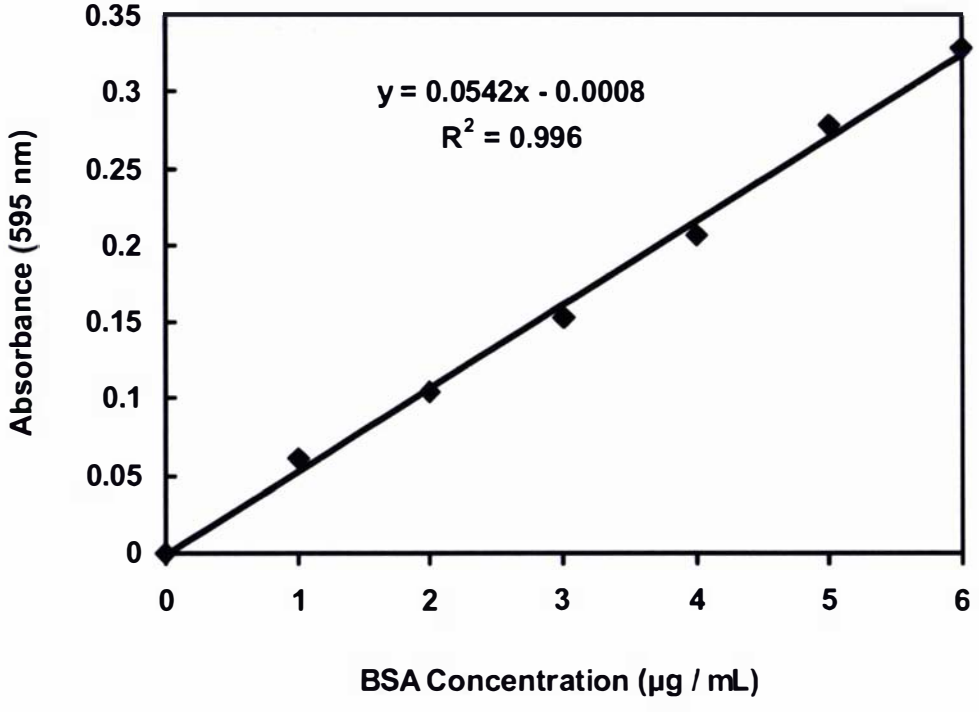

Figure 2.4 A typical protein standard curve used to estimate the protein concentration of samples for 2D-electrophoresis

2.3.8 Protein Analysis by SDS-PAGE Gels

SDS-PAGE was used to separate analytically different proteins during purification on the basis of molecular mass according to the method of Laemmli (1970).

2.3.8.1 Linear Slab Gel SDS-PAGE

Reagents:

- 40% (w/v) acrylamide stock solution (Bio-Rad). (Stored at 4°C)
- 2 × resolving (separating) gel buffer: (0.75 M Tris-HCl, pH 8.8, 0.2% (w/v) SDS). (Stored at 4°C)
- 2 ×stacking gel buffers: (0.25 M Tris-HCl. pH 6.8, 0.2% (w/v) SDS). (Stored at 4°C)
- 2 × SDS gel loading buffer: (24 mM Tris-HCl, pH 6.8, 20% (v/v) glycerol, 5% (w/v) SDS, 5% (v/v) 2-mercaptoethanol and 0.04% (w/v) bromophenol blue). (Stored at -20°C)
- 5 × SDS running buffer: (0.125 M Tris, 1 M glycine, 0.5% (w/v) SDS, pH *ca.* 8.3, stored at room temperature)
- 10% (w/v) ammonium persulphate (APS). (Univar, Auburn, NSW, Australia)
- *N,N,N',N'*-tetramethylethylenediamine (TEMED). (Riedel-de haen ag seelze, Hannover, Germany). (stored at 4°C)
- Prestained molecular mass standards (low range, Bio-Rad). (stored at -20°C)
- Water-saturated isobutanol

The separating gel solution (12%) was prepared by mixing the ingredients in the order as shown in Table 2.3. The mixture was then poured between two glass plates of a gel sandwich until the level reached *ca.* 1 cm below where the bottom of the well-forming comb sits. Water-saturated isobutanol or Milli-Q water was then layered onto the gel surface to minimize atmospheric oxidation, and the gel was left to polymerise for *ca.* 30 min. During polymerisation of the separating gel, a stacking gel solution (4%) was prepared as outlined in Table 2.3.

Table 2.3 Compositions of separating and stacking gels used for SDS-PAGE with the mini-protean apparatus

Order of Addition	Components	Separating Gel (ml)	Stacking Gel (ml)
1.	40% (w/v) acrylamide-bis stock	3	1
2.	2 × separating gel buffer	5	-
2'.	2 × stacking gel buffer	-	5
3.	Distilled water	2	4
4.	10%(w/v) ASP	0.1	0.1
5.	TEMED	0.01	0.01

After polymerisation of the separating gel, the layer of water-saturated isobutanol was discarded, the stacking gel solution added, and the well-forming comb inserted carefully. After polymerisation of the stacking gel, the gel sandwich apparatus was transferred to the Mini-Protean II® cell (Bio-Rad), 1 × SDS running buffer was added to both inner and outer compartments of the gel apparatus and then the comb removed gently in preparation for loading samples.

Protein samples were prepared by mixing the appropriate sample amount with an equal volume of 2 × SDS gel loading buffer and then incubating the mixture in a boiling water bath for 3 min. After centrifugation at 10,000 × *g* for up to 1 min, the samples were cooled to room temperature for loading. Routinely, one or two lanes were reserved for loading an aliquot (8 µl) of prestained molecular mass standards. Electrophoresis was conducted at 200 V for 50 to 60 min at room temperature.

2.3.8.2 Gradient (10-20%) and (8-15%) Slab Gel SDS-PAGE

Reagents:

- Sucrose
- 4× resolving (separating) gel buffer: (1.5 M Tris-HCl, pH 8.8, 0.4% (w/v) SDS). (Stored at 4°C)

A linear gradient gel of acrylamide from 10-20% or 8-15% was prepared by mixing two solutions containing different concentrations of acrylamide, designated heavy and light, in a Hoefer SG100 gradient maker (Hoefer Scientific Instruments, San Francisco,

CA., USA) and pumping the mixture using a 2120 Varioperpex® II peristalsis pump (LKB Vertriebs Ges.m.b.H., Vienna, Austria) into the large glass plates (16.5 × 22 cm). Two range of resolving gel solutions were prepared as outlined in Table 2.4

Table 2.4 Composition of resolving and stacking gel solutions used in SDS-PAGE gradient gels (10-20%) and (8-15%)

Components	Separating Gel Heavy Solution (ml)		Separating Gel Light Solution (ml)		Stacking Gel (ml)
	20%(w/v)	15%(w/v)	10%(w/v)	8%(w/v)	
1. Sucrose	3 g	3 g	-		-
2. Distilled water	3.5	6	10	11	8
3. 4 × separating gel buffer	5	5	5	5	-
4. 2 × stacking gel buffer	-		-		10
5. 40% (w/v) acrylamide	10	7.5	5	4	2
6. 10%(w/v) ASP	0.1	0.1	0.1	0.1	0.2
7. TEMED	0.003	0.003	0.003	0.003	0.02

After the separating gel was poured, a layer of water was added on the top of the gel, and the gel was left to polymerise either for *ca.* 60 min at room temperature or overnight at 4°C. After polymerization of the separating gel, the layer of water was discarded, the top of the separating gel was rinsed briefly with stacking buffer. A well-forming comb was inserted, then the stacking gel solution was pipetted onto the separating gel and left to set for *ca.* 30 min. The protein samples were prepared as described in section 2.3.8.1. Electrophoresis was conducted at 65 mA through the stacking gel and then 30 mA through separating gel, and was usually terminated after 5 to 6 h.

2.3.9 Western Analysis

The basic method described by Towbin *et al.* (1979) with some modifications was used for western analysis.

2.3.9.1 Transfer of Proteins from the Polyacrylamide Gel to PVDF Membranes Using Electrophoresis

Reagents:

- Transfer Buffer: (25 mM Tris, 190 mM glycine, pH 8.3 and 10% (v/v) methanol)

Proteins separated by SDS-PAGE gel were electrophoretically transferred from the gel to PVDF membrane (Immobilin-P, Millipore Corporation, Bedford, MA, USA) using a Trans-Blot Electrophoretic Transfer Cell (Bio-Rad). The transfer cassette holder with gel and membrane was assembled as shown in Figure 2.5.

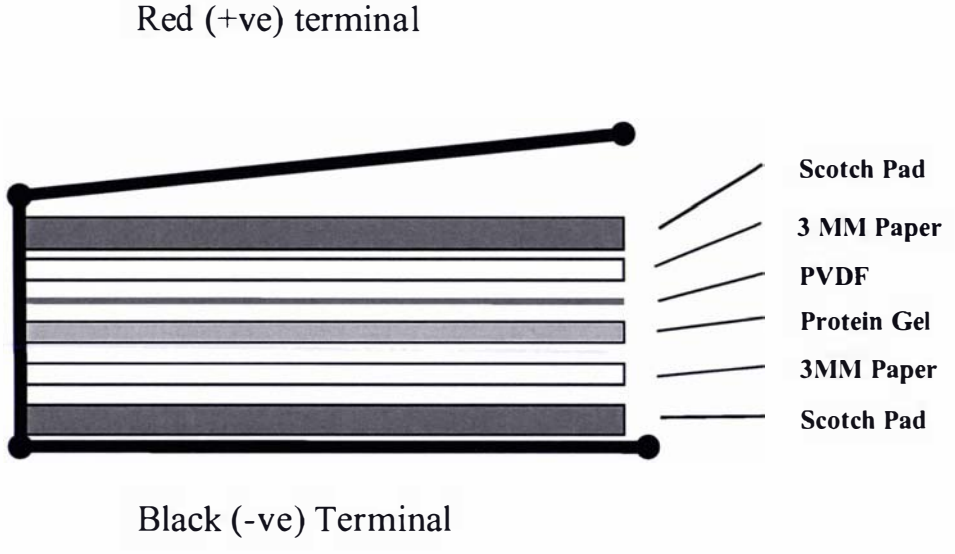

Figure 2.5 A diagrammatic setup for electrophoretic transfer of proteins from an acrylamide gel to PVDF membrane

2.3.9.2 Immunodetection of Proteins on PVDF Membrane

Reagents:

- PBSalt: (50 mM sodium phosphate, pH 7.4 containing 250 mM NaCl)
- PBST: (1× PBSalt containing 0.05% (v/v) Tween 20)
- 0.2% (w/v) blocking solution: (0.2 g I-Block™ dissolved in 100 ml 1× PBSalt by microwave heating for 40 seconds). (Tropix, Massachusetts, USA)
- Primary anti-TRACO2 rabbit IgG antibody (Hunter *et al.* 1999)
- Secondary antibody: anti-rabbit alkaline phosphatase conjugate and IgG raised in goat (Sigma)

- Substrate: (150 mM Tris-HCl, pH 9.7 containing 0.01% (w/v) 5-bromo-4-chloro-3-indolyl phosphate (BCIP), 0.02% (w/v) ρ-nitro blue tetrazolium chloride (NBT), 1% (v/v) dimethyl sulfoxide (DMSO), 8 mM $MgCl_2$; made fresh and stored in the dark until use)

Following electrophoretic transfer, the PVDF membrane was carefully peeled from the gel and placed protein-side up into a suitable clean container, and blocked in a 0.2% (w/v) blocking solution at room temperature for 1 h, or at 4°C overnight. The blocking solution was then discarded and the membrane rinsed with 1× PBST with shaking. The membrane was then incubated with a 1: 2,000 dilution of the primary anti-TRACO2 rabbit IgG antibody in 1× PBST at room temperature for 1 h with gentle shaking. After this, the primary antibody solution was discarded and the membrane washed (3 × 10 min) with 1× PBST and the secondary antibody at a concentration of 1: 10,000 in 1× PBST at room temperature for 1 h with gentle shaking. After this time, the secondary antibody solution was discarded and the membrane washed (3 × 10 min) with 1× PBST, and then with 150 mM Tris-HCl (pH 9.7) (2 × 5 min), and the membrane was developed in the dark with the addition of substrate. When sufficient color had developed, the reaction was stopped immediately by discarding the substrate solution and rinsing the membrane several times in RO water. The membrane was then 'photographed' as soon as possible either digitally with an Alpha Imager™ 2000 Documentation and Analysis System (Alpha Innotech Corporation, San Leandro, CA, USA) or using a Polaroid Land Camera with Polaroid 667 film (Fabrique au Royanne-Uni. UK, Ltd., Hertfordshire, England).

2.3.10 Protein Analysis by 2D-Electrophoresis

Two-dimensional electrophoresis (2D-Electrophoresis) is a powerful and widely used method for the analysis of complex protein mixtures extracted from cells, tissues, or other biological samples. Proteins are separated by isoelectric point (pI) in the first dimension using immobilized pH gradients and isoelectric focusing (IPG-IEF) and then in a second dimension by molecular mass using SDS-PAGE (O'Farrell, 1975; Klose, 1975; Görg *et al.*, 1985; 1988).

2.3.10.1 Protein Sample Preparation

The appropriate amount of protein sample was mixed with at least 3 volumes of ice-cold acetone at -20°C for 3 h, the precipitated proteins were collected by centrifugation at 35,300 × *g* for 12 min at 4°C, and any residual acetone was removed by air-drying.

2.3.10.2 Immobilized pH Gradients-Isoelectric Focusing (IPG-IEF) on the IPGphor

Reagents:

- Rehydration Buffer: (8 M Urea, 2% (w/v) CHAPS with a 'grain' of bromophenol blue)
- IPG Buffer (same pH range as the IPG strip)

Prior to IPG strip rehydration, the protein pellet obtained in section 2.3.10.1 was resuspended with rehydration buffer for solublizing and denaturing proteins, and then the appropriate amount of IPG buffer added to give a final concentration of *ca.* 0.5% of protein. The required number of strip holders for the Immobiline DryStrips (Amersham-Pharmacia Biotech, UK: 70 mm linear, pH 3-10, or 180 mm linear, pH 4-7) were put onto the cooling plate's electrode contact area of the IPGphor (Amersham-Pharmacia Biotech), and then 165 µl of sample containing rehydration solution (for 70 mm long IPG strips) or 350 µl of sample (for 180 mm long IPG strips) was pipetted carefully into a central point in the strip holder channel away from the sample application wells at the electrodes. The IPG strips were lowered, gel side down, onto the rehydration solution without trapping any air bubbles, and overlayered with 1 ml of silicone oil before the plastic cover was applied. Once the safety lid was closed, rehydration and IEF are carried out automatically according to the programmed settings until *ca.* 45,000 Vh were reached (Table 2.5). This step occurred preferably overnight, without further handling steps. As indicated in Table 2.5, low voltage (30-50 V) was applied during the rehydration step for improved sample entry of high molecular mass proteins into the polyacrylamide gel matrix. After isoelectric focusing, IPG gel strips were either stored between two sheets of plastic film at –80°C or immediately equilibrated using the method of Görg *et al.* (1987).

Table 2.5 Voltage settings for rehydration and IEF of dry strips using the IPGphor

Immobiline DryStrip	Phase	Voltage (V)	Current (mA)	Power (W)	Duration (h:min)
700 mm pH 3-10	1	50	2	5	16
	2	500	2	5	1
	3	1000	2	5	1
	4	2000	2	5	1
	5	8000	2	5	10
1800 mm pH 4-7	1	30	2	5	16
	2	500	2	5	1
	3	1000	2	5	1
	4	8000	2	5	10

2.3.10.3 SDS-PAGE of IEF-Strips

Reagents:

- Stock equilibration buffer:(0.04 M Tris-HCl, pH 6.8, containing 6 M urea, 25% (w/v) glycerol, 2% (w/v) SDS and 0.01% (w/v) bromophenol blue) (stored at –20°C)
- Equilibration solution I: (to 10 ml of stock equilibration buffer, add 100 mg of DTT)
- Equilibration solution II: (to 10 ml of stock equilibration buffer, add 250 mg of iodoacetamide)

Gel strips after IEF were equilibrated on a rocking table for 15 min at room temperature in equilibration solution I, followed by 15 min in equilibration solution II. The iodoacetamide was added to alkylate thiol groups on proteins, preventing their reoxidation during electrophoresis and DTT added to prevent point streaking and other silver-staining artifacts (Görg *et al.,* 1987). Equilibration with iodoacetamide was also used to minimize unwanted reactions of cysteine residues in the separated proteins, as cysteine-containing peptides not protected by alkylation may be under-represented in MALDI-TOF mass spectra (Sechi and Chait, 1998). Approximately 5 mm was trimmed from each end of gel strips to better fit the apparatus. The second dimension (SDS-PAGE) was performed in a 15% (w/v) acrylamide slab gel without stacking gel. A small amount of 1% (w/v) agarose in electrophoresis buffer was pippetted between the

gels plates to hold the strips in place and ensure a good connection between the strip and the separating gel. The 70 mm strips were electrophoresed using minigels using the SDS-PAGE protocol described previously (section 2.3.8.1). Larger gels (180 mm) were run at 30 mA per gel constant current in a Protean® II Cell apparatus (Bio-Rad) until the dye front reached the bottom of the gel at 4°C (about six h).

2.3.10.4 Visualisation of SDS-PAGE Gels

2.3.10.4.1 Coomassie Brillant Blue Staining

Reagents:

- CBB stain solution: (0.1% (w/v) Coomassie Brilliant Blue R-250, 40% (v/v) methanol and 10% (v/v) acetic acid)
- CBB destain solution: (30% (v/v) ethanol)

After electrophoresis, the separated protein bands or spots (after 2D-electrophoresis) were detected by CBB staining. Gels were immersed in CBB stain for 30 min (minigels) or overnight for larger gels with gentle shaking, followed by destaining until protein bands or spots became visible. The gels were usually photographed or scanned immediately, and then sealed using plastic film for storage at room temperature.

2.3.10.4.2 Silver Staining

Reagents:

- Fixer solution: (50% (v/v) methanol, 10% (v/v) acetic acid)
- Sensitiser solution: (0.01% (w/v) sodium thiosulphate)
- Silver nitrate solution: (0.2% (w/v) silver nitrate)
- Developer solution: (500 µl of 37% (w/v) formalin and 2 ml of 0.02% (w/v) $Na_2S_2O_3 \cdot 5H_2O$ with 0.6% (w/v) Na_2CO_3 in 100 ml)
- Stop solution: (5% (v/v) methanol, stored at 4°C)
- Storage solution: (30% (v/v) methanol, 3% (v/v) glycerol)

The silver staining procedure was performed similarly to the method described by Swain and Ross (1995) that was published earlier by Rabilloud *et al.* (1988). After electrophoresis, the gel slab was fixed in the fixer solution for 30 min. The gel was then washed in Milli-Q water (3 × 5 min) to remove the remaining acid, and the gel sensitized by incubating in sensitiser solution for 2 min followed by several washes

with Milli-Q water. After rinsing, the gel was submerged in silver nitrate solution and incubated for 20 min followed by thorough rinsing with plenty of Milli-Q water before being placed in the developer solution. After the desired intensity of staining was achieved, the reaction was terminated by discarding the reagent, followed by washing the gel with cooled stop solution. Silver stained gels were stored in a storage solution and sealed in plastic film until analyzed further.

2.3.10.5 Sample Preparation for MALDI TOF Mass Spectrometry

For acquisition of mass spectrometric peptide maps of the proteins, some spots of interest were excised into small pieces with a sterile scalpel. The gel piece for each spot was washed by vortexing for 5 min in 400 µl of sterile deionized water, the water discarded and the gel pieces dried in a vacuum centrifuge for 30 min (Savant Speed Vac, Holbrook, NY). The samples were then sent to Australian Proteome Analysis Facility (Macquarie University, Sydney, Australia) for MALDI-TOF mass spectrometric analysis.

2.3.11 Determination of Phosphorylation/ Dephosphorylation of Target Proteins

2.3.11.1 Extraction of ACC Oxidase for Phosphorlation/Dephosphorylation Studies

Reagents:

- + P extraction buffer: (100 mM Tris-HCl, pH 7.5, 10 mM magnesium acetate, 2 µM okadaic acid (OKA), 10 mM DTT, 30 mM sodium ascorbate, 10% (v/v) glycerol, proteinase inhibitor cocktail tablets (Complete™, Roche Molecular Biochemicals, Mannheim, Germany))
- – P extraction buffer: (100 mM Tris-HCl, pH 7.5, 10 mM DTT, 30 mM sodium ascorbate, 10% (v/v) glycerol, proteinase inhibitor cocktail tablets)
- Elution buffer: (50 mM Tris-HCl, pH 7.5, 10% (v/v) glycerol, 10 mM DTT, 30 mM sodium ascorbate)
- Ammonium sulphate

Approximately 2 g of leaf tissue was frozen in liquid nitrogen and ground quickly to a fine powder with a pre-cooled mortar and pestle, and 1 g aliquots of powdered leaf tissue were extracted in 2.5 volumes of chilled + P extraction buffer or – P extraction buffer on ice for 45 min. After centrifugation at 26, 000 × *g* for 10 min at 4°C, the

resulting supernatant was measured and adjusted to 80% saturation (w/v, 516 g/L at 0°C) with solid ammonium sulphate. The extract was incubated on ice with gentle stirring for about 1 h until all the ammonium sulphate was dissolved and the protein pelleted by centrifugation at 26,000 × *g* for 10 min at 4°C. The supernatant was discarded and the protein precipitate resuspended in 2 ml of resuspension and elution buffer, and then desalted by passage through PD-10 desalting columns (Amersharm Biosciences) containing Sephadex G-25 medium at 4°C. The resulting elute was apportioned into a 800 µl aliquots for phosphorylation and dephosphorylation treatment, and the excess extract was aliquotted into a separate tube to be used for protein assay.

2.3.11.2 Phosphorylation/Dephosphorylation Treatment for ACC Oxidase

Reagents:

- + P incubation buffer: (50 mM Tris-HCl, pH 7.5, 40 µM ATP, 400 µM MgAcetate, 2 µM OKA)
- – P incubation buffer: (100 mM Tris-HCl, pH 7.5, 150 mM NaCl, 1mM $MgCl_2$, 100 µM $MnCl_2$, 1 mM DTT, 0.04 units of purified PP2A from human red blood cells (Upstate Biotechnology))

The samples (800 µl) eluted from PD-10 columns were incubated in either the + P or – P incubation buffers at 30°C for 15 min. The reaction in the – P buffer was then stopped by the addition of 2 µl of OKA. The triplicate samples (250 µl) were assayed for ACC oxidase activity as soon as possible (section 2.3.6). Excess sample was aliquotted into another tube to be used for western analysis.

2.4 Molecular Methods

2.4.1 Chemicals

All general chemical reagents used in this section were molecular biology or analytical grade, obtained from either BDH or Sigma. All solutions and buffers were prepared with Milli-Q water (as described in section 2.3.1) and sterilized by autoclaving at 103 kPa for times dependent upon the volume of liquid (500 ml or less, 20 min; 1 L, 30 min; 2 L, 45 min), or by filtering through a sterile 0.22 μM nitrocellulose filter (Millex®-GS sterilizing filter unit, Millipore Corp., Bedford, MA, USA).

2.4.2 Growth of Bacterial Culture

2.4.2.1 Preparation of LB Media and LB-Amp^{100} Plate

Reagents:

- LB (Luria-Bertani) broth (pH 7.0): 1% (w/v) bacto-tryptone (DIFCO Laboratories, Detroit, MI, USA), 0.5% (w/v) bacto-yeast extract (DIFCO Laboratories), 1% (w/v) NaCl
- Amp^{100}: Ampicillin (100 mg/ml)
- 1.5% (w/v) agar (Life Technologies, Gathersbury, MD, USA)
- 100% (v/v) glycerol

Liquid bacterial cultures of *E. coli* were grown with vigorous shaking (210-230 rpm) at 37°C in LB broth. The LB medium was kept at room temperature until required, and supplemented with antibiotics as required.

For LB-Amp^{100} plates, agar was added to LB growth medium to make 1.5% (w/v) and the mixture sterilized as described (section 2.4.1) before. When the agar medium had cooled down to *ca.* 40°C, ampicillin was added to give a final concentration of 100 μg/ml and the medium poured into sterile plates in a lamina flow bench. After solidification, plates were sealed using parafilm and kept at 4°C until required.

Cultures of *E. coli* were maintained on solidified media and stored for short-term periods at 4°C. Every three to five months, the stored cultures on solidified media were replaced by fresh inoculations from frozen long-term glycerol stocks storage cultures. In order to store bacterial cells, cultures were preserved as frozen glycerol stocks

consisting of 700 µl of *E. coli* cells in LB broth and 300 µl of 100% (v/v) glycerol stored in cryotubes (Nunc). The tubes were snap frozen in liquid N_2 and immediately placed at -80°C until required.

2.4.2.2 Preparation of Competent Cells

Reagents:

- 60 mM $CaCl_2$
- 100 (v/v) glycerol
- LB broth

E. coli cells used for transformation were prepared from *E. coli* strain DH5α (GIBCO BRL). From a single *E. coli* colony, bacterial cells were cultured in 10 ml of LB broth at 37°C overnight with shaking (225 rpm), and then 0.4 ml of the culture was removed to inoculate 40 ml of fresh LB broth. Incubation was continued at 37°C until cell growth reached an optical density at 600 nm of 0.4. The culture was then poured into a prechilled centrifuge tube and the bacteria pelleted by centrifugation at 2000 × *g* for 5 min at 4°C. After discarding the supernatant, the bacterial pellet was resuspended in 10 ml of cold 60 mM $CaCl_2$, followed by the addition of a further 10 ml of 60 mM $CaCl_2$, and the cells incubated on ice for 30 min. The cell suspension was centrifuged at 2,000 × *g* for 5 min at 4°C, and the cell pellets resuspended in 4 ml $CaCl_2$, containing 15% (v/v) glycerol. Aliquots (300 µl) of the cell suspension were transferred to microfuge tubes and stored at -80°C until required for transformation.

2.4.3 RNA Isolation

RNA is tolerant of a variety of solvent, salt and temperature conditions. It is highly resistant to shear and can be vortex-mixed without detriment (Strommer *et al.*, 1993). The major concern of working with RNA is the presence of contaminating ribonucleases, both endogenous (mainly located in vacuoles) and in the environment, which can be difficult to eliminate or inactivate.

To prevent RNA degradation during extraction, all glassware used was well-washed using mixed acid over night, then rinsed in Milli-Q water and wrapped with tinfoil and baked in a dry air oven at 180°C for at least 4 h. All disposable plastics were either

new, or treated overnight in 0.3% (v/v) H_2O_2 (Andrew Industrial Ltd), then rinsed well using Milli-Q water and autoclaved in tinfoil. Solutions used for RNA work were not used for other purpose and clean disposable gloves were always used and regularly changed. The Milli-Q water used was always collected directly from the Milli-Q apparatus, and autoclaved in baked bottles. If pH adjustment of a solution was necessary, the pH electrode was incubated in 50 mM NaOH for 10 to 15 min and rinsed with sterile water. Any gel apparatus used was sterilized with 0.1 M NaOH for a minimum of 20 min before washing with autoclaved Milli-Q water.

2.4.3.1 Extraction of Total RNA

Reagents:

- TRI Reagent® (Molecular Research Center, Inc., Cincinnati, OH, USA)
- 100 (v/v) chloroform
- 100 (v/v) isopropanol
- High salt precipitation solution (0.8 M sodium citrate and 1.2 M NaCl)
- 75% (v/v) ethanol

Total RNA was isolated using TRI reagent according to the method developed by Chomczynski and Sacchi (1987) with some modifications. Half to 1 g of leaf tissue which was stored at -80°C or immediately frozen in liquid nitrogen after harvest was weighed out in a liquid nitrogen pre-chilled mortar and ground to a fine powder using a pestle in the presence of liquid nitrogen. The fine tissue powder was then transferred, with a pre-chilled spatula, into a 50 ml sterile screw-capped disposable polypropylene tube, and 5 ml TRI reagent was added. The extraction mix was homogenized using a glass rod before being centrifuged at 12,000 × *g* for 1 min at 4°C to remove extracellular membranes, polysaccharides and denatured proteins. The supernatants were transferred into another fresh tube and left at room temperature for 5 min to permit complete dissociation of nucleoprotein complexes. One ml of chloroform was added, and then shaken vigorously for 15 s. After keeping the suspension at room temperature for 10 min, the mixture was centrifuged for 15 min at 12,000 × *g* at 4°C. The mixture was separated into a lower red, phenol-chloroform interphase containing the DNA and proteins, and a colorless upper aqueous phase containing the RNA. The RNA containing solution was carefully pipetted into a fresh sterile disposable 50 ml polypropylene tube, and then 1.25 ml each of isopropanol and a high salt precipitation

solution (0.8 M sodium citrate and 1.2 M NaCl) were added, mixed well and then incubated for 5-10 min at room temperature. The tubes were then centrifuged at 12,000 × *g* for 8 min at 4°C to pellet the RNA (white or clear pellet) while leaving polysaccharides in the supernatant. The supernatants were removed and the RNA pellets were washed with 5-6 ml of 75% (v/v) ethanol. The tubes were centrifuged at 7,500 × *g* for 5 min at 4°C and then the supernatants were carefully removed to prevent loss of the RNA pellets.

The pellets were then dried briefly by inverting the tubes on clean paper towels and the pellets then resuspended in 150 µl of sterile water prior to transfer to 1.5 ml Eppendorf tubes. The RNA was quantified (section 2.4.3.3) and stored at -20°C until required. For long-term storage, RNA was stored at -80°C as an ethanol precipitate.

2.4.3.2 Extraction of Poly(A)$^+$mRNA

Reagents:

- PolyATtract mRNA Isolation System IV Kit (Promega, Madison, WI, USA)
- 20 × SSC, pH 7.0 (supplied in kit comprising 17.53% (w/v) NaCl, and 8.82% (w/v) sodium citrate)

Messenger RNA was extracted from total RNA using biotinylated oligo (dT) bound to Streptavidin MagneSphere™ particles, according to the manufacturer's instructions

One hundred to five hundred micrograms of total RNA was made up to 500 µl in a 1.5 ml Eppendorf tube with sterile water and incubated at 65°C for 10 min to denature the secondary structure of the RNA. A 3 µl aliquot of biotinylated-oligo (dT) oligonucleotide solution and 13 µl of 20 × SSC buffer were added and gently mixed, and the solution was incubated for 10 min at room temperature until completely cooled. The Streptavidin MagneSphere™ Particles (SA-PMPs) were resuspended by flicking the bottom of the tube, and captured with the magnetic stand. The SA-PMPs were washed three times with 300 µl aliquots of 0.5 × SSC, each time capturing the beads with the magnetic stand and discarding the supernatant. The SA-PMPs were then resuspended in 100 µl of 0.5 × SSC, and the entire contents of the annealing reaction added. The mixture was incubated at room temperature for 10 min to allow binding between the biotin and streptavidin beads. The SA-PMP-mRNA complexes were then

washed four times by resuspending them in 300 µl aliquots of 0.1 × SSC. After the final wash, as much of the supernatant as possible was removed without disturbing the SA-PMP-mRNA complexes. The bound Poly $(A)^+$mRNA was eluted from the SA-PMPs by incubating twice, for 5 min, in 50 µl of sterile water, recapturing the SA-PMPs with the magnetic stand after each incubation and combining both supernatants in a fresh Eppendorf tube. Poly $(A)^+$mRNA was quantified using an Ultrospec 3000 UV/visible spectrophotometer (Pharmacia Biotech) at 260 nm and 280 nm as described (section 2.4.3.3).

2.4.3.3 Quantification of RNA in Solution

RNA concentrations were determined by measuring the absorbance of each solution at 260 nm (A_{260}) and 280 nm (A_{280}) using an Ultrospec 3000 UV/visible spectrophotometer (Pharmacia Biotech). Samples were diluted appropriately and transferred to 200 µl quartz curettes and measured against water blank. For RNA, an OD_{260} of 1.0 corresponds to approximately 40 µg/ml (Sambrook *et al.*, 1989). The RNA concentration was calculated using the formula as follows:

A_{260nm} × dilution factor × 40 = RNA concentration (µg /ml)

The purity of the RNA was determined by measuring the A_{260nm}/ A_{280nm} ratio. Relatively pure RNA solutions have an A_{260nm}/ A_{280nm} ratio of 2.0 (Sambrook *et al.*, 1989), a value that decreases with the presence of contaminants such as proteins and phenol (if used in the RNA extraction).

2.4.4 Amplification of DNA by RT-PCR

2.4.4.1 DNase Treatment of RNA

Reagents:

- DNaseI (1U/µl)(Roche Diagnostics GmbH, Germany)
- RNase inhibitor (Roche)
- 100 mM DTT (supplied with expand reverse transcriptase) (Roche)
- DNaseI buffer (100 mM sodium acetate, 5 mM $MgSO_4$) (pH 5.0)

RNA was treated with DNaseI to remove DNA from RNA samples prior to applications such as RT-PCR according to the manufacturer's instructions. DNaseI degrades both double-stranded and single-stranded DNA and it is used in applications where maintaining the integrity of RNA is critical. Thirty μg of RNA (quantified in section 2.4.3.3) was incubated with 4 μl of DNaseI buffer, 2 μl of RNase inhibitor, 2 μl of 100 mM DTT and 4 μl of DNaseI in a total volume of 40 μl (made up with RNase-free water) for 30 min at 37°C. The mixture was then incubated at 75°C for 10 min to inactive the DNaseI, and the DNaseI treated RNA sample could be added to an RT-PCR reaction immediately following treatment, or stored at -20°C until required.

2.4.4.2 Generation of cDNA Using Reverse Transcriptase

Reagents:

- Superscript™ II RNase H-Reverse Transcriptase (200 U/μl) (Life Technologies)
- 5 × first strand buffer (supplied with Superscript)
- 0.1 M DTT (supplied with Superscript)
- Ribonuclease Inhibitor (10 U/μl) (Life Technologies)
- 10 mM dNTP mix (10 mM each of dATP, dGTP, dCTP and dTTP at neutral pH) (Life Technologies)

First strand copy DNA (cDNA) synthesis was performed using Superscript™ II RNase H-Reverse Transcriptase. For each reaction, 5 μg of DNaseI-treated total RNA (section 2.4.4.1) and 1 μl (1000 ng) of 17 mer oligo-dT primers were mixed in a microfuge tube and adjusted to a volume of 10 μl with sterile water before denaturation at 70°C for 10 min. Subsequently, the tube was placed immediately on ice for 2 min, and the contents collected in the bottom of the microfuge tube by a brief centrifugal pulse. A reaction buffer was then added, comprising 4 μl of 5 × first strand buffers, 2 μl of 100 mM DTT, 2 μl of 10 mM dNTP mix, 1 μl of ribonuclease inhibitor and the volume made up to 19 μl with RNase-free water. After mixing, the contents were incubated at 42°C for 2 min, and then 1 μl of reverse transcriptase was added. The reaction content was mixed by pipetting up and down and then incubated at 42°C for 1 h. To inactivate the reverse transcription enzyme, the temperature was increased to 70°C for 15 min. The synthesized first strand cDNA solution was used immediately, or kept at -20°C until required for amplifying cDNAs.

In this study, when the first strand cDNA was used for 3'-RACE, 5 µl of a 10 µM stock of the oligo-dT adapter primer (ADAPdT) (Figure 2.6) was used instead of the oligo-dT primer. For mRNA templates, 1 µg of poly $(A)^+$RNA made up to 5 µl in RNase-free water was used.

5'-GTGGATCCTACTGCAGCTAATTTTTTTTTTTTTTTT-3'

***Bam*H I** ***Pst* I**

Figure 2.6 Sequence of the ADAPdT primer

2.4.4.3 Amplification of cDNAs by PCR

Each primer (Life Technologies Inc.) was dissolved in sterile water at a concentration of 100 mM and stored at -20°C until required. A working stock was prepared by diluting to a concentration of 10 µM. In a 50 µl volume of PCR mixture, 2 µl of primer was used, giving a final primer concentration of 400 nM

2.4.4.3.1 Degenerate Primers Used in RT-PCR

Nested PCR reactions were performed with two sets of degenerate oligonucleotide primers. The primers are known to bind a highly conserved region amongst the ACC oxidase genes and were provided originally by Professor S.F. Yang (University of California, Davis, USA). The sequence of each primer is given in Figure 2.7.

ACOF1: First round forward primer (Shifted by 3 nucleotides in the 5' direction for E101)

```
                                    Q
                                    H
Amino acids      D    A    C    E    N    W    G
5' GTGAATTC GAY GCN TGY SAN AAY TGG GG 3'
     Eco R1      2    4    2  2 4    2    ◄——  Degeneracy = 256 ×
```

ACOR1: First round reverse primer (Shifted by 12 nucleotides in 3' direction for E102)

```
5' TCG TCT AGA TC RAA NCK MGG YTC YTT 3'
       Xba I     2    4  4 2    2    2    ◄——  Degeneracy = 256 ×
```

E101: Second round forward primer

```
                         Q
                    A    C    E    N    W    G    F
5' GTGAATTC GCN TGY GAR AAY TGG GGH TT 3'
     Eco R1      4    2    2    2         3    ◄——  Degeneracy = 96 ×
```

E102: Second round reverse primer

```
5' TCG TCT AGA GYT CYT TNG CYT GRA AYT T 3'
       Xba I     2    2    4    2    2    2    ◄——  Degeneracy = 256 ×
```

Where: R = A, C; H (A, C, T; W (A, T; D (A, G, T; Y (C, T; S (C, G;

N (A, C, G, T; M (A, C

Figure 2.7 Sequence of the primers used in RT-PCR to amplify putative ACC oxidase sequence

2.4.4.3.2 Gene-Specific Primers Used in RT-PCR

Gene-specific primers (Figure 2.8) were designed depending on the DNA sequence of TR-ACO3 to amplify regions of TO-ACO genes from a first strand cDNA template, where either one or two rounds of PCR were required.

TRACO3RA: RT reaction primer

5' CAAAGCCAAAATGAGTCTG 3'

TRACO3FA: First round forward primer (Shifted by 7 nucleotides in 5' direction for TRACO3FB)

5' ATGRVRAACTTCCCAGT 3'

TRACO3RB: First round reverse primer (Shifted by 23 nucleotides in 3' direction for TRACORC)

5' GCAATTGAACCCAAATTCAC 3'

TRACO3FB: Second round forward primer

5' ATGRVRAACTTCCCAGTKRTYRAC 3'

TRACO3RC: Second round reverse primer

5' TCATGCTTTCAGTGCTTCAAATC 3'

Figure 2.8 Sequences of gene-specific primers based on *TR-ACO3*

2.4.4.3.3 Primers Used for 3'-RACE

Nested PCR amplification was carried out using the two sets of gene-specific primers and the adapter primer (ADAP) as the forward and reverse primers, respectively (Figure 2.6). The gene-specific primers were designed from a region near to the 3'-end of the reading frame with the following criteria: (1) the 3-end of the primer should be unique in the sequence to eliminate the chance of secondary priming, and (2) the 3'-end should be a bit of unstable, finishing in A's and T's, which effectively prevents false priming as well as broadening the optimal annealing temperature (Rychlik, 1993). The primers used in 3'-RACE are given in Figure 2. 9.

TOACO2FA: First round forward primer

5' TATCTATCCAGCAACAACATTGATTG 3'

TOACO3FA: First round forward primer

5' AATCTACCCTGCTCCAGAATTGTTGG 3'

TOACO2FB: Second round forward primer

5' TGAAGAGAATAATGAAGTTTACCC 3'

TOACO2FC: Second round forward primer

5' ATCTTTATGCTGGATTAAAGTTCC 3'

TOACO3FB: Second round forward primer

5' AAACAGAGGAAAAAAACAATGTG 3'

TOACO3FC: Second round forward primer

5' AGATCTATGCTGCTTTGAAATTTC 3'

ADAP: reverse primer

5' GTGGATCCTACTGCAGCTAA 3'
***Bam* HI** ***Pst* I**

Figure 2.9 Sequences of primers used in 3'-RACE

2.4.4.3.4 PCR Conditions

Reagents:

- PCR Master Mix (Promega)

To carry out PCR amplification, the PCR reaction cocktail was prepared in order to reduce pipetting errors and save time. The cocktail consists of 25 µl of commercial PCR Master Mix, 2 µl of a 10 mM concentration of the first set of each of forward and reverse primers, and sterile water to make the final volume 45 µl. The PCR Master Mix is a premixed, and is a ready-to-use solution containing *Taq* DNA polymerase, dNTPs, $MgCl_2$ and reaction buffers at optimal concentrations for efficient amplification of DNA templates by PCR. To each of the PCR tubes, 45 µl of the cocktail was added, followed by 5 µl of the appropriate first strand cDNA solution. The tubes were preheated to 92°C for 2 min in a PTC 200 Peltier Thermal Cycler and the PCR reaction was performed for 35 cycles. Each cycle consist of 30 s at 92°C (denaturation), 30 s at 42°C (annealing), and 1 min 15 s at 72°C (extension) with a final incubation step at 72°C for 5 min to complete the extension of the cDNAs. The PCR reaction solutions were kept at 4°C on hold in the PCR thermalcycler before removed.

The second round PCR reactions were performed using the nested second set of primers, and 5 µl of the first round PCR products was used as DNA template. All other components in the cocktail were as described previously, and PCR performed under the same conditions as described previously except the annealing temperature increased from 42°C to 50°C.

For the second round PCR with gene-specific-primers and the 3'-RACE procedure, the annealing temperature was raised from 42°C to 50°C for the first round reaction, and from 50°C to 55°C for the second round.

2.4.5 Cloning of PCR Products into Plasmid Vector

2.4.5.1 Ethanol Precipitation of DNA or RNA

Reagents:

- 3 M sodium acetate pH 5.6
- 100% (v/v) ethanol: (99.7 to 100% ethanol)
- 70% (v/v) ethanol

Ethanol precipitation was used to concentrate nucleic acids by precipitation out of solution followed by resuspending in the desired volume. It was also used to partially purify DNA or RNA from salt solutions. Nucleic acid was routinely precipitated from solution by adding a 0.1 volume of 3 M sodium acetate (pH 5.6), and either 2.5 volumes (for DNA) or 3 volumes (for RNA) of ice cold 100% (v/v) ethanol. Precipitations were performed at -20°C for 3 h or overnight at 4°C (when maximal yield was required). The nucleic acid was then pelleted by centrifugation at 20 800 × g for 20 min at 4°C, the supernatant discarded and the residual salts removed by rinsing the pellet with ice cold 70% (v/v) ethanol. After discarding the 70% (v/v) ethanol, any residual ethanol was collected by pulse-centrifugation and removed with a micropipette. The pellet was air dried or dried in a heating block at 40°C for 4 min and then resuspended in sterile water.

2.4.5.2 Quantification of DNA in Solution

Reagents:

- Dye stock, containing 1mg/ml Hoechst 33258 dye (Amersham Biosciences, USA)
- 10 × TNE buffer: (0.1 M Tris-HCl, 2.0 M NaCl, and 10 mM EDTA, pH 7.4)
- 1 × TNE working buffer: (10 mM Tris-HCl, 0.2 M NaCl, 1 mM EDTA, pH 7.4)
- Assay solution: 0.1 μg/ml concentrated dye stock in 1 × TNE working buffer
- DNA standard: A calf thymus DNA standard of 100 μg/ml DNA in 10 mM Tris-HCl, 50 mM EDTA, pH 8.0 (Amersham Biotech)

DNA was quantified using a Hoefer TKO-100 Mini-Fluorometer (Amersham Biotech, USA). The fluorometer was calibrated to zero and 2 μl of a 100 μg/ml DNA standard added in 2 ml of assay solution, and then the mixture was pipetted in and out of the

cuvette with a disposable pipette. A 2 µl sample of unknown concentration was then tested.

2.4.5.3 Agarose Gel Electrophoresis of DNA

Reagents:

- UltraPURE™ agarose (Life Technologies)
- 10× TBE buffer: (0.89 M Tris, 0.89 M boric acid, 25 mM EDTA, pH 8.0)
- 10 × SUDS: (0.1 M EDTA, pH 8.0, 50% (v/v) glycerol, 1% (w/v) SDS, 0.025% (w/v) bromophenol blue)
- Ethidium bromide: (10 mg/ml)
- 1 kB Plus DNA ladder (Life Technologies)

Agarose gel electrophoresis is used to separate DNA fragments by size for either identification or purification. In solution (pH 8.0), DNA molecules are negatively charged and will migrate towards the positive electrode when an electrical current is applied. Migration is dependent on the size of the DNA fragments and their conformation both of which affect the movement of fragments in the agarose matrix. Horizontal 0.8 to 1.2% (w/v) agarose gels using 0.5 × TBE buffer were used routinely to separate DNA fragments generated by PCR (section 2.4.4) and restriction enzyme digestion (section 2.4.8.2.) To make the gel, an appropriate amount of agarose powder was heated and dissolved in a suitable volume of 0.5 × TBE buffer. After the gel solution had cooled to approximately 55°C, the solution was immediately poured into a gel-forming apparatus. DNA samples were mixed with 0.1 volumes of 10 × SUDS, and separated by electrophoresis at 70 to 100 V. After electrophoresis, the gel was stained with 0.1 µg/ml ethidium bromide for 20 to 30 min, and then destained (with water) for a further 20 min. The sizes of DNA bands were determined by measuring the distance a fragment had migrated from the well and comparing it with mobility of the 1 kB Plus DNA ladder on the same gel. The DNA fragments were visualized on a short wavelength (340 nm) UV Transilluminator (UVP Inc., San Gabriel, CA, USA), and photographed either digitally with an Alpha Imager™ 2000 Documentation and Analysis System (Alpha Innotech Corporation, San Leandro, CA, USA) or using a Polaroid Land Camera with Polaroid 667 film (Fabrique au Royanne-Uni. UK, Ltd.,

Hertfordshire, England).

2.4.5.4 DNA Recovery from Agarose Gels

Reagents:

- UltraClean™ DNA Purification Kit (MO BIO Laboratories, Inc. Carlsbad, CA. USA)

DNA fragments separated by electrophoresis in a 1% (w/v) agarose gel (section 2.4.5.3) were identified under UV light, excised from the gel with a sterile scalpel blade and placed in a pre-weighed micofuge tube. A 0.5 volume aliquot (by weight) of ULTRA TBE MELT solution and 4.5 volumes of ULTRA SALT solution were added and the mixture incubated at 55°C until the gel pieces were completely melted. Six µl of ULTRA BIND solution was then added to the melted gel and the mixture incubated at room temperature for 5 min. The mixture was then separated by centrifugation for 5 s, the supernatant removed and the pellet resuspended in 1 ml of ULTRA WASH by vortering for 5-10 s. After removed of the ULTRA WASH solution by centrifugation, the traces of wash solution was removed with a narrow pipette tip. The pellet was resuspended in a 12 µl aliquot of sterile water and the mixture was incubated at room temperature for 5 min, and then the DNA eluted by centrifugation at 10 000 × *g* for 1 min.

2.4.5.5 DNA Ligation

DNA ligation was performed in a final volume of 10 µl, and the protocol used was as outlined in the Promega pGEM®-T and pGEM®-T Easy vector systems technical manual.

The amount of PCR product (for a 1:3 molar ratio) required for ligation was calculated using the formula provided in the manufacturer's instructions.

$$\text{X ng of insert} = 3 \times \frac{\text{ng of vector} \times \text{kB size of insert}}{\text{kB size of vector}}$$

The PCR product was ligated with 50 ng pGEM®-T Easy vector (Figure 2.10 and Figure 2.11) in a reaction mix that contained 1 µl of T_4 DNA Ligase, 0.5 volumes of 2 × Rapid Ligation Buffer and the mixture made to 10 µl with sterile water. The ligation reaction was incubated at 4°C overnight.

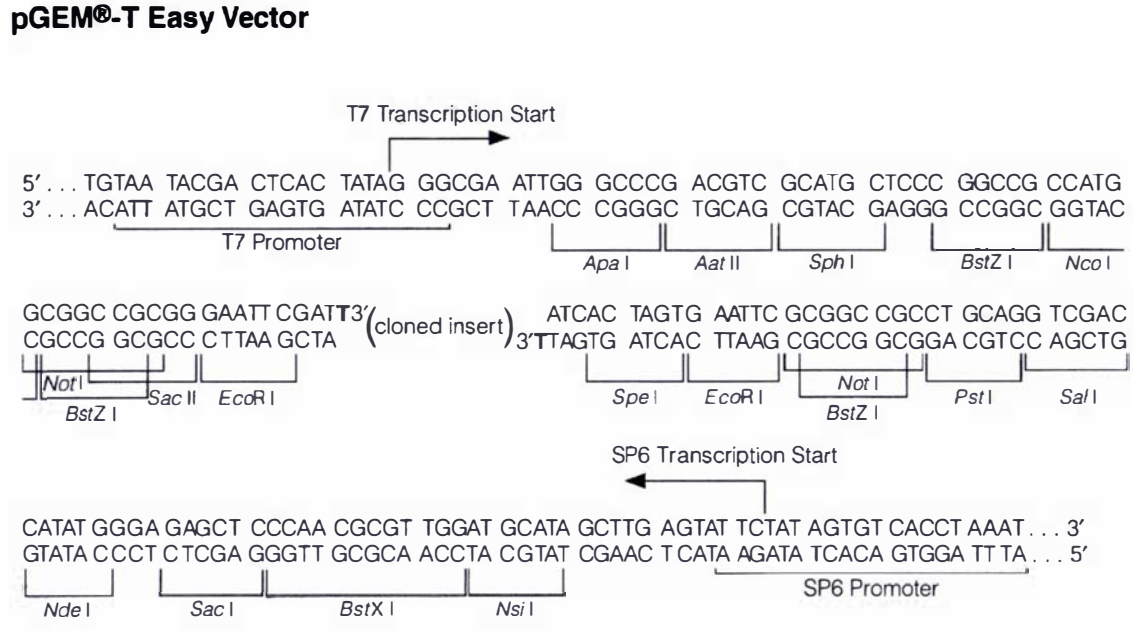

Figure 2.10 Sequence of the promoter and multiple cloning site of the pGEM®-T Easy vector

The top strand of the sequence shown corresponds to the RNA synthesized by T7 RNA Polymerase. The bottom strand corresponds to the RNA synthesized by SP6 RNA Polymerase (from Promega, 1999).

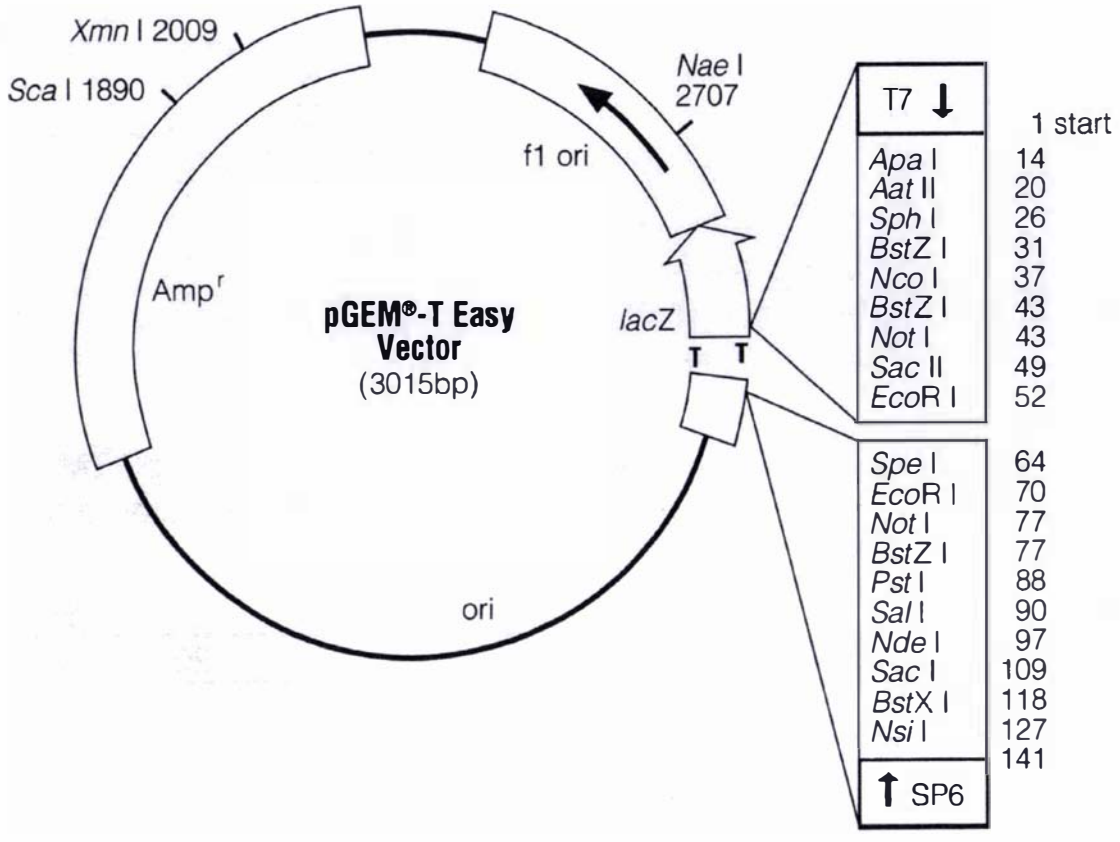

Figure 2.11 pGEM®-T Easy vector circle map and sequence reference points

pGEM®-T Easy vector sequence reference points:

T7 RNA Polymerase transcription initiation site	1
SP6 RNA Polymerase transcription initiation site	141
T7 RNA Polymerase promoter (-17 to +3)	2999-3
SP6 RNA Polymerase promoter (-17 to +3)	139-158
Multiple cloning region	10-128
lacZ start codon	180
lac operon sequences	2836-2996, 166-395
lac operator	200-216
β-lactamase coding region	1337-2197
phage 11 region	2380-2835
binding site of pUC/M13 Forward Sequencing Primer	2956-2972
binding site of pUC/M13 Reverse Sequencing Primer	176-192

2.4.5.6 Transformation of *E. coli* with the pGEM®-T Easy Vector

Reagents:

- LB broth: (refer section 2.4.2.1)
- 0.1 M IPTG stock solution (filter-sterilized and stored aliquot at -20°C)
- X-Gal (50 mg/ml, dissolved in *N,N'*- dimethyl-formamide)

The ligated pGEM®-T Easy vector was transformed into competent cells of *E. coli* strain DH5α (section 2.4.2.2) using the heat-shock method provided with the pGEM®-T Easy vector system. Competent DH5α *E. coli* cells prepared earlier were taken from -80°C storage and placed in an ice bath until just thawed. The entire ligation (50 µl) was added to the cells, and maintained on ice for 20 min. After this time, the cells were heat-shocked at exactly 42°C for 45 to 50s, placed back on ice for 2 min, then 950 µl of LB media maintained at room temperature was added, and the transformation mixture incubated at 37°C for 1.5 h with shaking at 150 rpm. One hundred µl of 0.1 M IPTG and 20 µl of 50 mg/ml X-Gal were spread over the surface of an LB Amp^{100} plate and allowed to absorb for 30 min at 37°C prior to use. Two hundred µl of each transformant mix was then spread onto these LB Amp^{100} plates with IPTG and X-Gal, the plates incubated overnight at 37°C and then transferred to a refrigerator at 4°C. *Lac* operon blue/white colony selection was used to identify transformants.

2.4.6 Characterization and Sequencing of Cloned DNA in *E. coli*

2.4.6.1 Plasmid Isolation from *E. coli* by the Alkaline Lysis Method

Reagents:

- Resuspension solution: (25 mM Tris-HCl, pH 8.0, 50 mM glucose, 10 mM EDTA)
- Alkaline lysis solution: (0.2 M NaOH, 1% (w/v) SDS)
- Neutralization solution: (3 M potassium acetate, 2 M glacial acetic acid)
- Isopropanol
- 70% (v/v) ethanol

Plasmid DNA was isolated from transformed *E. coli* by the alkaline lysis method using

the method of Sambrook *et al.* (1989). Single white colonies were picked and each grown overnight in 5 ml of LB medium with antibiotics as required. In this study, ampicillin at a final concentration of 100 μg/ml was typically used, after which, the cultures were grown with shaking of 200 rpm at 37°C. The cultures were then pelleted by centrifugation at 3 000 × *g* for 5 min at room temperature to harvest the bacterial cells. After the supernatants were removed, the tubes were inverted on paper towels for 10 min to allow the medium to drain completely from the pellets. Subsequently, 100 μl of freshly prepared resuspension solution was added to resuspend the pellets by pipetting up and down. After transfer of cell suspension into a microfuge tube, 400 μl of alkaline lysis solution was added and the suspension mixed by slow inversion, and lysed on ice for 10 min. Following the ice incubation, 300 μl of neutralization solution was added to the tubes and the mixture vortexed vigorously. The contaminating chromosomal DNA and protein was precipitated on ice for 15 min and subsequently pelleted by centrifugation at 20 800 × *g* for 5 min at room temperature. The supernatants were transferred into fresh tubes and mixed, by vortexing, with 1 ml of isopropanol to precipitate the DNA. The DNA was pelleted by centrifugation at 20 800 × *g* for 5 min at room temperature, the pellet was washed twice with ice-cold 70% (v/v) ethanol, dried and resuspended in 40 μl of sterile water, and stored at -20°C

2.4.6.2 Digestion of Plasmid DNA with Restriction Enzyme

Reagents:

- Restriction enzyme *Eco*R1 (GIBCO BRL, Life Technologies)
- 10 × Restriction buffer H (GIBCO BRL, Life Technologies)
- RNase A (10 mg/ml) (Sigma)
- 10 × SUDS: (0.1 M EDTA, pH 8.0, 50% (v/v) glycerol, 1% (w/v) SDS, 0.025% (w/v) bromophenol blue)

Digestion of plasmid DNA was performed for confirmation that transformed bacteria colonies contained inserts of the expected size. Typically, aliquots (1 to 2 μg) of plasmid DNA obtained by alkaline lysis (section 2.4.6.1) were routinely digested in a reaction mix containing 5 U of *Eco*R1, 0.1 volumes of 10 × Restriction buffer H, 10 μg RNase A and sterile water to make the final volume 15 μl. The reaction mixtures were

incubated for 3-4 h at 37°C, and 0.1 volumes of 10 × SUDS added to terminate the digestion. The DNA fragments were then separated and visualized using 1% (w/v) agarose gel electrophoresis (section 2.4.5.3) to confirm the existence of cDNA inserts. Plasmid preparations, treated the same way as described above but without adding the *Eco*R1 restriction enzyme, were included as uncut plasmid controls.

2.4.6.3 Purification of Plasmid DNA for Sequencing

Reagents:

- QIAprep® Spin Miniprep Kit (Qiagen Inc. Valencia, CA. USA)
- RNase A (10 mg/ml) (Sigma Chemical Co. Saint Louis, MO. USA)

Plasmid DNA was isolated and purified from 5 ml cultures of *E. coli* by using the QIAprep® Spin Miniprep plasmid preparation kit from Qiagen. Cells were pelleted by centrifugation at 3000 × *g* for 2 min at room temperature. The supernatant was drained and cells were resuspended in 250 µl of Buffer P1 and transferred to a microfuge tube, and cells were lysed with 250 µl of Buffer P2 by gently inverting the tube 4-6 times to mix. Buffer N3 was then added (350 µl) and the tube inverted immediately, but gently, 4-6 times to precipitate contaminating chromosomal DNA and protein. The precipitate was pelleted by centrifugation at 20800 × *g* for 10 min at room temperature, and the supernatant transferred to the QIAprep spin column by pipetting. After centrifuging for 30-60s and discarding the flow-through, the QIAprep spin column was washed by adding 0.75 ml of Buffer PE followed by centrifugation for 30-60s. After the QIAprep spin column was placed in a fresh 1.5 ml microfuge tube, DNA was eluted by adding 50 µl of Buffer EB to the center of the column and then centrifuging for 1 min. The plasmid DNA was separated on a 1% (w/v) agarose gel to assess quantity and purity, and then stored at -20°C until used.

2.4.6.4 Automated Sequencing of DNA

Reagents:

- Universal M13 forward and reverse primers (New England Biolab)
- ABI PRISM™ Big Dye Terminator Cycle Sequencing Ready Reaction Kit (Applied Biosystems)

- AmpiTaq®DNA Polymerase, FS (Perkin Elmer, Foster City, CA, USA)

All DNA sequencing was carried out by the Massey University DNA Analysis Service (MUSeq), Palmerston North, New Zealand. For pGEM®-T Easy plasmids, the intact plasmid DNA at a concentration of 200 ng/µl was provided and sequenced with M13 forward and reverse primers using a ABI PRISM™ Big Dye Terminator Cycle Sequencing Ready Reaction Kit with AmpiTaq®DNA Polymerase, and the fragments analyzed with an automated ABI PRISM™ 377 DNA sequencer (Applied Biosystems, Foster City, CA, USA).

2.4.7 DNA Sequence Analysis

2.4.7.1 Sequence Alignment

The sequence data obtained in this thesis were analyzed either using the Clustal X (1.5b) (Thompson *et al.,* 1994) or the relevant programmes of the Vector NT1 Suite 7 software package. The GenBank database was used to search for identical nucleic acid sequences of cloned cDNA sequences and the predicted polypeptide amino acid sequences from the cloned cDNA coding region were compared with the protein sequences held in the NCBI protein databases.

2.4.7.2 Sequence Phylogeny

A majority rule consensus tree was built using a heuristic search with default parameters of a pre-release β-version of the phylogenetic analysis using parsimony (PAUP version 4.0, Sinauer Associates Inc. Publishers, Sunderland Massachussetts© 1998 Smithsonian Institute).

2.4.8 Southern Analysis

The Southern analysis procedure was performed using the downward alkaline transfer method as described by Chomczynski (1992).

2.4.8.1 Isolation of Genomic DNA

Reagents:

- Nucleon PhytoPure Plant DNA Extraction Kit (Amersham Pharmacia Biotech, Uppsala, Sweden)
- TE buffer: (10 mm Tris-HCl, pH 8.0, 1 mM EDTA, pH 8.0)
- Tris buffered phenol: (6 ml of 1 M Tris-HCl, pH 8.0, 7.5 ml 2m NaOH, 130 ml H_2O, 500 g phenol crystals)
- RNase (Roche)

Genomic DNA was isolated by a modified method based on the Nucleon PhytoPure Plant DNA Extraction Kit. Approximately 2 g of young leaf tissue was placed into a 50 ml sterile screw-capped disposable polypropylene tube, deep frozen in liquid nitrogen and ground to a fine powder. Three volumes of Nucleon PhytoPure Reagent 1 (6 ml) and 60 µl of 2-mercaptoethanol were immediately added to the frozen powder and the mixture stirred with a disposable pipette tip until all the reagent ingredients had fully dissolved. After this time, 2 ml of Nucleon PhytoPure Reagent 2 was added and the tube was inverted several times until a homogeneous mixture was obtained. The mixture was incubated at 55°C for 10 min with regular manual agitation, and then cooled on ice for 20 min. Approximately 8 ml of phenol: chloroform: isoamyl alcohol (25:24:1) was added and the mixture vigorously shaken for 30s. The aqueous phase was separated from the organic phase by centrifugation at 13,000 rpm for 5 min at room temperature. The supernatant was transferred to a fresh tube and approximately 6 ml of isopropanol (pre-cooled to -20°C) was added. The tube was gently inverted several times to mix the contents until the DNA precipitated, and then the DNA was collected by centrifugation at 13,000 rpm for 10 min at room temperature. The supernatant was discarded and the pellet washed in 5 ml of 75% (v/v) ethanol (pre-cooled to -20°C), followed by centrifuging at 13,000 rpm for 5 min at room temperature. The supernatant was discarded and the tube was inverted for 10 min to drain, and then placed into a heating block set at 65°C for 30s to remove residual ethanol. While still in the heating block, 200 µl of sterile water containing 5 µl RNase, preheated to 65°C, was added to dissolve the DNA pellet and destroy any remaining RNA. The DNA was quantified (section 2.4.5.2) and stored in aliquots at -20°C until required.

2.4.8.2 Digestion of Genomic DNA

Reagents:

- *Eco*R1: (10 U/µl)
- *Xba* I: (10 U/µl)
- *Hind* III: (10 U/µl)
- 10 × Restriction buffer: (supplied with the appropriate enzyme)

Thirty micrograms of RNA-free genomic DNA in 200 µl of reaction solution that contained 20 µl of 10 × restriction buffer was digested with 80 U of either *Eco*R1, *Xba* I or *Hind* III at 37°C overnight. After this, a further 30 U of enzyme was added and the DNA digested for another 5 h. The digested DNA was then precipitated by the addition of 0.1 volumes of 3 M sodium acetate and 2.5 volumes of ice-cold 100% ethanol, and then incubated at -20°C overnight. The DNA was pelleted by centrifugation at 20 800 × *g* for 10 min, the supernatant discarded, the pellet washed once with ice-cold 80% (v/v) ethanol and once with ice-cold 100% (v/v) ethanol. The air-dried DNA was then dissolved in 20 µl of sterile water, one-tenth volume of 10 × SUDS gel loading buffer added and the solution mixed and incubated at 37°C for at least 1h to dissolve the DNA completely. The DNA samples were fractionated on a 1% (w/v) agarose gel by electrophoresis at 25 V overnight (section 2.4.5.3).

2.4.8.3 Southern Blotting of Genomic DNA

Reagents:

- Depurination solution: (0.25 M HCl)
- Denaturation solution: (1.5 M NaCl, 0.5 M NaOH)
- Neutralizing solution: (1.0 M Tris, pH 8.0, 1.5 M NaCl)
- Transfer buffer: (20 × SSC) (3 M NaCl, 0.3 M Sodium citrate, pH 7.0)

Following electrophoresis, genomic DNA fragments were transferred to a nylon membrane by the downward alkaline capillary transfer method of Chomczynski (1992), except for an additional depurination step. The agarose gel was soaked in depurination solution with gentle shaking for 20 min, rinsed twice with RO water and transferred to the denaturation solution for a further 20 min on a shaker. Following two more rinses

with Milli-Q water, the gel was equilibrated in neutralizing buffer for 20 min on a shaker. After this, the gel was finally immersed in 10 × SSC buffer for 20 min. The positively charged membrane (Hybond™-N^+, Amersham, UK) was pre-wetted with RO water, then rinsed in 10 × SSC buffer for 1 min, and the blotting system set up as shown in Figure 2.12. The whole construction was then covered in clingfilm to prevent evaporation of transfer solution from the wick, and transfer occurred overnight. Upon completion of transfer, the blot was carefully taken apart down to the gel. A soft pencil was pushed through the wells, and used to mark the position of each well on the membrane. The gel was then removed and the membrane was washed in 10 × SSC buffer for 5 min to remove any gel adhering to the membrane. After decanting the 10 × SSC buffer, the membrane was post-fixed by UV-crosslinker (UV Stratalinker®2400; Stratagene, La Jolla, CA, USA) set at 1200 mJ/cm^2. The membrane was placed between two sheets of dry 3MM paper and allowed to dry, then sealed in a plastic bag and stored at 4°C until required.

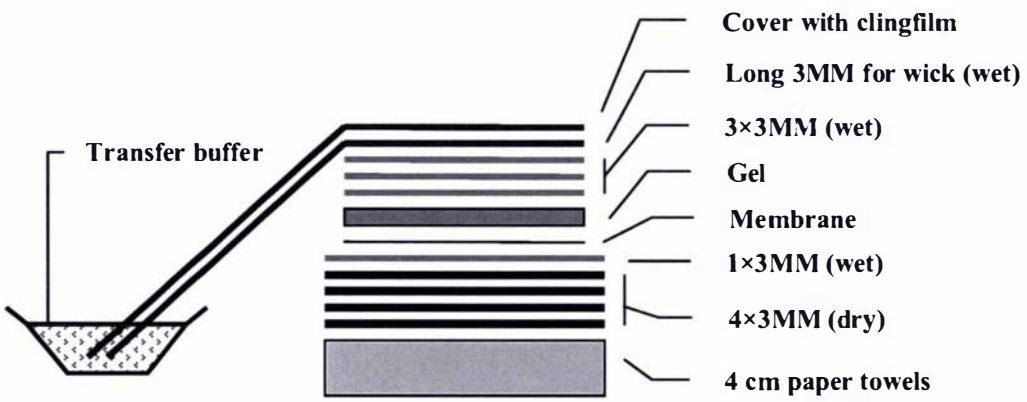

Figure 2.12 Arrangement of the apparatus used to transfer DNA and RNA samples to Hybond™-N^+ membranes

2.4.8.4 Labeling DNA for Southern and Northern Analysis with [α-^{32} P] -dATP

Reagents:

- Megaprime™ DNA Labeling Kit (Amersham)
- [α-^{32} P] -dATP (Amersham)
- 0.2 M EDTA, pH 8.0
- Reaction buffer: (supplied in kit)

Labeling of 3'-UTR probes was performed with [α-^{32} P] -dATP using the Megaprime™ DNA Labeling Kit. DNA was diluted to a concentration of approximately 5 ng/μl, and 5 μl of this diluted DNA was combined with 5 μl of nonamer primers. The mixture was then denatured in a boiling water bath for 5 min. Following pulse centrifugation to collect the contents, 4 μl each of the unlabelled dNTPs (dGTP, dCTP, and dTTP), 5 μl of reaction buffer, 2 μl of DNA polymerse was added, and the final volume was adjusted to 45 μl with sterile water. Five μl of [α-^{32} P] -dATP was then added and the mixture incubated at 37°C for 10 min. After completion of the labeling reaction, the reaction was stopped by the addition of 5 μl of 0.2 M EDTA, pH 8.0. The radiolabelled DNA was then purified through a ProbeQuant™ Sephadex G-50 Micro Column (Pharmacia Biotech). This involved vortexing the column to resuspend the Sephadex, loosening the lid, snapping off the bottom closure and centrifugation of the column in a microfuge tube at 735 × *g* for 1 min to remove the void volume. The column was transferred to a new microfuge tube and the labelled sample was layered onto the Sephadex and the sample purified away from unincorporated nucleotides, reaction dyes and salts by centrifugation at 735 × *g* for 2 min. The solution containing labelled DNA was denatured for 5 min in a boiling water bath, cooled on ice for 2 min and then added directly to the hybridization solution (pre-equilibrated at 65°C) bathing the membrane (section 2.4.8.5).

2.4.8.5 Hybridisation and Washing of DNA and RNA Blots

Reagents:

- Church hybridization solution: (0.25 M $Na_2PO_4 \cdot 2H_2O$, pH 7.2, 7%(w/v) SDS, 1%(w/v) BSA fraction V, 1 mM EDTA, pH 8.0)
- Hybridization wash solution: (20 mM $Na_2PO_4 \cdot 2H_2O$, pH 7.2, 5%(w/v) SDS, 0.5%(w/v) BSA fraction V, 1 mM EDTA, pH 8.0)
- 20 × SSPE: (0.2 M NaH_2PO_4, pH 6.5, 3.6 M NaCl, 20 mM EDTA)
- 2 × SSPE: (2 × SSPE pH 6.5, 0.1% (w/v) SDS)
- 1 × SSPE: (1 × SSPE pH 6.5, 0.1% (w/v) SDS)
- 0.2 × SSPE: (0.2 × SSPE pH 6.5, 0.1% (w/v) SDS)
- 0.1 × SSPE: (0.1 × SSPE pH 6.5, 0.1% (w/v) SDS)

The method used for labeling and washing of Hybond-N^+ membranes was based on that of Church and Gilbert (1984). The membrane was rolled up, nucleic acid facing inwards, and placed in a Hybaid™ screw top glass tube (Hybaid Ltd., Teddington, Middlesex, UK) containing 25 ml of Church hybridization solution in a rotary oven at 65°C. The denatured labelled probe (section 2.4.8.4) was added to the hybridization solution and circulated over the membrane overnight at 65°C. A series of washes were then undertaken, each at 65°C. In the first, 100 ml of hybridization wash solution was used to wash the membrane for 20 min. This was followed by a 20 min wash in 2 × SSPE, 20 min in 1 × SSPE wash, 20 min in 0.2 × SSPE and finally a 40 min wash in the 0.1 × SSPE. The membrane was then placed onto 3 MM paper, covered with clingfilm. The wrapped membrane was placed into a FujiFilm BAB cassette (2), nucleic acid facing upwards, and a FujiFilm Imaging Plate (coated with accelerated phosphorescent fluorescent material) was placed on top. The cassette was closed and stored for exposure. After exposure, the imaging plate was analyzed using a FujiFilm Fluoro Image Analyzer FLA-5000.

2.4.8.6 Stripping Southern and Northern Blots

Reagents:

- Stripping solution: (0.1 × SSPE, 0.1% (w/v) SDS)
- 0.1 × SSPE

Nylon membranes were stripped according to the method of Memelink *et al.* (1994). Stripping solution was boiled for *ca* 5 min and the solution poured onto the membrane and allowed to cool to room temperature. After discarding the solution, the procedure was repeated at least three times until the radioactive counts were low. The membrane was finally rinsed with 0.1 × SSPE to remove the SDS, sealed in a plastic bag, and kept at 4°C until required.

2.4.9 Northern Analysis

Northern analysis uses DNA: RNA hybridization to determine the steady state levels and size of mRNA gene transcripts. This procedure is based on the use of formaldehyde/formamide as denaturants. In this study, poly $(A)^+$mRNA was purified and used to determine transcript abundance and expression patterns. All equipment used in these procedures was RNase free and all solutions were prepared with sterile water.

2.4.9.1 Electrophoresis of RNA

Reagents:

- 10 × MOPS/EDTA buffer: (500 mM MOPS, pH 7.0, 10 mM EDTA, pH 7.5)
- Gel loading buffer: (For 1ml: Dissolve 400 mg sucrose, 5 mg xylene cyanol, 5 mg bromophenol blue, 100 µl 10 × MOPS/EDTA buffer, 178 µl formaldehyde, 10 µl ethidium bromide (10 mg/ml) and 500 µl formamide)
- Running buffer: (1 × MOPS/EDTA buffer)
- 37- 40% (v/v) formaldehyde
- 0.24 to 9.5 kb RNA Ladder (Life technologies)

Poly $(A)^+$ mRNA was separated on a 1% (w/v) denaturing agarose gel in a Bio-Rad DNA Sub Cell ™ (15 × 15 cm in size). The gel contained 7% (v/v) formaldehyde and was made with 1 × MOPS/EDTA buffer. All components used were mixed in a sterile Schott bottle, swirled around gently to rehydrate the agarose and then microwaved until the agarose was completely melted. The gel solution was then cooled to *ca.* 50-55°C prior to adding formaldehyde. The gel solution was poured immediately into a gel forming apparatus that had been pretreated with 3% (v/v) H_2O_2, and the gel was then

allowed to set.

All RNA samples were kept on ice during preparation. About 2.0-2.5 μg of Poly $(A)^+$ mRNA was ethanol precipitated and resuspended in 15 μl of gel loading buffer, and then the samples and standard RNA size ladder were denatured at 70°C for 10 min, immediately cooled on ice for at least 2 min before loading into wells. Gel electrophoresis was conducted using 1 × MOPS/EDTA as running buffer, first at 80 V for 30 min, and then overnight at 25 V.

2.4.9.2 Northern Blotting

RNA was transferred to a Hybond™-N^+ membrane by the method of Chomczynski (1992) as described for Southern blotting (section 2.4.8.3), except the gel was not pre-treated by depurination and denaturation, and the transfer was carried out for a shorter time (4-6 h).

2.5 Statistical Analysis

Experimental data collection and statistical analysis were performed with an Excel spreadsheets programme (version 2000; Microsoft, USA). Sample means with an estimate of the standard error (SE) have been used in this thesis. The existence of significant differences between data was tested using an Analysis of Variance (ANOVA), performed using Excel 2000 when a significant ANOVA result occurred. A difference between means at the 5 % ($P \leq 0.05$) was considered significant with a difference at the 1 % level ($P \leq 0.01$) being highly significant.

3. Chapter Three: Purification and Characterization of ACC Oxidase Isoforms in Leaf Tissue of White Clover (*Trifolium repens* L.)

3.1 Leaf Growth from Stolons of White Clover

White clover (genotype 10F, cultivar Grasslands Challenge), under the experimental conditions used in this thesis, was grown to obtain stolons with sub-tending leaves representing all developmental stages, from initiation at the stolon apex through maturation to senescence, and then necrosis (Figure 1.3). Changes in the ethylene evolution from attached leaves and chlorophyll content of each leaf during ontogeny using this growth system have been measured previously by Hunter (1998) (Figure 1.4). In the study by Hunter, leaves subtending nodes from 1 to 15 (designated leaves 1 to 15) were used for analysis and were representative of typical stolon growth. The first leaf to have emerged completely from the apical sheath was designated leaf 1, and subsequent numbers represent the stages through maturation and senescence to leaf 15.

3.2 Chlorophyll Content of Leaf Tissue during Leaf Initiation, Maturation and Senescence of White Clover

To confirm the developmental stage of leaves using the stolon growth system, chlorophyll content at each node was measured (section 2.2.2). Changes in leaf chlorophyll content of a typical harvest are presented in Figure 3.1. The total chlorophyll content increased as newly initiated leaf tissue unfolded and expanded (leaves 1 to 3), remained at a relatively constant level of *ca* 1300 to 1400 μg per g fresh leaf tissue during the mature green stage (leaves 4 to 7), and then, typically, leaves 8 to 11 were the first to display visual signs of chlorosis (onset of leaf senescence). After the onset of chlorophyll loss, the levels declined further as the leaf tissue aged (leaves 12 to 15) to reach *ca.* 270 μg per g fresh leaf tissue at leaf 15. As the leaf tissue aged, the general trend shows that chlorophyll *a* was degraded slightly faster than chlorophyll *b*, which was indicated by the ratio of chlorophyll *a:b* changing from 2.71 at leaf 5 to 2.40 at leaf 15 (Figure 3.1).

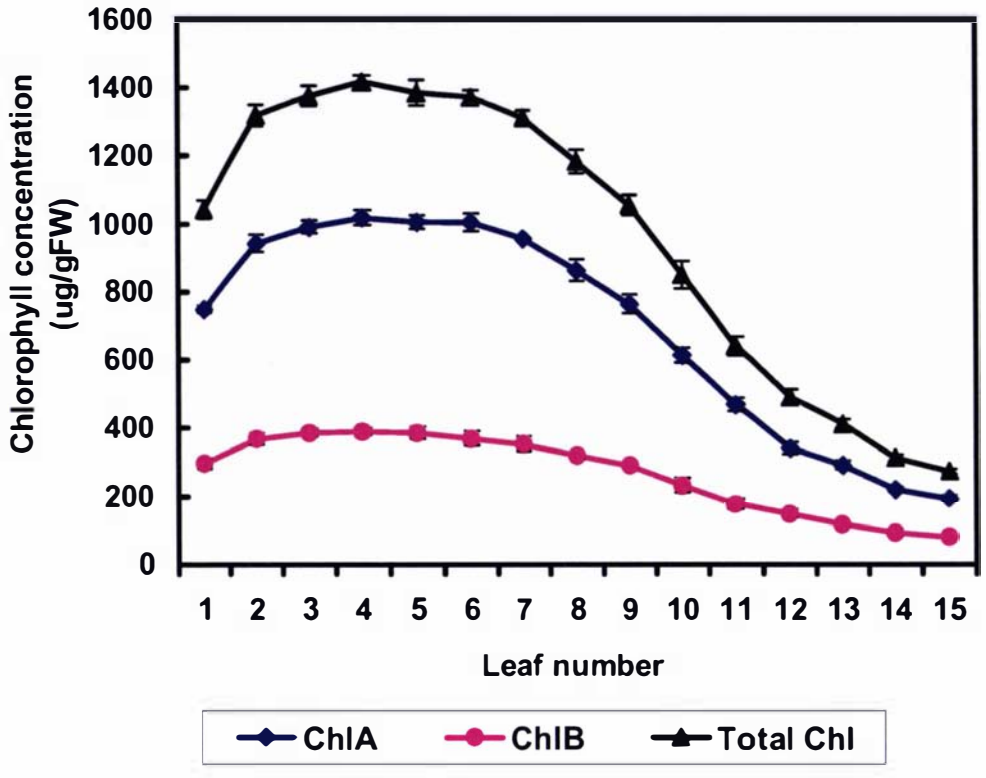

Chlorophyll a:b Ratio	2.52	2.56	2.56	2.61	2.60	2.72	2.70	2.69	2.62	2.64	2.64	2.30	2.49	2.38	2.40

Figure 3.1 Changes in chlorophyll concentration during leaf ontogeny in white clover

Results are mean values ± s.e., n=9

3.3 Extraction of ACC Oxidase from Leaves of White Clover

3.3.1 Extraction of ACC Oxidase from Newly Initiated Green and Senescent Leaves

ACC oxidase was extracted from leaves of white clover plants using modifications of the methods of McGarvey and Christoffersen (1992) and Kuai and Dilley (1992), exactly as described by Gong and McManus (2000). The same extraction scheme was used to extract the ACC oxidase from both newly initiated green and senescent leaf tissues (section 2.3.2). Mild extraction conditions were employed to isolate the water-soluble, active enzyme from both leaf tissues to try to minimize modification of the protein or degradation.

The extraction and separation procedure used in this thesis included ammonium sulphate precipitation and subsequent Sephadex G-25 gel filtration chromatography to remove residual ammonium sulphate and putative low molecular mass (<5 kDa) inhibitors. Table 3.1 summarizes the recovery of protein after these two extraction and separation stages from both newly initiated green and senescence leaf tissue. Although the protein recovery after ammonium sulphate precipitation and Sephadex G-25 chromatography was higher in the senescent leaf preparation when compared with the newly initiated green leaf preparation, the total protein was higher in the newly initiated green leaf preparation.

Table 3.1 Comparison of protein recovery in newly initiated green and senescent leaves in crude extracts and after ammonium sulphate precipitation and Sephadex G-25 gel filtration chromatography

Purification Step	Total Protein* (mg)		Protein Recovery (% of Total Protein)	
	IG**	SE**	IG	SE
Crude Extract	1516.4	1068.6	100	100
$(NH_4)_2SO_4$ Precipitation and Sephadex G-25 Chromatography	1156.8	880.8	76.3	82.4

*Total protein based on extraction from 100 g of fresh leaf tissue.

**IG and SE represent newly initiated green and senescent leaf tissue, respectively.

3.3.2 Separation of ACC Oxidase Protein from Crude Extracts Using Ammonium Sulphate Precipitation

In order to determine the efficiency of ammonium sulphate for the isolation of ACC oxidase, the saturation range was optimized (Table 3.2).

From the range tested, 50% to 70% saturated ammonium sulphate led to the highest recovery of both protein and ACC oxidase activity. However, in this thesis, a range of 40% to 80% saturated ammonium sulphate (and not 50% to 70%) was used to ensure that most of the ACC oxidase protein was precipitated.

Table 3.2 Recovery of protein and ACC oxidase activity using ammonium sulphate precipitation

Saturated Solution (%)	ACC Oxidase Activity (% of total activity)	Protein Precipitation (% of total protein)
30 to 50	14.90	43.4
50 to 70	80.44	49.4
70 to 90	4.69	7.2

3.4 Purification of ACC Oxidase from Newly Initiated Green Leaves Using FPLC

3.4.1 Selection of Leaf Tissue for ACC Oxidase Purification

At the beginning of the purification, protein extracts of pooled mature green leaves incorporating nodes from 4 to 7 were used. In these extracts, 3 to 4 bands were recognized by western analysis. In most fractions, two bands of *ca.* 35-36 kDa and *ca.*37 kDa were recognized with near equal intensity by the anti-TR-ACO2 antibody (lanes 34-36, Figure 3.2 A; lanes 8-11, Figure 3.2 B). In other lanes, 3 to 4 bands were recognized (lanes 33-36, Figure 3.2 A; lanes 7-10, Figure 3.2 B). This suggested that the two ACC oxidase isoforms putatively coded for by *TR-ACO2* and *TR-ACO3* were being purified because both genes are expressed in nodes 4 to 7 (Hunter *et al.,* 1999). Therefore, in order to more specifically purify an ACC oxidase isoform that may be encoded for by *TR-ACO2*, newly initiated green leaves (nodes 2 to 4) were used in further experiments. Similarly, to more specifically purify an ACC oxidase isoform encoded by *TR-ACO3*, nodes 12 to 15 were used.

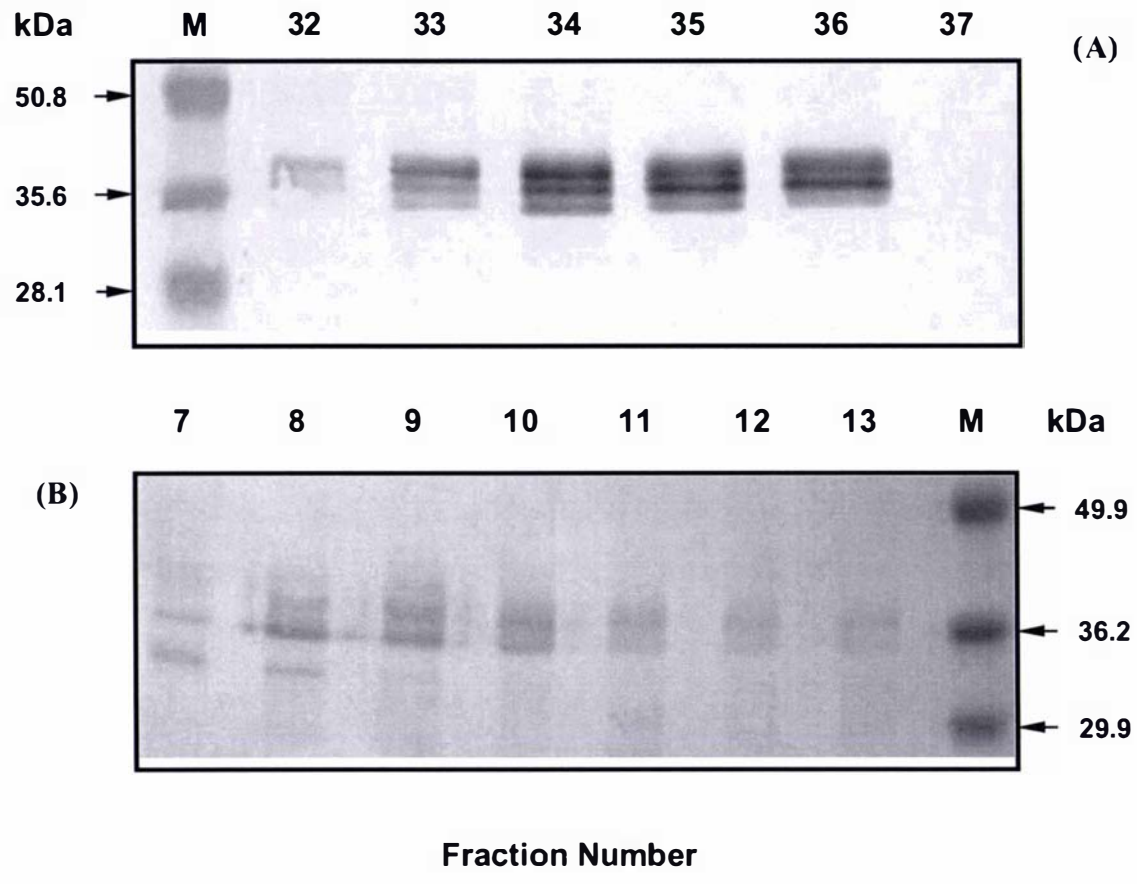

Figure 3.2 Western analysis using the anti-TR-ACO2 antibody of active fractions eluted from a Phenyl Superose Hydrophobic Interaction (A) and a Mono Q Ion-Exchange (B) column.

Enzyme extracts were subjected to 40% to 80% ammonium sulphate precipitation and Sephadex G-25 column chromatography prior to column chromatography of pooled leaves from nodes 4 to 7. Lane (M) are prestained molecular mass markers (molecular masses are indicated).

3.4.2 Sephadex G-25 Gel Filtration Chromatography of Crude Extract from Newly Initiated Green Leaves

After protein precipitation using ammonium sulphate, the protein suspension was then chromatographed through a Sephadex G-25 gel filtration column, the eluted protein collected as 2 ml fractions, and fractions that contained protein (fractions 8 to 18 in the example shown; Figure 3.3) were pooled and concentrated using Amicon Centriprep-10 tubes.

3.4.3 Hydrophobic Interaction Chromatography Using a Phenyl Sepharose Column

The first separation using FPLC utilized hydrophobic interaction column chromatography using a Phenyl Sepharose HiLoad 26/10 column (Pharmacia) pre-equilibrated with Buffer A [2M $(NH_4)_2SO_4$ in 50mM Tris-HCl, pH 7.5, containing 5.0% (v/v) glycerol, 30mM sodium ascorbate, 2mM DTT, 10μM PA]. Bound protein was eluted automatically using a linear reverse gradient of ammonium sulphate from 100% Buffer A: 0% Buffer B (Buffer A without ammonium sulphate) to 0% Buffer A: 100% Buffer B. Using this separation method, ACC oxidase protein from the newly initiated green leaves eluted in fractions 31 to 38 as determined by western analysis (Figure 3.4). The anti-ACC oxidase antibodies recognized a major protein of *ca.*37 kDa, with a minor protein of *ca.* 35 kDa. In fractions 32 to 34, the *ca.* 37 kDa and *ca.* 35 kDa were recognized, while the 37 kDa protein was recognized predominantly in fractions 35 to 38. Using this hydrophobic interaction column, the majority of protein eluted first within a decreasing linear gradient of ammonium sulphate in the buffer, while fractions 33 to 38, containing ACC oxidase and designated NIGI (extract from newly initiated green leaf tissues) in this thesis, eluted with no ammonium sulphate in the buffer (Figure 3.4). This suggests that the ACC oxidase protein has a high degree of surface hydrophobicity.

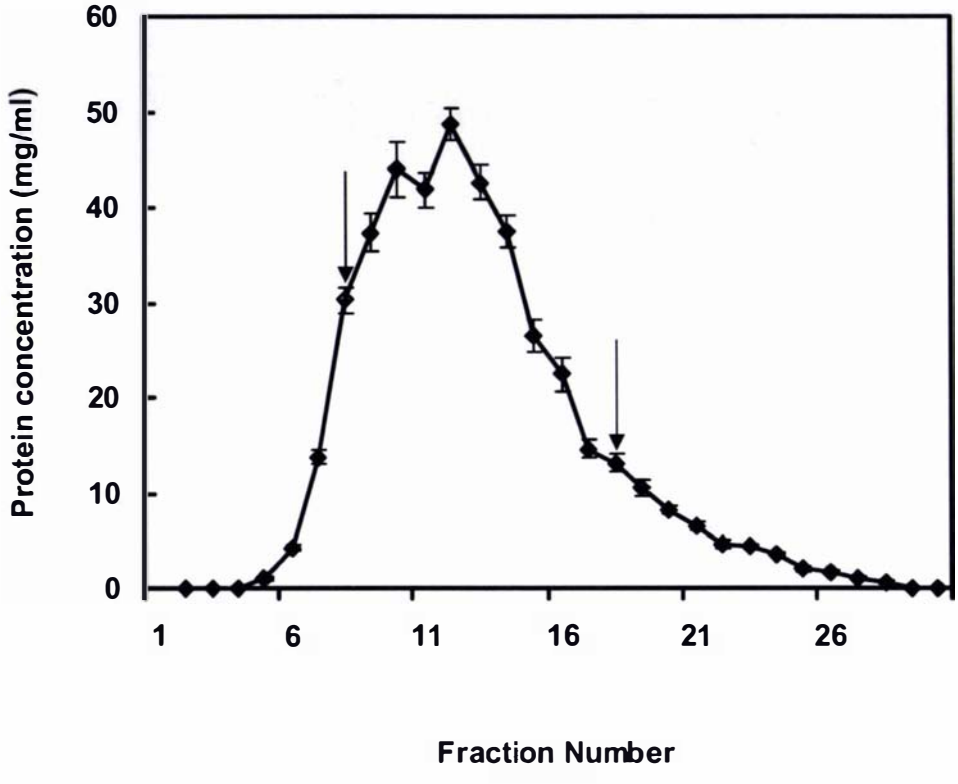

Figure 3.3 Protein elution profile from a Sephadex G-25 gel filtration column of a newly initiated green leaf protein extract

The arrows indicate the fractions pooled for further purifications.

Results are mean values ± s.e., n=3

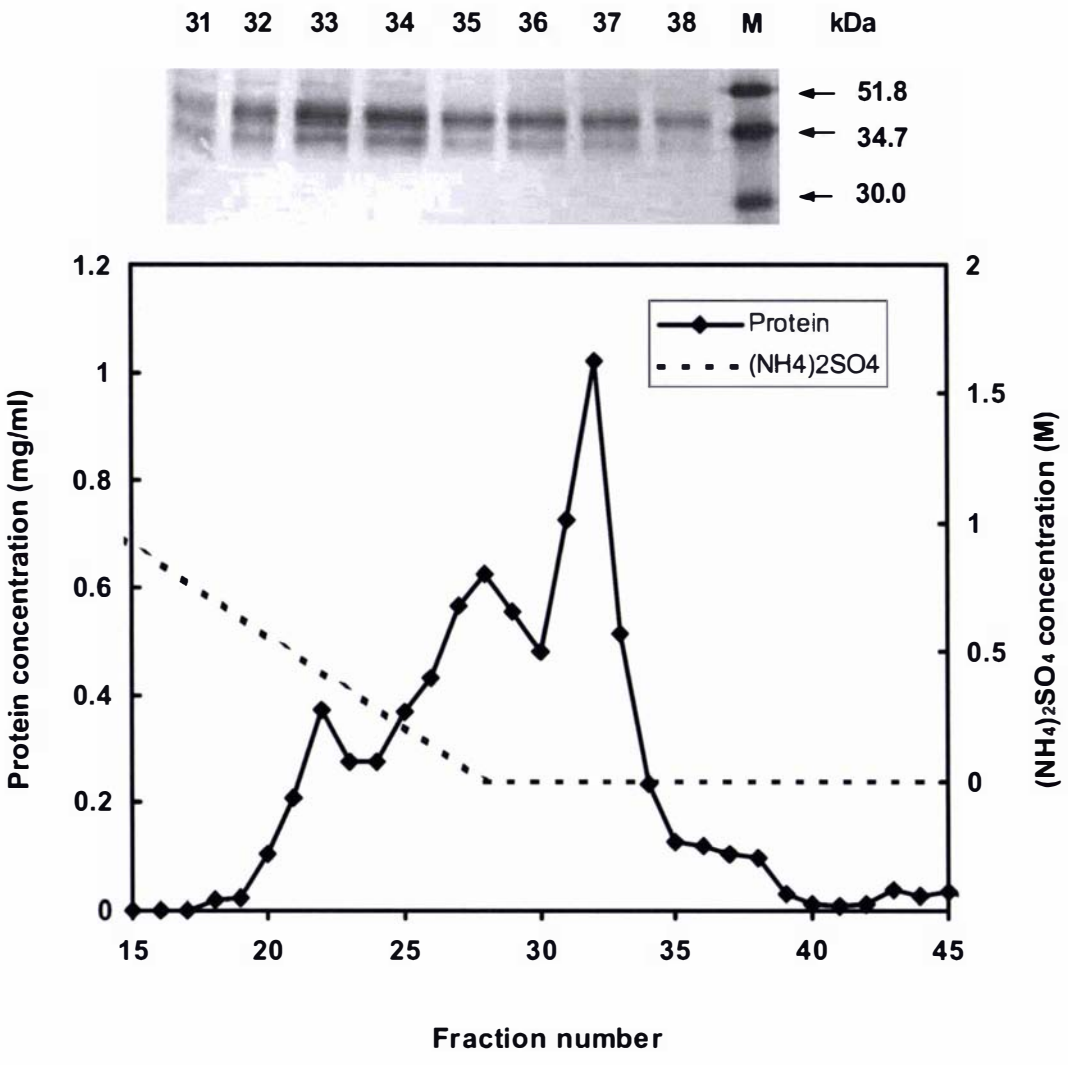

Figure 3.4 Separation of a newly initiated green leaf protein extract, after ammonium sulphate precipitation and Sephadex G-25 column chromatography, through a Phenyl Superose Hydrophobic Interaction column

The top panel represents western analysis of the fraction numbers indicated. Aliquots (2μg) from each fraction were separated using SDS-PAGE, transferred to PVDF membrane and challenged with anti-TR-ACO2 antibodies. Lane (M) are prestained molecular mass markers (molecular masses are indicated). The separation of fractions 1 to 14 is not shown.

3.4.4 Anion Exchange Chromatography Using a Mono Q Column

Anion exchange (Mono Q) column chromatography was used as the second purification step to further purify the NIGI isoform identified after hydrophobic column chromatography. The Mono Q anion exchange column was pre-equilibrated with Buffer A (50mM Tris-HCl, pH 7.5, containing 5.0% (v/v) glycerol, 30mM sodium ascorbate, 2mM DTT, 10μM PA) at a flow rate of 0.5 ml/min. Fractions 33 to 38 from the Phenyl Sepharose column were pooled, and then applied to a Mono Q anion exchange column. Bound proteins were eluted using a linear increasing gradient of sodium chloride from 100% Buffer A: 0% Buffer B (Buffer A containing 1.0 M NaCl, pH 7.5) to 20% Buffer A: 80% Buffer B at a flow rate of 0.5 ml/min (section 2.3.5.2).

The result showed that ACC oxidase protein can bind to the resin and be eluted from it with a linear sodium chloride gradient of 0 to 0.8 M (Figure 3.5.). The most intense antibody recognition was observed in fractions 8 to 11 with one major protein of *ca.* 37 kDa was recognized in fraction 8 by the anti-TR-ACO2 antibody. However, in fractions 9 and 10, the anti-ACC oxidase antibody again recognized two protein bands of *ca.* 37 kDa and *ca.* 36 kDa. Fractions with ACC oxidase recognition eluted at a sodium chloride concentration of 210 mM to 290 mM (fractions 8 to 10, Figure 3.5) suggesting that this isoform has a net negative charge (an anionic form) at pH 7.5.

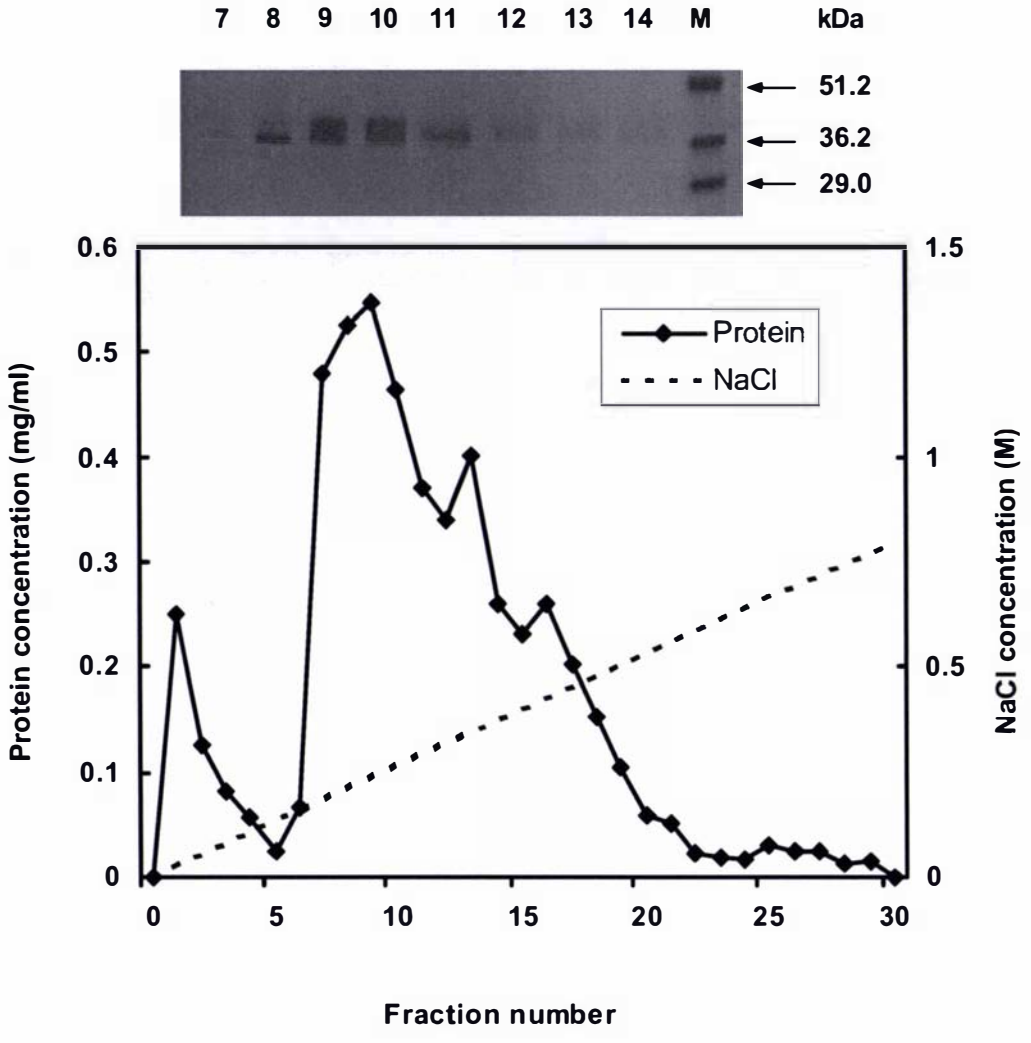

Figure 3.5 Separation of fractions 33 to 38 from the Phenyl Superose column through a Mono Q Anion Exchange column

The top panel represents western analysis of the fraction numbers indicated. Aliquots (2μg) from each fraction were separated using SDS-PAGE, transferred to PVDF membrane and challenged with anti-TR-ACO2 antibodies. Lane (M) are prestained molecular mass markers (molecular masses are indicated).

3.4.5 Gel Filtration Chromatography Using a Superose 12 Column

Gel filtration chromatography on a Superose 12 HR10/30 column (Pharmacia) was used as the final purification step. The column was equilibrated with Buffer A [50mM Tris-HCl, pH 7.5, containing 5.0% (v/v) glycerol, 30mM sodium ascorbate, 2mM DTT, 10μM PA and 150mM NaCl] at a flow rate of 0.3 ml/min (section 2.3.5.3). The inclusion of 150 mM NaCl in the equilibration and elution buffers was found to give good separation of proteins in previous purifications of ACC oxidase from white clover (Gong, 1999).

Fractions (8 to 11) from the Mono Q column containing ACC oxidase, as identified by antibody recognition using western analysis, were pooled, concentrated and then loaded onto the gel filtration column. Proteins were eluted with the same buffer, and subjected to SDS-PAGE and western analysis to identify fractions containing ACC oxidase (Figure 3.6). The most intense recognition fraction was eluted at fraction 21 which corresponded to an elution volume of 13.2-13.8 ml. Western analyses showed that this fraction cross-reacted with the anti-TR-ACO2 antibody as two major bands of proteins, one of greater mass of 34.7 kDa, while the second recognized band had a molecular mass of close to 34.7 kDa. In lanes 21 and 22, a band of less than 34.7 kDa was recognized.

3.4.6 SDS-PAGE Analysis of Partial Purified Isoform NIGI

The partially purified ACC oxidase protein after the three-column purification steps was assessed further using SDS-PAGE followed by Coomassie staining or western analysis using the anti-TR-ACO2 antibody (Figure 3.7). At this stage of the purification, *ca.* six major proteins ranging in molecular mass from 30.5 kDa to 55.5 kDa can be identified. Western analysis using the anti-TR-ACO2 antibody recognized a major protein that was large than 34.7 kDa and minor band of slightly larger molecular mass. The major protein recognized by the anti-TR-ACO2 antibody was transferred to PVDF membrane and submitted for N-terminal amino acid sequencing. However, no sequence was obtained, probably because the protein was blocked at the N-terminal (Dr. Carne, University of Otago, *pers. comm.*).

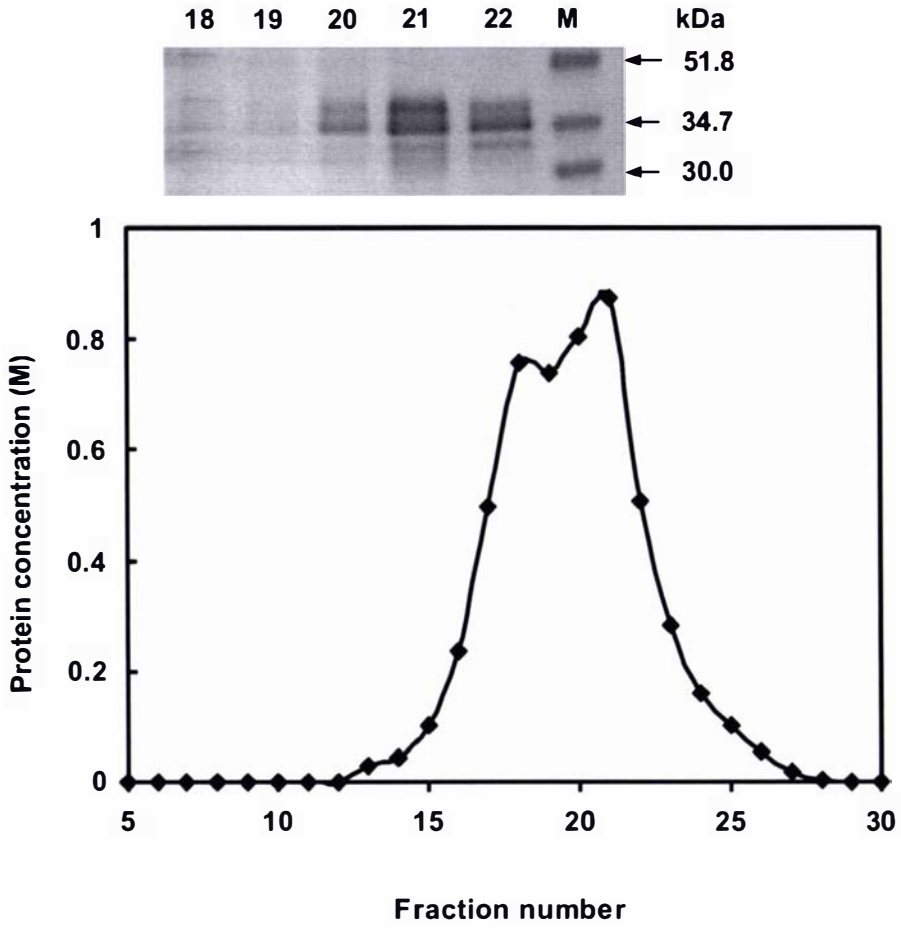

Figure 3.6 Separation of fractions 8 to 11 from the Mono Q column through a gel filtration column

The top panel represents western analysis of the fraction numbers indicated. Aliquots (2μg) from each fraction were separated using SDS-PAGE, transferred to PVDF membrane and challenged with anti-TR-ACO2 antibodies. Lane (M) are prestained molecular mass markers (molecular masses are indicated). The separation of fractions 1 to 4 is not shown.

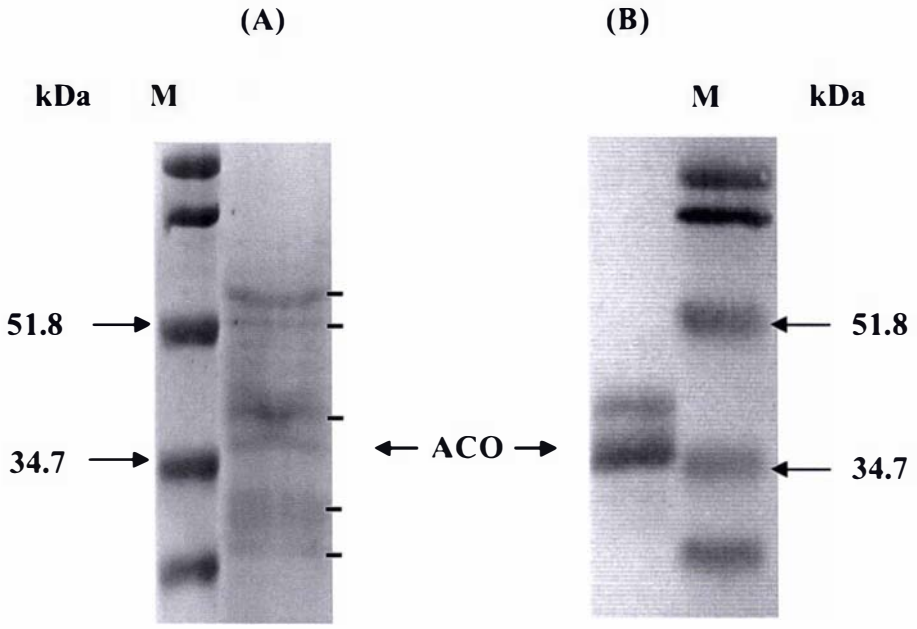

(A) Coomassie staining, (B) Western analysis

Figure 3.7 SDS-PAGE analysis of the partially purified NIGI isoform (fraction 21) obtained after separation through a gel filtration column

Aliquot 10 μg and 2 μg from fraction 21 were separated using SDS-PAGE, respectively. The Coomassie staining was used in A, the sample B was transferred to PVDF membrane and challenged with anti-TR-ACO2 antibodies. Lane (M) are prestained molecular mass markers (molecular masses of two of the standards are indicated).

3.4.7 Purification of ACC Oxidase Isoform NIGI Using Two-dimensional Electrophoresis

The partially purified NIGI protein (fraction 21 after gel filtration chromatography) was further separated in the first dimension depending on isoelectric point (pI) by isoelectric focusing (IEF) and in the second dimension according to molecular mass by SDS-PAGE. Several experiments were performed to optimize the IEF and SDS-PAGE conditions prior to separation of NIGI. In order to locate the ACC oxidase protein in the 2D-separations, duplicate samples were separated, one for protein staining and one for western analysis. Approximately 60-100 μg of protein was separated for silver staining or Coomassie Brillant Blue staining, and 15-40 μg of protein was separated for western analysis.

In these initial experiments, isoelectric focusing was performed in a series of linear immobilized pH gradients (IPGs) over a separation distance of 7 cm, including IPGs 3-10 and IPGs 4-7 and the use of 15% acrylamide in the second dimension.

In general, narrow IPGs are easier to use as pH gradients for 2D gel electrophoresis, when compared to wide gradients (ie pH 3-10) (data not shown). The resulting 2D pattern (Figure 3.8) shows the major protein spots between pH 4 and 6 (2.33 cm separation distance / pH unit). A single spot with molecular mass of approximately 36 kDa, with an estimated isoelectric point of 5.1 can be seen after silver staining, which is confirmed as an ACC oxidase using western analysis. Several other proteins can be visualized in the NIGI mixture, but these are mainly of lower molecular mass when compared with the putative ACC oxidase protein.

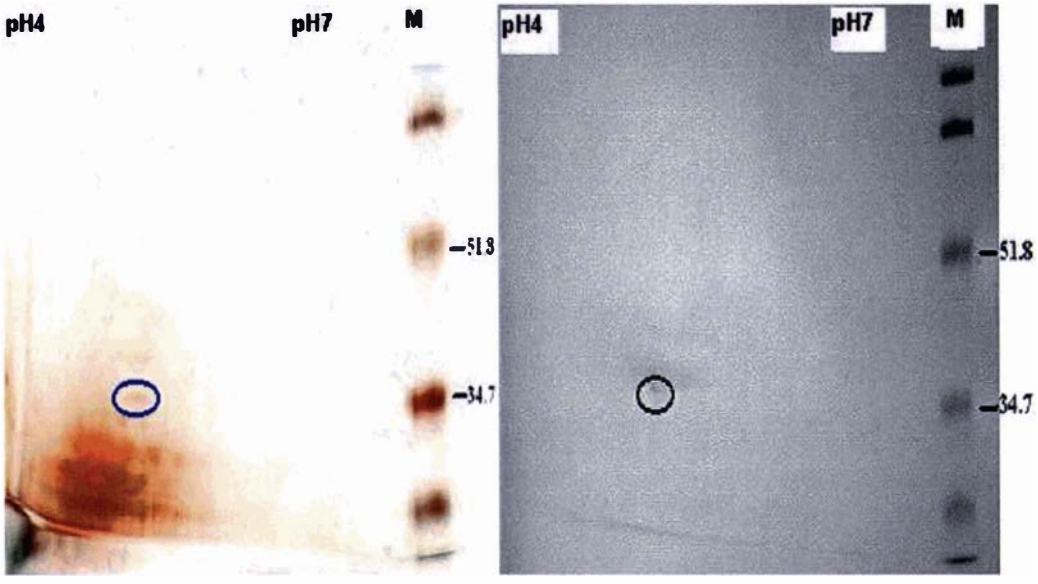

(A) (B)

Figure 3.8 Separation of fraction 21 (after gel filtration column chromatography) using Two-Dimensional electrophoresis

Separated proteins were detected by (A) silver staining, and (B) western analysis using the anti-TR-ACO2 antibody. Lane (M) are prestained molecular mass markers (molecular masses of two of the standards are indicated).

3.5 Purification of ACC Oxidase from Senescent Leaves Using FPLC

In parallel with the extraction of ACC oxidase from newly initiated green leaves of white clover, senescent leaves (nodes 12-15) were also extracted, and subjected to ammonium sulphate precipitation.

3.5.1 Sephadex G-25 Gel Filtration Chromatography of Crude Extracts from Senescent Leaves

After precipitation using ammonium sulphate, the protein suspension from the senescent leaf protein extract was chromatographed through a Sephadex G-25 gel filtration column and fractions that contained protein (fractions 6 to 20 in the example shown; Figure 3.9) were pooled and concentrated using Amicon Centriprep-10 tubes.

3.5.2 Hydrophobic Interaction Chromatography Using a Phenyl Sepharose Column

The concentrated protein extracts were then separated using the FPLC system. The first FPLC step, hydrophobic interaction chromatography, also produced the efficient and reproducible separation of the proteins from the senescent leaf protein extract (Gong, 1999). Western analysis with anti-TR-ACO2 antibodies recognized a major protein band of *ca.* 35 kDa in fractions 32 to 35 (Figure 3.10), designated SEI. However, in fractions 33 and 35, the anti-TR-ACO2 antibody again recognized two protein bands of 35 kDa and 37 kDa. The chromatograph in Figure 3.10 shows that a large amount of protein with no ACC oxidase eluted within a decreasing linear gradient of ammonium sulphate, while the ACC oxidase proteins eluted in later fractions with no ammonium sulphate in the buffer. This result also suggests a very strong surface hydrophobicity of the ACC oxidase protein in this extract.

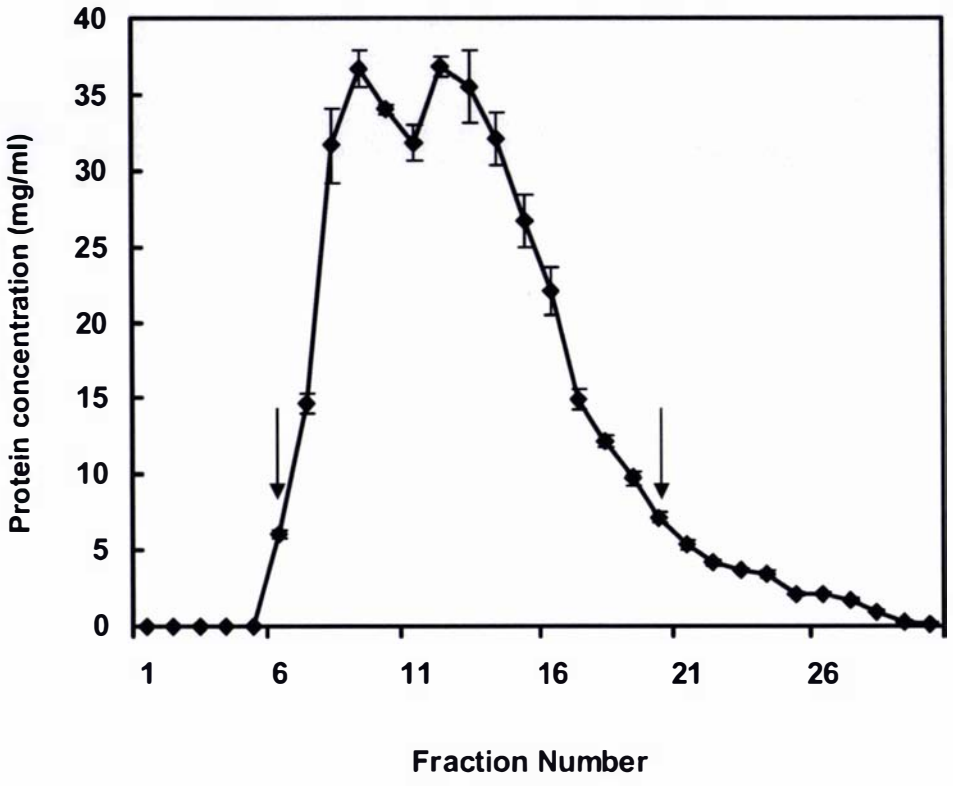

Figure 3.9 Protein elution profile from a Sephadex G-25 gel filtration column of a senescent leaf protein extract

The arrows indicate the range of fractions pooled for further purifications.

Results are mean values ± s.e., n=3

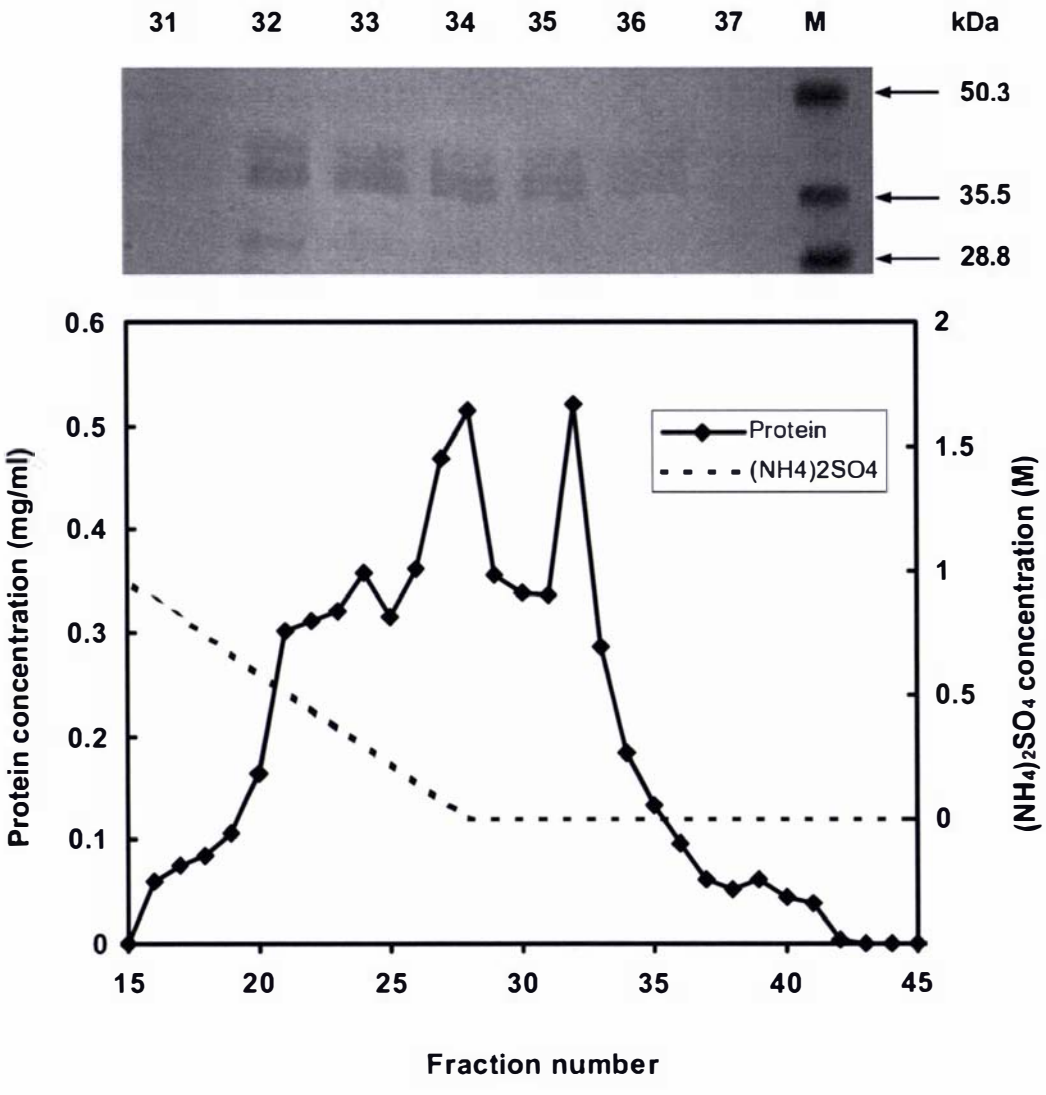

Figure 3.10 Separation of a senescent leaf protein extract, after ammonium sulphate precipitation and Sephadex G-25 column chromatography, through a Phenyl Superose Hydrophobic Interaction column

The top panel represents western analysis of the fraction numbers indicated. Aliquots (2μg) from each fraction were separated using SDS-PAGE, transferred to PVDF membrane and challenged with anti-TR-ACO2 antibodies. Lane (M) are prestained molecular mass markers (molecular masses are indicated). The separation of fractions 1 to 14 is not shown.

3.5.3 Anion Exchange Chromatography Using a Mono Q Column

Following hydrophobic interaction chromatography, the most intensely immuno-recognized fractions (fractions 32 to 35) were pooled and concentrated, and then loaded onto a Mono Q column (Figure 3.11). The result showed that the elution profile for ACC oxidase protein extract from senescent leaves using the same elution program as the extract from newly initiated green leaves is similar. The more intense antibody recognition was observed in fractions 10 to 12, and in these fractions, a major protein of *ca.* 35 kDa was recognized by the TR-ACO2 antibodies. Fractions with ACC oxidase recognition eluted at a sodium chloride concentration of 260 to 320 mM (fractions 10 to 12, Figure 3.11), suggesting that these isoforms carry a net negative charge at pH 7.5.

3.5.4 Gel Filtration Chromatography Using a Superose 12 Column

Gel filtration chromatography on a Superose 12 HR10/30 column was used as the final purification step for the senescent leaf extract ACC oxidase isoforms. Fractions (10 to 12), with higher intense antibody recognition after Mono Q column chromatography were concentrated and then loaded onto the pre-equilibrated gel filtration column. ACC oxidase protein eluted predominantly in fraction 22 from gel filtration column as determined by antibody recognition (Figure 3.12), and a single band of *ca.* 35 kDa was recognized most intensely by the anti-TR-ACO2 antibody.

3.5.5 Purification of ACC Oxidase Isoform SEI Using 2D Electrophoresis

The partial purified ACC oxidase protein preparation was further separated using 2D electrophoresis (Figure 3.13) using a linear IPG of 4-7 over a separation distance of 7 cm. The results revealed that at least a single spot was also visualized after silver staining and western analysis. The single spot had a calculated pI of *ca.* 5.2 and an apparent molecular mass of *ca.* 35 kDa. Again, a large number of lower molecular mass proteins were visualized after silver staining when compared with the putative ACC oxidase protein but none of these were recognized by the anti-TR-ACO2 antibody.

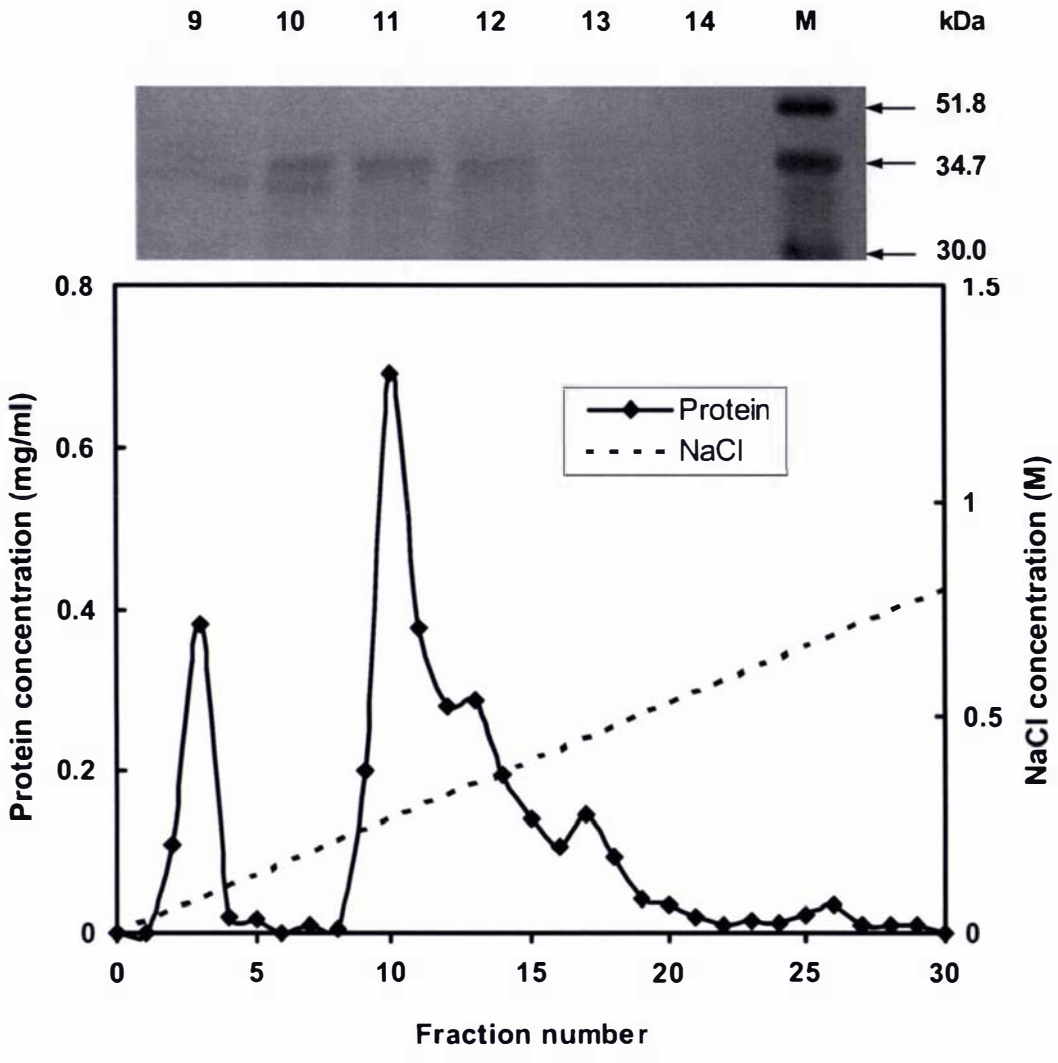

Figure 3.11 Separation of fractions 32 to 35 from the Phenyl Superose column through a Mono Q Anion Exchange column

The top panel represents western analysis of the fraction numbers indicated. Aliquots (2μg) from each fraction were separated using SDS-PAGE, transferred to PVDF membrane and challenged with anti-TR-ACO2 antibodies. Lane (M) are prestained molecular mass markers (molecular masses are indicated).

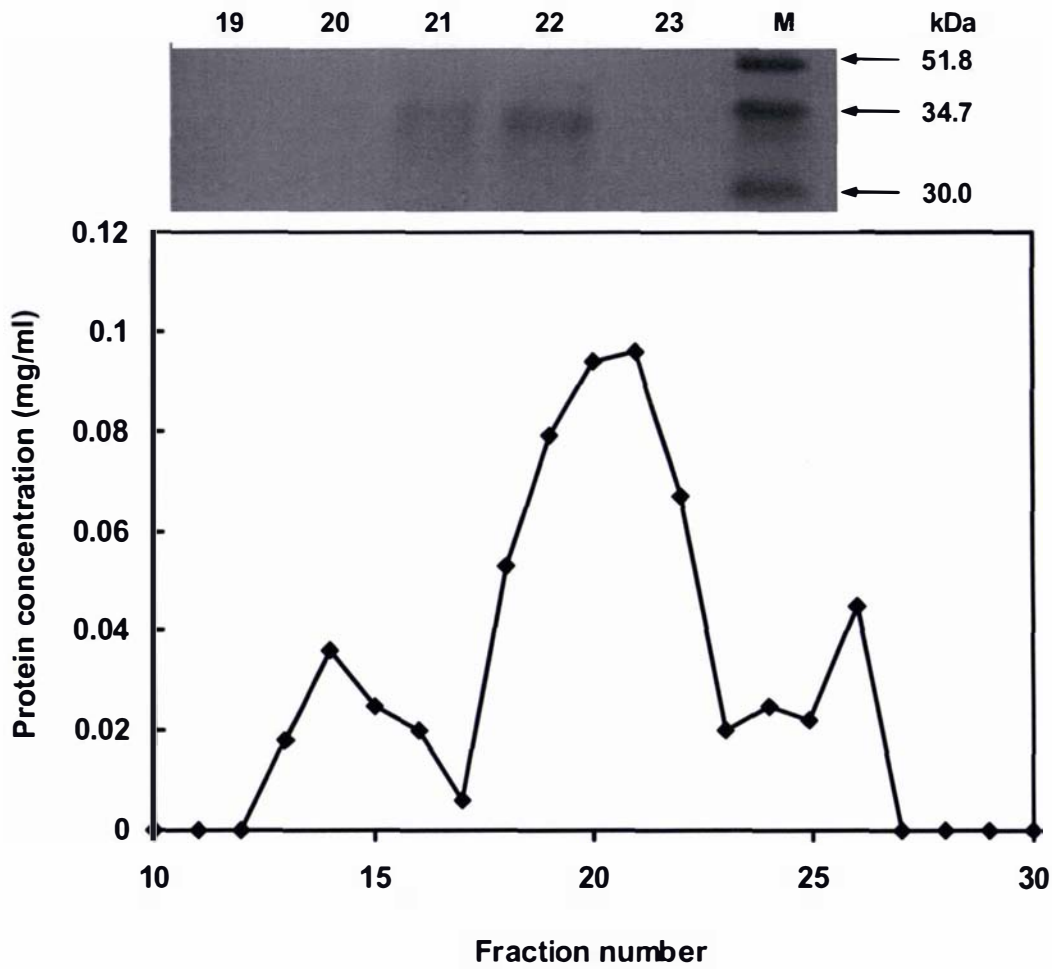

Figure 3.12 Separation of fractions 10 to 12 from the Mono Q column through a gel filtration column

The top panel represents western analysis of the fraction numbers indicated. Aliquots (2μg) from each fraction were separated using SDS-PAGE, transferred to PVDF membrane and challenged with anti-TR-ACO2 antibodies. Lane (M) are prestained molecular mass markers (molecular masses are indicated). The separation of fractions 1 to 9 is not shown.

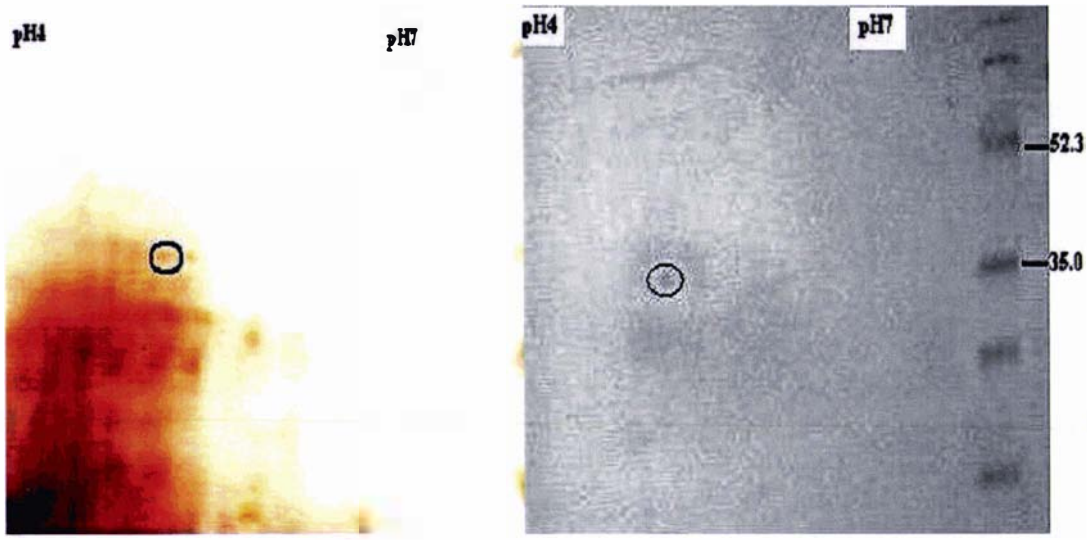

(A) **(B)**

Figure 3.13 Separation of fraction 22 (after gel filtration column chromatography) using Two-Dimensional electrophoresis

Separated proteins were detected by (A) silver staining, and (B) western analysis using the anti-TR-ACO2 antibody. Lane (M) are prestained molecular mass markers (molecular masses of two of the standards are indicated).

3.6 Matrix-Assisted Laser Desorption Ionization-Time of Flight (MALDI-TOF) Mass Spectrometric Analysis and Database Searching

In order to obtain more intensely stained protein spots for MALDI-TOF mass spectrometric analysis, more protein was loaded and isoelectric focusing was performed in linear IPGs of 4-7 over a separation distance of 18 cm (6 cm of separation distance/pH unit). Using this 2D gel electrophoresis system, approximately 600-800 μg of protein for silver staining or Coomassie Brillant Blue staining, and 40-80 μg of protein for western analysis was resolved.

For these separations, 2D gel electrophoresis was performed after purification of proteins using two FPLC columns (hydrophobic interaction chromatography and anion exchange column chromatography). To attempt to locate putative ACC oxidase protein spots, duplicate gels were run for all samples and one of the duplicate separations transferred to a PVDF membrane for western analysis with the anti-TR-ACO2 antibody.

For the putative protein NIGI, the 2D gel separations in Figure 3.14, Figure 3.15 and Figure 3.16 were identical runs which showed the position of protein spots with relatively close molecular masses but with different isoelectric points. Six protein spots, designated G1, G2, G3, G4, G5 and G6 were selected for identification, based on recognition by the anti-TR-ACO2 antibody. All of the separations had molecular masses of approximately 36 kDa to 38 kDa and isoelectric points ranging from pH 5.0 and 5.4. These were tentatively identified as isoforms of the putative ACC oxidase protein, NIGI, and the properties of each are summarized as Table 3.3.

Similar results were obtained from the partially purified ACC oxidase protein preparation from senescent leaves (Figure 3.17 and Figure 3.18). Spots, designated S1, S2, S3, S4 and S5, were all putative ACC oxidase proteins as determined by recognition by the anti-TR-ACO2 antibody with isoelectric points ranging from pI 5.0 to 5.5, and estimated molecular masses from 34 kDa to 35.5 kDa. Spot S6 was also selected because it always appeared a single high abundance protein in this gel position, although it was not recognized using western analysis. The properties of these protein spots are summarized as Table 3.3.

Table 3.3 Summary of the properties of selected protein spots used for MALDI-TOF mass spectrometric analysis

Sample	pI	Molecular Mass (kDa)	Figure Reference
G1	5.0	37.0	Figure 3.14
G2	5.1	36.5	Figure 3.14
G3	5.4	37.5	Figure 3.14
G4	5.1	37.0	Figure 3.15
G5	5.1	37.0	Figure 3.16
G6	5.4	38.0	Figure 3.16
S1	5.0	34.0	Figure 3.17
S2	5.2	35.5	Figure 3.17
S3	5.3	34.5	Figure 3.17
S4	5.2	35.0	Figure 3.18
S5	5.1	34.0	Figure 3.18
S6	5.7	24.5	Figure 3.18

All protein spots after silver staining or Coomassie Brilliant Blue staining were analyzed by MALDI-TOF analysis undertaken by the Australian Proteome Analysis Facility. For each protein, masses of 600 to 3500 mass units were obtained and the peak list obtained is included as Appendix I. Search parameter of mass tolerance was ± 1 Da (Moritz *et al.*, 1996)

For database searches, the obtained monoisotopic peptide masses were searched against the SWISS-PROT and TREMBL database with PeptIdent on Expasy. No matches were found with proteins in either database. However, when the obtained peptide masses were searched manually against the translated sequences deduced from *TR-ACO2* and *TR-ACO3* with MS-Digest (http://prospector.ucsf.edu/ucsfhtml4.0/ msdigest.htm), it was found that there are four spots that can be identified as ACC oxidase protein. The coverage of the predicted protein sequence by tryptic fragments ranged from 24.5% (for G4) to 37.6% (for G5) for the ACC oxidase protein isoform NIGI against the theoretical digest of TR-ACO2. Similarly, the coverage of the predicted protein sequence by tryptic fragments ranged from 13.4% (for S2) to 18.0% (for S4) for the ACC oxidase protein isoforms SEI from the senescent leaf extract against the theoretical digest of TR-ACO3. The data obtained from the MALDI-TOF mass spectrometric analysis is summarized as Table 3.4, and the peptide matches in TR-ACO2 and TR-ACO3 are shown as Figure 3.19. No significant peptide matches were obtained for G1, G2, G3, and G6, and S1, S3, and S5 (data not shown). It is interesting to note that for TR-ACO3, two N-terminal sequences (designated as TR-ACO3-1 and TR-ACO3-2 respectively) have now been identified (B. Chen, *pers. comm.*). There are only two different amino acid residues in the N-terminal at positions 4 and 22 between TR-ACO3-1 and TR-ACO3-2. However, as can be seen in the Figure 3.19, only TR-ACO3-1 was identified by MALDI-TOF mass spectrometric analysis.

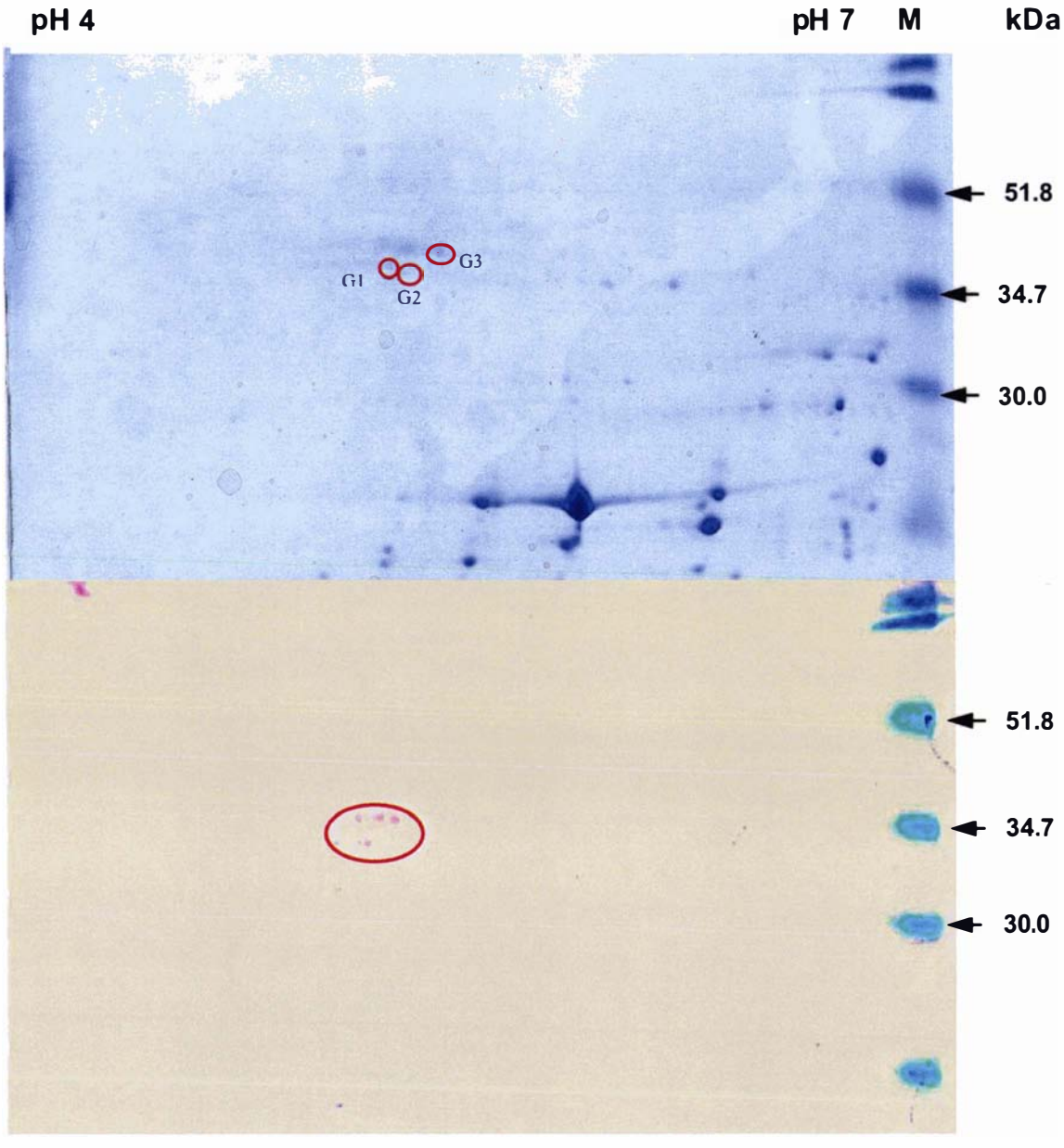

Figure 3.14 Separation I of NIGI (after Hydrophobic Interaction and Anion Exchange column chromatography) using Two-Dimensional electrophoresis

Separated proteins were detected by Coomassie staining (A) and Western analysis (B). Lane (M) are prestained molecular mass markers (molecular masses of three of the standards are indicated).

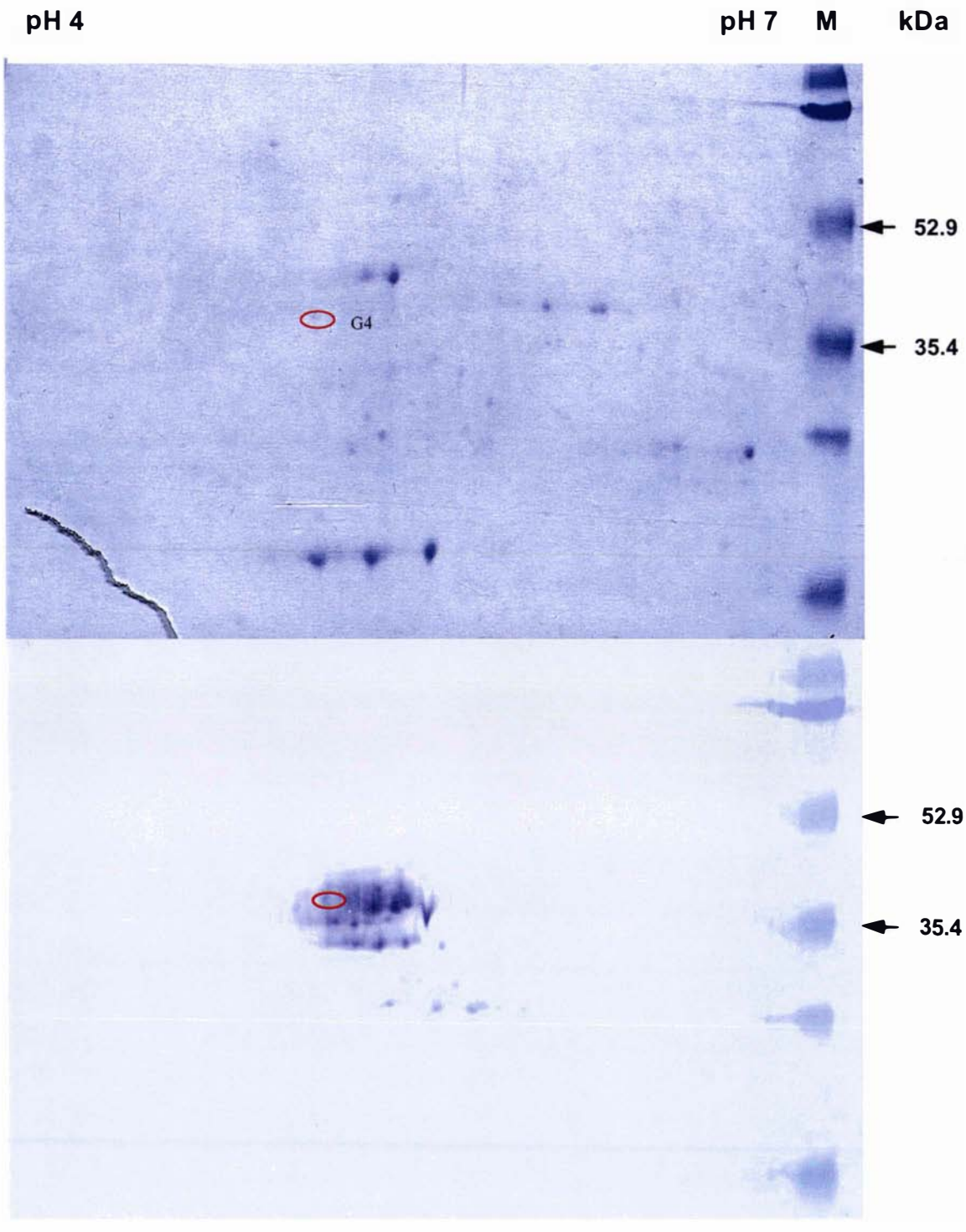

Figure 3.15 Separation II of NIGI (after Hydrophobic Interaction and Anion Exchange column chromatography) using Two-Dimensional electrophoresis

Separated proteins were detected by Coomassie staining (A) and Western analysis (B). Lane (M) are prestained molecular mass markers (molecular masses of two of the standards are indicated).

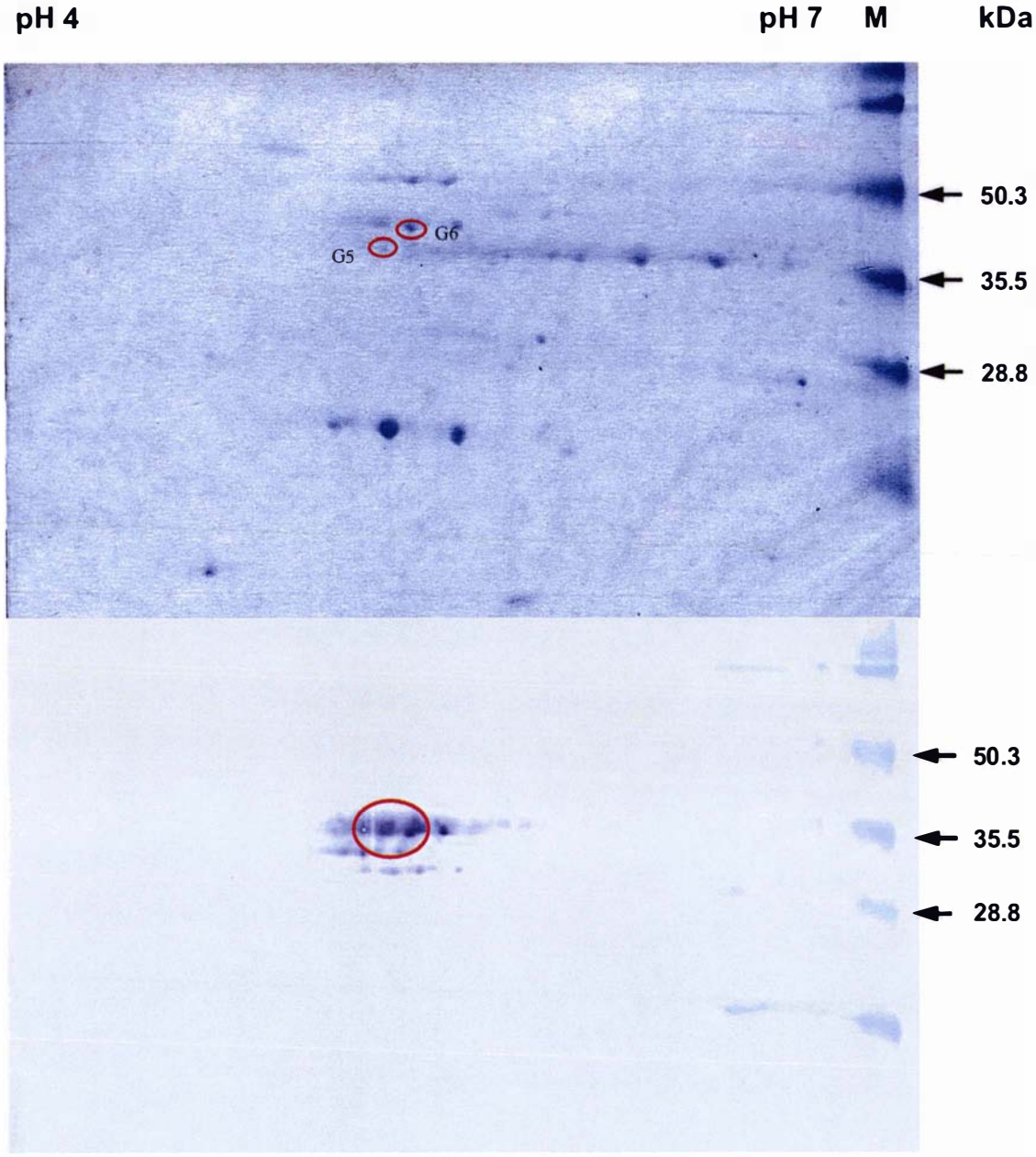

Figure 3.16 Separation III of NIGI (after Hydrophobic Interaction and Anion Exchange column chromatography) using Two-Dimensional electrophoresis

Separated proteins were detected by Coomassie staining (A) and Western analysis (B). Lane (M) are prestained molecular mass markers (molecular masses of three of the standards are indicated).

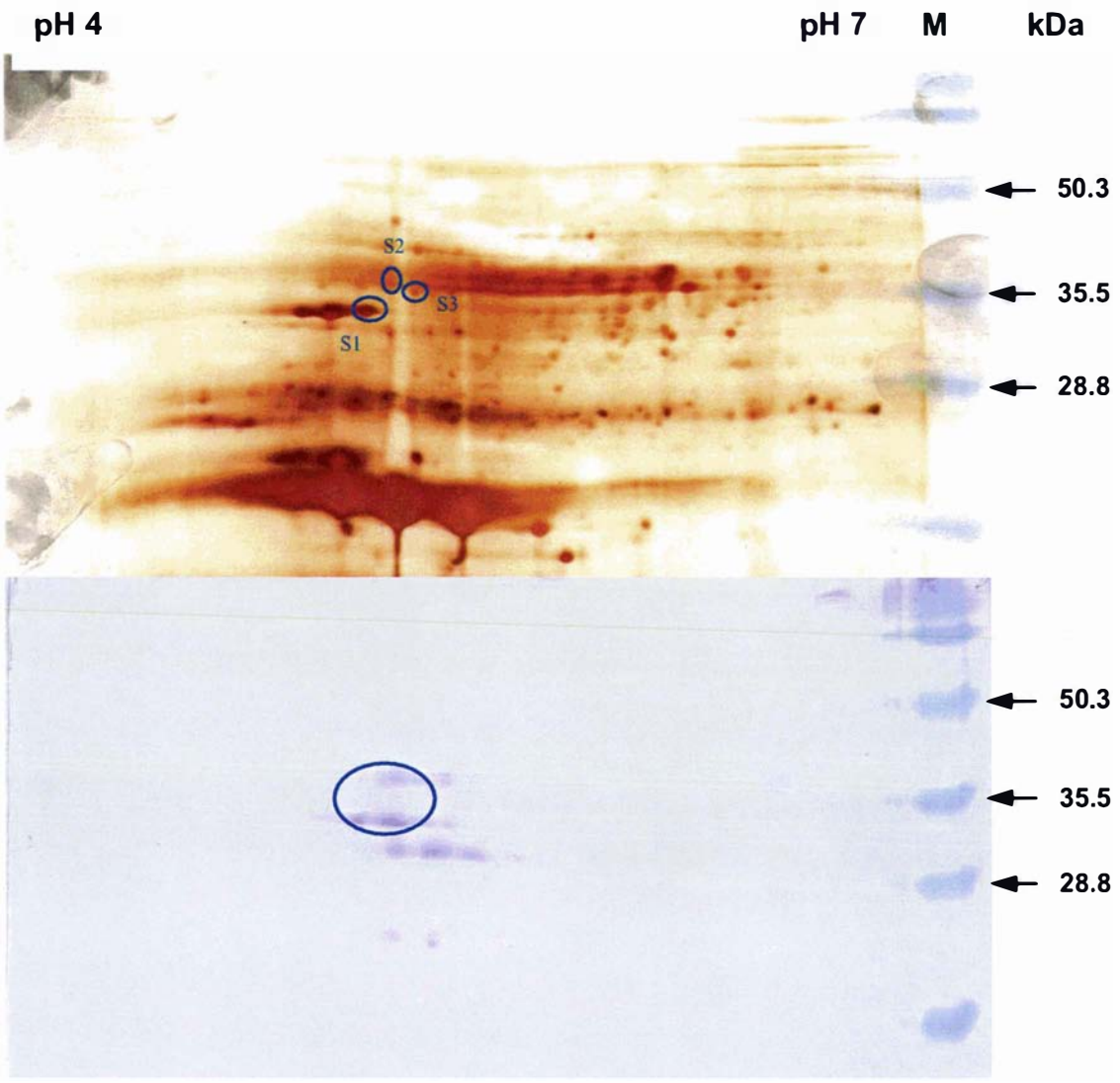

Figure 3.17 Separation I of SEI (after Hydrophobic Interaction and Anion Exchange column chromatography) using Two-Dimensional electrophoresis

Separated proteins were detected by Silver staining (A) and western analysis (B). Lane (M) are prestained molecular mass markers (molecular masses of three of the standards are indicated).

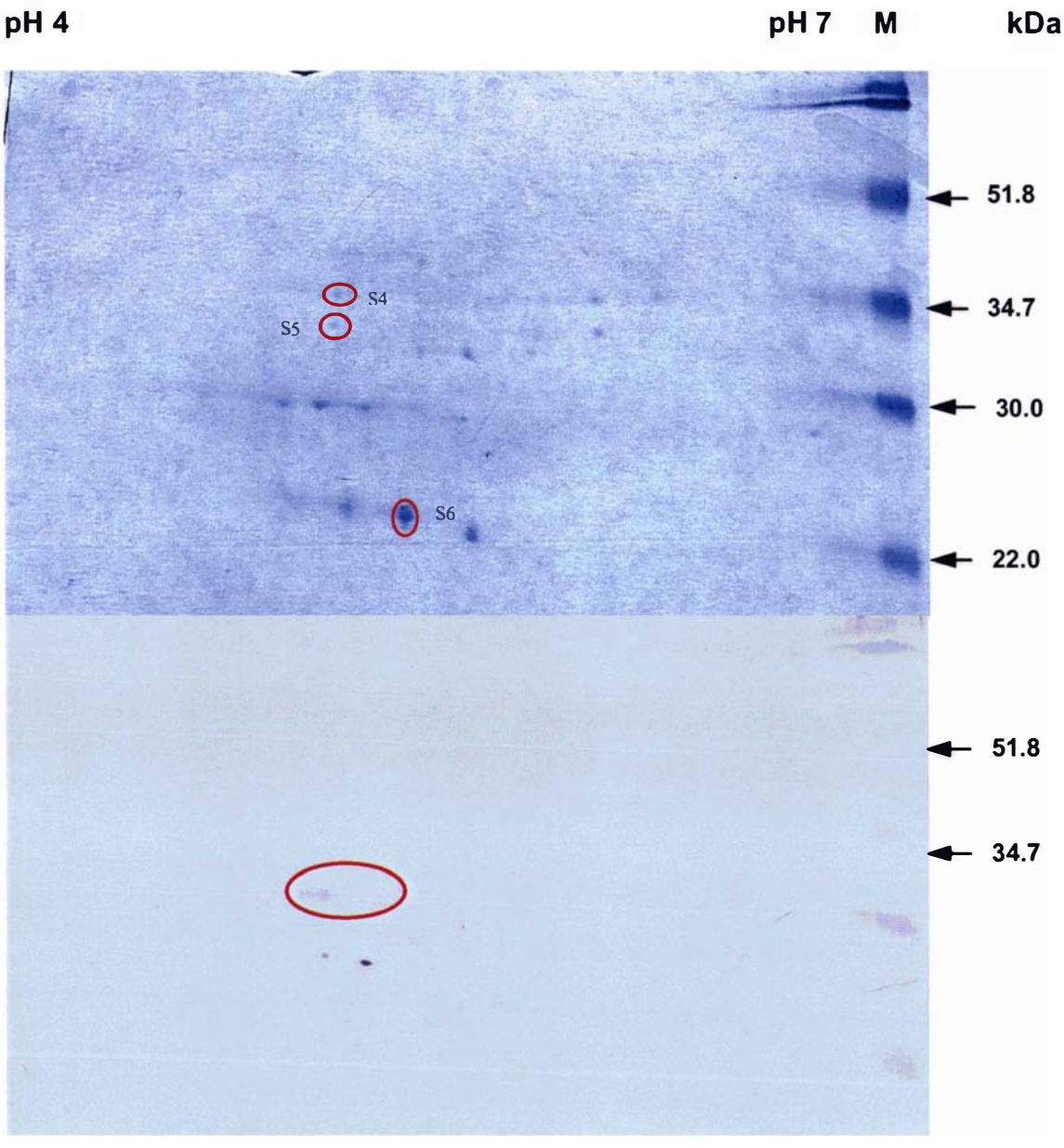

Figure 3.18 Separation II of SEI (after Hydrophobic Interaction and Anion Exchange column chromatography) using Two-Dimensional electrophoresis

Separated proteins were detected by Coomassie staining (A) and Western analysis (B). Lane (M) are prestained molecular mass markers (molecular masses of four of the standards are indicated).

Table 3.4 Identification of ACC oxidase proteins by MALDI-TOF mass spectrometry

Spot	Masses (M) of Fragments (Da)	Putative Protein	pI		Molecular Mass (kDa)		Coverage (%)*
			O**	T**	O**	T**	
G_4	1359.592 (1360.690); 1450.716 (1451.652); 1612.653 (1612.944); 1708.684 (1709.825); 2493.980 (2492.787)	(NIGI) (*T.repens*)	5.1	5.3	37.0	35.7	24.5
G_5	1436.635 (1436.627); 1450.656 (1451.652); 1553.676 (1554.799); 1714.875 (1714.928); 2073.932 (2072.297); 2241.118 (2242.099); 2448.139 (2448.899)	(NIGI) (*T.repens*)	5.1	5.3	37.0	35.7	37.6
S_2	993.6764 (993.2182); 1307.809 (1307.584); 1536.790 (1535.842); 1993.971 (1992.339)	(SEI) (*T.repens*)	5.2	5.5	35.5	35.2	13.4
S_4	857.5460 (857.1636); 864.3818 (864.4501); 877.1140 (876.0095); 1137.525 (1137.645); 1642.826 (1642.855)	(SEI) (*T.repens*)	5.2	5.5	35.0	35.2	18.0

Values in brackets are the theoretical masses for matched trypic fragments.
*Percentage coverage of the whole protein sequence from the peptides identified.
** O, observed; T, theoretical (by MS-Digest from *TR-ACO2* or *TR-ACO3*)

```
TR-ACO2      (1) MENFPIINLENLNGEERKATMEKIKDACENWGFFELVNHGISHDLMDTVE
TR-ACO3-1    (1) MMNSPIISLERLNGVERKDTMEKIKDACQNWGFFELVNHGIPHDLMDTLE

TR-ACO2     (51) RLTKEHYRICMEQRFKDLVANKGLEAVQTEVKDMDWESTFHLRHLPESNI
TR-ACO3-1   (51) RLTKEHYRKCMEQRFKELVSSKGLDAVQTEVKDMDWESTFHVRHLPESNI

TR-ACO2    (101) SEVPDLTDEYRKAMKEFALKLEKLAEELLDLLCENLGLEKGYLKKAFYGS
TR-ACO3-1  (101) SELPDLSDEYRKVMKEFSLRLEKLAEELLDLLCENLGLEKGYLKKAFYGS

TR-ACO2    (151) KGPTFGTKVANYPPCPKPDLVKGLRAHTDAGGIILLFQDDKVSGLQLLKD
TR-ACO3-1  (151) RGPTFGTKVANYPQCPNPELVKGLRAHTDAGGIILLFQDDKVSGLQLLKD

TR-ACO2    (201) GKWVDVPPMHHSIVINLGDQLEVITNGKYKSVEHRVIAQSDGTRMSIASF
TR-ACO3-1  (201) DEWIDVPPMRHSIVVNLGDQLEVITNGKYKSVEHRVIAQTNGTRMSIASF

TR-ACO2    (251) YNPGSDAVIYPATTLIE----ENNEVYPKFVFEDYMNLYAGLKFQAKEPR
TR-ACO3-1  (251) YNPGSDAVIYPAPELLEKETEEKTNVYPKFVFEEYMKIYAALKFQAKEPR

TR-ACO2    (297) FEAFKESSNVKLGPIATV
TR-ACO3-1  (301) FEALKA------------


TR-ACO3-2    (1) MMNFPIISLERLNGVERKDTMAKIKDACQNWGFFELVNHGIPHDL (45)
```

Figure 3.19 Peptide matching results for TR-ACO2 and TR-ACO3 sequences from white clover by MALDI-TOF mass spectrometry

The matched fragments are highlighted in grey, and represent a combination of G4 and G5 for the TR-ACO2, and S2 and S4 for TR-ACO3.

3.7 Investigation of the Rhythm of ACC Oxidase Activity from Mature Green Leaf Tissue of White Clover

Previous preliminary observations have suggested that *TR-ACO2* may be under circadian control (Hunter, 1998). Diurnal changes in plant responses (whether anatomical, physiological, biochemical or molecular) describe those that occur daily or over a day/night cycle. When the observed behavior is inherent and independent of external periodicity then it is described as a circadian rhythm. In order to determine whether *TR-ACO2* expression is under a circadian or diurnal rhythm, circadian changes in transcript levels of *TR-ACO2* gene, and changes of ACC oxidase activity *in vitro* and ACC oxidase protein accumulation were examined.

ACC oxidase activity was measured in extracts of mature green leaves (section 2.3.6), harvested every three h over a 24 h time period, and activity varied over the 24 h time period during a short day (the leaf tissues were harvested in May 2002) (Figure 3.20). Two ACC oxidase activity peaks were observed. The first maximum of activity was at 12:00 am and the minimum activity was recorded at 9:00 pm, while the second period of maximum activity occurred at 12:00 pm. In parallel, the top panel of Figure 3.20 is an immunodetection assay using the anti-TR-ACO2 antibody, and shows that the ACC oxidase protein accumulation was highest at noon (12:00 am) and midnight and lowest at 9:00 pm. A similar result was observed when ACC oxidase activity is calculated as specific activity (Figure 3.21). These results suggest that ACC oxidase extracted from mature green leaves shows a circadian-type rhythm in terms of enzyme activity and protein accumulation.

ACC oxidase activity and ACC oxidase protein accumulation was also measured in mature green leaf extracts during a long day (December 2002) (Figure 3.22). ACC oxidase activity was highest at 12:00 am and lower between 6:00-9:00 pm, and high again at midnight (12:00 pm). Calculation of ACC oxidase as specific activity assay also showed the same pattern of activity (Figure 3.23). The top panel of Figure 3.22 represents an immunodetection assay using the anti-TR-ACO2 antibody, and shows that ACC oxidase protein accumulation was highest at midnight and lowest at 3:00-9:00 pm. However, there is no significant difference between noon (12:00 am) and 9:00 pm, but there was also high accumulation of TR-ACO2 at 9:00 am.

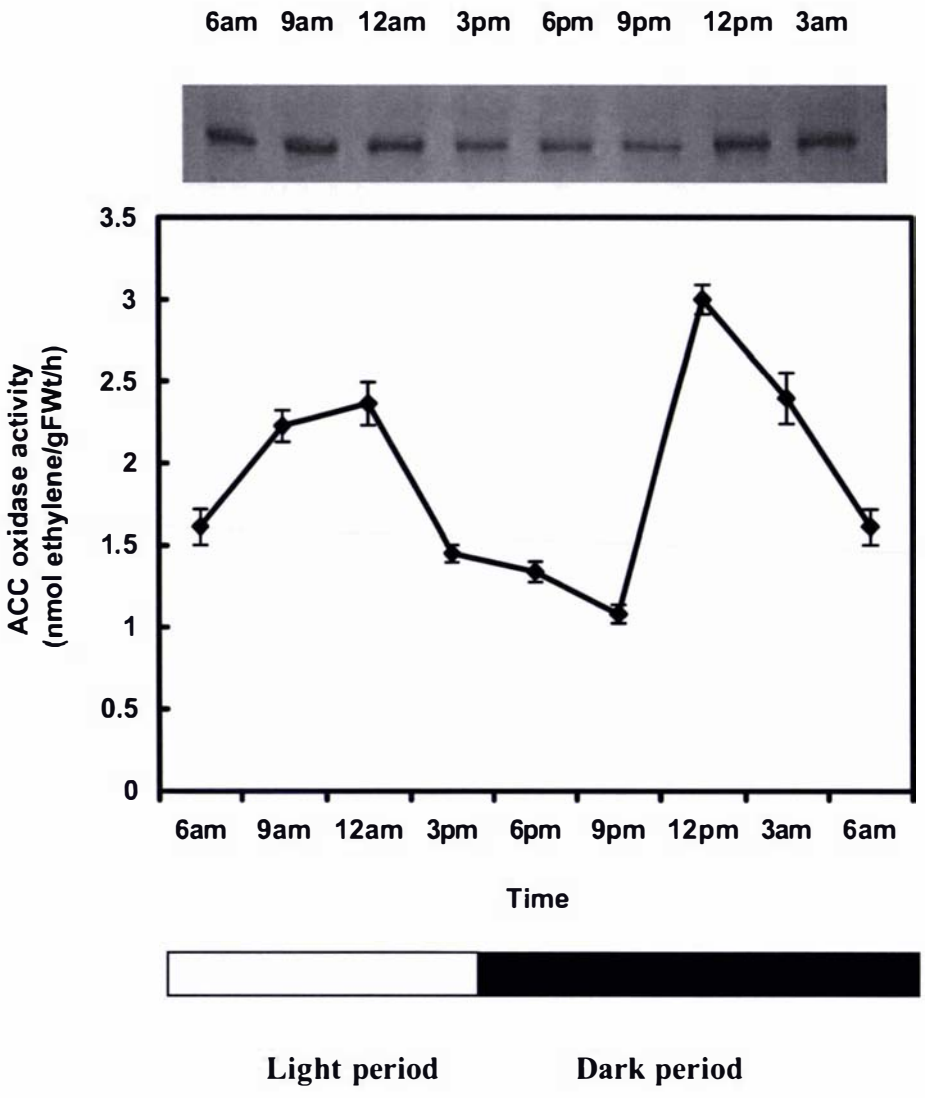

Figure 3.20 Changes in ACC oxidase activity measured *in vitro* over a 24 hour period in green leaf tissue extracts harvested at the time points indicated during the short day

Values are means ± s.e., n=3

The top panel represents western analysis of extracts at the time points indicated. Aliquots (30 μg) of extracts from each time point were separated using SDS-PAGE, transferred to PVDF membrane and challenged with anti-TR-ACO2 antibodies.

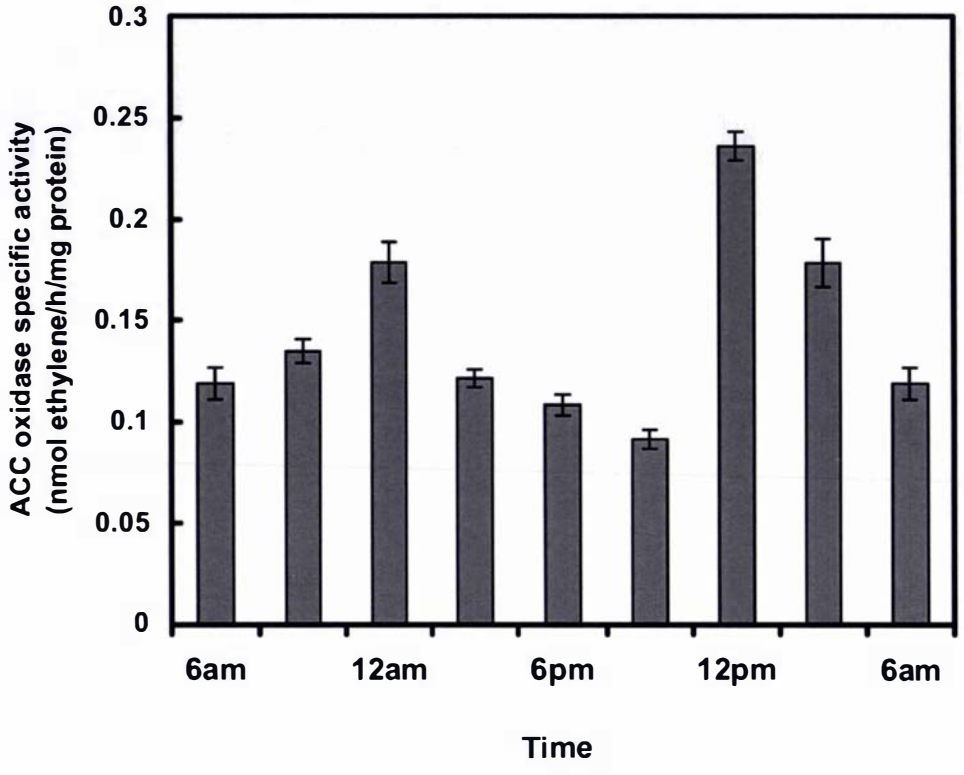

Figure 3.21 Changes in ACC oxidase specific activity measured *in vitro* over a 24 hour period in green leaf tissue extracts harvested at the time points indicated during the short day

Results are mean values ± s.e., n=3

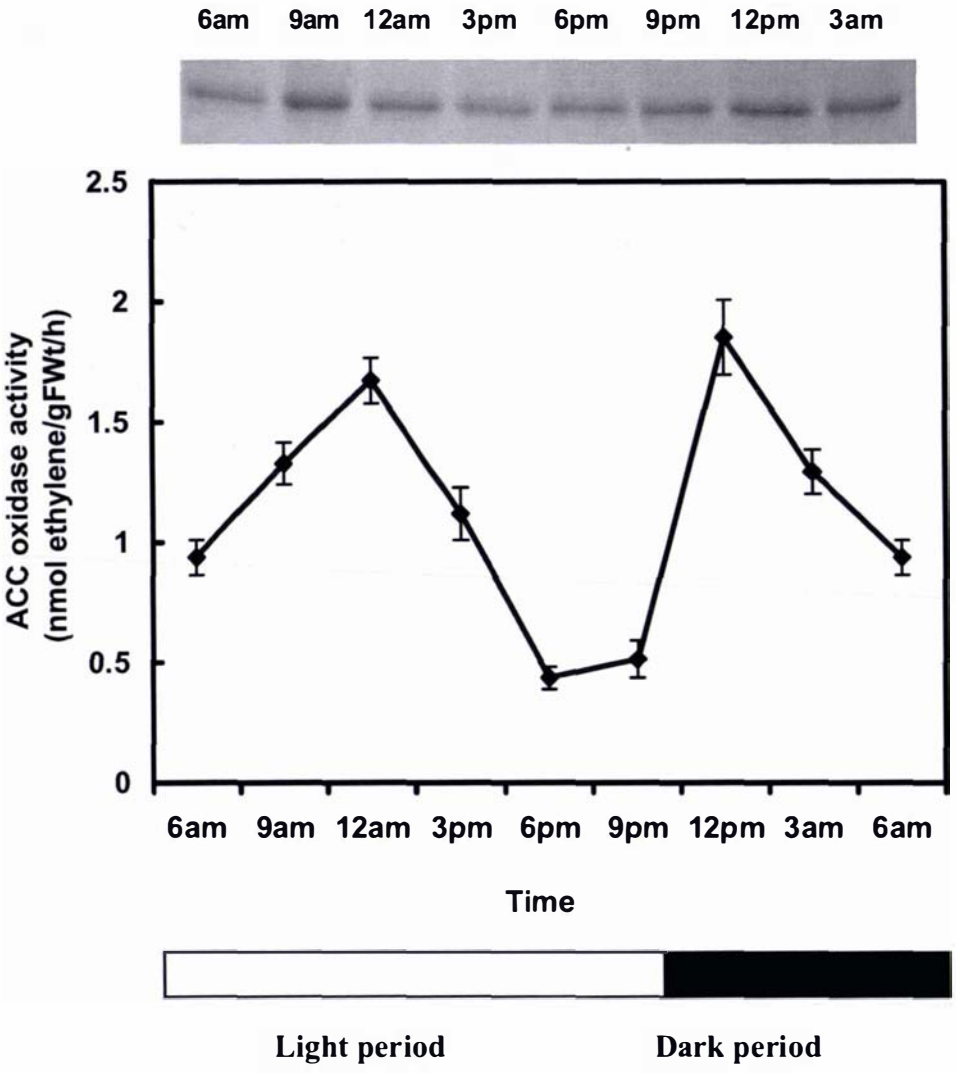

Figure 3.22 Changes in ACC oxidase activity measured *in vitro* over a 24 hour period in green leaf tissue extracts harvested at the time points indicated during the long day

Values are means ± s.e., n=3

The top panel represents western analysis of extracts at the time points indicated. Aliquots (30 μg) of extracts from each time point were separated using SDS-PAGE, transferred to PVDF membrane and challenged with anti-TR-ACO2 antibodies.

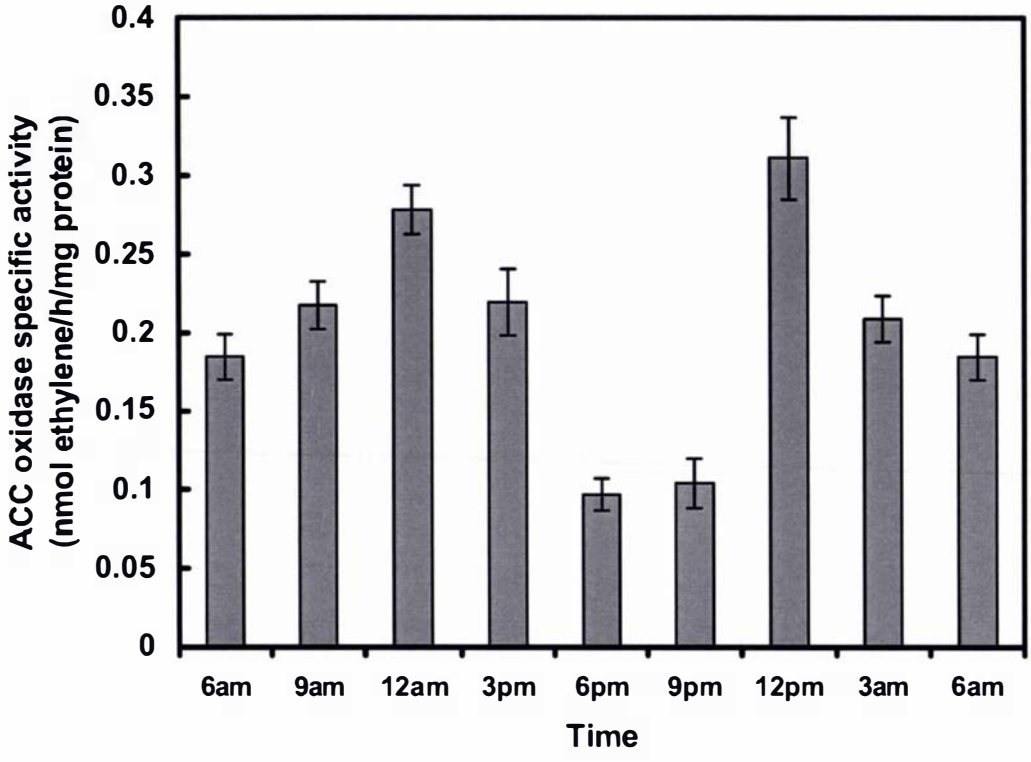

Figure 3.23 Changes in ACC oxidase specific activity measured *in vitro* over a 24 hour period in green leaf tissue extracts harvested at the time points indicated during the long day

Results are mean values ± s.e., n=3

To examine whether these observed changes in activity were also reflected in changes in the transcript level of the *TR-ACO2* gene, northern blot analysis was performed using mRNA isolated from mature green leaves harvested at three time points (12:00 am, 9:00 pm and 12:00 pm) during long day conditions.

The purity and yield of the total RNA in each extract was assessed by spectrophotometry (Table 3.5). All the samples had an A_{260}/A_{280} ratio of 1.85 indicating that RNA in the samples may still have been contaminated with other cellular constituents, and may affect the estimates of yield.

Table 3.5 Spectrophotometric assessments of purity and yield in RNA preparations

Time Point	Ratio (A_{260}/A_{280})	Total RNA Yield (µg/g)	Ratio (A_{260}/A_{280})	mRNA Yield (µg/g)
12:00 am	1.854	204.7	2.355	4.19
9:00 pm	1.825	204.9	2.340	5.06
12:00 pm	1.888	105.8	2.315	4.80

A poly $(A)^+$mRNA extraction procedure was used to purify mRNA from the total RNA extracts (section 2.4.3.2). The purity and yield of mRNA in each extract is shown in Table 3.5. These ratios of A_{260}/A_{280} readings indicate that all the samples contained relatively pure mRNA and aliquots containing 2 µg of mRNA was used for northern analysis.

A single RNA transcript of *ca.* 1.35 kb was detected in all samples (Figure 3.24). The level of this transcript was comparatively high in RNA isolated from leaves harvested at 12:00 pm, but lower in RNA isolated from tissue harvested at 12:00 am and 9:00 pm. Thus the expression pattern of *TR-ACO2* does match the ACC oxidase protein accumulation and the ACC oxidase activity measured at both 9:00 pm and 12:00 pm. However, the level of transcript appeared to be approximately the same in RNA isolated from leaf tissue harvested at 12:00 am and 9:00 pm.

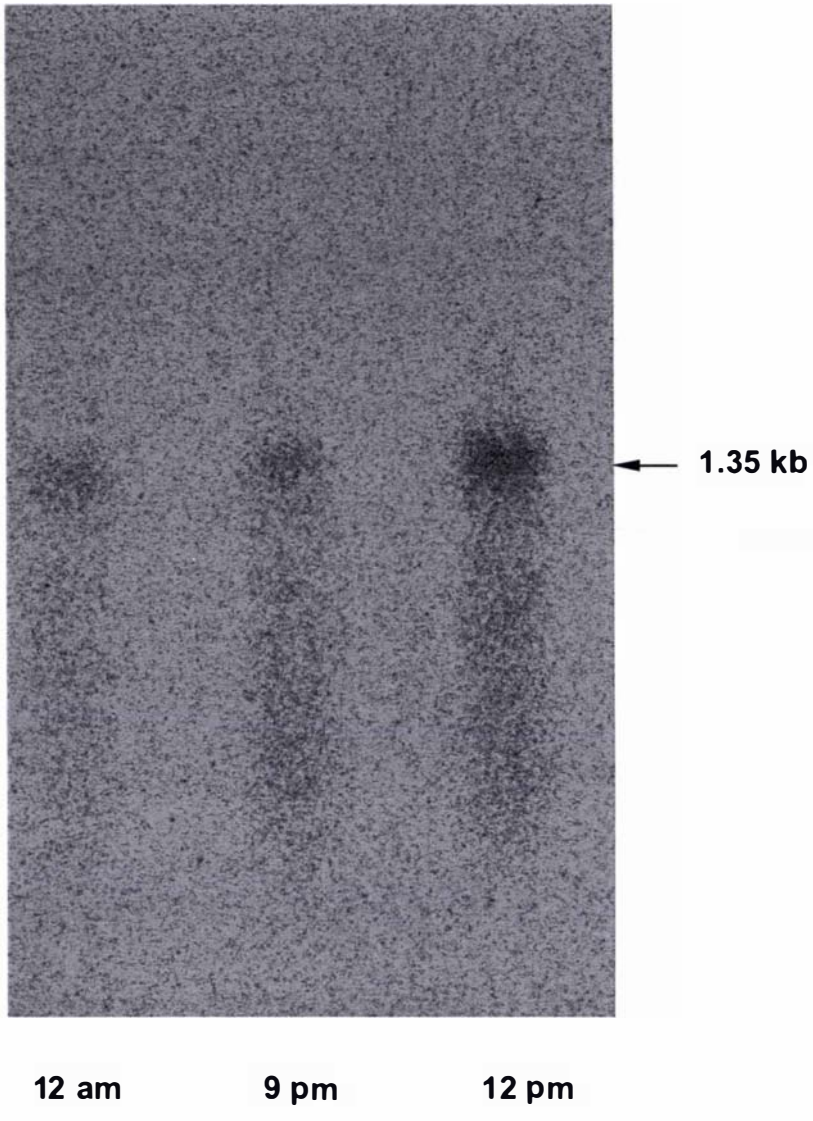

Figure 3.24 Northern analysis of *TR-ACO2* gene expression in mRNA isolated from mature green leaves of white clover at the times indicated

Northern blots were probed with the [α-^{32} P] -dATP labelled 3'-UTR of *TR-ACO2*. The size of the transcript is indicated to the right of the figure in kb.

3.8 Regulation of ACC Oxidase Activity from White Clover between Phosphorylation and Dephosphorylation

The preceding section has shown that at the translation level at least, ACC oxidase activity may be under a circadian control. Because phosphorylation and dephosphorylation of proteins often serves as a regulator of activity during diurnal and circadian rhythm in higher plants (Luan, 2003; Yang, *et al.*, 2002; Sugano, *et al.*, 1998; Naidoo, *et al.*, 1999), this section of the thesis focuses on the influence of phosphorylation and dephosphorylation *in vitro* on ACC oxidase enzyme activity.

Before experimental data on the effect of phosphorylation/dephosphorylation on enzyme activity was obtained, the TR-ACO2 and TR-ACO3 sequences were submitted to the NetPhos 2.0 predication server at the Centre for Biological Sequence Analysis (http://www.cbs.dtu.dk/services/NetPhos/; Blom *et al.*, 1999) to predict the occurrence of putative phosphorylation sites. NetPhos evaluates all Ser, Thr, and Tyr residues and their surrounding amino acid residues, and reports a score reflecting the likelihood of phosphorylation at that residue (Figure 3.25B and C). This comparison gives possible phosphorylation sites in TR-ACO2 and TR-ACO3 as scores above 0.8. The data are summarized as Table 3.6 with scores close to the maximum score of 1.0 suggesting that both TR-ACO2 and TR-ACO3 have a high likelihood of containing specific residues that are phosphorylated. After this database assessment, experiments were performed, utilizing changes in enzyme activity over a 24 h period, to investigate the role of phosphorylation/dephosphorylation in regulating this activity.

Initial attempts at measuring ACC oxidase activity in a crude tissue homogenate in HEPES buffers for both extraction and incubation procedures proved unsatisfactory because the activity levels were very low. However, activity could be measured after passage of the crude tissue homogenate through Sephadex G-25 column, and the results broadly indicated that the activity of dephosphorylated ACC oxidase was a little higher than the phosphorylated form of the enzyme although this difference was not significant statistically (Figure 3.26).

However, to compare changes of ACC oxidase activity in response to phosphorylation and dephosphorylation more accurately, higher activity levels were required. A series of experiments were designed to characterize aspects of the extraction and incubation

```
TR-ACO2     (1) MENFPIINLENLNGEERKATMEKIKDACENWGFFELVNHGISHDLMDTVE
TR-ACO3     (1) MMNSPIISLERLNGVERKDTMEKIKDACQNWGFFELVNHGIPHDLMDTLE

TR-ACO2    (51) RLTKEHYRICMEQRFKDLVANKGLEAVQTEVKDMDWESTFHLRHLPESNI
TR-ACO3    (51) RLTKEHYRKCMEQRFKELVSSKGLDAVQTEVKDMDWESTFHVRHLPESNI

TR-ACO2   (101) SEVPDLTDEYRKAMKEFALKLEKLAEELLDLLCENLGLEKGYLKKAFYGS
TR-ACO3   (101) SELPDLSDEYRKVMKEFSLRLEKLAEELLDLLCENLGLEKGYLKKAFYGS

TR-ACO2   (151) KGPTFGTKVANYPPCPKPDLVKGLRAHTDAGGIILLFQDDKVSGLQLLKD
TR-ACO3   (151) RGPTFGTKVANYPQCPNPELVKGLRAHTDAGGIILLFQDDKVSGLQLLKD

TR-ACO2   (201) GKWVDVPPMHHSIVINLGDQLEVITNGKYKSVEHRVIAQSDGTRMSIASF
TR-ACO3   (201) DEWIDVPPMRHSIVVNLGDQLEVITNGKYKSVEHRVIAQTNGTRMSIASF

TR-ACO2   (251) YNPGSDAVIYPATTLIE----ENNEVYPKFVFEDYMNLYAGLKFQAKEPR
TR-ACO3   (251) YNPGSDAVIYPAPELLEKETEEKTNVYPKFVFEEYMKIYAALKFQAKEPR

TR-ACO2   (297) FEAFKESSNVKLGPIATV
TR-ACO3   (301) FEALKA------------
```

(A)

(B)

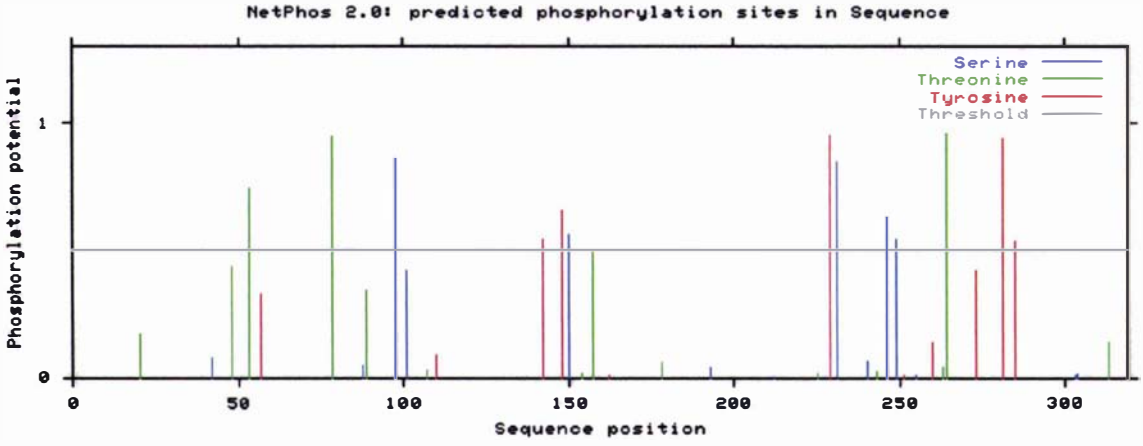

(C)

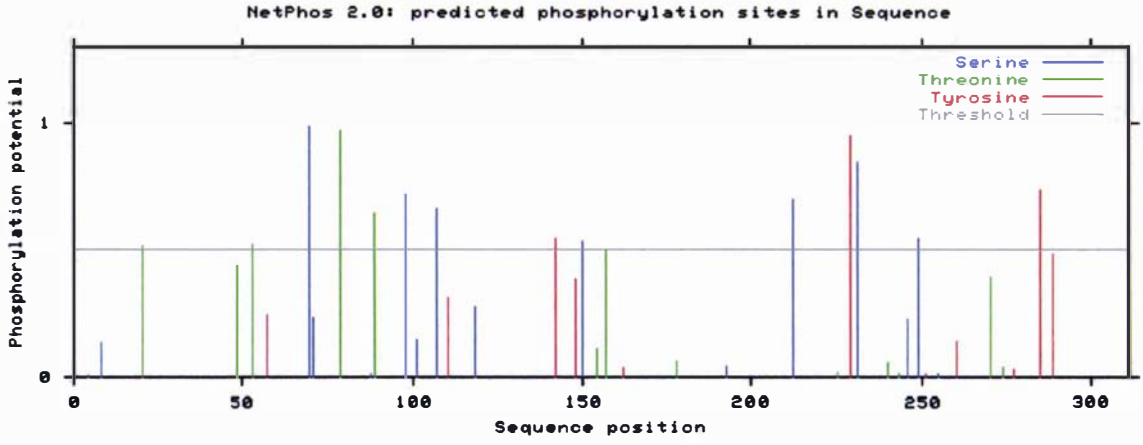

Figure 3.25 Comparison of putative phosphorylation sites in TR-ACO2 with TR-ACO3 as determined by the NetPhos 2.0 programme

The residues indicated have a score of grade than 0.8 (A). Scores of all Ser, Thr or Tyr residues in the TR-ACO2 sequence (B) and TR-ACO3 sequence (C).

Table 3.6 Summary of high-scoring phosphorylation sites predicted for serine, threonine, and tyrosine residues in TR-ACO2 and TR-ACO3

Name of Amino Acid	Position		Score	
	TRACO2	TRACO3	TRACO2	TRACO3
Serine	-	70	-	0.990
	98	-	0.856	-
	231	231	0.845	0.845
Threonine	79	79	0.947	0.970
	264	-	0.955	-
Tyrosine	229	229	0.950	0.950
	281	-	0.941	-

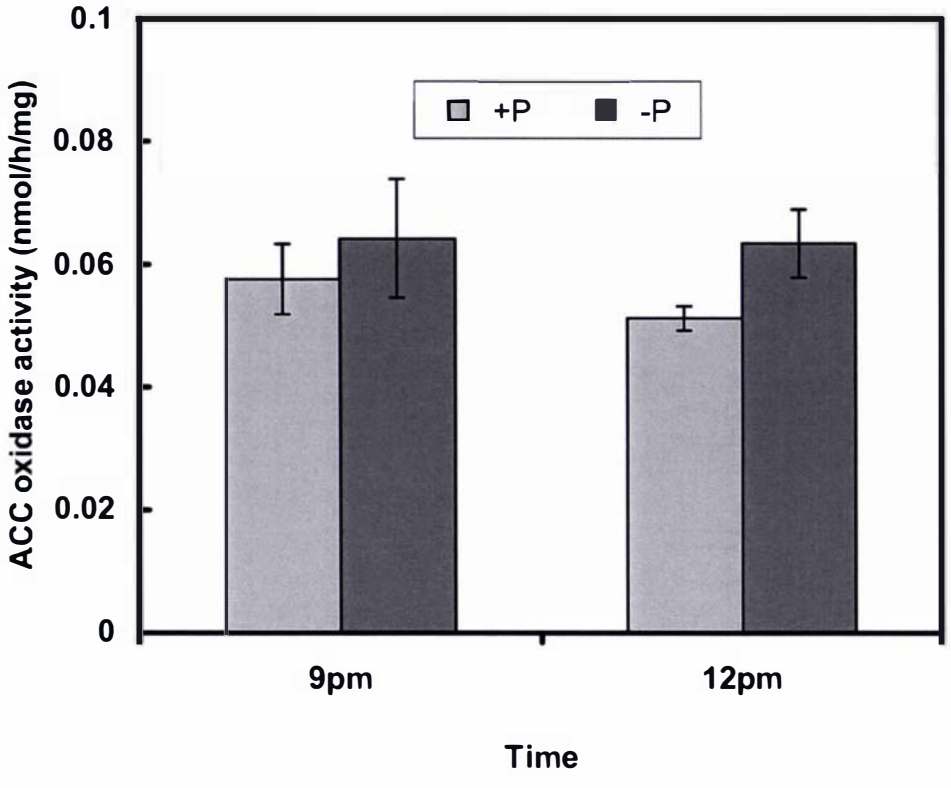

Figure 3.26 Comparison of ACC oxidase activity in extracts harvested at the time shown and subjected to phosphorylation or dephosphorylation treatments using a HEPES buffer system

Results are mean values ± s.e., n=3

systems used for both phosphorylation and dephosphorylation prior to measurement of enzyme activity. This was useful in terms of optimizing activity, and identifying factors important for the activity assay that may need to be tightly controlled in order to obtain reproducible results. The composition of the extraction and incubation buffers was tested in terms of recovering maximal enzyme activity. As shown in Figure 3.27, the ACC oxidase activity using the Tris buffer system resulted in much higher activity when compared with the HEPES buffer system.

In order to determine if the incubation temperature directly affected ACC oxidase activity, and whether each component of the extraction and incubation medium also influenced activity, each component was added separately to the standard (control) incubation buffer system (50 mM Tris-HCl, pH7.5, containing 10% (v/v) glycerol, 30 mM sodium ascorbate and 2 mM DTT) (Figure 3.28). No significant difference in activity was found in the presence of OKA, Mg^{2+}, ATP, and Mn^{2+} when compared with the control assay. In terms of the effect of the incubation temperature at 30°C, the activity of the enzyme was reduced by less than 10%, except when Mn^{2+} was present where a decrease of 20% was observed when compared with the extraction temperature at 4°C.

Together these results provide the composition of the extraction and incubation buffer for both phosphorylation and dephosphorylation treatments to give maximum recoverable activity of ACC oxidase.

To determine how phosphorylation and dephosphorylation affects ACC oxidase activity, mature green leaves of white clover were extracted using the appropriate extraction buffer, the homogenate centrifuged, the supernatant proteins precipitated with ammonium sulphate, and the resulting pellets were dissolved in elution buffer and then desalted with PD 10 columns that were pre-equilibrated with elution buffer. For phosphorylation of ACC oxidase, the protein sample was incubated in an incubation buffer (including OKA) for 15 min at 30°C. For dephosphorylation of ACC oxidase, the protein sample was incubated at 30°C with 2 units of purified PP2A. Following incubation, the reaction was stopped by the addition of OKA, and ACC oxidase activity determined, as well as enzyme abundance using western analysis.

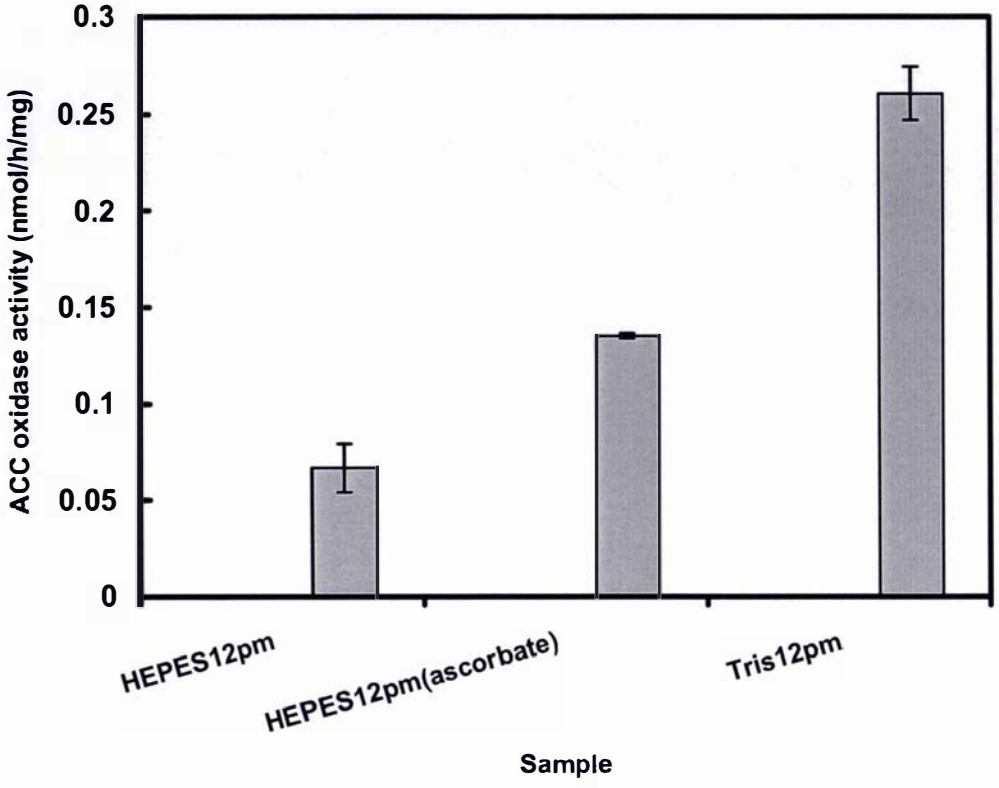

Figure 3.27 Comparison of ACC oxidase activity in extracts harvested at the time indicated using a HEPES or a Tris buffer system

Results are mean values ± s.e., n=3

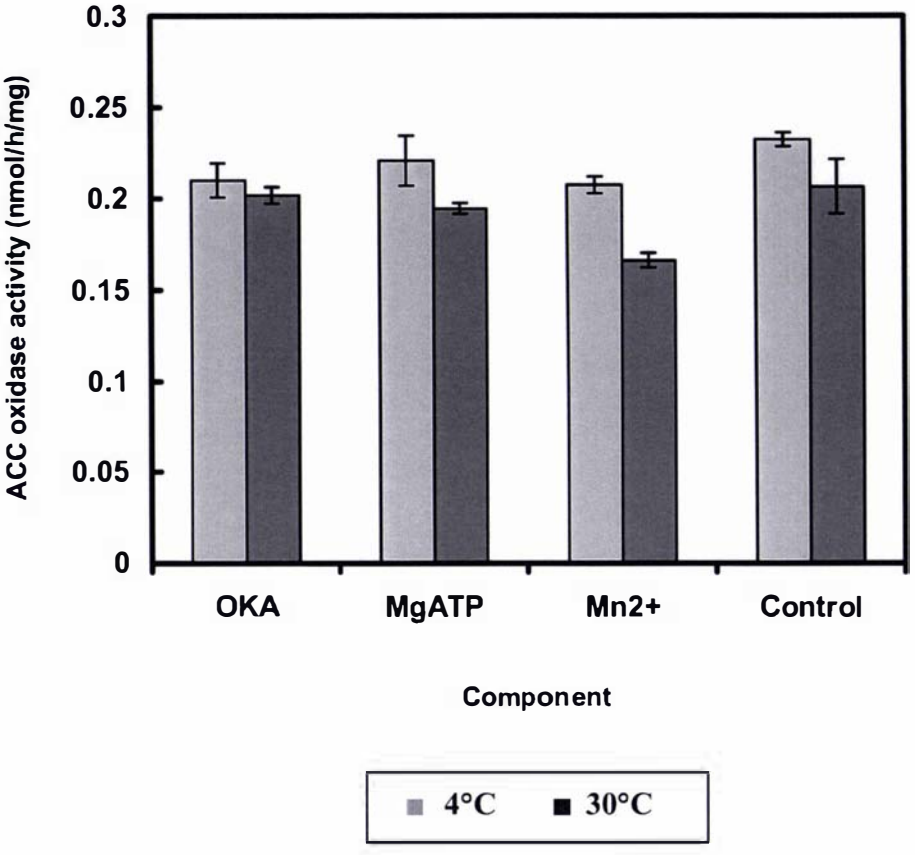

Figure 3.28 Comparison of ACC oxidase activity in Tris-buffer extracts harvested at 12 pm.

The components of the incubation buffer were added separately (as indicated) to a standard ACC oxidase buffer (50 mM Tris-HCl, pH7.5, containing 10% (v/v) glycerol, 30 mM sodium ascorbate and 2 mM DTT).

Results are mean values ● s.e., n=3

The results showed that during the maximum period of ACC oxidase activity (12:00 am and 12:00 pm), dephosphorylation did affect enzymatic activity (Figure 3.29). At these two time points, the ACC oxidase activity after dephosphorylation increased by 36% (12:00 am) and 56% (12:00 pm), when compared with the phosphorylated enzyme. In contrast, activity at (9:00 pm) exhibited only a 21% change between the phosphorylated and dephosphorylated enzyme treatments.

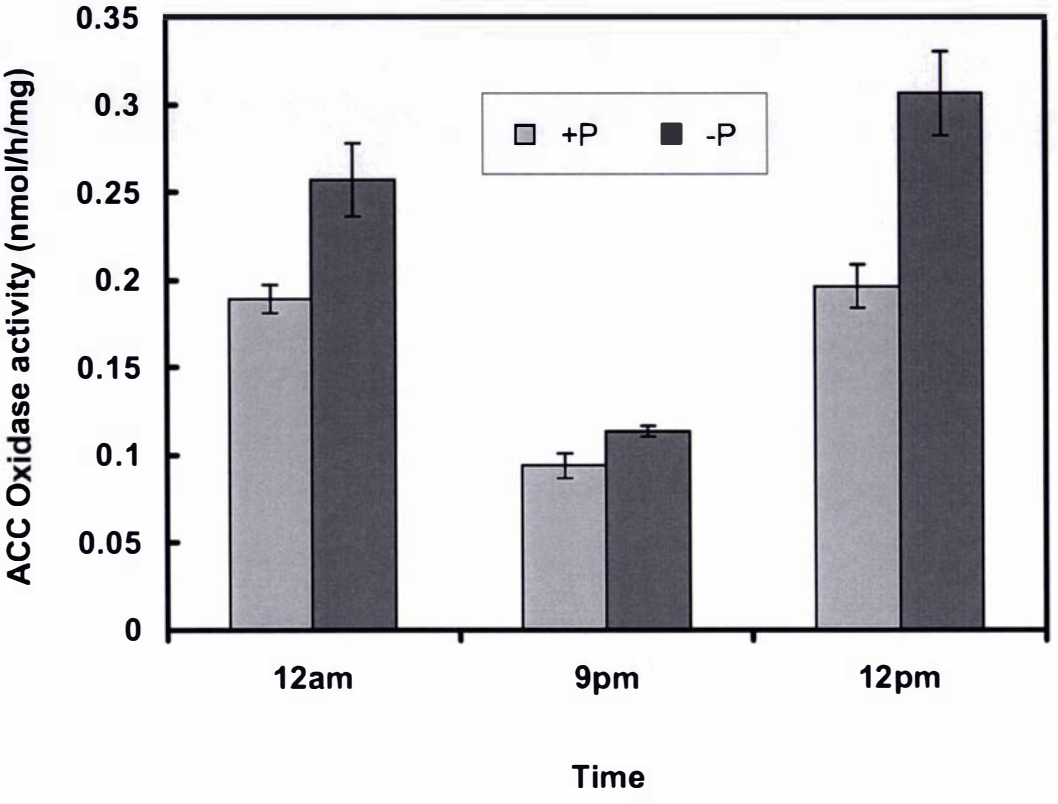

Figure 3.29 Comparison of ACC oxidase activity in extracts harvested at the time shown after phosphorylation and dephosphorylation treatments

Results are mean values ± s.e., n=3

To investigate whether the phosphorylation status of ACC oxidase has any effect on its molecular mass, the protein extracts used for the activity assays shown as Figure 3.29 were examined using SDS-PAGE and western blot analysis.

Using the SDS-PAGE mini-protein gel system, with 30 μg of protein sample loaded and western blot analysis using the anti-TR-ACO2 antibodies, the molecular mass of ACC oxidase of the dephosphorylated enzyme exhibited a slightly lower mass than the phosphorylated enzyme (Figure 3.30).

In order to further confirm this finding, two concentration ranges of linear gradient SDS-PAGE gels were used followed by western blot analysis. Using a 10-20% gradient gel with 80 μg of protein sample, the results of the mini-gel were repeated in that the dephosphorylated enzyme had a lower molecular mass (Figure 3.31). Using the 8-15% gradient gel with 40 μg of protein sample, it is clearer that the molecular mass of ACC oxidase protein after phosphorylation is higher than the dephosphorylated enzyme (Figure 3.32).

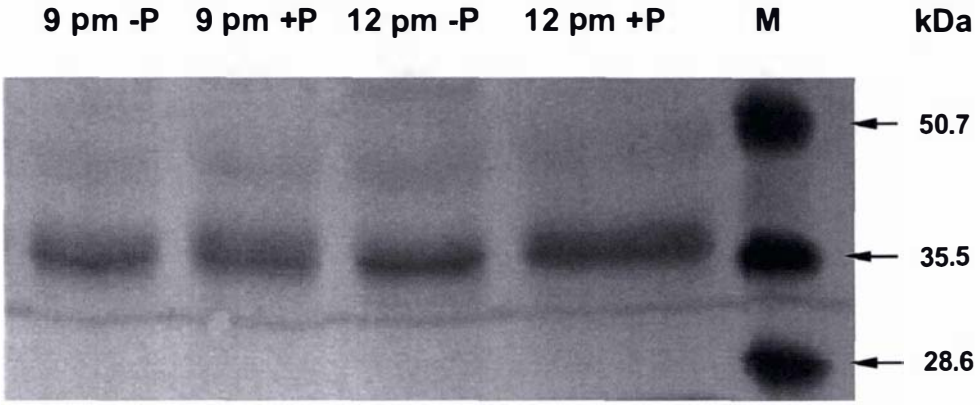

Figure 3.30 Comparison of the molecular mass of ACC oxidase in extracts harvested at the time indicated after phosphorylation (+P) or dephosphorylation (-P) treatment

Aliquots (30 μg) from each time point after phosphorylation or dephosphorylation treatment were separated using the mini-gel SDS-PAGE system, electroblotted onto PVDF membrane and challenged with anti-TR-ACO2 antibodies. Lane (M) are prestained molecular mass markers (molecular masses are indicated).

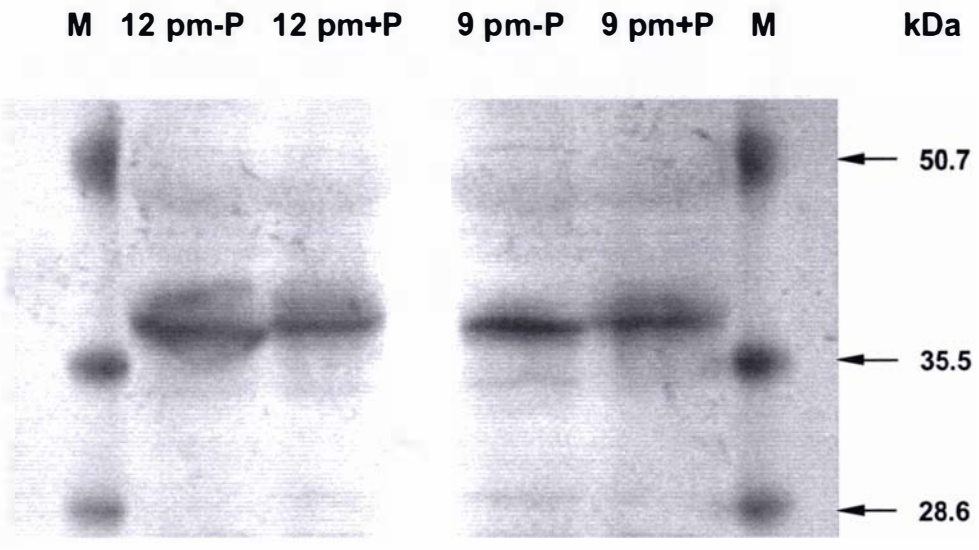

Figure 3.31 Comparison of the molecular mass of ACC oxidase in extracts harvested at the time indicated after phosphorylation (+P) or dephosphorylation (-P) treatment and separated using a 10 to 20% SDS-PAGE gradient gel

Aliquots (80 μg) from each time point after phosphorylation or dephosphorylation treatment were separated using the gradient gel SDS-PAGE system, electroblotted onto PVDF membrane and challenged with anti-TR-ACO2 antibodies. Lane (M) are prestained molecular mass markers (molecular masses are indicated).

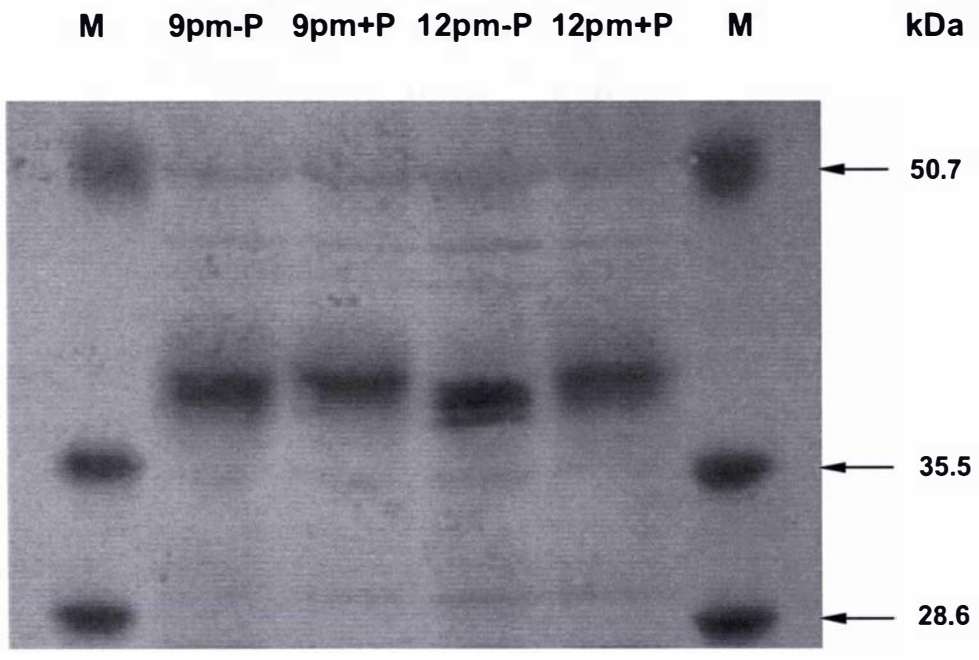

Figure 3.32 Comparison of the molecular mass of ACC oxidase in extracts harvested at the time indicated after phosphorylation (+P) or dephosphorylation (-P) treatment and separated using a 8 to 15% SDS-PAGE gradient gel

Aliquots (40 μg) from each time point after phosphorylation or dephosphorylation treatment were separated using the gradient gel SDS-PAGE system, electroblotted onto PVDF membrane and challenged with anti-TR-ACO2 antibodies. Lane (M) are prestained molecular mass markers (molecular masses are indicated).

4. Chapter Four: Molecular Characterization of ACC Oxidase during Leaf Maturation and Senescence in *Trifolium occidentale*

4.1 Physiological Analysis of Clonal Growth of *T. occidentale*

4.1.1 Physiology of Leaf Development in *T. occidentale*

In this thesis, *T. occidentale* is being assessed as a model system for the study of leaf ontogeny in a pasture legume species related to white clover. Therefore, it was necessary that some basic physiological properties should be investigated and compared with white clover before determining whether orthologues of *TR-ACO2* and *TR-ACO3* occur in *T. occidentale.*

T. occidentale (genotype 18Z, AgResearch Grasslands, Palmerston North, New Zealand), when grown under the same experimental conditions used for white clover (section 2.1.2), grows as a single stolon from a major root with leaves that, at harvest time, display all stages of development from leaf initiation at the apex, through mature green to senescence, and then necrosis (Figure 1.5).

Generally, stolons had 14 to 18 unfolded leaves. Leaf 1 was defined as the first fully unfolded leaf that had emerged completely from the apical sheath.

The growing method used produced a highly reproducible pattern of leaf development along the stolon for both *T. occidentale* and white clover. The leaf fresh weight and leaf area have been determined initially to characterize the basic physiology of leaf tissue at each developmental stage (Figure 4.1 and 4.2). For *T. occidentale,* the fresh weights (Fwt) of the trifoliate leaves at each node increased rapidly during leaf expansion (leaf 2 to leaf 5) and reached the first peak at leaf 5 (*ca.* 13.2 mg) (Figure 4.1). The values of leaves 6 to 10 remained similar (around 10 mg) during the mature green leaf stage. In leaf 11, the fresh weight of the tissue increased further to the second peak (*ca.* 13.6 mg) and then decreased after leaf 11. In contrast, the fresh weights of leaf tissue of white clover were much higher than *T. occidentale*, and a similar trend was observed in terms of changes in fresh weight with development, although the second peak at leaf 12 was

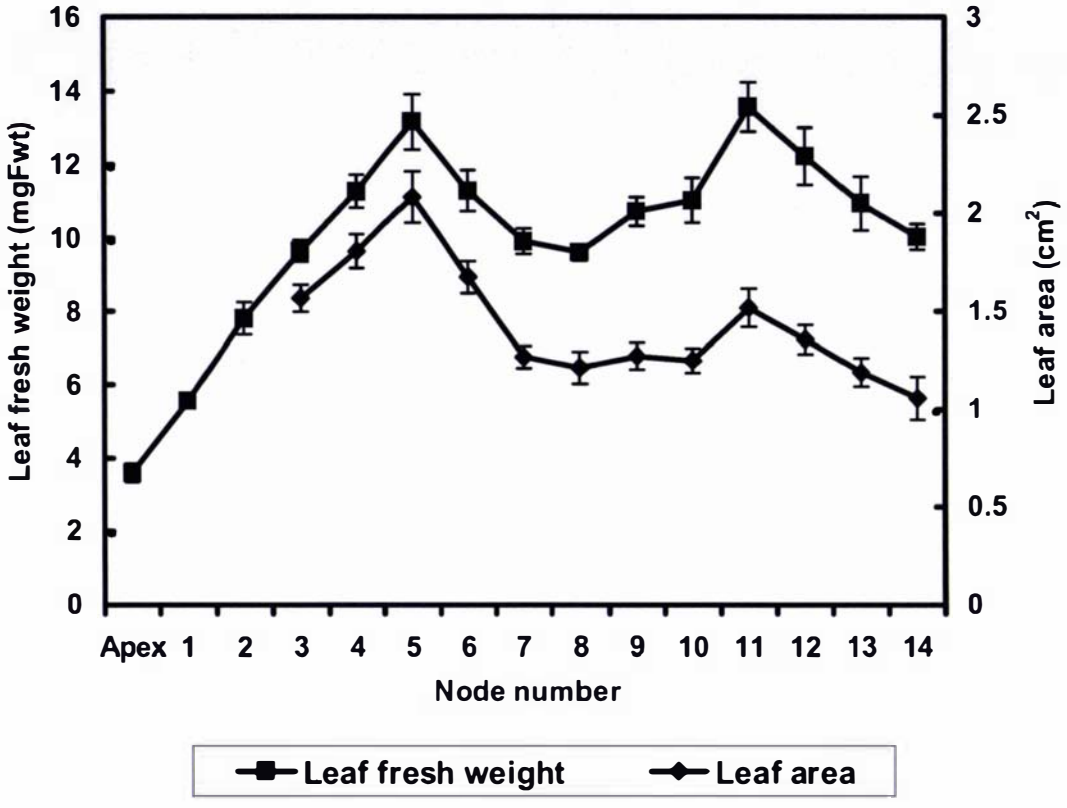

Figure 4.1 Changes in fresh weight and area of leaves of *T. occidentale* during leaf ontogeny

Results are mean values ± s.e., n=5

not as pronounced. The weights of the newly initiated leaves were low (leaf 1, *ca.* 76 mg), but increased to between 230 to 260 mg at leaves 3 to 6. The values of leaves 7 to 11 remained at a constant level of *ca.* 200 mg during the mature green leaf stage. In leaf 12, the fresh weight of tissue increased to 216 mg and then declining gradually after leaf 12 (Figure 4.2).

The area of a trifoliate leaf at each node was determined (section 2.2.1) from leaf 3 (the first fully expanded leaf) for both *T. occidentale* and white clover using a leaf area meter (as shown in Figure 4.1 and Figure 4.2). For *T. occidentale*, the mean values of leaf area increased as newly initiated leaf tissue (leaves 3 to 5) and reached the first peak at leaf 5 (2.08 cm^2). The values of leaves 7 to 11 remained at a constant level of *ca.*1.25 cm^2 during the mature green and onset of senescence developmental stages. In leaf 11, the leaf area increased to the second peak (1.52 cm^2), after which, as determined by the methodology used in this thesis to measure area, the area decreased as leaf senescence ensued as determined by the visible onset of chlorosis (Figure 4.1). For white clover, a similar pattern was observed with values of leaf area of *ca.* 12 to 14 cm^2 observed during the mature green and onset of senescence stages (between leaf 3 and leaf 12) (Figure 4.2). Again, as determined by the methodology used in this thesis to measure area, the appeared leaf area decreased.

The ratio of leaf fresh weight to leaf area at each node of *T. occidentale* was determined and found to increase, which suggests that the leaf area decreased noticeably when compared to fresh weight of trifoliate leaves during leaf ontogeny (Figure 4.3). This tendency is also observed when the fresh weight of leaf discs (diameter = 5 mm) excised from the basal region of a leaflet of the trifoliate leaf was measured (Figure 4.3). The fresh weight of these tissues also increased over the developmental stages examined. The ratio of leaf fresh weight to leaf area and the fresh weight of leaf discs (diameter = 10 mm) was also determined for white clover (Figure 4.4). Here, a similar trend was observed only for fresh weight of leaf discs, which also increased during leaf ontogeny. The ratio of leaf fresh weight to leaf area in white clover showed two broad peaks, one at leaf 6 and one at leaf 16.

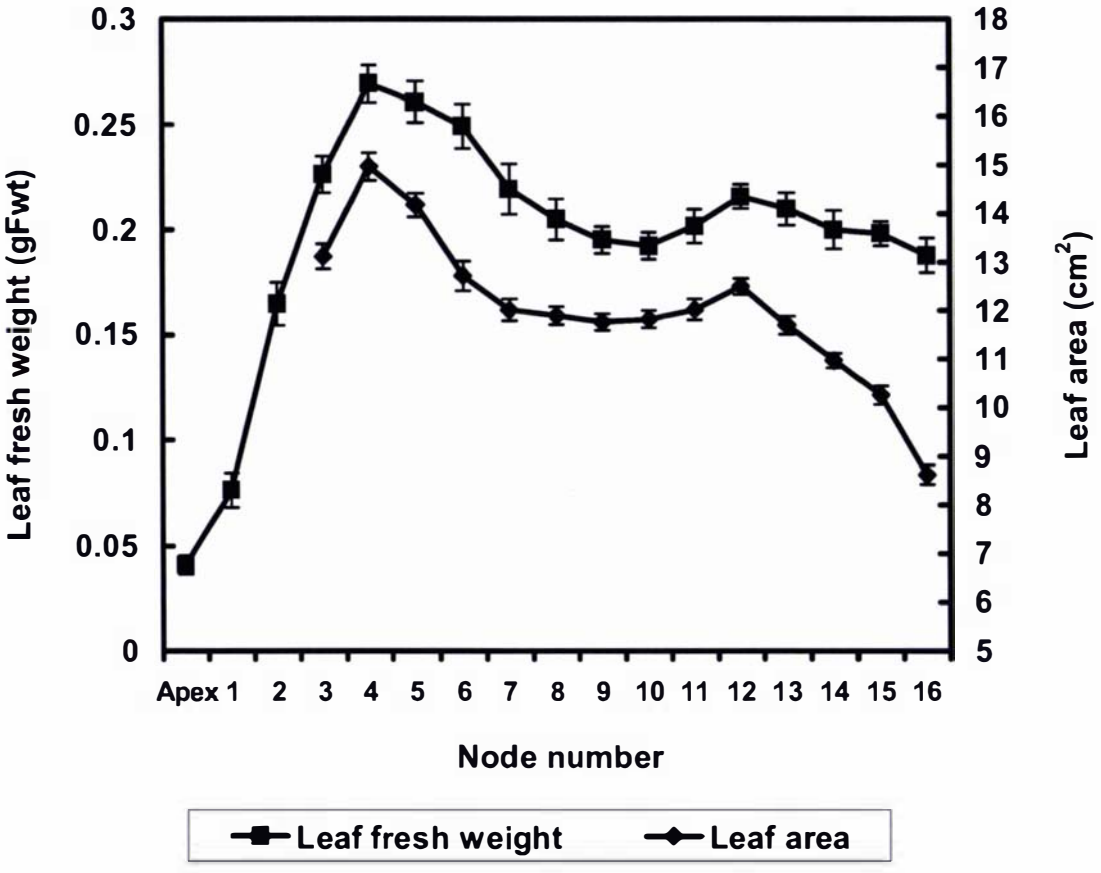

Figure 4.2 Changes in fresh weight and area of leaves of white clover during leaf ontogeny

Results are mean values ± s.e., n=5

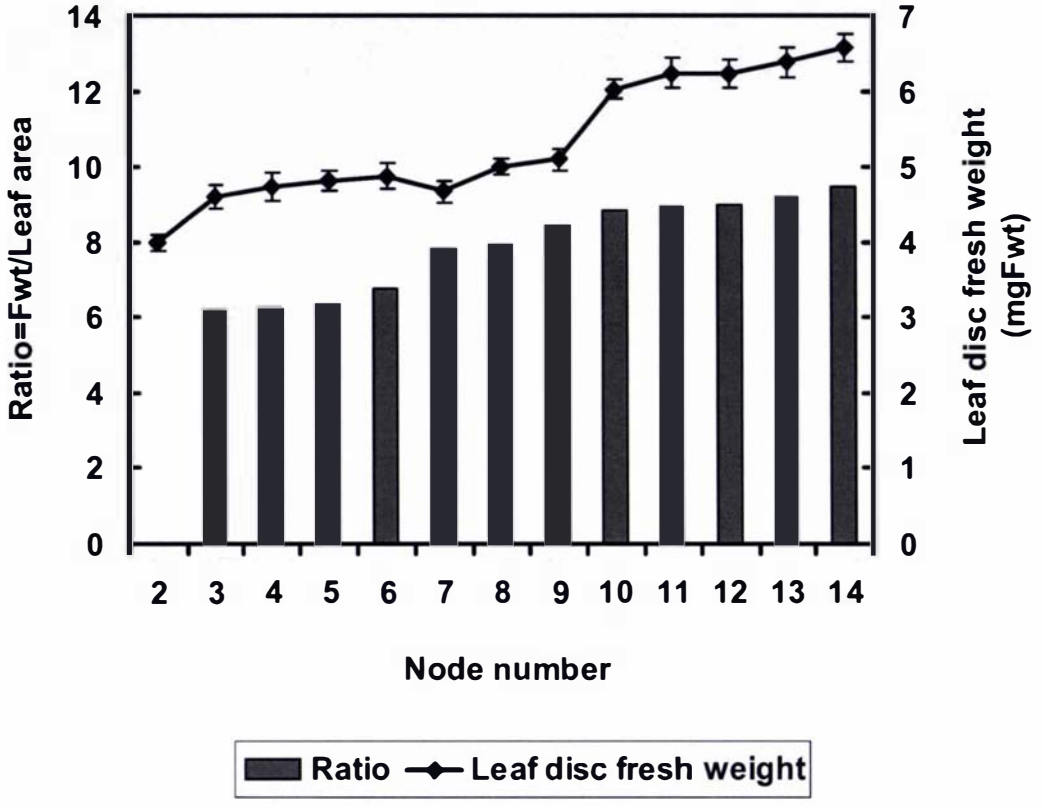

Figure 4.3 Changes in the ratio of mean leaf fresh weight to leaf area, and fresh weight of leaf discs from the basal portion of the leaf blade at each node of *T. occidentale*

Results of the fresh weight of leaf discs are mean values ± s.e., n=5

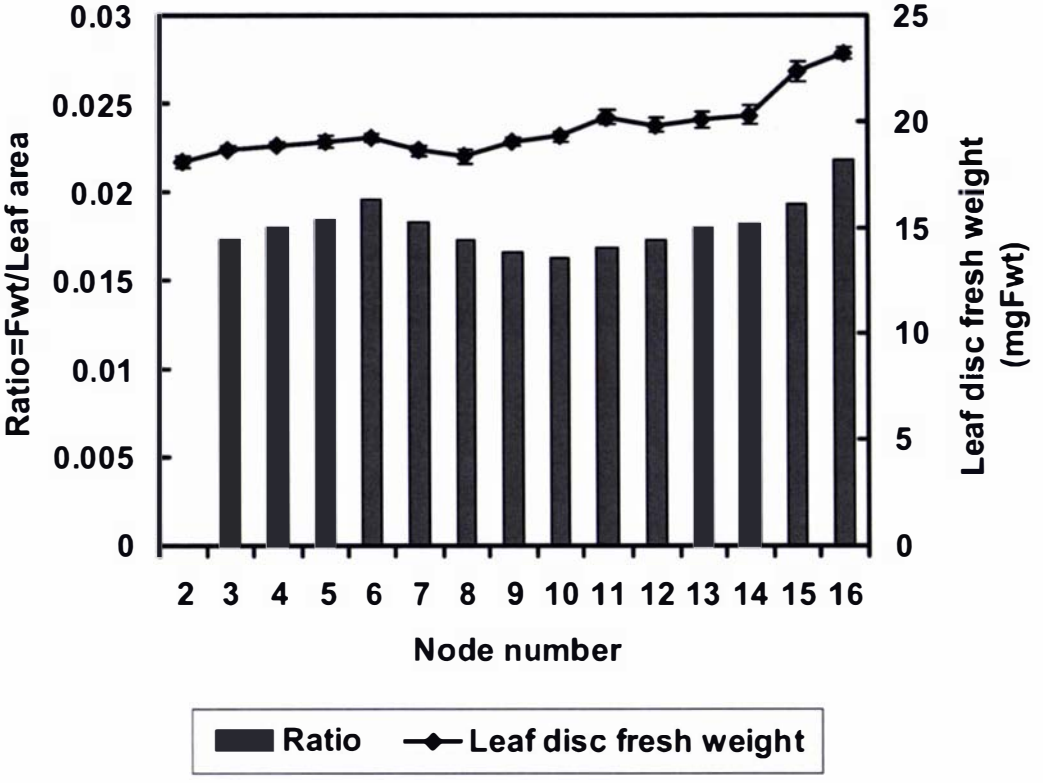

Figure 4.4 Changes in the ratio of mean leaf fresh weight to leaf area, and fresh weight of leaf discs from the basal portion of the leaf blade at each node of white clover

Results of the fresh weight of leaf discs are mean values ± s.e., n=5

4.1.2 Chlorophyll Content of Leaf Tissue during Leaf Initiation, Maturation and Senescence of *T. occidentale*

Although the onset of leaf senescence can be determined visually, for a more accurate determination chlorophyll content of leaves at each node was measured (section 2.2.2). The chlorophyll profile from three stolons with different numbers of leaves is shown in Figure 4.5. The total chlorophyll content increased as newly initiated leaf tissue unfolded and expanded (leaf 1 to 3). For mature green leaves, the chlorophyll levels remained relatively constant of *ca.* 950 to 1020 μg per g fresh leaf tissue (leaf 4 to 8), and then, typically, leaves 9 to 11 were the first to display visual signs of chlorosis (onset of the senescence stage). After the onset of chlorophyll loss, the levels declined in a relatively linear fashion (leaves 12 to 14) to reach *ca.* 350 μg per g fresh leaf tissue at leaf 14 before the first dead leaf. As the leaf tissue aged, the general trend shows that chlorophyll *a* was degraded slightly faster than chlorophyll *b* during the later stage of senescence with ratio, which is indicated by the ratio of chlorophyll *a:b* changing from 2.42 at leaf 4 to *ca.* 2.20 between leaf 10 to14 (Figure 4.5).

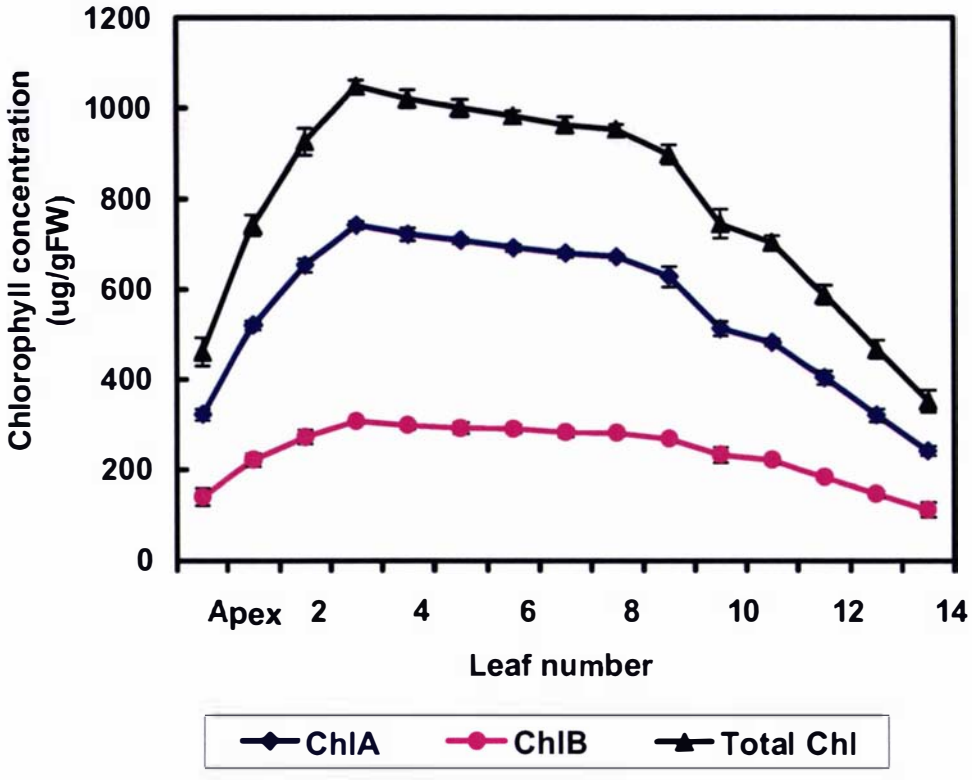

Chlorophyll a:b Ratio	2.32	2.35	2.40	2.41	2.42	2.42	2.38	2.40	2.39	2.34	2.20	2.18	2.20	2.20	2.18

Figure 4.5 Changes in chlorophyll concentration during leaf ontogeny in *T. occidentale*

Results are mean values ± s.e., n=3

4.1.3 Changes in Nitrogen Content during Leaf Ontogeny in *T. occidentale* and White Clover

Nitrogen is an important component of protein in higher plants. The natural abundance of nitrogen in higher plants can be a good indicator of their physiology and responses to the environment (Handley and Raven, 1992; Yoneyama, 1995).

Average nitrogen content of leaves was determined throughout leaf ontogeny in *T. occidentale* (Figure 4.6) and white clover (Figure 4.7). The objective of the experiment was to determine the relationship between nitrogen concentration and leaf senescence and chlorophyll concentration in both species.

For both white clover and *T. occidentale*, the leaf nitrogen concentration of individual leaf samples declined as the leaves aged, with the highest values in the newly initiated green leaves, which then declines to reach the lowest values in the senescent leaves. It should be noted that due to tissue shortage of *T. occidentale*, only single determination of average nitrogen content was completed. Therefore, only the decrease observed in white clover is likely to be significant.

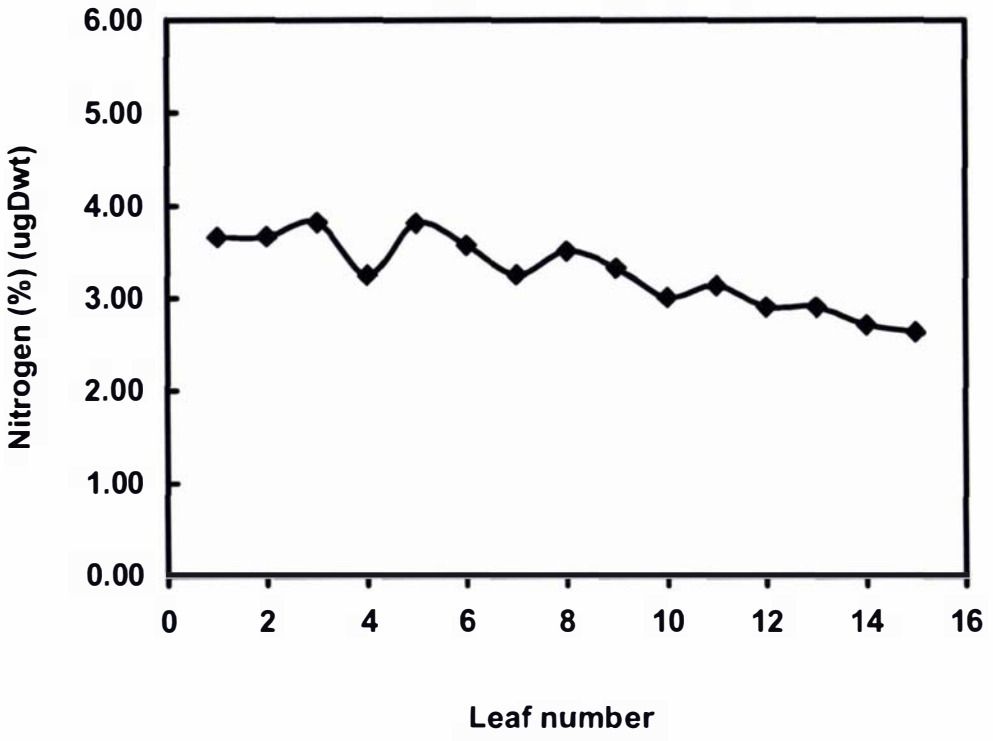

Figure 4.6 Changes in average nitrogen content during leaf ontogeny in *T. occidentale*

n=1

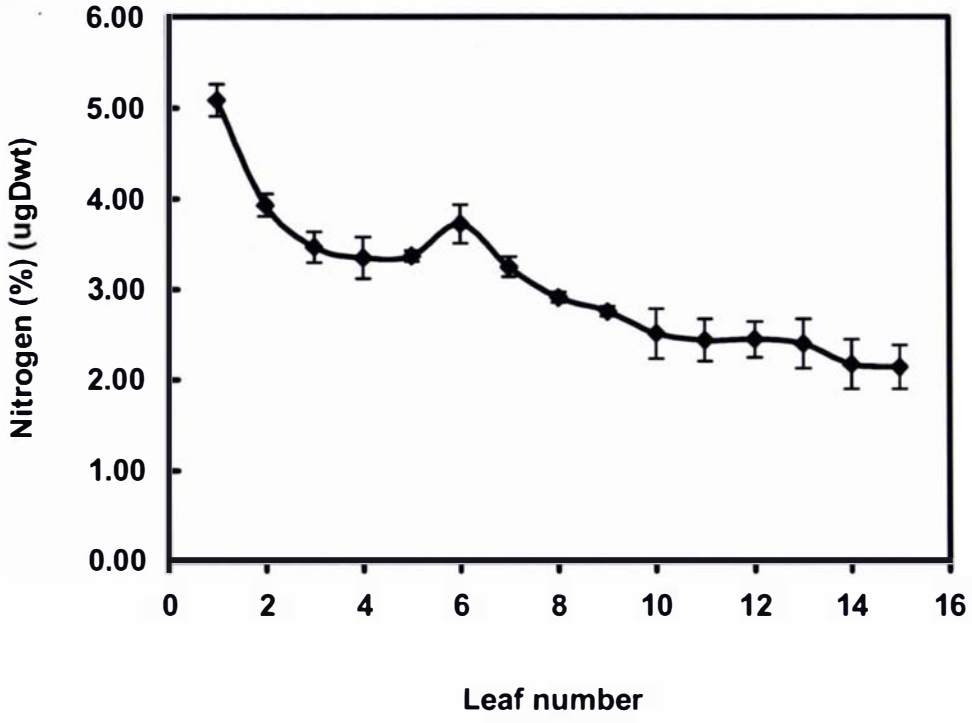

Figure 4.7 Changes in average nitrogen content during leaf ontogeny in white clover

Results are mean values ± s.e., n=3

4.2 Molecular Cloning of Protein-Coding Regions of ACC Oxidase Genes in *T. occidentale*

4.2.1 RT-PCR Amplification of Putative ACC Oxidase Gene Transcripts

In order to determine whether orthologues of *TR-ACO2* and *TR-ACO3* occur in *T. occidentale*, gene products encoding ACC oxidases expressed in newly initiated green leaves and those at the onset of senescence were cloned using the reverse transcriptase-dependant polymerase chain reaction (RT-PCR). To do this, tissues at similar developmental stages were pooled to comprise the two stages of development. The first developmental stage (newly initiated; nodes 2 to 4) comprised leaves that had reached maximum chlorophyll content. The second developmental stage (onset of senescence; nodes 9 to 10) comprised leaves where the chlorophyll concentration decreased significantly.

Initially, ACC oxidase cDNAs were amplified by PCR using nested degenerate primers (see Figure 2.7) known to bind to highly conserved regions within ACC oxidase genes. The primer sequences were provided by Professor S. F. Yang (University of California, Davis, USA). The first round primers (ACOF1 and ACOR1) generated cDNA transcripts from total RNA, and aliquots of this first round PCR were used as templates for amplification with the second round primers (E101 and E102). The amplified products after the first round of PCR were unable to be detected after electrophoresis on a 1% (w/v) agarose gel and ethidium bromide staining (data not shown). However, after two rounds of PCR, amplification products of approximately 830 bp were obtained (Figure 4.8). In addition, the same amount of RNA without undergoing RT treatment as a template was used as a control for the two rounds of PCR. No *ca* 830 bp PCR product was amplified (Figure 4.9 lane 1), indicating that the *ca* 830 bp DNA band was a genuine RT-PCR product. As well, larger cDNA fragments (*ca* 1300 to 1600 bp) were also obtained, which might be non-specific amplified products due to the genomic DNA contamination. These larger sized fragments were not sequenced or analyzed further.

The second round PCR products of *ca.* 830 bp were recovered from the 1% (w/v) agarose gel, then cloned into the pGEM®-T Easy vector (Figure 2.11) and transformed into the *E. coli* strain DH5α. The white colonies from the transformation, which used

LB Amp^{100} plates with IPTG and X-Gal, were picked and cultured in LB Amp^{100} broths. Plasmids were isolated (section 2.4.6.1) and purified (section 2.4.6.3), and the presence of an insert of approximately 830 bp was confirmed by restriction enzyme digestion with *Eco*R1 followed by agarose gel electrophoresis. The larger DNA fragment (*ca.* 3000 bp) was the pGEM®-T Easy vector (Figure 4.9). The 830 bp insert was isolated using the same procedure as described above and DNA sequences were determined using an automated sequencer. All of the DNA sequences obtained from both newly initiated and senescent leaves belong to the same gene, which has high identity with *TR-ACO2* expressed in green leaves of white clover. This result suggested that either the nested degenerate primers did not amplify any homologues specifically expressed in senescent leaves or a homologue of *TR-ACO3* gene does not occur in senescent leaves of *T. occidentale.*

In order to amplify and clone the putative ACC oxidase gene specifically expressed in senescent leaves, gene-specific primers were designed based on the known DNA sequence of *TR-ACO3* (Figure 2.8).

A putative ACC oxidase gene was amplified using RT-PCR with cDNA templates generated by RT-treatment of total RNA extracted from leaves of *T. occidentale* at the onset of senescence. The TRACO3FA and TRACO3RB primers were used for a first round of PCR amplification and TRACO3FB and TRACO3RC primers were used for the second round PCR. The amplified product of approximately 920 bp (the expected size) was only detected after two rounds of PCR (Figure 4.10). The PCR products were cloned into the pGEM®-T Easy vector, transformed into the *E. coli* strain DH5α and inserts sized after restriction enzyme digestion of plasmid DNA with *Eco*R1 and agarose gel electrophoresis. The large DNA fragments were the vector or uncompleted digests of plasmid DNA, such as in lane 3 (as shown in Figure 4.11).

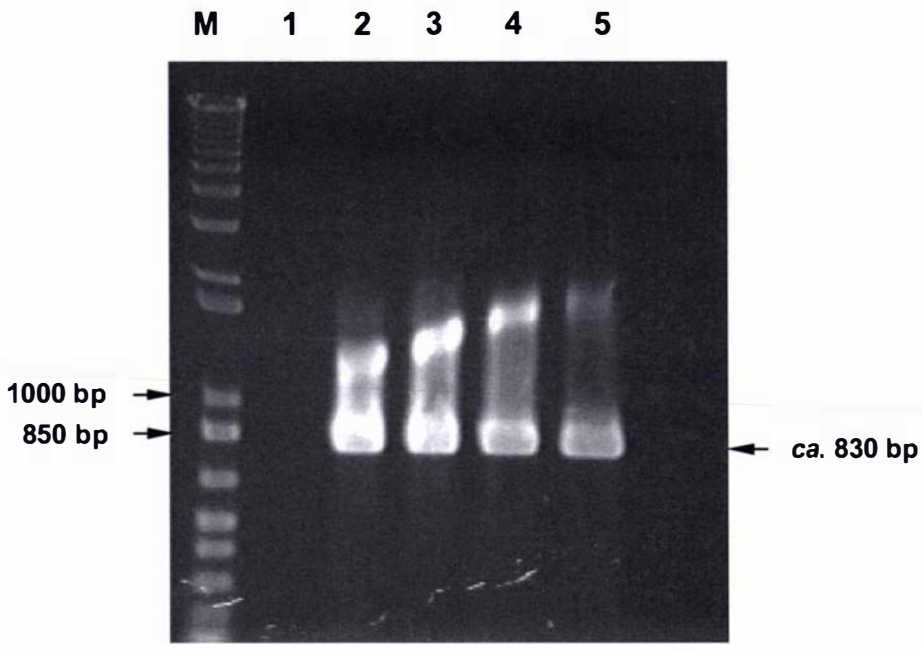

Figure 4.8 PCR amplification of a putative ACC oxidase cDNA using RT-generated cDNA templates from total RNA isolated from newly initiated green leaves

Nested degenerate primers were used for two rounds of PCR amplification. PCR products were separated on 1% (w/v) agarose gel and visualized with ethidium bromide.

Lane M: GIBCO BRL 1 kb DNA ladder. The molecular weights of two of the standards are indicated to the left of the figure. The approximate size of the amplification product is indicated by an arrow to the right of the figure.

Lane 1: The control using the same amount of RNA without RT-treatment as a template

Lanes 2 to 5: The separated products from the second round PCR

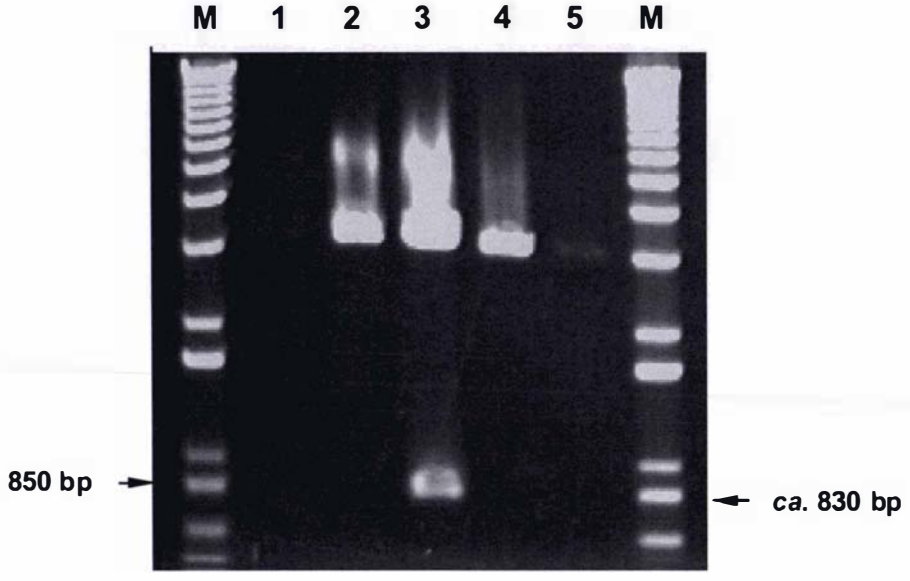

Figure 4.9 Cloning of putative cDNAs encoding ACC oxidase in newly initiated green leaves of *T. occidentale* generated using RT-PCR

Restriction digest of plasmids isolated from *E. coli* to confirm cloning of the *ca.* 830 bp cDNA fragments. Inserts obtained from *Eco*R1-digestion of plasmids containing putative ACC oxidase sequences were separated on 1% (w/v) agarose gel and visualized with ethidium bromide.

Lane M: GIBCO BRL 1 kb DNA ladder. The molecular weight of one of the standards is indicated to the left of the figure. The approximate size of the amplified cDNA is indicated by an arrow to the right of figure.

Lanes1 to 5: Restriction enzyme digestion of plasmids isolated from *E. coli* to confirm cloning of the *ca.* 830 bp cDNA fragments.

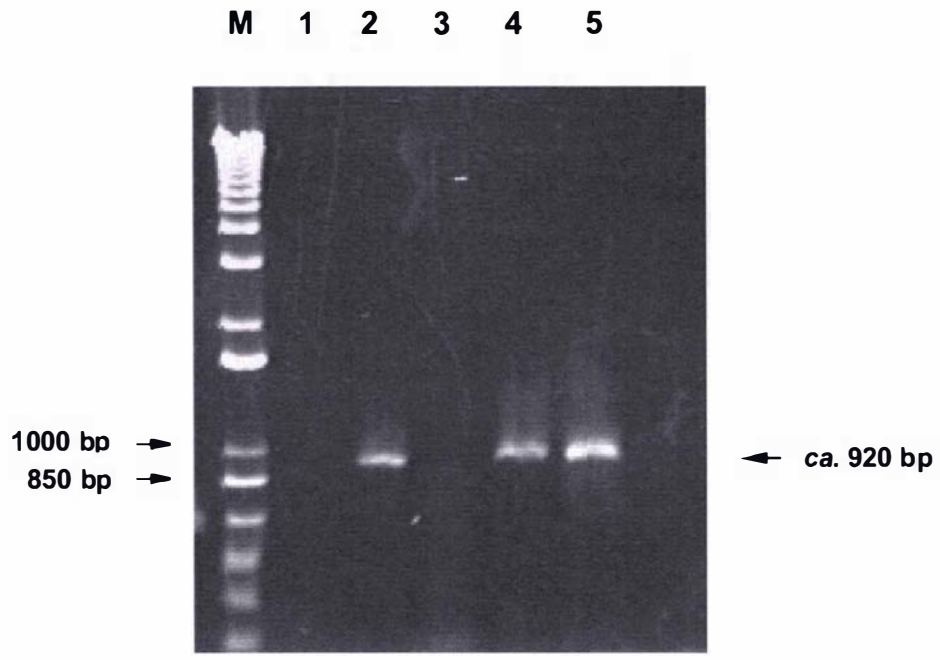

Figure 4.10 PCR amplification of a putative ACC oxidase cDNA using RT-generated cDNA templates from total RNA isolated from senescent leaves

Gene-specific primers were used for two rounds of PCR amplification. PCR products were separated on 1% (w/v) agarose gel and visualized with ethidium bromide.

Lane M: GIBCO BRL 1 kb DNA ladder. The molecular weights of two of the standards are indicated to the left of the figure. The approximate size of the amplification product is indicated by an arrow to the right of the figure.

Lane 1: The control using the same amount of RNA without RT-treatment as a template

Lanes 2 to 5: The separated products from the second round PCR.

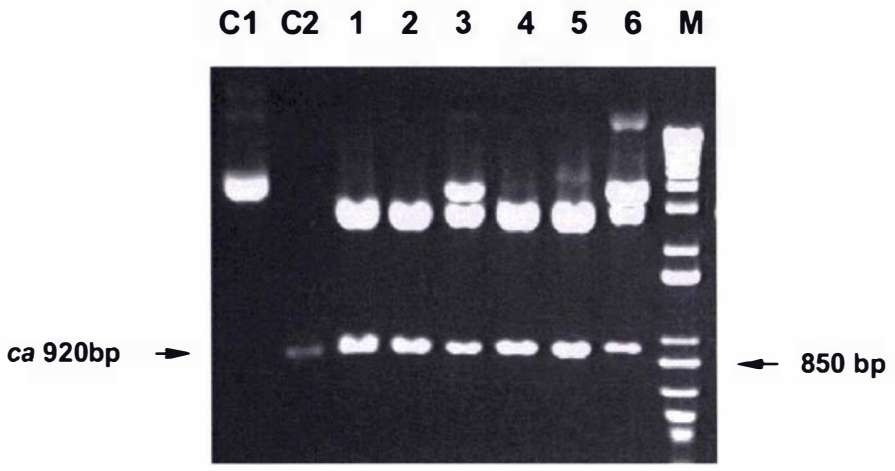

Figure 4.11 Cloning of putative cDNAs encoding ACC oxidase in senescent leaves of *T. occidentale* generated using RT-PCR

Restriction enzyme digestion of plasmids isolated from *E. coli* to confirm cloning of the *ca.* 920 bp cDNA fragments. Inserts obtained from *Eco*R1-digestion of plasmids containing putative ACC oxidase sequences were separated on 1% (w/v) agarose gel and visualized with ethidium bromide.

Lane M: GIBCO BRL 1 kb DNA ladder. The molecular weight of one of the standards is indicated to the right of the figure. The approximate size of the amplified cDNA is indicated by an arrow to the left of figure.

Lane C1: The control using the same amount of plasmid DNA without digestion.

Lane C2: The control using second round PCR products.

Lanes1 to 6: Restriction enzyme digestion of plasmids isolated from *E. coli* to confirm cloning of the *ca.* 920 bp cDNA fragments.

4.2.2 Confirmation of Putative ACC Oxidase Gene Transcripts by Sequence Analysis

A total of 18 clones were sequenced: eight from RNA isolated from newly initiated green leaves and amplified using nested degenerate primers, and ten from RNA isolated from leaves at the onset of senescence using the gene-specific primers based on the DNA sequence of *TR-ACO3*. A sequence alignment comparison, using the Clustal X (1.5 b) or Vector NTI Suite 7 program, indicated that all of these sequences displayed highest sequence homology to ACC oxidase gene sequences in the GenBank database. Within these sequences, an alignment comparison revealed that all of the sequences could be separated into two distinct groups. Each of the sequences within a group showed greater than 99% homology and so both groups were considered to represent two distinct ACC oxidase cDNA products. In terms of a comparison with the GenBank database, it was found that the *TR-ACO2* and *TR-ACO3* genes from white clover have the highest similarity with these genes, and so the ACC oxidase sequences cloned from *T. occidentale* were designated as *TO-ACO2* and *TO-ACO3*.

The consensus sequence identity of the two ACC oxidase cDNAs identified in *T. occidentale* and the two related genes from white clover are compared and summarized at both the nucleotide and amino acid level in Table 4.1. The consensus nucleotide sequences of *TO-ACO2* and *TO-ACO3* and deduced amino acid consensus TO-ACO2 and TO-ACO3 sequences are shown in Figure 4.12 and Figure 4.13, respectively.

As shown in Table 4.1, the sequence identity of *TO-ACO2* was 97% and 81% with *TR-ACO2* and *TR-ACO3*, respectively, while the identity of *TO-ACO3* was 97% and 82% with *TR-ACO3* and *TR-ACO2*, respectively. The *TO-ACO2* gene has 82% identity to *TO-ACO3* at the nucleotide level (Table 4.1). The deduced amino acid sequences of the two ACC oxidase genes in *T. occidentale* showed that the sequence identity of TO-ACO2 was 98% and 84% with TR-ACO2 and TR-ACO3, respectively, and TO-ACO3 was 96% and 85% with TR-ACO3 and TR-ACO2, respectively (Table 4,1). The TO-ACO2 is 84% identical to TO-ACO3 at the amino acid level (Figure 4.14). This high similarity at the amino acid level, as well as the nucleotide sequence level, confirms that the RT-PCR-based gene cloning successfully generated ACC oxidase gene homologues of white clover in *T. occidentale.*

Table 4.1 Identity values of four ACC oxidase genes identified in *T. occidentale* and *T. repens* in both nucleotide and amino acid level

Nucleotide Level	*TO-ACO2*	*TO-ACO3*	*TR-ACO2*	*TR-ACO3*
TO-ACO2	-	82%	97%	81%
TO-ACO3	82%	-	82%	97%
TR-ACO2	97%	82%	-	84%
TR-ACO3	81%	97%	84%	-
Amino Acid Level	**TO-ACO2**	**TO-ACO3**	**TR-ACO2**	**TR-ACO3**
TO-ACO2	-	84%	98%	84%
TO-ACO3	84%	-	85%	96%
TR-ACO2	98%	85%	-	85%
TR-ACO3	84%	96%	85%	-

ACC oxidase is known to have some conserved amino acid residues and require some crucial amino acid residues for maximal activity of the enzyme (Kadyrzhanova *et al.*, 1997; 1999; Dilley *et al.*, 2003). As shown in Figure 4.12 and 4.13, both TO-ACO2 and TO-ACO3 contain the amino acids which have been shown to be important for ACC oxidase activity. These include histidine residues at positions 177 and 234 (H^{177} and H^{234}), and aspartate residue at position 179 (D^{179}), which have been shown to be essential for ACC oxidase activity because they are ligands for Fe^{2+}. Although there are three conserved cysteine residues at positions 28, 133, and 165 (C^{28}, C^{133}, and C^{165}), respectively, only C^{28} is very important for activity since at least one SH group is needed. Other residues also shown to be important for maximal activity include the arginine residue at position 244, the serine residue at position 246, and the threonine residue at position 157 (R^{244}, S^{246}, and T^{157}) as they are ligands for the ACC carboxyl group. Moreover, there are seven completely conserved lysine residues at positions 72, 144, 158, 172, 199, 230 and seventh residue that varies slightly in position in TO-ACO2 and TO-ACO3, which occurs at position 289 in TO-ACO2 and 293 in TO-ACO3 (K^{72}, K^{144}, K^{158}, K^{172}, K^{199}, K^{230}, K^{289}, and K^{293}). The presence of these residues in TO-ACO2 and TO-ACO3 strongly suggest that both transcripts encode functional ACC oxidases

TO-ACO2 (822bp)

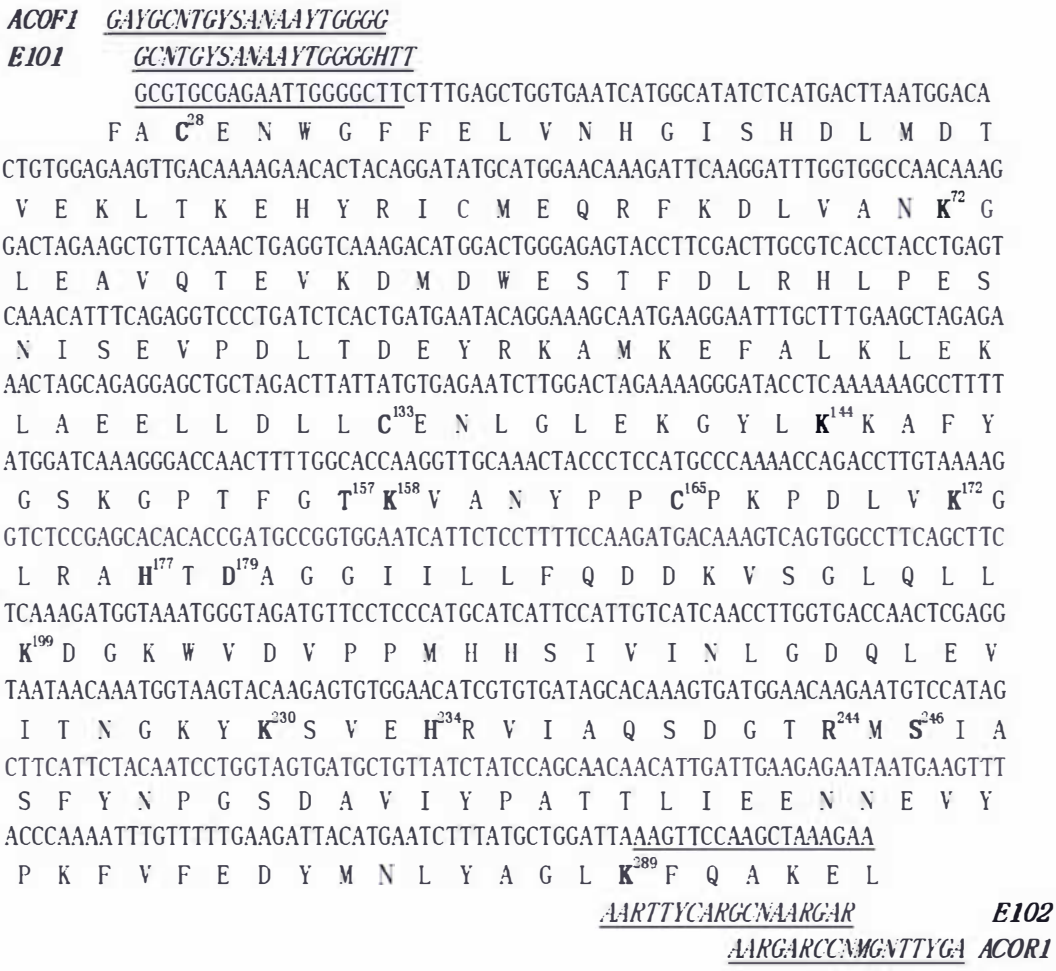

Figure 4.12 Nucleotide and deduced amino acid sequence of the protein-coding region of the consensus *TO-ACO2* gene.

The two nested sets of degenerate primers used for RT-PCR are given in italics. The first cysteine in the sequence is designated at position 28 as determined by a consensus of published studies. Residues shown to be important for maximal enzyme activity or to be completely conserved by structure/function analysis are indicated (bold, number).

TOACO3 (922bp)

Figure 4.13 Nucleotide and deduced amino acid sequence of the protein-coding region of the consensus *TO-ACO3* gene.

The two nested sets of degenerate primers used for RT-PCR are given in italics. The first cysteine in the sequence is designated at position 28 as determined by a consensus of published studies. Residues shown to be important for maximal enzyme activity or to be completely conserved by structure/function analysis are indicated (bold, number).

Reference molecule: TO-ACO2 (271 aa) Homology
Sequence 2: TO-ACO3 (306 aa) 84%

```
TOACO2    -------------------------ACENWGFFELVNHGISHDLMDTVE
TOACO3    MGNFPVVDLERLNGVERKDTMEKIKDACENWGFFELVNHGIPHDLMDTLE

TOACO2    KLTKEHYRICMEQRFKDLVANKGLEAVQTEVKDMDWESTFDLRHLPESNI
TOACO3    RLTKEHYRKCMEQRFKELVSSKGLDAVQTEVKDMDWESTFHVRHLPESNI

TOACO2    SEVPDLTDEYRKAMKEFALKLEKLAEELLDLLCENLGLEKGYLKKAFYGS
TOACO3    SELPDLSDEYRKVMKEFSLRLEKLAEELLDLLCENLGLEKGYLKKAFYGS

TOACO2    KGPTFGTKVANYPPCPKPDLVKGLRAHTDAGGIILLFQDDKVSGLQLLKD
TOACO3    RGPTFGTKVANYPQCPNPELVKGLRAHTDAGGIILLFQDDKVSGLQLLKD

TOACO2    GKWVDVPPMHHSIVINLGDQLEVITNGKYKSVEHRVIAQSDGTRMSIASF
TOACO3    DEWIDVPPMRHSIVVNLGDQLEVITNGKYKSVEHRVIAQTNGTRMSIASF

TOACO2    YNPGSDAVIYPATTLIEENNE----VYPKFVFEDYMNLYAGLKFQAKE--
TOACO3    YNPGSDAVIYPAPELLEKETEEKNNVYPKFVFEEYMKIYAALKFHAKEPR

TOACO2    ------
TOACO3    FEALKA
```

Figure 4.14 Comparison the Amino Acid Sequence of TO-ACO2 with TO-ACO3

Regions of differences are highlighted in grey.

(-): Represents no sequence data obtained.

A phylogenetic tree constructed from the alignment of the deduced amino acid sequences of TO-ACO2 and TO-ACO3 with twenty-two other ACC oxidases (from a GenBank search) also confirmed that the two ACC oxidase genes (*TO-ACO2* and *TO-ACO3*) generated from *T. occidentale* were not only much closer to each other, but also had the highest grouping with *TR-ACO2* and *TR-ACO3* from white clover, respectively (Figure 4.15, Table 4.2). The dendrogram shows the clustering relationships of *TO-ACO2* and *TO-ACO3* within a single branch of the tree, as well as the clustering relationships between *TO-ACO2* and *TR-ACO2*, and *TO-ACO3* and *TR-ACO3*. This is further evidence for *TO-ACO2* and *TO-ACO3* representing authentic ACC oxidase sequences.

Table 4.2 Comparison of the two ACC oxidase cDNAs identified in *T. occidentale* with sequences available in the GenBank database

Reference Sequence	Sequences with High Identity	Accession Number
TO-ACO2	*Trifolium repens TR-ACO2*	AF115262
	Medicago truncatula ACO mRNA	AY062251
	Trifolium repens TR-ACO3	AF115263
	Phaseolus lunatus ACO mRNA	AB062359
	Phaseolus vulgaris ACO mRNA	AF053354
TO-ACO3	*Trifolium repens TR-ACO3*	AF115263
	Phaseolus lunatus ACO mRNA	AB062359
	Phaseolus vulgaris ACO mRNA	AF053354
	Medicago truncatula ACO mRNA	AY062251
	Trifolium repens TR-ACO2	AF115262

(Searched on 22nd, April 2004; the sequences with high identity were ranked)

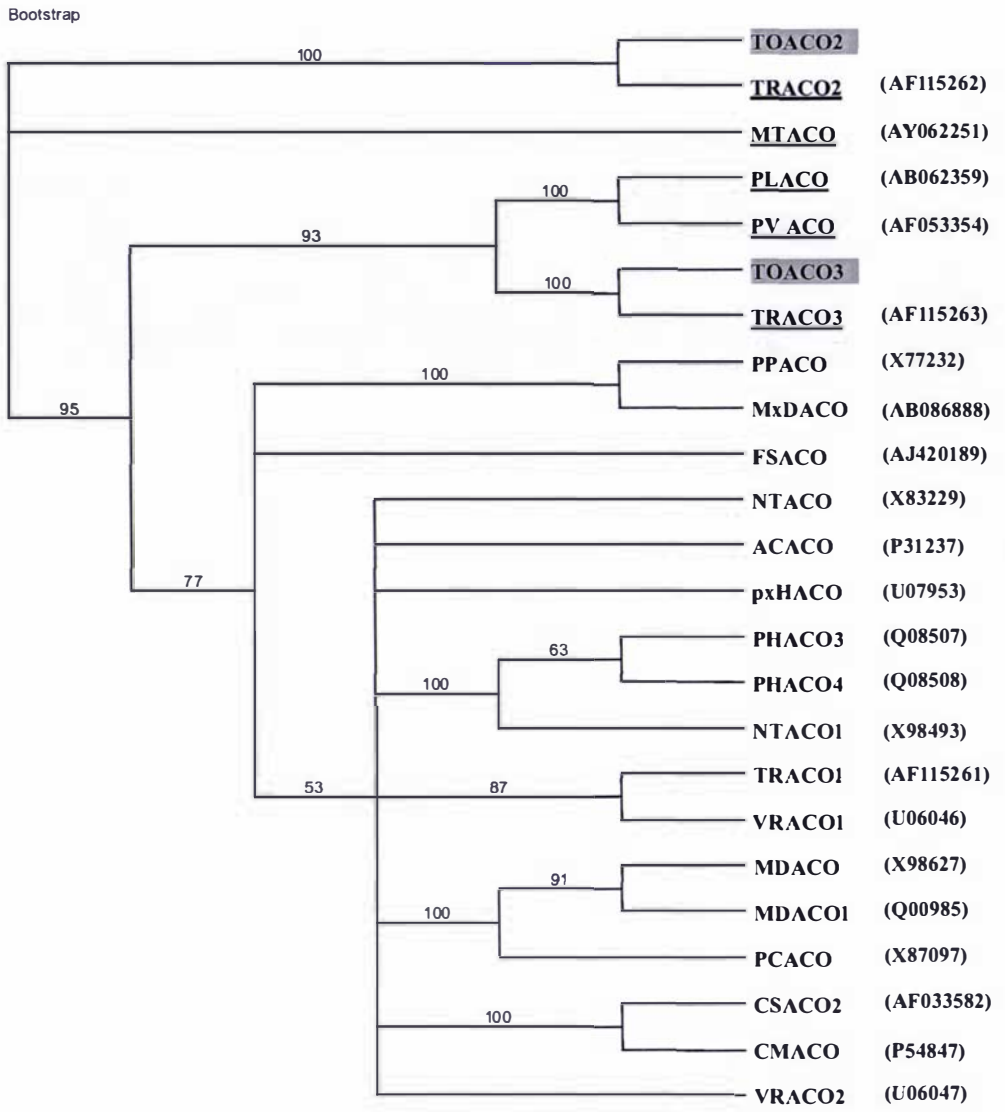

Figure 4.15 Phylogenetic analysis of the ACC oxidase amino acid sequences from *T. occidentale* with other ACC oxidase genes in the GenBank database

The phylogenetic tree was constructed from alignment of GenBank sequences with deduced amino acid sequences for *TO-ACO2* and *TO-ACO3* and the first five highest identities with *TO-ACO2* and *TO-ACO3* are underlined. The accession number for each gene is given in parenthesis. The full name for each entry is given in Appendix II.

4.3 Confirmation by Genomic Southern Analysis That *TO-ACO2* and *TO-ACO3* Are Encoded by Distinct Genes

To further confirm that *TO-ACO2* and *TO-ACO3* were two distinct ACC oxidase genes, Southern analysis was undertaken. Previous experience with Southern analysis of the genome of white clover had shown that gene-specific probes, which comprise the 3'-untranslated regions of each gene, were required (Hunter, 1998). Initial attempts to amplify the 3'-UTR regions using gene-specific primers (section 2.4.4.3.3), for both *TO-ACO2* and *TO-ACO3* were unsuccessful. However, because *TR-ACO2* and *TR-ACO3* had highest homology with *TO-ACO2* and *TO-ACO3*, respectively, it was decided to use the 3'-UTR regions of *TR-ACO2* and *TR-ACO3*, created by Hunter (1998). Prior to their use, the probes were confirmed by sequence analysis, and these probes was used both for Southern and northern analysis.

To perform Southern analysis, genomic DNA isolated from *T. occidentale* was digested in separate aliquots with *Eco*R1, *Xba* I and *Hind* III (section 2.4.8.2). After electrophoresis, the gel was blotted onto the Hybond™-N^+ membrane (section 2.4.8.3). Subsequently, the duplicate blots were probed with either [α-^{32} P] -dATP labelled 3'-UTR sequences of *TR-ACO2* or *TR-ACO3* (section 2.4.8.4).

The Southern hybridization and washing procedure as described in section 2.4.8.5 with the [α-^{32} P] -dATP labelled probes indicated that *TO-ACO2* and *TO-ACO3* are each members of a multigene family in *T. occidentale* (Figure 4.16). Multiple hybridizing bands were observed in every restriction enzyme digestion lane. These data suggest that the sequences hybridizing to probes are present in multiple copies in the genome. The banding patterns for TO-ACO2 and TO-ACO3 were similar in the *Eco*R1, *Xba* I and *Hind* III lines digests. Taken together, genomic Southern analysis could not indicate that the two ACC oxidase genes might be encoded by distinct genes in *T. occidentale.*

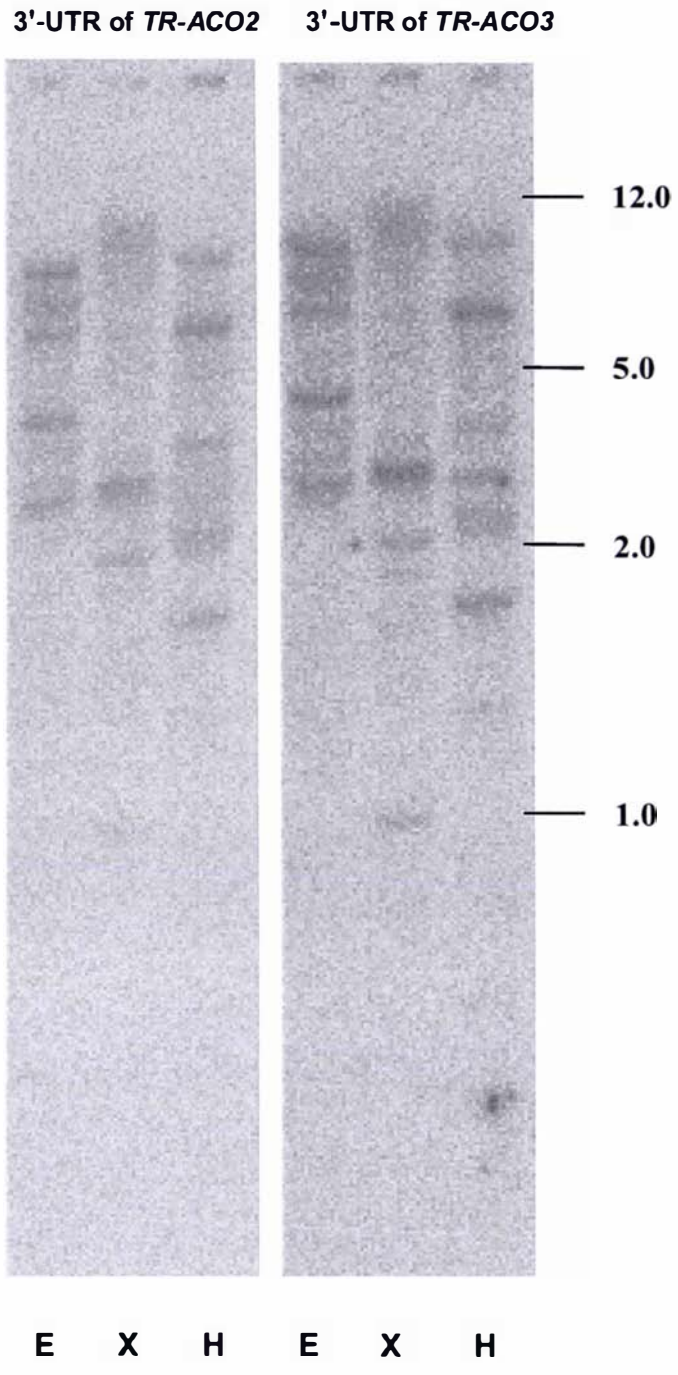

Figure 4.16 Southern analysis of *T. occidentale* genomic DNA

Thirty μg aliquots of genomic DNA were digested with restriction enzymes *Eco*R1 (E), *Xba* I (X) or *Hind* III (H) overnight, separated on a 1% (w/v) agarose gel and blotted onto Hybond™-N^+ membrane with alkaline transfer buffer. The membrane was probed with [α-^{32} P] -dATP labelled probes, and exposed in a FujiFilm BAB (2) cassette with an Imagine® Plate. Molecular sizes are indicated.

4.4 Expression of ACC Oxidase Genes during Leaf Ontogeny

The expression of *TO-ACO2* and *TO-ACO3* genes during both leaf maturation and senescence was studied using northern analysis, with the same 3'-UTR probes used as for Southern analysis (Figure 4.17A). Leaf tissue was pooled into five developmental stages for these studies, depending on the chlorophyll concentration (see section 4.1.2). The five stages used were: (i) newly initiated green leaves (represented by leaf tissue pooled from leaf 1 to 3); (ii) onset of mature green stage (leaf 4 to 6); (iii) mature green stage (leaf 7 to 8); (iv) onset of senescence stage (leaf 9 to 11); and (v) senescence stage (leaf 12 to 14).

As shown in Figure 4.17A, the 3'-UTR probes hybridized to a single RNA transcript of *ca* 1.35 kb. The transcript recognized by the 3'-UTR of *TR-ACO2* accumulated predominantly in newly initiated green leaves and mature green leaves, while the transcript recognized by the 3'-UTR of *TR-ACO3* showed maximal expression in the senescent leaf tissues. The gels used were loaded with total RNA and stained with ethidium bromide (Figure 4.17B). It can be seen that approximately the same amount of total RNA had been fractionated in each lane. So, the differential transcript accumulation patterns observed were not caused by uneven loading of the RNA.

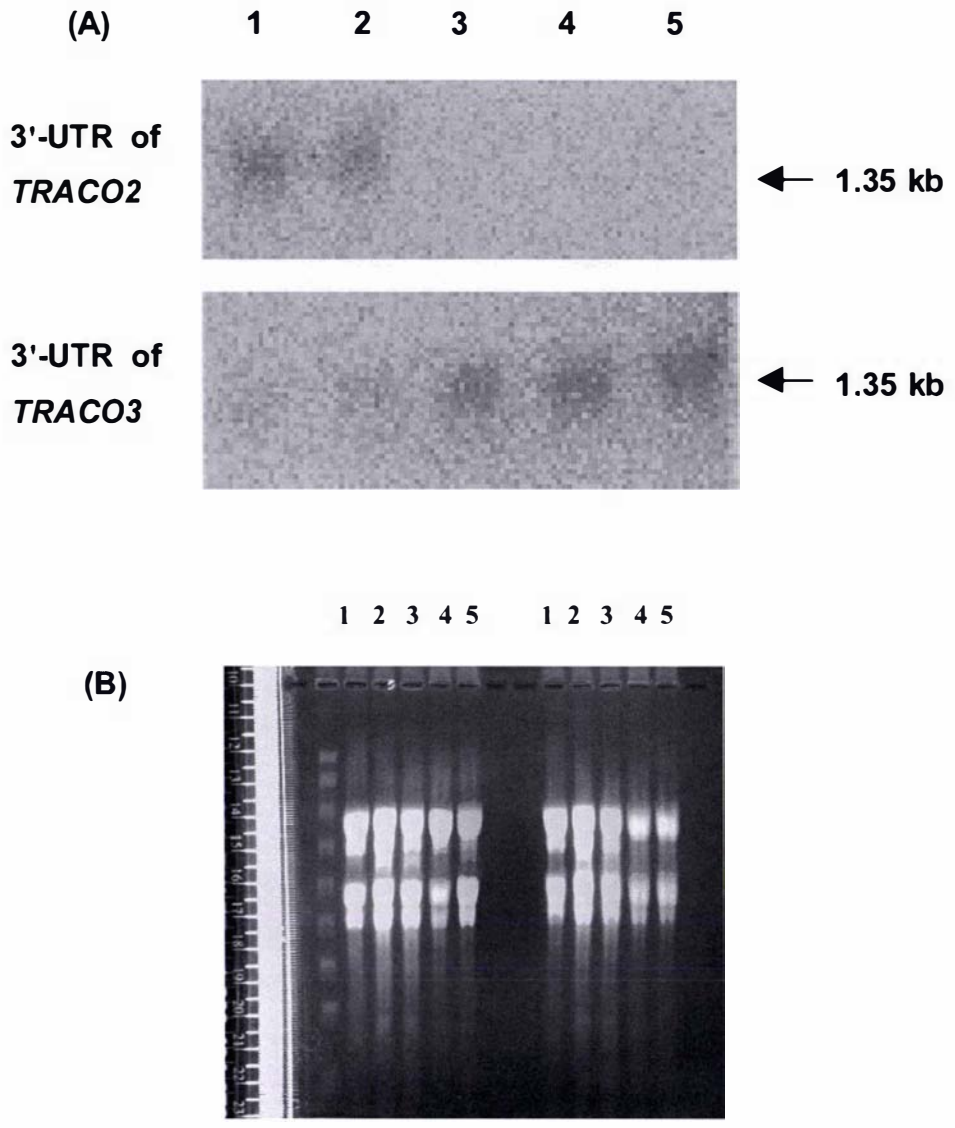

Figure 4.17 Northern analysis of ACC oxidase gene expression during leaf ontogeny in *T. occidentale*

Thirty μg of total RNA was separated on a 1.2% (w/v) agarose-formaldehyde gel, blotted onto the Hybond™-N^+ membrane with alkaline transfer buffer, and probed with [α-^{32} P] -dATP labelled probes. The membrane was washed at high stringency (0.1 × SSPE at 65°C), and was exposed in a FujiFilm BAB (2) cassette with an Imagine® Plate.

(A) Lane 1: Newly initiated green leaf tissue (leaf 1 to 3); Lane 2: Onset of mature green leaf tissue (leaf 4 to 6); Lane 3: Mature green leaf tissue (leaf 7 to 8); Lane 4: Onset of senescence leaf tissue (leaf 9 to 11); Lane 5: Senescence leaf tissue (leaf 12 to 14). The visualization of RNA on northern gel by ethidium bromide was shown in (B).

4.5 Changes in Protein Concentration and ACC Oxidase Activity during Leaf Maturation and Senescence of *T. occidentale*

Changes in ACC oxidase protein accumulation during leaf maturation and senescence of *T. occidentale* was examined by western analysis as described in section 2.3.9. Ten microgram aliquots of protein extracted from leaves 1 to 14 were pooled according to specific development stages. A total of five samples were separated on a SDS-PAGE gel, transferred to a PVDF membrane and the ACC oxidase protein detected with the anti-TR-ACO2 antibody.

The TR-ACO2 antibody raise against the ACC oxidase protein recognized a protein of *ca.* 37 kDa (Figure 4.18), which is in the range reported for ACC oxidases from other plant species (from 36 kDa to 41 kDa). As shown in the Figure 4.18, the accumulation of ACC oxidase protein increased from newly initiated green leaf tissue (lane 1) to mature green leaf tissue (lane 3) at which point accumulation was highest, while accumulation in senescent leaf tissue (lane 5) was lowest.

Table 4.3 summarizes the data obtained from image analysis to quantify the signal band intensity (Figure 4.18). The protein was highest in mature green leaves (sample 3) and then declined as the leaves became chlorotic.

Furthermore, changes in ACC oxidase activity *in vitro* during leaf ontogeny in *T. occidentale* was measured (Figure 4.19). The ACC oxidase activity initially increased until a peak of activity was measured in mature green leaf tissue after which activity declined dramatically. Taken together, the changes of ACC oxidase activity during leaf ontogeny do support the trend observed for ACC oxidase protein accumulation using western analysis and image analysis in *T. occidentale.*

Figure 4.18 Changes in ACC oxidase protein accumulation during leaf ontogeny in *T. occidentale* determined using western analysis

Lane 1: Newly initiated green leaf tissue (leaf 1 to 3); Lane 2: Onset of mature green leaf tissue (leaf 4 to 6); Lane 3: Mature green leaf tissue (leaf 7 to 8); Lane 4: Onset of senescence leaf tissue (leaf 9 to 11); Lane 5: Senescence leaf tissue (leaf 12 to 14). Aliquots (30 μg) from each sample were separated using the SDS-PAGE gel system, electroblotted onto PVDF membrane and challenged with anti-TR-ACO2 antibodies. Lane (M) are prestained molecular mass markers (molecular masses are indicated).

Table 4.3 The intensity and band area of the 37 kDa protein bands recognized by the anti-TR-ACO2 antibody in Figure 4.19

Developmental Stage	AU*	Area (mm^2)	AU/ mm^2
1.	9.709 e + 07	11.13	8719241.70
2.	1.014 e +08	11.57	8764255.77
3.	1.215 e + 08	13.91	8736128.17
4.	8.869 e + 07	10.17	8723712.97
5.	8.341 e +07	9.68	8614703.96

*AU value is displayed as an absorption unit that corresponds to the intensity of bands.

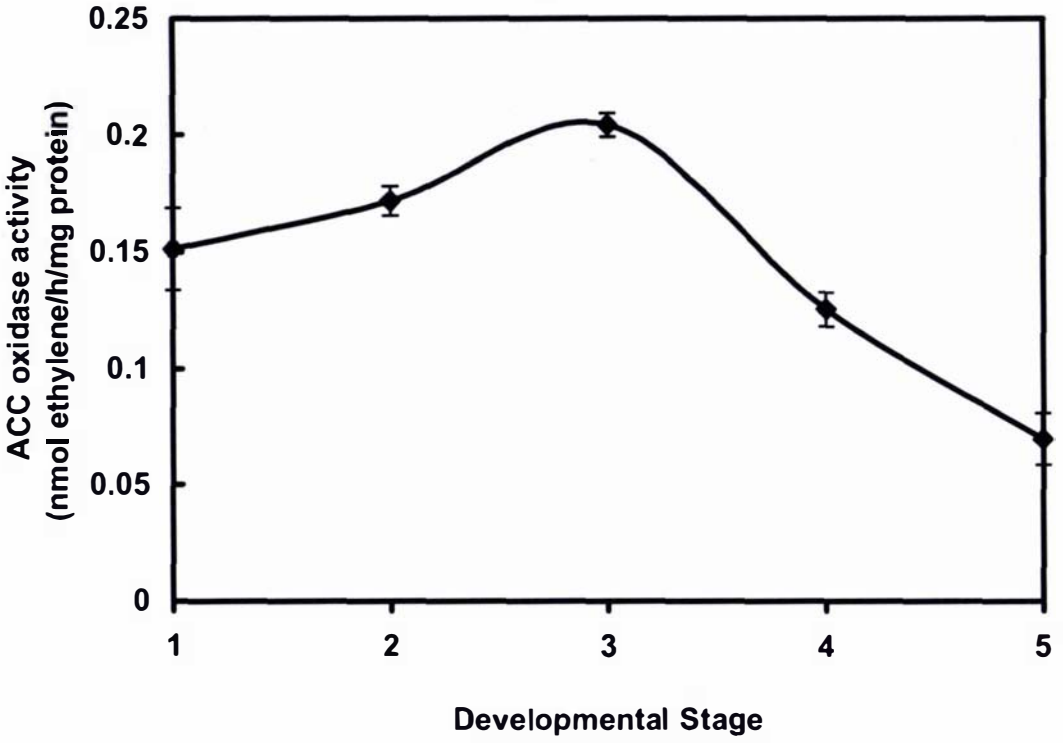

Figure 4.19 Changes in ACC oxidase activity during leaf ontogeny in *T. occidentale*

Developmental stages: 1: Newly initiated green leaf tissue (leaf 1 to 3); 2: Onset of mature green leaf tissue (leaf 4 to 6); 3: Mature green leaf tissue (leaf 7 to 8); 4: Onset of senescence leaf tissue (leaf 9 to 11); 5: Senescence leaf tissue (leaf 12 to 14).

Results are mean values ± s.e., n=3

5. Chapter Five: Discussion

5.1 Overview

Thus far, three distinct ACC oxidase genes during leaf ontogeny in white clover (*T. repens* L.) have been identified (Hunter *et al.,* 1999). Of the three ACC oxidase genes identified, one designated *TR-ACO2*, is expressed in newly initiated and mature green leaves while *TR-ACO3* is expressed predominantly in the senescent leaf tissue. In a separate study, two isoforms (designated MGI and SEII) were purified to homogeneity and some basic biochemical properties, such as apparent K_m and V_{max} for the substrate ACC were characterized (Gong and McManus, 2000). MGI was purified from mature green leaf tissues, while SEII was one of two isoforms identified in senescent leaf tissues (Gong, 1999). However, the study by Gong was not extended to determine whether *TR-ACO2* coded for MGI or *TR-ACO3* coded for SEII.

The research in this thesis is, therefore, divided into two main parts. The first part is concerned with the purification and characterization of ACC oxidase isoforms in leaf tissue of white clover, which extends the study of Gong (1999). This section includes further purification of ACC oxidase isoforms using 2D gel electrophoresis, and the identification of proteins using MALDI-TOF mass spectrometry to determine which isoform *TR-ACO2* or *TR-ACO3* codes for. As well, to more fully understand the role of ethylene in regulating leaf senescence (and therefore the persistence of white clover in pastures), more information is needed on the regulation of these ACC oxidase isoforms during leaf maturation and senescence. This includes the investigation of the rhythm of ACC oxidase activity in mature green leaf tissue, and the regulation of ACC oxidase activity by phosphorylation and dephosphorylation.

The second part of this thesis is concerned with molecular characterization of ACC oxidase during leaf maturation and senescence in *T. occidentale*. This is a diploid clover species, and has a smaller genome when compared with *T. repens* (Badr *et al.*, 2002). As a diploid, selfing species, *T. occidentale* may represent a better genome system when compared with *T. repens* (an outcrossing, allotetraploid species) to carry out more detailed analysis of the regulation of ACC oxidases at the genetic level. Thus the second section of the thesis focused on the isolation of two distinct ACC oxidase

genes during leaf maturation in *T. occidentale* using RT-PCR. These were investigated by Southern analysis, gene expression and protein accumulation studies during leaf ontogeny.

5.2 Part I: Purification and Characterization of ACC Oxidase Isoforms in Leaf Tissue of White Clover (*Trifolium repens* L.)

5.2.1 Stolon Leaf Growth of White Clover

Stolons of white clover were used in this thesis to provide leaf tissue for isolation, purification, and characterization of ACC oxidase isoforms from different leaf development stages (Figure 1.3). Under the controlled experimental conditions used (section 2.1.2), when the rates of leaf initiation and emergence are constant and the changes from node to node represent changes in time (Thomas, 1987), a single harvest time represents all stages of development from leaf initiation, through maturation to senescence, and necrosis.

Previously determined physiological data characterizing changes in ethylene evolution during leaf ontogeny (Hunter, 1998) were used to target specific leaf developmental stages on the stolon. During white clover leaf ontogeny, there are two stages of significant ethylene production. The first stage coincides with leaf initiation at the apex. Ethylene production then typically declines to reach a minimum value by leaf three, and is maintained at this level through the mature green stage of leaf development. After which, a second stage of significant ethylene evolution is observed that coincides with chlorophyll loss.

As well as ethylene evolution, leaf development is also generally measured in terms of chlorophyll loss because leaf senescence is accompanied by the metabolism of chlorophyll and chlorophyll breakdown (Nooden *et al.*, 1997; Hörtensteiner, 1999). For example, oilseed rape has been used extensively as a model plant for the recent elucidation of structures of chlorophyll catabolites during the leaf senescence (Hörtensteiner and Kräutler, 2000). Also, chlorophyll content has been used to examine changes in photosynthetic capacity and as an indicator to identify different developmental stages during leaf ontogeny of white clover (Butcher, 1997; Hunter, 1998; Yoo *et al.*, 2003). The data presented in this thesis also show that the total

chlorophyll content increases during the leaf expansion stage (leave 1 to 3) to reach to a maximum level at leaf 4. It then remains at a relatively constant level until leaf 7, after which it decreases as the rate of degradation overtakes the rate of biosynthesis, and the leaf starts to show visible signs of senescence after leaf 8 (Figure 3.1). So, chlorophyll content can be used as an indicator for further studies when sampling the leaf tissues. After these measurements, leaves at individual nodes along the stolon were grouped into four developmental stages (newly initiated green, mature green, onset of senescence and senescent).

5.2.2 Extraction and Purification of ACC Oxidase isoforms from Newly Initiated Green and Senescent Leaves of White Clover

Since the discovery in 1979 that ACC is the direct precursor to ethylene formation (Adams and Yang, 1979), progress toward the characterization of ACC oxidase has been slow, due largely to the lack of purified enzyme and suitable *in vitro* assays. The first *in vitro* observation of ACC oxidase was from melon fruit due to the discovery of the absolute requirement for the ferrous ion and ascorbate for its *in vitro* activity (Ververidis and John, 1991). There then followed a number of reports on the extraction and partial purification, or purification to homogeneity of the enzyme from a number of other fruit tissues including apple (Dong *et al.*, 1992; Kuai and Dilley, 1992; Dupille *et al.*, 1993; Pirrung *et al.*, 1993), banana (Moya-Leon and John, 1995), cherimoya (Escribano *et al.*, 1996), papaya (Dunkley and Golden, 1998) and pear (Kato and Hyodo, 1999), breadfruit (Williams and Golden, 2002), as well as senescing carnation petals (Nijenhuis-De Vries *et al.*, 1994; Kosugi *et al.*, 1997). Although the purification and characterization of ACC oxidase from fruits has progressed very quickly after an activity assay *in vitro* using appropriate cofactors has been developed, fewer ACC oxidases have been partially purified, or purified to homogeneity from vegetative plant tissue (Gong, 1999).

To determine which ACC oxidase isoform that accumulates during leaf maturation and senescence in white clover is encoded by which gene (*TR-ACO2* or *TR-ACO3*), ACC oxidase enzyme samples of high purity are required to use MALDI-TOF mass spectrometry. Before starting a large-scale extraction and purification of ACC oxidases, the saturation range of ammonium sulphate for the isolation of the protein was optimized, and leaf tissue for both MGI and SEII was selected.

The initial extraction methodology is a key in this study because this step is considered not only to largely reduce the total volume of protein extract from plant tissues but also to allow some purification with almost no loss of enzyme activity (Dupille *et al.*, 1993). Protein precipitation by salting out (increasing the ionic strength) with ammonium sulphate makes use of the surface hydrophobic property of the protein molecule. The concentration of ammonium sulphate used in this extraction step is different from that used by other researchers with different plant species. For example, Dupille *et al.* (1993) used 30% to 90% saturated ammonium sulphate for protein precipitation from the crude extract of apple fruit, while Pirrung *et al.* (1993) precipitated the ACC oxidase protein from the same tissue with 50% to 80% saturated ammonium sulphate. McGarvey and Christoffersen (1992) reported that 30% to 50% ammonium sulphate precipitation was necessary and sufficient to separate the enzyme from avocado fruit. Likewise, Dunkley and Golden (1998) only used 50% ammonium sulphate to precipitate enzyme from crude extracts of papaya fruit. In addition, Smith *et al.* (1992) carried out ammonium sulphate fractionation for the separation the enzyme from melon fruit and used 70% to 90% saturation. Furthermore, protein precipitated from senescing carnation flowers by ammonium sulphate added at 50% to 65% saturation was also observed (Kosugi *et al.*, 1997). In common with Dupille *et al.* (1993), a concentration of ammonium sulphate of between 30% to 90% saturation was used in the ACC oxidase separation from crude extract of white clover leaf tissues (Gong, 1999). So, it was necessary to more precisely define the saturation range of ammonium sulphate for the enzyme purification step to be optimized still further. In this study, a series of different concentrations of ammonium sulphate were tried, and ACC oxidase activity assayed (Table 3.2). It was found that 50% to 70% saturated ammonium sulphates achieved the highest recovery of both total protein and ACC oxidase activity. Consequently, all further experiments were conducted on a range of 40% to 80% saturated ammonium sulphate to make sure that most of the ACC oxidase protein was recovered from crude extract of white clover leaf tissues. The concentration range was the same as that of Escribano *et al.* (1996) used in the purification of the enzyme from cherimoya fruit.

Meanwhile, recovery of ACC oxidase activity *in vitro* in the supernatant of the 26,000 × *g* centrifugation with the common extraction buffer supports the now general thought that ACC oxidase is not membrane bound, but a cytosolic protein (Gong,

1999). Whether ACC oxidase is localized to the cytosol or cell membrane has been debated for many years (see section 1.5.2.2). The results in this thesis indicate that, under these conditions, ACC oxidase activity is soluble and not membrane-bound. Similar results were obtained by Ververidis and John (1991) with extracts from melon fruit; Moya-Leon and John (1995) from banana; Dunkley and Golden (1998) from *Carica papaya*. However, ACC oxidases from apple fruits have been observed to be membrane-associated because the majority of ACC oxidase activity in the apple homogenate was associated with the pellet fraction and could be solubilized by polyvinylpolypyrrolidone (PVPP) or Triton X-100 (Fernández-Maculet and Yang, 1992; Kuai and Dilley, 1992; Dupille, *et al.,* 1993). Peck *et al.* (1992) found that intact cells and protoplasts of transformed yeast expressing ACC oxidase contained equal amounts of the protein whereas vacuoles did not contain any detectable levels. By generating a gradient of specific radioactivity of ACC between cell compartments, Bouzayen *et al.* (1990) showed that ethylene originated from both apoplasmic and intracellular ACC. Rombaldi *et al.* (1994) reported that ACC oxidase is located at the cell wall in the pericarp of ripening tomato and climacteric apple using immunocytological methods. In addition, Ramassamy *et al.* (1998) combined cell fractionation and immunocytological methods and found that ACC oxidase is mainly located at and associated with the external face of the plasma membrane. Recently, Chung *et al.* (2002) re-examined the subcellular localization of ACC oxidase in apple fruit by immunogold labeling with a highly specific antibody raised against the recombinant apple enzyme and demonstrated that apple ACC oxidase was located mainly, if not solely, in the cytosol of apple fruit mesocarp cell. In addition, it should be noted that ACC synthase, which is considered to be a cytosolic enzyme, is also associated with the pellet fraction of apple fruit and can be solubilized in active form with Triton X-100 (Yip *et al.*, 1991). More recently, Chung *et al.* (unpublished data) found that ACC oxidase from the flower of the pollinated *Phalaenopsis* orchid can be readily extracted with only water, suggesting that the association of ACC oxidase with the pellet fraction in apple fruit might be an artifact of extraction (Chung *et al.*, 2002).

In terms of selection of leaf tissue of white clover for isolation and purification of the MGI and SEII isoforms identified by Gong (1999), preliminary experiments using mature green leaves (nodes 4 to 7) showed that two ACC oxidase bands of *ca.* 35 and 37 kDa were recognized with nearly equal intensity by the anti-TR-ACO2 antibody

after purification from both Phenyl Superose hydrophobic interaction and anion exchange Mono Q column (Figure 3.2). This may represent TR-ACO2 and TR-ACO3 as both genes are expressed in mature green leaves (Hunter *et al.*, 1999). Therefore, nodes 2 to 4 (newly initiated green leaves) and 12 to 15 (senescent leaves) were used to purify MGI and SEII isoforms respectively in further experiments.

The initial purification methodology adopted the previous procedures which involved four chromatography steps: hydrophobic interaction on phenyl Sepharose, anion exchange on Mono Q, chromatofocusing on Mono P and finally gel filtration on Superose 12 (Gong, 1999). However, after using this series of FPLC columns, it became apparent that the amount of the partially purified protein was not sufficient for MALDI-TOF mass spectrometric analysis (data not shown). So, it was considered necessary to change the purification procedure. The new purification strategy was based on the aim that the target protein recovery should be increased as much as possible using the FPLC system followed by two-dimensional electrophoresis (2D-Electrophoresis) for further purification. Therefore, chromatofocusing on Mono P was omitted because this mode of separation could be achieved in the first dimension of 2D gel electrophoresis.

The results shown in Figure 3.4 and Figure 3.10 suggest that the ACC oxidase protein has a high degree of surface hydrophobicity (after eluting at 100% buffer B), and so the hydrophobic interaction step should afford significant purification of the enzyme, in which ACC oxidase has been purified from white clover leaves and purifications of 10.2-fold (for mature green leaves) and 15.9-fold (for senescent leaves) were achieved using hydrophobic interaction chromatography (Gong and McManus, 2000). Although the possible biological role for this property of ACC oxidase is unclear now, these results may be attributed to the fact that the protein possesses an amphipathic helix that is inferred on the basis of hydrophobic amino acids present every four to five positions within the highly helical region of the ACC oxidase in apple fruit (Pirrung *et al.*, 1993). In terms of the analysis of deduced amino acid sequence of TR-ACO2 and TR-ACO3, it was found that there are 45% and 44% hydrophobic amino acids in the sequences of TR-ACO2 and TR-ACO3, respectively (Figure 3.25). Moreover, the different point of elution of the two ACC oxidase isoforms isolated from nodes 2 to 4 and 12 to 15 on this column with the same elution program also indicates that they have different

hydrophobicity. This difference is presumably associated with the fact that there is a different number and content of hydrophobic amino acid residues in the surface of two ACC oxidase isoforms, and this is further evidence that the two ACC oxidase isoforms are distinct. Furthermore, the different molecular masses of the two isoforms determined by western analysis also indicate that these two isoforms are distinct, and were designated NIGI and SEI. The ACC oxidase isoform, NIGI is from newly initiated green leaves, and SEI is from senescent leaves, and is the only isoform recognized by western analysis from the elution profile. The NIGI isoform was eluted with no ammonium sulphate in buffer B using hydrophobic interaction chromatography but was recognized as a major band of *ca.* 37 kDa in fractions 35 to 38 by the anti-TR-ACO2 antibody. This result is the same as MGI, which was identified and purified by Gong (1999). As for the SEI isoform, the proteins were also eluted with no ammonium sulphate in the elution buffer (buffer B). A major protein band of *ca.* 35 kDa in fractions 32 to 35 was recognized by western analysis. This observation is similar to the SEII isoform separated using Phenyl Superose hydrophobic interaction column (Gong, 1999).

Following the purification step using hydrophobic interaction column chromatography, anion exchange column chromatography was used and the results are shown in Figure 3.5 and Figure 3.11. These suggested that the NIGI and SEI isoforms from white clover leaf tissues exist as the anionic form at pH 7.5. In addition, both Figure 3.5 and Figure 3.11 showed that two protein peaks were obtained. The first peak represents unbound protein that was not recognized by western analysis (data not shown), with the ACC oxidase isoform being recognized in the second peak. The ACC oxidase isoform NIGI eluted at a sodium chloride concentration range from 210 mM to 290 mM with a determined molecular mass of 37 kDa, while isoform SEI was eluted at a sodium chloride concentration of 260 mM to 320 mM with a determined molecular mass of 35 kDa. These results showed that both NIGI and SEI isoforms were more negatively charged at pH 7.5 when compared with the ACC oxidase enzymes obtained from fruits of apple (125 mM; Dupille *et al.*, 1993) and banana (*ca.* 185 mM; Moya-Leon and John, 1995). The elution profile of NIGI (210-290 mM) broadly agree with the elution profile of MGI (265-371 mM) reported by Gong (1999). However, in this study, SEI is less negatively charged at pH 7.5 when compared with the previous purification work for SEII (371-480 mM), but much more negatively charged at pH 7.5 when compared

with another isoform identified SEI (106 mM) (Gong, 1999). The difference between SEI in this study and SEII in the study of Gong (1999) might be attributed to the different elution programs and a new column that has been used. In this study, the elution program has been changed from the sharp increase in the salt concentration to a gentler slope of a linear gradient to obtain better resolution. Furthermore, it should be noted that the pKa of a buffering substance varies with the temperature. When optimizing FPLC ion exchange, this effect should always be considered since the change in pKa can be quite significant (Pharmacia Lab. Operation Manual, 1985). For example, Tris has a pKa of 8.85 at 0 °C, and 8.06 at 25 °C. The working temperature was always maintained at 4 °C in this study, but the separation by Gong was achieved at 20°C. So, the different working temperature might be another reason for different elution profiles.

The last purification step of the ACC oxidase isoforms involved the use of gel filtration chromatography on a Superose 12 column. The results are shown in Figure 3.6 and Figure 3.12. For the NIGI isoform (Figure 3.6), the most intensely recognized fraction was eluted at fraction 21 which cross-reacted with the anti-TR-ACO2 antibody as two major protein bands. One of these was the NIGI isoform with a determined molecular mass of 37 kDa, which was the same as the MGI isoform purified by Gong (1999) with same elution point from the column and precise molecular mass using SDS-PAGE. The other protein band with a determined molecular mass of 35 kDa is due to either co-purification of two isoforms or post-translational modification of the NIGI protein. As for the SEI isoform (Figure 3.12), the most intensely recognized fraction eluted at fraction 22 which corresponded to an elution volume of 13.8-14.5 ml with a single band of *ca.* 35 kDa proteins recognized by the anti-TR-ACO2 antibody. A more weakly recognized band of *ca.* 35 kDa was observed at fraction 21. This result differs a little when compared with SEII (Gong, 1999). In the study by Gong (1999), SEII eluted in fraction 21 as did MGI. An explanation may be that the elution conditions for gel filtration column chromatography may not be exactly the same as with previous study by Gong (1999). However, the molecular mass of NIGI isoform is larger than SEI, so it is reasonable that NIGI may elute a little earlier than SEI when the same elution program is used. This is because gel filtration chromatography acts like a molecular sieve, and separates proteins solely on the basis of their different molecular masses (Scopes, 1994).

To ascertain the purity of the NIGI preparation after gel filtration chromatography, and to attempt to obtain a sequence from the N-terminal of the isoform, fraction 21 was subjected to SDS-PAGE, and then transferred to PVDF membrane. The 37 kDa protein band was excised from the membrane and submitted for N-terminal amino acid sequencing. Unfortunately, no data were obtained from sequence analysis. This may be due to either the protein concentration being too low, or the N-terminal of the protein was blocked after the series of protein purification steps (D. Carne, University of Otago, *per. comm.*). Similarly, the failure of Dong *et al.* (1992) to obtain a sequence of the ACC oxidase from apple fruit by Edman methods suggested that the protein is blocked at the amino terminus. Pirrung *et al.* (1993) proposed that an acetyl group may be the most reasonable assignment for the amino-terminal blocking group. In this study, because the SEI isoform is only recognized by the anti-TR-ACO2 antibody and the protein band was too weak, it was not submitted for N-terminal amino acid sequencing (data not shown).

The extraction and purification of both NIGI and SEI isoforms in this study suggests that ACC oxidase is not an abundant enzyme in both newly initiated green and senescent leaf tissues of white clover. In the current study, the initial purification step from the crude extract began with *ca.* 1,000 mg of total protein. However, after a series of further purification steps, the amount of protein available for further investigation was very low. In the previous purification of ACC oxidase isoforms from white clover by Gong (1999), a very low recovery based on total protein in crude extract (from 0.00034% to 0.00077%) was also obtained. Using these values for a comparative calculation, theoretical yields of 3.4 μg to 7.7 μg may be expected. Moreover, a molecular study of ACC oxidase from leaf tissue of white clover indicates that two rounds of PCR is required to amplify cDNA sequences for visualization by ethidium bromide staining (Hunter, 1998). Contrary to this observation, some other observations indicated that the ACC oxidase from apple fruit is abundant (Dong *et al.* 1992; Pirrung *et al.* 1993): "it is present at a significant level even in the crude extract" (Pirrung *et al.* 1993). This is probably due to the fact that apple is a climacteric fruit, and Dong *et al.* (1992) pretreated fruit by storage at low temperature (4°C) and monitored ethylene production to detect when fruit was at the climacteric stage and should contain maximal ACC oxidase activity. Furthermore, the ethylene production rate from fruit tissue may be higher than leaf tissue. For example, the specific activity

for the purified enzyme from apple fruit is 1200 nmol ethylene/h/mg protein (Dong *et al.* 1992), while the purified isoforms MGI and SEII displayed specific activities of 25.2 and 29.8 nmol ethylene/h/mg protein, respectively (Gong, 1999).

5.2.3 2D Gel Electrophoresis and MALDI-TOF Mass Spectrometric Analysis for Isoforms NIGI and SEI

Two-dimensional (2D) gel electrophoresis is one of the most powerful techniques for the separation and subsequent identification of proteins in complex biological mixtures since about thirty years ago (O'Farrell, 1975). Over the last decade there have been marked developments, both in 2D gel electrophoresis technology, and in the sensitive methods for the isolation and identification of proteins separated by 2D gel electrophoresis, which have greatly enhanced the power of this technique. More recently, MALDI-TOF mass spectrometric analysis has been used to identify proteins of known amino acid sequences that are listed in the available protein and DNA databases. The combination of MALDI-TOF mass spectrometry, in-gel enzymatic digestion of proteins separated by 2D gel electrophoresis and searches of molecular mass in peptide-mass databases is a powerful and well-established method for protein identification, especially for proteomic analyses. For successful protein identification by MALDI-TOF mass spectrometry of peptide mixtures, critical parameters include highly specific enzymatic cleavage, high mass accuracy and sufficient numbers and sequence coverage of the protein by peptides, which can be analyzed (Soskic and Godovac-Zimmermann, 2001). Fortunately, mass fingerprinting is now feasible for this study because the entire coding sequence of *TR-ACO2* and *TR-ACO3* is known.

In the initial experiments, isoelectric focusing was performed in a linear IPG of 4-7 over a separation distance of 7 cm, and mini gels were used for the second dimension. The protein samples after gel filtration column chromatography were loaded (about 80 μg). One of the major problems encountered during separation of ACC oxidase using 2D gel electrophoresis is believed to be its weak recognition by the anti-TR-ACO2 antibody. As shown in Figure 3.8 and Figure 3.13, although a single spot could be identified for each sample, and they were confirmed as ACC oxidase by western analysis, the intensity of the spots was too faint to submit for MALDI-TOF mass spectrometric analysis. This probably due to the fact that ACC oxidase is not an

abundant enzyme in both newly initiated green and senescent leaf tissues of white clover as mentioned above. In addition, plant material does not typically provide a ready source of proteins for investigation by 2D gel electrophoresis. In general, protein content and concentration are low compared to those found in microorganisms and animal cells (based on fresh and dry weight). Moreover, plant extracts contain numerous compounds (salts, organic acids, phenolics, proteases, pigments, terpenes etc.) that have a negative effect on protein extraction and on isoelectric focusing (IEF) (Jacobs *et al.*, 2001)

In this study, in order to obtain more intense putative ACC oxidase protein spots for MALDI-TOF mass spectrometric analysis, a linear IPG of 4-7 over a separation distance of 18 cm was performed and more protein (800 to 1200 μg) was loaded. For these separations using 2D gel electrophoresis, the loaded samples were obtained after separation through only two FPLC columns (hydrophobic interaction chromatography and anion exchange column chromatography). The function of chromatofocusing on a Mono P column and gel filtration column chromatography can be replaced by the first and second dimensional of 2D gel electrophoresis, respectively. Therefore, this strategy can avoid a potential protein consuming process and increase recovery of the target protein.

Corresponding protein spots were excised from Coomassie or silver stained gels after 2D gel electrophoresis with a higher protein loading. Although database searching against the SWISS-PORT and TREMBL database with tryptic peptides from twelve spots did not identify the target proteins (ACC oxidase), there were four of the twelve spots, G4, G5, S2 and S4 which can be identified as ACC oxidase proteins when the obtained peptide masses were compared manually against the sequences of fragments deduced from *TR-ACO2* and *TR-ACO3* using the MS-Digest program (http://prospector.ucsf.edu/ucsfhtml4.0/ msdigest.htm). Critically in these searches, for spots G4 and G5, the coverage of the predicted protein sequence (TR-ACO2) by tryptic digestion was 24.5% and 37.6%, respectively, while the observed pI (5.1) and molecular mass (37 kDa) for both spots is close to the theoretical pI (5.3) and computed mass (35.7 kDa) of TR-ACO2. As to spots S2 and S4, the percentage coverage of the whole protein sequence (TR-ACO3) for the peptides identified was 13.4% and 18.0%, respectively. The observed pI (5.2) for both spots and molecular masses (35.5 kDa for

S2 and 35.0 for S4) is also close to the theoretical pI (5.5) and computed mass (35.2 kDa). In common with this thesis, Wilson (2000) reported that several proteins showing senescence-related changes in abundance from the leaf tissues of white clover could be identified by MALDI-TOF mass fingerprinting, with percentage coverage ranging from 15% to 35%. More recently, Bykova *et al.* (2003) identified some phosphoproteins involved in important plant mitochondrial processes from potato tubers (*Solannum tuberosum* L.) by using 2D gel electrophoresis for separation followed by MALDI-TOF mass spectrometry for identification. Of the two proteins identified, NAD-isocitrate dehydrogenase could be identified with 18% coverage, while pyruvate dehydogenase E1α subunit could be identified with 15% coverage. In these cases, the target proteins could be identified unambiguously with a combination of the high mass accuracy of tryptic fragments with the known molecular mass and isoelectric point of the target protein.

All four of these proteins were of relatively low abundance, as determined by the faintness of the intensity of target spots when compared with other spots in the same gel. In general, low abundance proteins generate fewer tryptic fragments and therefore there is less chance of successful matches when searching for identical proteins. The reason might be that some peaks are suppressed by others in MALDI-TOF spectra and the higher abundance proteins also tend to generate more tryptic masses, which improves the accuracy of matches.

In addition, another complicating factor might be the presence of several proteins in close proximity to the spots selected. This is because additional masses were found in each peak list. Virtually all of the protein spots probably contain at least two, sometimes more contaminating proteins. Although it was still possible to successfully identify proteins, the additional masses may affect both the search statistics and the search results.

Sequence information was obtained by analysis of a total of eleven and nine peptides generated by trypsin digestion for NIGI and SEI isoforms, respectively. The determined molecular masses of both ACC oxidase isoforms was in close agreement with those calculated from predicted sequence analysis data. Table 3.4 summarizes the data obtained from MALDI-TOF mass spectrometric analysis showing sequence coverage, measured and computed masses and isoelectric points, in which the sequence coverage

is higher than the partial amino acid sequences of ACC oxidase from apple fruit (*ca.* 11%) (Dupille *et al.*, 1993). This is the first demonstration, to the author's knowledge, of ACC oxidase protein separation and identification in both newly initiated green and senescent leaves of white clover by 2D gel electrophoresis and subsequent MALDI-TOF mass spectrometric analysis

Indeed, the position of these proteins (NIGI and SEI) in the 2D gel electrophoresis patterns indicates that they have relatively close molecular masses and isoelectric points when compared with the theoretical data. Taken together, the results of the MALDI-TOF analysis suggests that the spots G4 and G5, as representatives of NIGI, are encoded by *TR-ACO2*, while spots S2 and S4 as representatives of SEI, are encoded by *TR-ACO3*. So, as an extension of the study of Gong (1999), the initial objective of determining which isoform *TR-ACO2* or *TR-ACO3* codes for has been achieved. However, as one can see in Table 3.4, the comparison between the theoretical and observed molecular mass and isoelectric point indicated that there was a clear shift between the theoretical and observed values, which may be due to post-translational modification of ACC oxidase protein of white clover, such as phosphorylation. So, experiments were then undertaken to investigate any post-translational modification of ACC oxidase protein from white clover.

5.2.4 Post-Translation Modification of ACC Oxidase in White Clover

In general, post-translation modification of proteins can involve phosphorylation, glycosylation, acylation, ubiquitination, and protein processing (Battey *et al.*, 1993). However, protein phosphorylation is one of the more important post-translational mechanisms in higher plants, and regulating the phosphorylation state of proteins is a mechanism that is extensively utilized for circadian control, as well as regulating the terminal molecular targets of the clock (Nimmo, 1998; Naidoo *et al.*, 1999; Sugano *et al.*, 1998). For example, two enzymes, nitrate reductase (NR) and sucrose phosphate synthase (SPS), that are regulators of basic metabolic processes in plants, are known to be regulated in a circadian fashion in a variety of species (McClung and Kay, 1994). In tomato, the evidence suggests that phosphorylation cycles mediate circadian regulation of both enzymes, but through different means. SPS is regulated through circadian changes in its phosphorylation state, while cyclic NR activity is due to circadian regulation of its expression, in large part through phosphorylation-dependent

mechanisms that act to affect the level of mRNA encoding the enzyme (Jones and Ort, 1997; Jones *et al.,* 1998). However, Kaiser and Huber (2001) showed in their experiments with whole leaves of spinach and leaf discs, that there was a correlation between low activity state (high degree of phosphorylation) and rapid degradation of NR. In addition, some recent reports also indicated that the NR protein could been rapidly inactivated/activated by phosphorylation/dephosphorylation in higher plants in response to environmental stimuli and various treatments (Lillo *et al.*, 2004; Tucker *et al.*, 2004).

Because some previous preliminary observations have suggested that the expression of *TR-ACO2* might be under circadian regulation (Hunter, 1998) and the phosphorylation and dephosphorylation states of proteins often serves as a regulator of activity during the circadian rhythm in higher plants (Luan, 2003), the rhythm of ACC oxidase activity and phosphorylation and dephosphorylation states was studied in mature-green leaf tissue of white clover.

5.2.4.1 Circadian Regulation of ACC Oxidase Gene and Rhythmicity of ACC Oxidase Activity and Protein in Leaf Tissue of White Clover

By definition, a circadian rhythm is one that persists for a period of approximately 24 h under constant conditions in the absence of an external timing cue (Barak *et al.*, 2000). Production of the hormone ethylene, known to regulate plant growth and development, has been shown to cycle diurnally in sorghum, but this is a nice demonstration that the rhythm is endogenous, and circadian. Interestingly, loss of phytochrome B preferentially increased the amplitude of ethylene expression rhythms at peak phases (Finlayson *et al.,* 1998). In *Stellaria longipes*, Kathiresan *et al.* (1996) found that ethylene evolution was shown to be controlled by a circadian rhythm that correlated with both ACC oxidase mRNA levels and enzymatic activity *in vitro*. A similar phenomenon in sorghum was shown in which ACC oxidase mRNA (*SbACO2*) accumulation and enzyme activity *in vitro* was circadian (Finlayson *et al.*, 1999). In white clover, ACC oxidase activity *in vitro* from a mature green leaf crude extract of white clover was observed to be the highest at 11:30 am and the lowest at 9:00 pm although this experiment has been performed only once (Hunter, 1998). This observation might indicate the existence of a rhythmic property of the ACC oxidase activity in white clover leaves. Therefore, it was necessary to further investigate to

show unequivocally whether the rhythmicity of ACC oxidase activity and protein accumulation does exist.

In order to explore whether *TR-ACO2* expression in leaf tissue of white clover is under a circadian rhythm, changes in ACC oxidase activity *in vitro* and ACC oxidase protein accumulation over a 24-h period in mature green leaf tissue extracts at three h intervals during the short and long day were determined. Also, changes in transcript levels of *TR-ACO2* at long day conditions were analyzed by northern blot analysis.

For experiments represented in Figure 3.20 and Figure 3.22, there are two ACC oxidase activity peaks observed during both the short and long day conditions. The pattern of fluctuation in ACC oxidase activity resulted in a high level at noon, reduced levels until a minimum was reached at 9:00 pm, and then an increase to maximum activity at midnight. Interestingly, a similar pattern of ACC oxidase protein accumulation was obtained in the short day conditions. However, in the long day, the pattern of ACC oxidase protein accumulation does not match well with the pattern of fluctuation in ACC oxidase activity. These results suggest that ACC oxidase extracted from mature green leaves is under a circadian-type control both in terms of enzyme activity and protein accumulation, but control in the long day light period may differ from that in the short day. In addition, the data from this study also suggest that ACC oxidase might be not only translationally but also post-translationally regulated in the leaf tissues of white clover because such modifications are thought to be required to maintain the period of the circadian rhythm to approximately 24-h (Roden and Carré, 2001).

Northern analysis of mature green leaf tissue sampled at three time points during a long day detected a definite pattern of fluctuation in *TR-ACO2* transcript levels. *TR-ACO2* mRNA levels oscillates, with relatively higher expression at midnight (12:00 pm), but lower at noon (12:00 am) and 9:00 pm (Figure 3.24). However, there was no significant difference in transcript level between 12:00 am and 9:00 pm, where ACC oxidase protein also accumulated to the same level using western analysis. Therefore, the pattern of expression of *TR-ACO2* appears to match well with the ACC oxidase protein accumulation measured during the long day conditions, but expression at 9:00 am has yet to be determined. The fact was shown for the expression of *TR-ACO2* reinforces the suggestion that the ACC oxidase might be post-translationally regulated in the leaf tissues of white clover.

It is interesting to note that the *TR-ACO2* mRNA level, ACC oxidase protein content, and ACC oxidase activity displayed a circadian pattern. Together these results suggest that the ACC oxidases involved in ethylene biosynthesis in white clover may be controlled at multiple levels. Similar results were obtained from the circadian regulation of nitrate reductase expression, which may be at the transcriptional or translational as well as post-translational modification levels (Jones *et al.*, 1998; Tucker *et al.*, 2004). Such a regulatory pattern is also similar to that of monoterpene biosynthesis in peppermint glandular trichomes (McConkey *et al.*, 2000), which showed coincidental temporal changes in steady-state transcript abundance and enzyme activities. To our knowledge, this is the first report using transcriptional and translational evidence that ACC oxidase plays a circadian associated role in the leaf tissues of white clover, and extends the work of Hunter (1998) who first provided tentative evidence that the activity of ACC oxidase might be under a circadian-type regulation. Additional support comes from a recent report that ethylene production by intact cotton cotyledinary tissue is rhythmic with very similar patterns for a 24 h period and continuous light treatment suggesting that is a circadian rhythm, and also showed that ACC oxidase is the enzyme that is linked to the circadian clock (Jasoni *et al.*, 2002).

5.2.4.2 Phosphorylation and Dephosphorylation of ACC Oxidase in Leaf Tissue of White Clover

More is now known as to the significance of post-translational modification of proteins by phosphorylation in terms of the regulation of plant development and metabolism (Fallon and Trewavas, 1993). In addition to transcriptional regulation, post-transcriptional mechanisms and protein phosphorylation may also play important roles in regulating the circadian rhythm in higher plant (Sugano *et al.*, 1999; Wang *et al.*, 2004b). The post-translational modification of clock associated proteins in thought to be required to maintain the period of the circadian oscillator to approximately 24 h (Roden and Carré, 2001). In particular, phosphorylation is increasingly prominent as a mechanism of circadian post-translational regulation (McClung, 2000). In order to explore the effect of phosphorylation and dephosphorylation on ACC oxidase activity, and link this to a circadian rhythm, changes in ACC oxidase activity and ACC oxidase protein accumulation were determined. Also, putative phosphorylated and

dephosphorylated ACC oxidase proteins were analyzed by SDS-PAGE and western analysis.

In terms of biological sequence analysis using the NetPhos 2.0 predication server at the (http://www.cbs.dtu.dk/services/NetPhos/; Blom *et al.*, 1999), both TR-ACO2 and TR-ACO3 sequences have at least a theoretical possibility of phosphorylation (Figure 3.25). However, although protein phosphorylation might be involved in the regulation of ACC oxidase activity by theoretical analysis, there is no direct evidence of this to date.

To determine the effect of protein phosphorylation and dephosphorylation on ACC oxidase activity, leaf tissue was sampled at three key time points during the day and night. ACC oxidase activity during the maximum periods increased dramatically (36% at 12:00 am and 56% at 12:00 pm) after dephosphorylation. However, there were only 21% changes in activity between the phosphorylation and dephosphorylation state was observed at the minimum period (Figure 3.29). The findings of the present study suggest that ACC oxidase might be modified by protein phosphorylation in leaf tissue of white clover, and activity is regulated through the phosphorylation/ dephosphorylation states. In addition, this means that phosphorylation might be a mechanism of circadian post-translational regulation of ACC oxidase in leaf tissues of white clover. A similar result has been reported previously in tomato by Jones and Ort (1997) using inhibitors and phosphatases, which demonstrated that circadian regulation of sucrose phosphate synthase activity is the result of rhythmic cycling of the enzyme phosphorylation state. Moreover, it is now clear that nitrate reductase is inactivated and rapid degradated by phosphorylation, and activated by dephosphorylation in higher plants (Kaiser and Huber, 2001; Lillo *et al.*, 2004). Furthermore, a recent study has shown clearly that protein phosphorylation of ACC synthase occurs *in vivo* in tomato (Tatsuki and Mori, 2001). However, after inhibitors studies it was still unknown in this thesis whether ACC oxidase was directly phosphorylated or whether other proteins that control ACC oxidase activity or stability were phosphorylated.

To investigate this possibility in white clover, both SDS-PAGE mini-protein gel and gradient gel systems were used to determine whether the phosphorylation state of ACC oxidase alters its properties, such as molecular mass. The experiments determined that the molecular mass of ACC oxidase protein after dephosphorylation is lower

(*ca.* 1.0-1.5 kDa) when compared with the phosphorylated enzyme (Figure 3.30 to Figure 3.32). In the dephosphorylated state, the molecular mass is closer to the calculated molecular mass from the deduced amino acid sequence of TR-ACO2 (Table 3.4) because there is about 1.3 kDa difference between observed and theoretical molecular masses. The present study could help to elucidate why there are multiple spots at the same molecular mass (ie.with different isoelectric points) or spots with different molecular masses after 2D gel electrophoresis. The major reason might be due to ACC oxidase protein existing at different phosphorylation or dephosphorylation states. In maize, the tightly regulated acidic ribosomal protein (ARP) separates as three spots with different pIs as determined by IEF, and this has been shown to be due to different phosphorylated forms (Montoya-García *et al.*, 2002). Moreover, because the sequence surrounding the three potential phosphorylation sites (S^{98}, Y^{229}, S^{231}) identified using the NetPhos 2.0 in TR-ACO2 are conserved in a consensus sequence derived from 23 ACC oxidases (data not shown), phosphorylation might be a general feature of the ACC oxidase in other species besides white clover. In addition to the NetPhos 2.0 assessment of putative phosphorylation residues on ACC oxidase proteins, Kadyrzhanova *et al.* (1997) also proposed that Ser^{231} and Thr^{178} were putative phosphorylation sites. $Ser^{231}$is also identified by NetPhos 2.0 but not Thr^{178}. However, which residues are phosphorylated *in vivo* can also be determined by ^{32}P-labeling and immune-precipitation studies. Nevertheless, this is the first demonstration, to the author's knowledge, that ACC oxidase proteins may be phosphorylated and dephosphorylated, which may play a role in the function of the circadian rhythm in leaf tissue of white clover.

5.3 Part II: Molecular Characterization of ACC Oxidase during Leaf Maturation and Senescence in *Trifolium occidentale*

5.3.1 Physiological Analysis of *T. occidentale* Clonal Growth in the Model System and Compare with White Clover

Why was *Trifolium occidentale* chosen as another model system for this research project? The main reason is that *T. occidentale* is a diploid clover species and has a small genome when compared with white clover, which is an allotetraploid, and an outcrossing species (Thomas, 1987). Although white clover was used in this thesis to provide an ideal model system for purification and characterization of ACC oxidase isoforms during leaf ontogeny, as a diploid, selfing species, *T. occidentale* might be a better genome system for the use of standard genetics approaches. In addition, *T. occidentale* is a physically small plant, allowing many individuals to be grown in a small area, and hundreds of progeny can be produced per generation. Therefore, the focus on use of *T. occidentale* to study the role of the ACC oxidase multi-gene family in detail is due to the ease of the use of molecular genetics in this clover species when compared with white clover. However, before beginning such experiments, it is necessary to study the stolon growth of *T. occidentale* using the white clover growth system, and to determine whether the different expression of ACC oxidase genes during leaf maturation and senescence occur in the same way in *T. occidentale* as it does in white clover.

Stolons of the *T. occidentale* genotype 18Z were grown using the same method as the white clover genotype 10F (section 2.1.2), and produced leaves at a constant rate and exhibited a consistent pattern of leaf development allowing replication of plant material for analyses. In common with white clover, *T. occidentale* plants also have a stoloniferous growth habit. At a single harvest time, leaf tissue replicated across individual stolons can be collected as representing all stages of development from initiation to maturation, senescence and necrosis. Stolons of *T. occidentale* were used in this thesis to provide leaf tissue for molecular characterization of ACC oxidase during leaf maturation and senescence (Figure 1.5). Before determining whether orthologues of *TR-ACO2* and *TR-ACO3* occur in *T. occidentale*, some basic physiological

properties of leaf development have been examined and compared with white clover, including leaf fresh weight, leaf area, chlorophyll content, and nitrogen content.

In this study, for both *T. occidentale* and white clover when grown under the conditions used, it was found that the first four (for *T. occidentale*) or three (for white clover) leaves are still expanding, whereas leaf 5 (for *T. occidentale*) and leaf 4 (for white clover) have almost reached full size in terms of leaf fresh weight and leaf area. After leaf 11 (for *T. occidentale*) or leaf 12 (for white clover), both leaf fresh weight and leaf area display a decreasing trend. However, the leaf fresh weight changes display a more steady gradual decrease when compared with leaf area. This might be caused by the accumulation of inorganic substances, such as sodium, chlorine, calcium and magnesium that accumulate in senescing leaves during leaf senescence (Lin and Wang, 2001). That the leaf fresh weight increases as the leaf senesces was determined using leaf discs excised from the basal part of leaf blades (in order to be comparable among the nodes) at each node for both *T. occidentale* and white clover (Figure 4.3 and Figure 4.4). Therefore, leaf development on both model stolon systems is balanced between initiation of leaf tissue at the apex and senescence of leaves at the basal portion of stolons.

Chlorophyll content at each node of *T. occidentale* was also measured to confirm the developmental stage of leaves as mentioned above. The observation in this part also confirmed that developing leaves are denoted by an increase in the total chlorophyll content, mature green leaves by a relatively constant (maximum) level of chlorophyll and senescent leaves by a discernible decrease in chlorophyll levels (Figure 4.5). In addition, partitioning of total chlorophyll into chlorophyll *a* and chlorophyll *b* indicated that approximately 70% of total chlorophyll was chlorophyll *a* while 30% of total chlorophyll was chlorophyll *b*. Although chlorophyll *a* and *b* have identical structures except for the side chain at C-7 which is a methyl group in chlorophyll *a* and a formyl group in chlorophyll *b* (Rüdiger, 2002), when leaf tissue ages, chlorophyll *a* was degraded slightly faster than chlorophyll *b*, which is revealed by the ratio of chlorophyll *a:b* from 2.42 at leaf 4 to *ca.* 2.20 between leaf 10 to14 (Figure 4.5). Similar results have been reported in other plant species, for example, barley and oat (Young *et al.*, 1991), meadow fescue (Gut *et al.*, 1987), and wheat (Lu and Zhang, 1998a), in which the relative abundance of chlorophyll *b* increases as leaf senescence progresses due to a

preferential loss of chlorophyll *a* in senescing leaf tissue. Although the absolute reason for this is still unknown, a probable reason is that every chlorophyll molecule in higher plants is complexed with one of several membrane proteins, which proteins form stronger coordination bonds with chlorophyll *b* when compared with chlorophyll *a* (Ruban *et al.*, 1999). Moreover, the chlorophyll *b* molecules are hydrogen-bonded to amino acid sidechains, which further strengthens the interaction with the protein (Liu *et al.*, 2004). This differential degradation of chlorophyll components is proposed to support the operation of a chlorophyll *b-a* cycle in higher plants during leaf senescence (Thomas, 1997). However, for other species, such as maize (Lu and Zhang, 1998b), no decrease in the chlorophyll *a:b* ratio has been reported. Therefore, the function of chlorophyll cycle is believed to supply either chlorophyll *a* or chlorophyll *b*, according to the particular physiological need, and to satisfy that need at the cost of preformed chlorophyll. In other words, plants can potentially use the reactions of the chlorophyll cycle to adjust the ratio of chlorophyll *a:b* to the particular need under various physiological and environmental conditions (Rüdiger, 2002). Taken together, the results of the current study, and that of Butcher (1997) and Hunter (1998), in terms of the pattern of chlorophyll variation, are similar. The data demonstrated that leaves at each node could be categorized into four developmental stages (newly initiated green, mature green, onset of senescence and senescent), and can be used as an indicator for further studies when sampling the leaf tissues from *T. occidentale.*

Senescence is a complex, highly regulated developmental phase in the life of a leaf that results in the coordinated degradation of macromolecules and the subsequent mobilization of components to other parts of the plant (Buchanan-Wollaston, 1997). Chlorophyll and thylakoid proteins account for about 25% of the total nitrogen content of mature leaves (Evans, 1988; Peoples and Dalling, 1988). During senescence, plants undergo a switch from a "nitrogen assimilation" status to a "nitrogen remobilization" status when senescence takes place within the leaf (Feller and Fischer, 1994; Masclaux *et al.*, 2000). In order to investigate the relationship between nitrogen content and leaf senescence and chlorophyll concentration, an experiment was carried out to determine changes in the concentration of leaf nitrogen during ontogeny in both *T. occidentale* and white clover. In the present study, the consistent decline in leaf nitrogen concentration in both species has been shown to be associated with leaf senescence, with a loss of 31% and 42% of leaf nitrogen concentration in the developmental

transition from mature green to senescent in *T. occidentale* and white clover, respectively (Figure 4.6 and 4.7). The profile of nitrogen concentration in leaves might be associated both with the protein concentration (data not shown) and chlorophyll concentration as well as that in leaves that progress from the onset senescence to senescence. The decline in leaf nitrogen concentration presumably reflects the mobilization of nitrogen to developing parts of the stolon, and also partially reflects protein and chlorophyll degradation during leaf senescence. Therefore, the results suggested that leaf nitrogen played a significant role in leaf development and senescence. Peoples *et al.* (1983) found similar results in cowpea, in which the leaflets at lower vegetative nodes lost 44-57% of their nitrogen concentration during leaf senescence. Moreover, the leaf nitrogen concentration as a function of leaf age has been documented in leaves of cotton during ontogeny, in which the leaf nitrogen content also declined about 60% during leaf senescence (Bondada and Oosterhuts, 1998). Furthermore, the decrease in nitrogen with advancing leaf age may be a genetically programmed process (Buchanan-Wollaston, 1997), which results in translocation of nitrogen from old leaves to new leaves and reproductive structures (Field and Mooney, 1986).

5.3.2 Identification of ACC Oxidase Genes from *T. occidentale* Using RT-PCR

To identify ACC oxidase genes expressed during leaf ontogeny in *T. occidentale*, an RT-PCR approach was used with total RNA isolated from different developmental stages as templates. The reading-frames (protein-coding regions) of ACC oxidase genes were successfully amplified and the sequences showed high homology to ACC oxidases in the GenBank database. Based on nucleotide sequence identity, the ACC oxidase genes can be categorized into two groups, designated as *TO-ACO2* (Figure 4.12) and *TO-ACO3* (Figure 4.13) because they are *TR-ACO2*- and *TR-ACO3*-like sequences, respectively. These two sequences showed 82% identity in their nucleotide and 84% identity in their amino acid sequences to each other.

In this study, RT-PCR with nested degenerate primers made to conserved regions of ACC oxidase genes together with cloning and sequencing was successful at identifying *TO-ACO2*, but *TO-ACO3* was not identified by this method. This might be a function of the abundance of the transcript in the tissue used to isolate RNA for the RT-PCR. So, if the *TO-ACO3* transcript is present in only lower amounts when compared with

TO-ACO2 in leaf tissue it may be more difficult to amplify, and will therefore be cloned to a lesser extent. As a result, the cloning of such gene transcripts may only be achieved by screening large numbers of clones. But, because there is high nucleotide sequence identity between *TO-ACO2* and *TR-ACO2*, it was reasonable to assume that there might be also high homology between any putative *TO-ACO3* and *TR-ACO3*. So, to amplify and clone a putative *TO-ACO3*-like gene expressed specifically in senescent leaf tissues of *T. occidentale*, gene-specific primers based on the DNA sequence of *TR-ACO3* were used. These were effective at amplifying a *TR-ACO3*-like sequence, designated *TO-ACO3*. This successful identification may also imply that the use of gene-specific primers increases the sensitivity of amplification using PCR.

The ACC oxidase transcripts are present in very low abundance, as indicated by the necessity for two rounds of PCR to amplify cDNA sequences with a greater number of cycles (35 cycles for each round) before visualization by ethidium bromide staining. This result probably suggests that the level of ACC oxidase gene expression in leaf tissue of *T. occidentale* might not be as high as reported from other plant species, such as melon leaf tissues (Lasserre *et al.*, 1996; 1997). Here, the three ACC oxidase genes cDNA sequences can be amplified with only one round PCR with 25 cycles. Furthermore, the *TO-ACO2* and *TO-ACO3* genes were amplified with high frequency from cDNA templates made from RNA isolated from different developmental stages. The frequency of the gene cloned from RT-PCR products in this system could be correlated with the level of expression of each ACC oxidase gene in leaf tissues of *T. occidentale*. This suggests that *TO-ACO2* is expressed mainly in newly initiated green leaves, while *TO-ACO3* is expressed predominantly in the senescent leaf tissue. In common with this study, a similar pattern in which three genes of ACC oxidase are differentially expressed has also been reported for melon leaf tissues using RT-PCR analysis (Lasserre *et al.*, 1996; 1997).

It is clear now that ACC oxidase has some conserved amino acid residues and require some crucial amino acid residues for maximal activity of the enzyme (Kadyrzhanova *et al.*, 1997; 1999; Dilley *et al.*, 2003). Both *TO-ACO2* and *TO-ACO3* appear to encode functional enzymes, as their deduced amino acid sequences contain all the residues hitherto shown to be important for maximal activity of the enzyme. Therefore, this is evidence to further confirm that both transcripts encode functional

ACC oxidases. In addition, it was of interest to see whether *TO-ACO3* was more closely related to other senescence-associated ACC oxidases than it was to *TO-ACO2*. The phylogenetic analysis using a tree building programme (Figure 4.15) indicated that *TO-ACO2* and *TO-ACO3* fall within the same ACC oxidase group, and also confirmed that they are not only much closer to each other, but also grouped with *TR-ACO2* and *TR-ACO3* from white clover. However, the phylogenetic tree clearly showed that *TO-ACO3* was more closely related to *TR-ACO3* than *TO-ACO2*, while *TO-ACO2* more closed related to *TR-ACO2*. This result may suggest that these isoenzymes have arisen from a common ancestor (mature green or senescence-associated), and that the conditions associated with mature green and senescing tissue may select for an isoenzyme with particular sequence constraints (Hunter, 1998). However, more complete proof will await either the investigation after purification of the individual isoezymes corresponding to each gene identified by MALDI-TOF mass spectrometry, or expression and detection of ACC oxidase activity in heterologous systems.

In common with ACC synthases, ACC oxidase comprises a multigene family, which has been reported in many plant species by screening genomic libraries or screening cDNA libraries. In some plant species, the identification of all the genes in the family is considered to be complete. For example, four genes in *Petunia hybrida* (Tang *et al.*, 1993), four genes in tomato (Holdsworth *et al.*, 1987; Hamilton *et al.*, 1991; Bouzayen *et al.*, 1993; Barry *et al.*, 1996; Nakatsuka *et al.*, 1998), three genes in melon (Lasserre *et al.*, 1996), three genes in sunflower (Liu *et al.*, 1997), three genes in *Nicotiana glutinosa* (Kim *et al.*, 1998). In other plant species, the identification of all genes is still under progress, such as two genes in peach (Ruperti, *et al.*, 2001), and two genes in papaya (Chen *et al.*, 2003; Lopez-Gomez, *et al.*, 2004) having been identified. As a general feature, ACC oxidase genes are highly homologous in the coding regions both within the same family and between families from different plant species, but show some degree of divergence within the untranslated flanking sequences. For example, in petunia, the four ACC oxidase cDNAs displayed only 42 % to 43% homology in their 5'-untranslated regions (UTRs) and 50% to 57% homology in their 3'-UTRs (Tang *et al.*, 1994). Similarly, in the leaves of white clover, the three distinct ACC oxidase genes exhibit a high level of sequence divergence within their 3'-untranslated regions from 55% to 61% (Hunter *et al.*, 1999). Gene-specific probes have been used to study the differential expression of these genes in various tissues and

during different stages of development (Barry *et al.*, 1996; Lasserre *et al.*, 1996; Hunter *et al.*, 1999; Ruperti *et al.*, 2001; Mathooko *et al.*, 2001; Kato *et al.*, 2002).

Because the *TO-ACO2* and *TO-ACO3* gene sequences have highest homology with *TR-ACO2* and *TR-ACO3*, respectively, the 3'-UTRs of *TR-ACO2* and *TR-ACO3* (created by Hunter, 1998) were used as probes in genomic Southern analysis. The results shown in Figure 4.16 did not confirm that these two genes represented two different members of the *T. occidentale* ACC oxidase gene family and did not support the existence of a multi-gene family in this species.

5.3.3 Gene Expression of *TO-ACO2* and *TO-ACO3* during Leaf Ontogeny in *T. occidentale*

Expression studies of *TO-ACO2* and *TO-ACO3* genes during leaf development of *T. occidentale* have been conducted using 3'-UTRs of *TR-ACO2* and *TR-ACO3* as probes in northern analysis. Approximately equal amount of total RNA extracted from pooled leaves from each developmental stage were used for northern analysis. As reported by Bleeker (1998), total RNA declines significantly during leaf senescence, so differing amount of leaf tissues were required from different developmental stages to ensure equal quantities of total RNA.

In this study, hybridization with the 3'-UTR probes of the *TR-ACO* genes indicated that *TO-ACO2* is expressed predominantly in newly initiated and leaf tissue at the onset of the mature green stage, while *TO-ACO3* shows maximal expression in the senescent leaf tissue. The differential expression of *TO-ACO2* and *TO-ACO3* during leaf senescence is consistent with what has now been found in white clover (Hunter *et al.*, 1999), tomato (Barry *et al.*, 1996), and melon (Lasserre *et al.*, 1996; 1997). In white clover, for example, *TR-ACO1* is expressed almost exclusively in the developing apex, *TR-ACO2* shows maximal expression in mature green leaves, while gene expression of *TR-ACO3* is very low in mature green leaves, but increases prior to the large decline in chlorophyll and is expressed predominantly in the senescent leaf tissue. In melon, gene expression studies show that *CM-ACO3* is highest in young leaves and declines to be lowest in mature green leaves, and is very similar to *TO-ACO2* and *TR-ACO2* gene expression. In contrast, *CM-ACO1* is lowest in young leaves, highest in pale-green adult leaves, a pattern of expression that more closely resembles that of *TO-ACO3* and

TR-ACO3. In addition, of the four ACC oxidase genes detected in tomato, *LE-ACO1* and *LE-ACO3* gene transcripts accumulate during leaf senescence. However, *LE-ACO3* only accumulates transiently, at the onset of senescence, and its levels are much lower than *LE-ACO1*. By contrast, the *LE-ACO1* gene transcripts are high at all stages of senescence examined. *LE-ACO2* is mainly expressed in the anther cone, whereas *LE-ACO4* and *LE-ACO1* expression occurs during fruit ripening (Barry *et al.*, 1996; Nakatsuka *et al.*, 1998). More recently, Ruperti *et al.* (2001) reported that two ACC oxidase genes from peach are also expressed in a differential manner in flowers, fruit and leaves. Expression analyses indicate that the increase in *PP-ACO1* transcript accumulation appears to be mainly related to the ethylene burst occurring during ripening, abscission and leaf senescence. In contrast, *PP-ACO2* seems to be specifically associated with growth in both vegetative and reproductive organs. Furthermore, in papaya, expression analysis indicated that *CP-ACO2* is expressed only at the late stage of fruit ripening and leaf senescence, whereas *CP-ACO1* is induced before color break (mature) stage, which suggest that *CP-ACO2* is a late-stage-associated ACC oxidase occurring during organ senescence, such as fruit ripening and leaf senescence, while *CP-ACO1* is maturation-associated (Chen *et al.*, 2003).

This study has extended the gene expression studies by combining gene expression analysis with the determination for both ACC oxidase protein accumulation and enzyme activity during leaf maturation and senescence. The protein translation level was determined by western analysis using ammonium sulphate precipitated proteins. It revealed a single band (Figure 4.18), thus demonstrating that antibodies raised against white clover ACC oxidase cross-react with the protein isolated from *T. occidentale* with high specificity. It is not surprising in view of the great sequence homology between ACC oxidase related cDNAs from white clover (Hunter, 1998) and *T. occidentale*, in which TO-ACO2 shares 98% identity at the amino acid level to the TR-ACO2 protein while TO-ACO3 displays 96% identity with the TR-ACO3 protein. ACC oxidase protein accumulation was highest in mature green leaves and then declined as the leaves became chlorotic (Figure 4.18, Table 4.3), which correlated with ACC oxidase activity *in vitro*. This result showed that ACC oxidase activity initially increased and reached the highest point in mature green leaf tissue, after which, the activity declined dramatically during leaf senescence. Also, this result is quite similar to that observed in white clover (Hunter, 1998). Although the vast majority of natural and

cultivated forms of white clover are allotetraploid species, *T. occidentale* is diploid species. Originally, some studies proposed that the diploid *Trifolium nigrescens* is one of the ancestors of *T. repens*, while the other ancestor may be *T. occidentale*, which indicates a close relationship between *T. repens* and *T. occidentale* (Chen and Gibson 1971). However, more recently, reports suggest that the two genomes of the tetraploid white clover could have been derived from hybridization between *T. uniflorum* and *T. nigrescens*. However, the high values of genetic identity and the low values of genetic distance between *T. occidentale* and each of *T. uniflorum* and *T. nigrescens* suggest that introgression of genes from the former species into the genomes of the latter two species may also have taken place (Badr *et al.*, 2002). Taken together, both the biochemical properties investigations and molecular studies do support the hypothesis that there is close relationship between *T. occidentale* and white clover.

5.4 Conclusions

Plants of white clover (genotype 10F) and *T. occidentale* (genotype 18Z) were propagated by the method of Butcher (1996) to produce individual stolons, which contained leaf tissue representative of all developmental stages, from leaf initiation, maturation through to senescence. The leaf developmental pattern for both species was highly reproducible between vegetatively propagated clones.

In this thesis, following partial purification by a series of FPLC columns, 2D gel electrophoresis was used for further purification. Thus two distinct isoforms of ACC oxidase, designated NIGI and SEI, have been successfully identified and partially purified from newly initiated green and senescent leaf tissue of white clover. Both purified NIGI and SEI proteins were recognized by western analysis using an anti-TR-ACO2 antibody after SDS-PAGE or 2D gel electrophoresis. The position of NIGI and SEI proteins in 2D gel electrophoresis patterns indicated that they have relatively close molecular masses and isoelectric points when compared with theoretical data derived from the known amino acid sequence of *TR-ACO2* and *TR-ACO3*, respectively. Subsequently, sequence information from the MALDI-TOF mass spectrometric analysis suggested that the NIGI isoform is encoded by *TR-ACO2*, while the SEI isoform is encoded by *TR-ACO3*.

ACC oxidase activity *in vitro* and ACC oxidase protein accumulation over 24 h in mature green leaf tissue extracts during the short and long day have been shown to be under circadian control. In addition, northern analysis indicated that the *TR-ACO2* mRNA level also displayed a circadian pattern of variation. Taken together and in common with other species, ACC oxidase involved in ethylene biosynthesis in white clover is controlled at the both transcriptional and translational levels.

The investigation on the effect of protein phosphorylation and dephosphorylation on ACC oxidase activity indicated that activity during the maximum circadian period increased 36% at 12:00 am and 56% at 12:00 pm after dephosphorylation, respectively, but no significant changes between the phosphorylation and dephosphorylation state at 9:00 pm (the minimum period of activity) was observed. Moreover, both the SDS-PAGE mini-protein gel and gradient gel system showed that the molecular mass of ACC oxidase decreased after dephosphorylation when compared with the

phosphorylated enzyme. These results suggest that the phosphorylation and dephosphorylation of the ACC oxidase protein occurs *in vitro* and the state does affect enzymatic activity.

In the second part of this thesis, the coding regions of putative ACC oxidases gene transcripts were generated from leaf tissue of genotype 18Z of *T. occidentale* using RT-PCR. Sequence alignments indicated that the sequences could be grouped into two distinct classes, and these coding regions were designated *TO-ACO2* (*Trifolium occidentale* ACC oxidase 2) and *TO-ACO3* (*Trifolium occidentale* ACC oxidase 3). *TO-ACO2* and *TO-ACO3* shared 82% similarity in nucleotide sequence and 84% similarity in amino acid sequence. The *TO-ACO2* and *TO-ACO3* sequences were validated as encoding ACC oxidase by comparison with other ACC oxidases in the GenBank database and both TO-ACO2 and TO-ACO3 deduced amino acid sequences contain all the residues hitherto shown to be important for maximal activity of the enzyme. Further, *TO-ACO2* has 98% identity at the amino acid level and 97% identity at the nucleotide level to *TR-ACO2*, and *TO-ACO3* has 96% identity at the amino acid level and 97% identity at the nucleotide level to *TR-ACO3*. Genomic Southern analysis, using the 3'-UTRs of *TR-ACO2* and *TR-ACO3* as probes, suggests that the sequences are encoded for by distinct genes. To confirm this observation, Southern analysis would need to be repeated with 3'-UTRs of *TO-ACO2* and *TO-ACO3*.

Expression studies of *TO-ACO2* and *TO-ACO3* genes during leaf maturation and senescence of *T. occidentale* were examined using northern analysis. *TO-ACO2* and *TO-ACO3* are expressed differentially during leaf ontogeny. *TO-ACO2* is expressed predominantly in newly initiated and at the onset of mature-green leaf stage, while *TO-ACO3* shows maximal expression in the senescent leaf tissue. Again, these results are indicative, since they would need to be confirmed using the 3'-UTRs of *TO-ACO2* and *TO-ACO3*.

The changes of ACC oxidase activity during leaf ontogeny of *T. occidentale* coincided with the pattern observed for ACC oxidase protein accumulation using western analysis and image analysis.

5.5 Suggestions for Future Work

The work in this thesis includes two main parts. One is concerned with purification and characterization of the two distinct isoforms of ACC oxidase in leaf tissue of white clover. This includes the further purification of ACC oxidase isoforms using 2D gel electrophoresis, and sequencing of proteins using MALDI-TOF mass spectrometry to determine which isoform *TR-ACO2* or *TR-ACO3* codes for. As well, investigation of the rhythm of ACC oxidase activity from mature green leaves, and regulation of ACC oxidase activity between phosphorylation and dephosphorylation was investigated. The second part concerned the molecular characterization of ACC oxidase during leaf maturation and senescence in *T. occidentale.* This included the generation of the two distinct ACC oxidase genes from leaf tissue using RT-PCR, confirmation of both sequences using genomic Southern analysis, and investigation of gene expression using northern analysis and protein accumulation using western analysis. This study has uncovered many interesting avenues that can be pursued further. In terms of future studies, some suggestions are as follows:

- In this study, ACC oxidase protein content and ACC oxidase activity displayed a circadian pattern of variation in the mature green leaf tissues of white clover. These results suggest that the ACC oxidase involved in ethylene biosynthesis in white clover may be controlled at the both transcriptional and translational level. Further investigation would need to be confirmed the rhythmicity of ACC oxidase at the level of gene expression level using more time points in both long and short days.

- The phosphorylation /dephosphorylation experiments should be repeated with leaf tissues from a series of plant species and needs to address some important questions. These include how ACC oxidase is really regulated by its phosphorylation state, and further studies are needed to determine whether the phosphorylation of ACC oxidase is reversible and whether other ACC oxidase isozymes are phosphorylated.

- Further investigation is required on the purification and kinetic characterization of TO-ACO2 and TO-ACO3. Subsequently, sequence information can be achieved from the MALDI-TOF analysis.

- Further Southern analysis and northern analysis would need to be repeated with 3'-UTRs of *TO-ACO2* and *TO-ACO3*.

Bibliography

Abdi N, McGlasson WB, Holford P, Williams M, Mizrahi Y (1998) Responses of climacteric and suppressed climacteric plums to treatment with propylene and 1-methylcyclopropene. *Postharvest Biology and Technology* **14:** 29-39.

Abeles FB, Morgan PW, Saltveit ME (1992) Ethylene in plant biology, 2nd. Ed Abeles, F.B. Morgan, P.W. Saltveit, M.E. Academic Press, San Diego. CA.

Adams DO, Yang SF (1979) Ethylene biosynthesis: identification of 1-aminocyclopropane-1-carboxylic acid as an intermediate in the conversion of methionine to ethylene. *Proceedings of the National Academy of Sciences, USA* **76:** 170-174.

Alexander L, Grierson D (2002) Ethylene biosynthesis and action in tomato: a model for climacteric fruit ripening. *Journal of Experimental Botany* **53:** 2039-2055.

Allada R, Emery P, Takahashi JS, Rosbash M (2001) Stopping time: the genetics of fly and mouse circadian clocks. *Annual Review Neuroscience* **24:** 1091-1119.

Alonso JM, Hirayama T, Roman G, Nourizadeh S, Ecker JR (1999) EIN2, a bifunctional transducer of ethylene and stress responses in *Arabidopsis. Science* **284:** 2148-2152.

Amrhein N, Schneebeck D, Skorupka H, Tophof S, Stöckigt J (1981) Identification of a major metabolite of the ethylene precursor 1-aminocyclopropane-1-carboxylic acid in higher plants. *Naturwissenschaften* **68:** 619-620.

Arteca JM, Arteca RN (1999) A multi-responsive gene encoding 1-aminocyclopropane-1-carboxylate synthase (ACS6) in mature *Arabidopsis* leaves. *Plant Molecular Biology* **39:** 209-219.

Badr A, Sayed-Ahmed H, El-Shanshouri A, Watson LE (2002) Ancestors of white clover (*Trifolium repens* L.), as revealed by isozyme polymorphisms. *Theoretical and Applied Genetics* **106:** 143-148.

Baker MJ, Williams WM (1987) White Clover, Ed Baker, M.J., Williams, W.M. CAB International, Oxon, UK.

Balagué C, Watson CF, Turner AJ, Rougé P, Picton S, Pech JC, Grierson D (1993) Isolation of a ripening and wound-induced cDNA from *Cucumis melo* L. encoding a protein with homology to the ethylene-forming enzyme. *European Journal of Biochemistry* **212:** 27-34.

Barak S, Tobin EM, Andronis C, Sugano S, Green RM (2000) All in good time: the *Arabidopsis* circadian clock. *Trends in Plant Science* **5:** 517-522.

Barry CS, Blume B, Bouzayen M, Cooper W, Hamilton AJ, Grierson D (1996) Differential expression of the 1-aminocyclopropane-1-carboxylate oxidase gene family of tomato. *The Plant Journal* **9:** 525-535.

Barry CS, Llop-Tous MI, Grierson D (2000) The regulation of 1-aminocyclopropane-1-carboxylic acid synthase gene expression during the transition from system-1 to system-2 ethylene synthesis in tomato. *Plant Physiology* **123:** 979-986.

Battey NH, Dickinson HG, Hetherington AM (1993) Some roles of post-translational modification in plants. *In* Post-translational modification in plants, Ed Battey, NH, Dickinson, HG, Hetherington, AM. Cambridge University Press, Cambridge, UK. pp 1-15.

Bekman EP, Saibo NJM, Cataldo AD, Regalado AP, Ricardo CP, Rodrigues-Pousada C (2000) Differential expression of four genes encoding 1-aminocyclopropane-1-carboxylate synthase in *Lupinus albus* during germination, and in response to indole-3-acetic acid and wounding. *Planta* **211:** 663-672.

Benichou M, Martinez-Reina G, Romojaro F, Pech JC, Latche A (1995) Partial purification and properties of a 36-kDa 1-aminocyclopropane-1-carboxylate-*N*-malonyltransferase from mung bean. *Physiologia Plantarum* **94:** 629-634.

Bewley JD, Black M (1994) Seeds: Physiology of development and germination. 2nd. Plenum Press, New York, NY.

Bidonde S, Ferrer MA, Zegzouti H, Ramarsamy S, Latche A, Pech JC, Hamilton AJ, Grierson D, Bouzayen M (1998) Expression and characterization of three tomato 1-aminocyclopropane-1-carboxylate oxidase cDNAs in yeast. *European Journal of Biochemistry* **253:** 20-26.

Bleecker AB (1998) The evolutionary basis of leaf senescence: method to the madness? *Current Opinion in Plant Biology* **1:** 73-78.

Bleecker AB, Kende H (2000) Ethylene: A gaseous signal molecule in plants. *Annual Review of Cell and Developmental Biology* **16:** 1-18.

Bleecker AB, Kenyon WH, Somerville SC, Kende H (1986) Use of monoclonal antibodies in the purification and characterization of 1-aminocyclopropane-1-carboxylate synthase, an enzyme in ethylene biosynthesis. *Proceedings of the National Academy of Sciences, USA* **83:** 7755-7759.

Bleecker AB, Estelle MA, Somerville C, Kende H (1988) Insensitivity to ethylene conferred by a dominant mutation in *Arabidopsis thaliana*. *Science* **241:**1086-1089.

Blom N, Gammeltoft S, Brunak S (1999) Sequence and structure-based prediction of eukaryotic protein phosphorylation sites. *Journal of Molecular Biology* **294:** 1351-1362.

Blume B, Grierson D (1997) Expression of ACC oxidase promoter-GUS fusions in tomato and *Nicotiana plumbaginifolia* regulated by developmental and environmental stimuli. *The Plant Journal* **12:** 731-746.

Bondada BR, Oosterhuts (1998) Relationships between nitrogen content and net gas exchange components of a cotton leaf during ontogeny. *Photosynthetica* **35:** 631-635.

Bouzayen M, Latché A, Pech JC (1990) Subcellular localization of conversion of 1-aminocyclopropane-1-carboxylic acid into ethylene in plant cells. *Planta* **180:** 175-180.

Bouzayen M, Cooper W, Barry C, Zegzouti H, Hamilton AJ, Grierson D (1993) EFE multigene family in tomato plants: expression and characterization. *In* Cellular and Molecular Aspects of the Plant Hormone Ethylene, Ed Pech, J.C., Latché, A., Balagué, C. Kluwer Academic Publishers, Dordrecht, The Netherlands. pp 76-81.

Bradford MM (1976) A rapid and sensitive method for the quantitation of microgram quantities of protein utilizing the principle of protein-dye binding. *Analytical Biochemistry* **72:** 248-254.

Brock JL, Hay MJM, Thomas VJ, Sedcole JR (1988) Morphology of white clover (*Trifolium repens* L.) plants in pastures under intensive sheep grazing. *Journal of Agricultural Science* **111:** 273-283.

Brougham RW, Ball PR, Williams WM (1978) Ecology and management of white clover-based pastures. *In* Plant Relations in Pastures, Ed Wilson, J.R. CSIRO, Melbourne. pp 309-324.

Brown SA, Schibler U (1999) The ins and outs of circadian time-keeping. *Current Opinion in Genetics and Development* **9:** 588-594.

Buchanan-Wollaston V (1997) The molecular biology of leaf senescence. *Journal of Experimental Botany* **48:** 181-199.

Butcher SM (1997) Ethylene biosynthesis during leaf maturation and senescence in white clover. PhD. Thesis. Institute of Molecular BioSciences, Massey University, Palmerston North, New Zealand.

Butcher SM, Fountain DW, McManus MT (1996) Leaf senescence and clonal growth of white clover. *Agronomy Society of New Zealand Special Publication No. 11, Grassland Research and Practice Series* **6:** 171-173.

Bykova NV, Egsgaard H, Møller IM (2003) Identification of 14 new phosphoproteins involved in important plant mitochondrial processes. *FEBS Letters* **540:**141-146.

Cameron AC, Fenton CAL, Yu Y, Adams DO, Yang SF (1979) Increased production of ethylene from plant tissues treated with 1-aminocyclopropane-1-carboxylic acid. *HortScience* **14:** 178-180.

Capitani G, Hohenester E, Feng L, Storici P, Kirsch JF, Jansonius JN (1999) Structure of 1-aminocyclopropane-1-carboxylate synthase, a key enzyme in the biosynthesis of the plant hormone ethylene. *Journal of Molecular Biology* **294:** 745-756.

Casas JL, Garcia-Canovas F, Tudela J, Acosta M (1993) A kinetic study of simultaneous suicide inactivation and irreversible inhibition of an enzyme. Application to 1-aminocyclopropane-1-carboxylate (ACC) synthase inactivation by its substrate S-adenosylmethionine. *Journal of Enzyme Inhibition* **7:** 1-14.

Chae HS, Cho YG, Park MY, Lee MC, Eun MY, Kang BG, Kim WT (2000) Hormonal cross-talk between auxin and ethylene differentially regulates the expression of two members of the 1-aminocyclopropane-1-carboxylate oxidase gene family in rice (*Oryza sativa* L.). *Plant and Cell Physiology* **41:** 354-362.

Chae HS, Faure F, Kieber JJ (2003) The *eto1*, *eto2* and *eto3* mutations and cytokinin treatment increase ethylene biosynthesis in *Arabidopsis* by increasing the stability of ACS protein. *Plant Cell* **15:** 545-559.

Chang C, Meyerowitz EM (1995) The ethylene hormone response in *Arabidopsis*: a eukaryotic 2-component signalling system. *Proceedings of the National Academy of Sciences, USA* **92:** 4129-4133.

Chang C, Kwok SF, Bleecker AB, Meyerowitz EM (1993) *Arabidopsis* ethylene-response gene ETR1: similarity of product to two-component regulators. *Science* **262:** 539-544.

Chao QM, Rothenberg M, Solano R, Roman G, Terzaghi W, Ecker JR (1997) Activation of the ethylene gas response pathway in *Arabidopsis* by the nuclear protein ETHYLENE-INSENSITIVE3 and related proteins. *Cell* **89:** 1133-1144.

Chen CC, Gibson PB (1971) Karyotype of fifteen *Trifolium* species in section *Amoria*. *Crop Science* **11:** 441-445.

Chen CC, Gibson PB (1972) Barriers to hybridization of *Trifolium repens* with related species. *Canadian Journal of Genetics and Cytology* **14:** 591-595.

Chen YT, Lee YR, Yang CY, Wang YT, Yang SF, Shaw JF (2003) A novel papaya ACC oxidase gene (*CP-ACO2*) associated with late stage fruit ripening and leaf senescence. *Plant Science* **164:** 531-540.

Chomczynski P (1992) One-hour downward alkaline capillary transfer for blotting of DNA and RNA. *Analytical Biochemistry* **201:** 134-139.

Chomczynski P, Sacchi N (1987) Single-step method of RNA isolation by acid guanidinium thiocyanate-phenol-chloroform extraction. *Analytical Biochemistry* **162:** 156-159.

Chung MC, Chou SJ, Kuang LY, Charng YY, Yang SF (2002) Subcellular localization of 1-aminocyclopropane-1-carboxylic acid oxidase in apple fruit. *Plant and Cell Physiology* **43:** 549-554.

Church GM, Gilbert W (1984) Genomic sequencing. *Proceedings of the National Academy of Sciences, USA* **81:** 1991-1995.

Ciardi JA, Klee H (2001) Regulation of ethylene-mediated responses at the level of the receptor. *Annals of Botany* **88:** 813-822.

Ciardi JA, Tieman DM, Lund ST, Jones JB, Stall RE, Klee HJ (2000) Response to *Xanthomonas campestris pv. vesicatoria* in tomato involves regulation of ethylene receptor gene expression. *Plant Physiology* **123:** 81-92.

Coombe DE (1961) *Trifolium occidentale*, a new species related to *T. repens* L. *Watsonia* **5:** 68-87.

Coombe DE, Morisset P (1967) Further observations on *Trifolium occidentale*. *Watsonia* **6:** 271-275.

DeLong A, Mockaitis K, Christensen S (2002) Protein phosphorylation in the delivery of and response to auxin signals. *Plant Molecular Biology* **49:** 285-303.

Destefano-Beltran LJC, Van Caeneghem W, Gielen J, Richard L, Van Montagu M, Van Der Straeten D (1995) Characterization of three members of the ACC synthase gene family in *Solanum tuberosum* L. *Molecular & General Genetics* **246:** 496-508.

Dilley DR, Wang Z, Kadyrzhanova DK (2003) Mechanism of bicarbonate and ascorbic acid activation of 1-aminocyclopropane-1-carboxylate (ACC) oxidase. *In* Biology and Biotechnology of the Plant Hormone Ethylene III, Ed Vendrell, M., Klee, H., Pech, JC, Romojaro, F. IOS Press, Netherlands. pp 9-14.

Dolan L (1997) The role of ethylene in the development of plant form. *Journal of Experimental Botany* **48:** 201-210.

Dong JG, Fernández-Maculet JC, Yang SF (1992) Purification and characterization of 1-aminocyclopropane-1-carboxylate oxidase from apple fruit. *Proceedings of the National Academy of Sciences, USA* **89:** 9789-9793.

Dunkley HM, Golden KD (1998) ACC oxidase from *Carica papaya*: Isolation and characterization. *Physiologia Plantarum* **103:** 225-232.

Dunlap JC (1999) Molecular bases for circadian clocks. *Cell* **96:** 271-290.

Dupille E, Zacarias L (1996) Extraction and biochemical characterization of wound-induced ACC oxidase from citrus peel. *Plant Science* **114:** 53-60.

Dupille E, Rombaldi C, Leliévre JM, Cleyet-Marel JC, Pech JC, Latché A (1993) Purification, properties and partial amino acid sequence of 1-aminocyclopropane-1-carboxylate oxidase from apple fruits. *Planta* **190:** 65-70.

Ecker JR (1995) The ethylene signal transduction pathway in plants. *Science* **268:** 667-675.

Edery I (1999) Role of posttranscriptional regulation in circadian clocks: lessons from *Drosophila*. *Chronobiology International* **16:** 377-414.

English PJ, Lycett GW, Roberts JA, Jackson MB (1995) Increased 1-aminocyclopropane-1-carboxylic acid oxidase activity in shoots of flooded tomato plants raises ethylene production to physiologically active levels. *Plant Physiology* **109:** 1435-1440.

Escribano MI, Merodio C, John P (1996) Characterization of 1-aminocyclopropane-1-carboxylate oxidase partially purified from cherimoya fruit. *Journal of Agricultural and Food Chemistry* **44:** 730-735.

Evans JR (1988) Acclimation by the thylakoid membranes to growth irradiance and the partitioning of nitrogen between soluble and thylakoid proteins. *Australian Journal of Plant Physiology* **15:** 93-106.

Fallon KM, Trewavas AJ (1993) The significance of post-translational modification of proteins by phosphorylation in the regulation of plant development and metabolism. *In* Post-translational modification in plants, Ed Battey, N.H., Dickinson, H.G., Hetherington, A.M. Cambridge University Press, Cambridge, UK. pp 53-64.

Fejes E, Nagy F (1998) Molecular analysis of circadian clock regulated gene expression in plants: features of the 'output' pathways. *In* Biological Rhythms and Photoperiodism in Plants, Ed Lumsden, P.J., Millar, A.L. BIOS Scientific Publishers, Oxford, UK. pp 99-118.

Feller U, Fischer A (1994) Nitrogen metabolism in senescing leaves. *Critical Reviews in Plant Sciences* **13:** 241-273.

Fernández-Maculet JC, Yang SF (1992) Extraction and partial characterization of the ethylene-forming enzyme from apple fruit. *Plant Physiology* **99:** 751-754.

Field C, Mooney HA (1986) The photosynthesis-nitrogen relationship in wild plants. *In* On the economy of plant form and function, Ed Givnish, T.J. Cambridge University Press, Cambridge, UK. pp 25-55.

Finlayson SA, Reid DM, Morgan PW (1997) Root and leaf specific ACC oxidase activity in corn and sunflower seedlings. *Phytochemistry* **45:** 869-877.

Finlayson SA, Lee IJ, Morgan PW (1998) Phytochrome B and the regulation of circadian ethylene production in sorghum. *Plant Physiology* **116:** 17-25.

Finlayson SA, Lee I-J, Mullet JE, Morgan PW (1999) The mechanism of rhythmic ethylene production in sorghum. The role of phytochrome B and simulated shading. *Plant Physiology* **119:** 1083-1090.

Fluhr R, Mattoo AK (1996) Ethylene-biosynthesis and perception. *Critical Reviews in Plant Sciences* **15:** 479-523.

Fujiwara S, Ishida N, Tsuzuki M (1996) Circadian expression of the carbonic anhydrase gene, *Cah1*, in *Chlamydomonas reinhardtii*. *Plant Molecular Biology* **32:** 745-749.

Gane R (1934) Production of ethylene by some fruits. *Nature* **134:** 1008.

Garbers C, DeLong A, Deruere J, Bernasconi P, Soll D (1996) A mutation in protein phosphatase 2A regulatory subunit A affects auxin transport in *Arabidopsis*. *EMBO Journal* **15:** 2115-2124.

Gibson PB, Beinhart G (1969) Hybridization of *Trifolium occidentale* with two other species of clover. *Journal of Heredity* **60:** 93-96.

Golding JB, Shearer D, Wyllie SG, McGlasson WB (1998) Application of 1-MCP and propylene to identify ethylene-dependent ripening processes in mature banana fruit. *Postharvest Biology and Technology* **14:** 87-98.

Gomez-Gomez L, Carrasco L (1998) Hormonal regulation of *S*-adenosylmethionine synthase transcripts in pea ovaries. *Plant Molecular Biology* **30:** 821-832.

Gong D (1999) Characterization of 1-aminocyclopropane-1-carboxylate (ACC) oxidase isoforms during leaf maturation and senescence in white clover (*Trifolium repens* L.). PhD. Thesis. Institute of Molecular BioSciences, Massey University, Palmerston North, New Zealand.

Gong D, McManus MT (2000) Purification and characterization of two ACC oxidases expressed differentially during leaf ontogeny in white clover. *Physiologia Plantarum* **110:** 13-21.

Görg A, Postel W, Günther S, Weser J (1985) Improved horizontal two-dimensional electrophoresis with hybrid isoelectric focusing in immobilized pH gradients in the first dimension and laying-on transfer to the second dimension. *Electrophoresis* **6:** 599-604.

Görg A, Postel W, Günther S (1988) The current state of two-dimensional electrophoresis with immobilized pH gradients. *Electrophoresis* **9:** 531-546.

Görg A, Postel W, Weser J, Günther S, Strahler JR, Hanash SM, Somerlot L (1987) Elimination of point streaking on silver-stained two-dimensional gels by addition of iodoacetamide to the equilibration buffer. *Electrophoresis* **8:**122-124.

Grbic V, Bleecker AB (1995) Ethylene regulates the timing of leaf senescence in *Arabidopsis*. *The Plant Journal* **8:** 595-602.

Grichko VP, Glick BR (2001) Ethylene and flooding stress in plants. *Plant Physiology and Biochemistry* **39:** 1-9.

Guo L, Arteca RN, Phillips AT, Liu Y (1992) Purification and characterization of 1-aminocyclopropane-1-carboxylate *N*-malonyltransferase from etiolated mung bean hypocotyls. *Plant Physiology* **100:** 2041-2045.

Gut H, Rutz C, Matile P, Thomas H (1987) Leaf senescence in a non-yellowing mutant of *Festuca pratense*: degradation of carotenoids. *Physiologia Plantarum* **70:** 659-663.

Guzman P, Ecker JR (1990) Exploiting the triple response of Arabidopsis to identify ethylene-related mutants. *Plant Cell* **2:** 513-523.

Hall AE, Findell JL, Schaller GE, Sisler EC, Bleecker AB (2000) Ethylene perception by the ERS1 protein in Arabidopsis. *Plant Physiology* **123:** 1449-1458.

Hamilton AJ, Lycett GW, Grierson D (1990) Antisense gene that inhibits synthesis of the hormone ethylene in transgenic plants. *Nature* **346:** 284-287.

Hamilton AJ, Bouzayen M, Grierson D (1991) Identification of a tomato gene for the ethylene-forming enzyme by expression in yeast. *Proceedings of the National Academy of Sciences, USA* **88:** 7434-7437.

Handley LL, Raven JA (1992) The use of natural abundance of nitrogen isotopes in plant physiology and ecology. *Plant, Cell and Environment* **15:** 965-985.

Hardie DG (1999) Plant protein serine/threonine kinases: classification and functions. *Annual Review of Plant Physiology and Plant Molecular Biology* **50:** 97-131.

Harmer SL, Hogenesch JB, Straume M, Chang HS, Han B, Zhu T, Wang X, Kreps JA, Kay SA (2000) Orchestrated transcription of key pathways in *Arabidopsis* by the circadian clock. *Science* **290:** 2110-2113.

Harpham N, Berry A, Knee E, Rovedahoyos G, Raskin I, Sanders I, Smith A, Wood C, Hall M (1991) The effect of ethylene on the growth and development of wild-type and mutants *Arabidopsis thaliana* (L.) Heynh. *Annals of Botany* **68:** 55-61.

Harris ELV (1989) Concentration of the extract. *In* Protein Purification methods: A Practical Approach, Ed Harris, E.L.V., Angal, S. IRL Press, Oxford, UK. pp 154-157.

Hay MJM, Brock JL, Thomas VJ (1989) Characterization of individual white clover plants in grazed swards. *Proceedings of the New Zealand Grassland Association* **16:** 1051-1052.

Hay MJM, Newton PCD, Thomas VJ (1991) Nodal structure and branching of *Trifolium repens* in pastures under intensive grazing by sheep. *Journal of Agricultural Science* **116:** 221-228.

Hoffman NE, Yang SF (1980) Changes of 1-aminocyclopropane-1-carboxylic acid content in ripening fruits in relation to their ethylene production rates. *Journal of the American Society for Horticultural Science* **105:** 492-495.

Hoffman NE, Yang SF, McKeon TA (1982) Identification of 1-(malonylamino) cyclopropane-1-carboxylic acid, an ethylene precursor in higher plants. *Biochemical and Biophysical Research Communications* **104:** 765-770.

Hoffman NE, Fu JR, Yang SF (1983) Identification and metabolism of 1-(malonylamino)cyclopropane-1-carboxylic acid in germinating peanut seeds. *Plant Physiology* **71:** 197-199.

Holdsworth MJ, Bird CR, Ray J, Schuch W, Grierson D (1987) Structure and expression of an ethylene-related mRNA from tomato. *Nucleic Acids Research* **15:** 731-739.

Hörtensteiner S (1999) Chlorophyll breakdown in higher plants and algae. *Cellular & Molecular Life Sciences* **56:** 330-347.

Hörtensteiner S, Kräutler B (2000) Chlorophyll breakdown in oilseed rape. *Photosynthesis Research* **64:** 137-146.

Hua J, Chang C, Sun Q, Meyerowitz EM (1995) Ethylene insensitivity conferred by *Arabidopsis ERS* gene. *Science* **269:** 1712-1714.

Hua J, Sakai H, Nourizadeh S, Chen QG, Bleecker AB, Ecker JR, Myerowitz EM (1998) EIN4 and ERS2 are members of the ethylene putative receptor gene family in *Arabidopsis. The Pant Cell* **10:** 1321-1332.

Huai Q, Xia Y, Chen Y, Callahan B, Li N, Ke H (2001) Crystal structures of 1-aminocyclopropane-1-carboxylate (ACC) synthase in complex with aminoethoxyvinylglycine and pyridoxal-5'-phosphate provide new insight into catalytic mechanisms. *Journal of Biological Chemistry* **276:** 38210-38216.

Huang PL, Do YY (1998) Cloning and characterization of genes encoding 1-aminocyclopropane-1-carboxylate oxidase specific for fruit ripening in banana. *In* Biology and Biotechnology of the Plant Hormone Ethylene II, Ed Kanellis, A.K., Chang, C., Grierson, D., Klee, H., Pech, J.C., European Union Tmr-Euroconference Programme. pp 67.

Hunter DA (1998) Characterization of ACC oxidase during leaf maturation and senescence in white clover. Ph.D. Thesis. Institute of Molecular BioSciences, Massey University, Palmerston North, New Zealand.

Hunter DA, Yoo SD, Butcher SM, McManus MT (1999) Expression of 1-aminocyclopropane-1-carboxylate oxidase during leaf ontogeny in white clover. *Plant Physiology* **120:** 131-142.

Imaseki H (1999) Control of ethylene synthesis and metabolism. *In* Biochemistry and Molecular Biology of Plant Hormones, Ed Hooykaas, P.J.J., Hall, M.A., Libbenga, K.R., Elsevier Science B.V. pp 209-245.

Inskeep WP, Bloom PR (1985) Extinction coefficients of chlorophyll *a* and *b* in *N, N*-dimethylformamide and 80% acetone. *Plant Physiology* **77:** 483-485.

Jacobs DI, van Rijssen MS, van der Heijden R, Verpoorte R (2001) Sequential solubilization of proteins precipitated with trichloroacetic acid in acetone from cultured *Catharanthus roseus* cells yield 52% more spots after two-dimensional electrophoresis. *Proteomics* **1:** 1345-1350.

Janssens V, Goris J (2001) Protein phosphatase 2A: a highly regulated family of serine/threonine phosphatase implicated in cell growth and signalling. *Biochemical Journal* **353:** 417-439.

Jasoni RL, Cothren JT, Morgan PW, Sohan DE (2002) Circadian ethylene production in cotton. *Plant Growth Regulation* **36:** 127-133.

Jiang YM, Fu J (2000) Ethylene regulation of fruit ripening: Molecular aspects. *Plant Growth Regulation* **30:** 193-200.

Jiang YM, Joyce DC, Macnish AJ (1999) Responses of banana fruit to treatment with 1-methylcyclopropene. *Plant Growth Regulation* **28:** 77-82.

Jin E, Lee JH, Park JA, Kim WT (1999) Temporal and spatial regulation of the expression of 1-aminocyclopropane-1-carboxylate oxidase by ethylene in mung bean (*Vigna radiata*). *Physiologia Plantarum* **105:** 132-140.

John P (1997) Ethylene biosynthesis: the role of 1-aminocyclopropane-1-carboxylate (ACC) oxidase, and its possible evolutionary origin. *Physiologia Plantarum* **100:** 583-592.

Johnson PR, Ecker JR (1998) The ethylene gas signal transduction pathway: a molecular perspective. *Annual Review of Genetics* **32:** 227-254.

Jones ML, Woodson WR (1999) Differential expression of three members of the 1-aminocyclopropane-1-carboxylate synthase gene family in carnation. *Plant Physiology* **119:** 755-764.

Jones TL, Ort DR (1997) Circadian regulation of sucrose phosphate synthese activity in tomato by protein phosphatase activity. *Plant Physiology* **113:** 1167-1175.

Jones TL, Tucker DE, Ort DR (1998) Chilling delays circadian pattern of sucrose phosphate synthase and nitrate reductase activity in tomato. *Plant Physiology* **118:** 149-158.

Kadyrzhanova DK, McCully TJ, Jaworski SA, Ververidis P, Vlachonasios KE, Murakami KG, Dilley DR (1997) Structure-function analysis of ACC oxidase by site-directed mutagenesis. *In* Biology and Biotechnology of the Plant Hormone Ethylene, Ed Kanellis, A.K., Chang, C., Kende, H. and Grierson, D. Kluwer Academic Publishers, Dordrecht, The Netherlands. pp 5-13.

Kadyrzhanova DK, McCully TJ, Warner T, Vlachonasios KE, Wang Z, Dilley DR (1999) Analysis of ACC oxidase activity by site-directed mutagenesis of conserved amino acid residues. *In* Biology and Biotechnology of the Plant Hormone Ethylene II, Ed Kanellis, A.K., Chang, C., Klee, H., Bleecker, A.B., Pech, J.C. and Grierson, D. Kluwer Academic Publishers, Dordrecht, The Netherlands. pp 7-12.

Kaiser WM, Huber SC (2001) Post-translational regulation of nitrate reductase: mechanism, physiological relevance and environmental triggers. *Journal of Experimental Botany* **52:** 1981-1989.

Kakes P, Chardonnens AN (2000) Cyanotypic frequencies in adjacent and mixed populations of *Trifolium occidentale* Coombe and *Trifolium repens* L. are regulated by different mechanisms. *Biochemical Systematics and Ecology* **28:** 633-649.

Kakes P, Hakvoort HWJ (1994) On the origin of the cyanogenic polymorphism in *Trifolium repens* L. *Journal of Evolutionary Biology* **7:** 201-215.

Kathiresan A, Reid DM, Chinnappa CC (1996) Light and temperature entrained circadian regulation of activity and mRNA accumulation of 1-aminocyclopropane-1-carboxylic acid oxidase in *Stellaria longipes*. *Planta* **199:** 329-335.

Kato M, Hyodo H (1999) Purification and characterization of ACC oxidase and increase in its activity during ripening of pear fruit. *Journal of the Japanese Society for Horticultural Science* **68:** 551-557.

Kato M, Kamo T, Wang R, Nishikawa F, Hyodo H, Ikoma Y, Sugiura M, Yano M (2002) Wound-induced ethylene synthesis in stem tissue of harvested broccoli and its effect on senescence and ethylene synthesis in broccoli florets. *Postharvest Biology and Technology* **24:** 69-78.

Kende H (1993) Ethylene biosynthesis. *Annual Review Plant Physiology and Plant Molecular Biology* **44:** 283-307.

Kieber JJ, Rothenberg M, Roman G, Feldmann K, Ecker JR (1993) *CTR1*, a negative regulator of the ethylene response pathway in *Arabidopsis*, encodes a member of the Raf family of protein kinases. *Cell* **72:** 427-441.

Kim WT, Yang SF (1994) Structure and expression of cDNAs encoding 1-aminocyclopropane-1-carboxylate oxidase homologs isolated from excised mung bean hypocotyls. *Planta* **194:** 223-229.

Kim YS, Choi D, Lee MM, Lee SH, Kim WT (1998) Biotic and abiotic stress-related expression of 1-aminocyclopropane-1-carboxylate oxidase gene family in *Nicotiana glutinosa* L. *Plant and Cell Physiology* **39:** 565-573.

Klose J (1975) Protein mapping by combined isoelectric focusing and electrophoresis of mouse tissues. A novel approach to testing for induced point mutations in mammals. Humangenetik **26:** 231-243.

Kosugi Y, Oyamada N, Satoh S, Yoshioka T, Onodera EI, Yamada Y (1997) Inhibition by 1-aminocyclobutane-1-carboxylate of the activity of 1-aminocyclopropane-1-carboxylate oxidase obtained from senescing petals of carnation (*Dianthus caryophyllus* L.) flowers. *Plant & Cell Physiology* **38:** 312-318.

Kreps JA, Kay SA (1997) Coordination of plant metabolism and development by the circadian clock. *Plant Cell* **9:** 1235-1244.

Kruzmane D, Ievinsh G (1999) Characterization of 1-aminocyclopropane-1-carboxylic acid oxidase from barley (*Hordeum vulgare* L.) seedlings and pine (*Pinus sylvestris* L.). *Plant Science* **142:** 13-19.

Kuai J, Dilley DR (1992) Extraction, partial purification and characterization of 1-aminocyclopropane-1-carboxylic acid oxidase from apple fruit. *Postharvest Biology and Technology* **1:** 203-211.

Laemmli UK (1970) Cleavage of structural proteins during the assembly of the head of bacteriophage T4. *Nature* **227:** 680-685.

Lanahan MB, Yen HC, Giovannoni JJ, Klee HJ (1994) The never ripe mutation blocks ethylene perception in tomato. *Plant Cell* **6:** 521-530.

Lashbrook CC, Tieman DM, Klee HJ (1998) Differential regulation of the tomato *ETR* gene family throughout plant development. *The Plant Journal* **15:** 243-252.

Lasserre E, Bouquin T, Hernandez JA, Bull J, Pech JC, Balague C (1996) Structure and expression of three genes encoding ACC oxidase homologs from melon (*Cucumis melo* L.). *Molecular and General Genetics* **251:** 81-90.

Lasserre E, Godard F, Bouquin T, Hernandez JA, Pech JC, Roby D, Balague C (1997) Differential activation of two ACC oxidase gene promoters from melon during plant development and in response to pathogen attack. *Molecular and General Genetics* **256:** 211-222.

Lee MM, Lee SH, Park KY (1997) Effects of spermine on ethylene biosynthesis in cut carnation (*Dianthus caryophylls* L.) flowers during senescence. *Journal of Plant Physiology* **151:** 68-73.

Lelievre JM, Latche A, Jones B, Bouzayen M, Pech JC (1997) Ethylene and fruit ripening. *Physiologia Plantarum* **101:** 727-739.

Li S, Taylor KB, Kelley SK, Jedrzejas MJ (2001) Vitamin C inhibits the enzymatic activity of streptococcus pneumoniae hyaluronate lyase. *Journal of Biological Chemistry* **276:** 15125-15130.

Liang X, Abel S, Keller JA, Shen NF, Theologis A (1992) The 1-aminocyclopropane-1-carboxylate synthase gene family of *Arabidopsis thaliana. Proceedings of the National Academy of Sciences, USA* **89:** 11046-11050.

Lillo C, Meyer C, Lea US, Provan F, Oltedal S (2004) Mechanism and importance of post-translational regulation of nitrate reductase. *Journal of Experimental Botany* **55:** 1275-1282.

Lim PO, Woo HR, Nam HG (2003) Molecular genetics of leaf senescence in *Arabidopsis. Trends in Plant Science* **8:** 272-278.

Lin P, Wang WQ (2001) Changes in the leaf composition, leaf mass and leaf area during leaf senescence in three species of mangroves. *Ecological Engineering* **16:** 415-424.

Lin Z, Hackett R, Payton S, Grierson D (1998) A tomato sequence (AJ005077) encoding an *Arabidopsis* CTR1 homolog. *Plant Physiology* **117:** 1125.

Lincoln JE, Campbell AD, Oetiker J, Rottmann WH, Oeller PW, Shen NF, Theologis A (1993) LE-ACS4, a fruit ripening and wound-induced 1-aminocyclopropane-1-carboxylate synthase gene of tomato (*Lycopersicon esculentum*). *The Journal of Biological Chemistry* **268:** 19422-19430.

Liu JH, Lee-Tamon SH, Reid DM (1997) Differential and wound-inducible expression of 1-aminocyclopropane-1-carboxylate oxidase genes in sunflower seedlings. *Plant Molecular Biology* **34:** 923-933.

Liu Z, Taub CC, McClung CR (1996) Identification of an *Arabidopsis thaliana* ribulose-1, 5-bisphosphate carboxylase/oxygenase activase (RCA) minimal promoter regulated by light and the circadian clock. *Plant Physiology* **112:** 43-51.

Liu Z, Yan H, Wang K, Kuang T, Zhang J, Gui L, An X, Chang W (2004) Crystal structure of spinach major light-harvesting complex at 2.72 Å resolution. *Nature* **428:** 287-292.

Lopez-Gomez R, Morales-Dominguez F, Mendoza Alcazar O, Gomez-Lim MA (2004) Identification of a genomic clone to ACC oxidase from papaya (*Carica papaya* L.). *Journal of Agricultural and Food Chemistry* **52:** 794-800.

Lu C, Zhang J (1998a) Changes in photosystem II function during senescence of wheat leaves. *Physiologia Plantarum* **104:** 239-247.

Lu C, Zhang J (1998b) Modifications in photosystem II photochemistry in senescent leaves of maize plants. *Journal of Experimental Botany* **49:** 1671-1679.

Luan S (2003) Protein phosphatases in plants. *Annual Review of Plant Biology* **54:** 63-92.

Lurssen K, Naumann K, Schroder R (1979) 1-aminocyclopropane-1-carboxylic acid: an intermediate of the ethylene biosynthesis in higher plants. *Z. Pfanzen Physiology* **92:** 285-294.

MacDiarmid CWB, Gardner RC (1993) A cDNA sequence from kiwifruit homologous to 1-aminocyclopropane-1-carboxylic acid oxidase. *Plant Physiology* **101:** 691-692.

Martin MN, Saftner RA (1995) Purification and characterization of 1-aminocyclopropane-1-carboxylic acid N-malonyltransferase from tomato fruit. *Plant Physiology* **108:** 1241-1249.

Martin MN, Cohen JD, Saftner RA (1995) A new 1-aminocyclopropane-1-carboxylic acid conjugating activity in tomato fruit. *Plant Physiology* **109:** 917-926.

Masclaux C, Valadier M-H, Brugiére N, Morot-Gaudry JF, Hirel B (2000) Characterization of the sink/source transition in tobacco (*Nicotiana tabacum* L.) shoots in relation to nitrogen management. *Planta* **211:** 510-518.

Mathooko FM, Tsunashima Y, Owino WZO, Kubo Y, Inaba A (2001) Regulation of genes encoding ethylene biosynthetic enzymes in peach (*Prunus persica* L.) fruit by carbon dioxide and 1-methylcyclopropene. *Postharvest Biology and Technology* **21:** 265-281.

Mathooko FM, Inaba A, Nakamura R (1998) Characterization of carbon dioxide stress-induced ethylene biosynthesis in cucumber (*Cucumis sativus* L.) fruit. *Plant and Cell Physiology* **39:** 285-293.

Matilla AJ (2000) Ethylene in seed formation and germination. *Seed Science Research* **10:** 111-126.

Mattoo AK, Suttle JC (1991) The plant hormone ethylene. CRC Press, Boca Raton, Florida, USA. pp 337.

Mattoo AK, Mehta RA, Baker JE (1992) Copper-induced ethylene biosynthesis in terrestrial (*Nicotiana tabacum*) and aquatic (*Spirodela oligorrhiza*) higher plants. *Phytochemistry* **31:** 405-409.

Maunders MJ, Holdsworth MJ, Slater A, Knapp JE, Bird CR, Schuch W, Grierson D (1987) Ethylene stimulates the accumulation of ripening-related messenger-RNAs in tomatoes. *Plant, Cell and Environment* **10:** 177-184.

Mayne RG, Kende H (1986) Ethylene biosynthesis in isolated vacuoles of *Vicia faba* requirement for membrane integrity. *Planta* **167:** 159-165.

Mbeguie-A-Mbeguie D, Chahine H, Gomez RM, Gouble B, Reich M, Audergon JM, Souty M, Albagnac G, Fils-Lycaon B (1999) Molecular cloning and expression of a cDNA encoding 1-aminocyclopropane-1-carboxylate (ACC) oxidase from apricot fruit (*Prunus armeniaca*). *Physiologia Plantarum* **105:** 294-303.

McClung CR (2000) Circadian rhythms in plants: a millennial view. *Physiologia Plantarum* **109:** 359-371.

McClung CR (2001) Circadian rhythms in plants. *Annual Review of Plant Physiology and Plant Molecular Biology* **52:** 139-162.

McClung CR, Kay SA (1994) Circadian rhythms in *Arabidopsis thaliana*. *In Arabidopsis thaliana*, Ed Somerville, C.R. Meyerowitz, E. Cold Spring Harbor Press, Cold Spring Harbor, NY, USA. pp 615-637.

McConKey M, Geshenzon J, Croteau RB (2000) Developmental regulation of monoterpene biosynthesis in glandular trichomes of peppermint. *Plant Physiology* **122:** 215-223.

McGarvey DJ, Christoffersen RE (1992) Characterization and kinetic parameters of ethylene-forming enzyme from avocado fruit. *The Journal of Biological Chemistry* **267:** 5964-5967.

McKeon TA, Yang SF (1984) A comparison of the conversion of 1-amino-2-ethylcyclopropane-1-carboxylic acid stereoisomers to 1-butene by pea epicotyls and by a cell free system. *Planta* **160:** 84-87.

McKeon TA, Fernández-Maculet JC, Yang SF (1995) Biosynthesis and metabolism of ethylene. *In* Plant Hormones: Physiology, Biochemistry and Molecular Biology, 2nd, Ed Davies, P.J. Kluwer Academic, Dordrecht, The Netherlands. pp 118-139.

Mehta AM, Jordan RL, Anderson JD, Mattoo AK (1988) Identification of a unique isoform of 1-aminocyclopropane-1-carboxylic acid synthase by monoclonal antibody. *Proceedings of the National Academy of Sciences, USA* **85:** 8810-8814.

Memelink J, Swords KM, Staehelin LA, Hoge JH (1994) Southern, northern and western blot analysis. *In* Plant Molecular Biology Manual, 2nd. Ed Gelvin, S.B., Schilperoot, R.A. Kluwer Academic Press, London, UK. pp F-10.

Millar AJ, Kay SA (1991) Circadian control of *cab* gene transcription and mRNA accumulation in *Arabidopsis*. *Plant Cell* **3:** 541-550.

Mittag M, Lee DH, Hastings JW (1994) Circadian expression of the luciferin-binding protein correlates with the binding of a protein to the 3' untranslated region of its mRNA. *Proceedings of the National Academy of Sciences, USA* **91:** 5257-5261.

Mizutani F, Dong JG, Yang SF (1995) Effect of pH on CO_2-activated 1-aminocyclopropane-1-carboxylate oxidase activity from apple fruit. *Phytochemistry* **39:** 751-755.

Montoya-García L, Muñoz-Ocotero V, Aguilar R, Sánchez de Jiménez E (2002) Regulation of acidic ribosomal protein expression and phosphorylation in maize. *Biochemistry* **41:** 10166-10172.

Moran R, Porath D (1980) Chlorophyll determination in intact tissues using *N,N*-dimethylformamide. *Plant Physiology* **65:** 478-479.

Moritz RL, Eddes JS, Reid GE, Simpson RJ (1996) *S*-pyridylethylation of intact polyacrylamide gels and *in situ* digestion of electrophoretically separated proteins: A rapid mass spectrometric method for identifying cysteine-containing peptides. *Electrophoresis* **17:** 907-917.

Moya-Leon MA, John P (1995) Purification and biochemical characterization of 1-aminocyclopropane-1-carboxylate oxidase from banana fruit. *Phytochemistry* **39:** 15-20.

Mumbly M, Walter G (1993) Protein serine/threonine phosphatase: structure, regulation, and functions in cell growth. *Physiology Review* **73:** 673-699.

Munoz De Rueda P, Gallardo M, Matilla AJ, Sanchez-Calle IM (1995) Preliminary characterization of 1-aminocyclopropane-1-carboxylate oxidase properties from embryonic axes of chick-pea (*Cicer arietinum* L.) seeds. *Journal of Experimental Botany* **46:** 695-700.

Nadeau JA, Zhang XS, Nair H, O'Neill SD (1993) Temporal and spatial regulation of 1-aminocyclopropane-1-carboxylate oxidase in the pollination-induced senescence of orchid flowers. *Plant Physiology* **103:** 31-39.

Naidoo N, Song W, Hunter-Ensor M, Sehgal A (1999) A role for the proteasome in the light response of the timeless clock protein. *Science* **285:** 1737-1741.

Nakagawa N, Mori H, Yamazaki K, Imaseki H (1991) Cloning of complementary DNA for auxin-induced 1-aminocyclopropane-1-carboxylate synthase and differential expression of the gene by auxin and wounding. *Plant and Cell Physiology* **32:** 1153-1164.

Nakajima N, Imaseki H (1986) Purification and properties of 1-aminocyclopropane-1-carboxylate synthase of mesocarp of *Cucurbita maxima* Duch. fruits. *Plant and Cell Physiology* **27:** 969-980.

Nakajima N, Nakagawa N, Imaseki H (1988) Molecular size of wound-induced 1-aminocyclopropane-1-carboxylate synthase from *Cucurbita maxima* Duch. and change of translatable mRNA of the enzyme after wounding. *Plant and Cell Physiology* **29:** 989-998.

Nakatsuka A, Murachi S, Okunishi H, Shiomi S, Nakano R, Kubo Y, Inaba A (1998) Differential expression and internal feedback regulation of 1-aminocyclopropane-1-carboxylate (ACC) synthase, 1-aminocyclopropane-1-carboxylate oxidase, and ethylene receptor genes in tomato fruit during development and ripening. *Plant Physiology* **118:** 1295-1305.

Neal MW, Florini JR (1973) A rapid method for desalting small volumes of solution. *Analytical Biochemistry* **55:** 328-330.

Nijenhuis-De Vries MA, Woltering EJ, De Vrije T (1994) Partial characterization of carnation petal 1-aminocyclopropane-1-carboxylate oxidase. *Plant Physiology* **144:** 549-554.

Nimmo HG (1998) Circadian regulation of a plant protein kinase. *Chronobiology International* **15:** 109-118.

Nooden LD, Guiamet JJ, John I (1997) Senescence mechanisms. *Physiologia Plantarum* **101:** 746-753.

Oetiker JH, Olson DC, Shiu OY, Yang SF (1997) Differential induction of seven 1-aminocyclopropane-1-carboxylate synthase genes by elicitor in suspension cultures of tomato (*Lycopersicon esculentum*). *Plant Molecular Biology* **34:** 275-286.

O'Farrell PH (1975) High resolution two-dimensional electrophoresis of proteins. *Journal of Biological Chemistry* **250:** 4007-4021.

Olson DC, White JA, Edelman L, Harkins RN, Kende H (1991) Differential expression of two genes for 1-aminocyclopropane-1-carboxylate synthase in tomato fruits. *Proceedings of the National Academy of Sciences, USA* **88:** 5340-5344.

Osborne DJ (1989) Abscission. *Critical Reviews in Plant Sciences* **8:** 103-129.

Pandey S, Ranade SA, Nagar PK, Kumar N (2000) Role of polyamines and ethylene as modulators of plant senescence. *Journal of Biosciences* **25:** 291-299.

Park KY, Drory A, Woodson WR (1992) Molecular cloning of an 1-aminocyclopropane-1-carboxylate synthase from senescing carnation flower petals. *Plant Molecular Biology* **18:** 377-386.

Payton S, Fray RG, Brown S, Grierson D (1996) Ethylene receptor expression is regulated during fruit ripening, flower senescence and abscission. *Plant Molecular Biology* **31:** 1227-1231.

Peck SC, Kende H (1995) Sequential induction of the ethylene biosynthetic enzymes by indole-3-acetic acid in etiolated peas. *Plant Molecular Biology* **28:** 293-301.

Peck SC, Reinhardt D, Olson DC, Boller T, Kende H (1992) Localization of the ethylene-forming enzyme from tomatoes, 1-aminocyclopropane-1-carboxylate oxidase, in transgenic yeast. *Journal of Plant Physiology* **140:** 681-686.

Peiser G, Yang SF (1998) Evidence for 1-(malonylamino)cyclopropane-1-carboxylic acid being the major conjugate of aminocyclopropane-1-carboxylic acid in tomato fruit. *Plant Physiology* **116:** 1527-1532.

Peleman J, Saito K, Cottyn B, Engler G, Seurinck J, Van Montagu M, Inze D (1989) Structure and expression analysis of the S-adenosylmethionine synthetase gene family in *Arabidopsis thaliana*. *Gene* **84:** 359-369.

Peoples MB, Dalling MJ (1988) The interplay between proteolysis and amino acid metabolism during senescence and nitrogen reallocation. *In* Senescence and ageing in plants, Ed Noodén, L.D. Leopold, A.C. Academic Press, San Diego, CA., USA. pp 181-217.

Peoples MB, Pate JS, Atkins CA (1983) Mobilization of nitrogen in fruiting plants of a cultivar of cowpea. *Journal of Experimental Botany* **34:** 563-578.

Pirrung MC, Cao J, Chen C (1995) Ethylene biosynthesis 12. Analog approach to the active site topography of the ethylene-forming enzyme. Novel hydroxymate inhibitors. *Journal of Organic Chemistry* **60:** 5790-5794.

Pirrung MC, Kaiser LM, Chen J (1993) Purification and properties of the apple ethylene-forming enzyme. *Biochemistry* **32:** 7445-7450.

Pogson BJ, Downs CG, Davies KM (1995) Differential expression of two 1-aminocyclopropane-1-carboxylic acid oxidase genes in broccoli after harvest. *Plant Physiology* **108:** 651-657.

Poneleit LS, Dilley DR (1993) Carbon dioxide activation of 1-aminocyclopropane-1-carboxylate (ACC) oxidase in ethylene biosythesis. *Postharvest Biology and Technology* **3:** 191-199.

Preneta AZ (1989) Separation on the basis of size: gel permeation chromatography. *In* Protein Purification Methods: A practical Approach, Ed Harris, E.L., Angal, S. IRL Press, Oxford, UK. pp 293-306.

Prescott AG, John P (1996) Dioxygenases: molecular structure and role in plant metabolism. *Annual Review of Plant Physiology* **47:** 245-271.

Privalov P (1992) Protein Folding, Ed Freeman, W.H., N.Y., USA.

Rabilloud T, Carpentier G, Tarroux P (1988) Improvement and simplification of low-background silver staining of proteins by using sodium dithionite. *Electrophoresis* **9:** 288-291.

Ramassamy S, Olmos E, Bouzayen M, Pech JC, Latche A (1998) 1-aminocyclopropane-1-carboxylate oxidase of apple fruit is periplasmic. *Journal of Experimental Botany* **49:** 1909-1915.

Raz V, Fluhr R (1993) Ethylene signal is transduced *via* protein phosphorylation events in plants. *Plant Cell* **5:** 523-530.

Reid MS (1995) Ethylene in plant growth, development and senescence. *In* Plant Hormones: Physiology, Biochemistry and Molecular Biology. 2nd. Ed Davies, P.J. Kluwer Academic Publishers, Dordrecht, The Netherlands. pp 486-508.

Reinhardt D, Kende H, Boller T (1994) Subcellular localization of 1-aminocyclopropane-1-carboxylate oxidase in tomato cells. *Planta* **195:** 142-146.

Roach PL, Clifton IJ, Hensgens CMH, Shibata N, Schofield CJ, Hajdu J, Baldwin JE (1997) Structure of isopenicillin N synthase complexed with substrate and the mechanism of penicillin formation. *Nature* **387:** 827-830.

Roden LC, Carré IA (2001) The molecular genetics of circadian rhythms in *Arabidopsis*. Seminars in *Cellular and Developmental Biology* **12:** 305-315.

Roe S (1989) Separation based on structure. *In* Protein Purification Method: A Practical Approach, Ed Harris, E.L., Angal, S. IRL Press, Oxford, UK. pp 175-244.

Roman G, Lubarsky B, Kieber J, Rothenberg M, Ecker JR (1995) Genetic analysis of ethylene signal transduction in *Arabidopsis thaliana*: five novel mutant loci integrated into a stress response pathway. *Genetics* **139:** 1393-1409.

Rombaldi C, Lelièvre JM, Latché A, Petitprez M, Bouzayen M, Pech JC (1994) Immunocytolocalization of 1-aminocyclopropane-1-carboxylic acid oxidase in tomato and apple fruit. *Planta* **192:** 453-460.

Rottmann WH, Peter GF, Oeller PW, Keller JA, Shen NF, Nagy BP, Taylor LP, Campbell AD, Theologis A (1991) 1-aminocyclopropane-1-carboxylate synthase in tomato is encoded by a multigene family whose transcription is induced during fruit and floral senescence. *Journal of Molecular Biology* **222:** 937-961.

Ruban AV, Lee PJ, Wentworth M, Young AJ, Horton P (1999) Determination of the stoichiometry and strength of binding of xanthophylls to the photosystem II light harvesting complex. *Journal of Biological Chemistry* **274:** 10458-10465.

Rüdiger W (2002) Biosynthesis of chlorophyll *b* and the chlorophyll cycle. *Photosynthesis Research* **74:** 187-193.

Ruperti B, Bonghi C, Rasori A, Ramina A, Tonutti P (2001) Characterization and expression of two members of the peach 1-aminocyclopropane-1-carboxylate oxidase gene family. *Physiologia Plantarum* **111:** 336-344.

Rychlik W (1993) Selection of Primers for Polymerase Chain Reaction. *In* Methods in Molecular Biology: PCR Protocols: Current Methods and Applications, Ed White, B.A. Humana Press, Totowa, New Jersey, USA. pp 31-40.

Sackville-Hamilton NR, Harper JL (1989) The dynamics of *Trifolium repens* in a permanent pasture I. The population dynamics of leaves and nodes per shoot axis. Proceedings of the Royal society of London **237:** 133-173.

Sakai H, Hua J, Chen QG, Chang CR, Medrano LJ, Bleecker AB, Meyerowitz EM (1998) *ETR2* is a *ETR1*-like gene involved in ethylene signalling in *Arabidopsis*. *Proceedings of the National Academy of Sciences, USA* **95:** 5812-5817.

Salisbury FB, Ross CW (1985) Hormones and growth regulators. *In* Plant Physiology, 3rd. Ed Carey J.C. Wadsworth Publishing Company, Belmont, California, USA. pp 330-349.

Sambrook J, Fritsch EF, Maniatis T (1989) Molecular Cloning: A Laboratory Manual, 2nd. Cold Spring Harbor Laboratory Press, Cold Spring Harbor, NY., USA.

Sanders IO, Ishizawa K, Smith AR, Hall MA (1990) Ethylene binding and action in rice seedlings. *Plant and Cell Physiology* **31:** 1091-1099.

Sarquis JI, Morgan PW, Jordan WR (1992) Metabolism of 1-aminocyclopropane-1-carboxylic acid in etiolated maize seedlings grown under mechanical impedance. *Plant Physiology* **98:** 1342-1348.

Sato T, Oeller PW, Theologis A (1991) The 1-aminocyclopropane-1-carboxylate synthase of *Cucurbita*. *The Journal of Biological Chemistry* **266:** 3752-3759.

Satoh S, Esashi Y (1984) Changes in ethylene production and in 1-aminocyclopropane-1-carboxylic acid (ACC) and malonyl-ACC contents of cocklebur seeds during their development. *Plant and Cell Physiology* **25:** 1277-1283.

Satoh S, Esashi Y (1986) Inactivation of 1-aminocyclopropane-1-carboxylic acid synthase of etiolated mung bean hypocotyl segments by its substrate, *S*-adenosylmethionine. *Plant and Cell Physiology* **27:** 285-291.

Satoh S, Yang SF (1988) S-adenosylmethionine-dependent inactivation and radiolabeling of 1-aminocyclopropane-1-carboxylate synthase isolated from tomato fruits. *Plant Physiology* **88:** 109-114.

Schaffer R, Landgraf J, Accerbi M, Simon V, Larson M, Wisman E (2001) Microarray analysis of diurnal and circadian-regulated genes in *Arabidopsis*. *Plant Cell* **13:** 113-123.

Schaller GE, Bleecker AB (1995) Ethylene binding sites generated in yeast expressing the *Arabidopsis ETR1* gene. *Science* **270:** 1809-1811.

Schroder G, Eichel J, Breinig S, Schroder J (1997) Three differentially expressed *S*-adenosyl methionine synthetases from *Catharanthus roseus*: molecular and functional characterization. *Plant Molecular Biology* **33:** 211-222.

Scopes RK (1994) Protein Purification: Principles and Practice. 2nd. Springer-Verlag, N.Y., USA.

Sechi S, Chait BT (1998) Modification of cysteine residues by alkylation. A tool in peptide mapping and protein identification. *Analytical Chemistry* **70:** 5150-5158.

Shiomi S, Yamamoto M, Ono T, Kakiuchi K, Nakamoto J, Nakatsuka A, Kubo Y, Nakamura R, Inaba A, Imaseki H (1998) cDNA cloning of ACC synthase and ACC oxidase genes in cucumber fruit and their differential expression by wounding and auxin. *Journal of Japanese Society of Horticultural Science* **67:** 685-692.

Shiu OY, Oetiker JH, Yip WK, Yang SF (1998) The promoter of *LE-ACS7*, an early flooding-induced 1-aminocyclopropane-1-carboxylate synthase gene of the tomato, is tagged by a *Sol3* transposon. *Proceedings of the National Academy of Sciences, USA* **95:** 10334-10339.

Simpson GG, Dean C (2002) Flowering: *Arabidopsis*, the Rosetta stone of flowering time? *Science* **296:** 285-289.

Slater A, Maunders MJ, Edwards K, Schuch W, Grierson D (1985) Isolation and characterization of cDNA clones for tomato polygalacturonase and other ripening-related proteins. *Plant Molecular Biology* **5:** 137-147.

Smith RD, Walker JC (1993) Expression of multiple type 1 phosphoprotein phosphatase in *Arabidopsis thaliana. Plant Molecular Biology* **21:** 307-316.

Smith CJS, Slater A, Grierson D (1986) Rapid appearance of a mRNA correlated with ethylene synthesis encoding a protein of molecular weight 35000. *Planta* **168:** 94-100.

Smith JJ, Ververidis P, John P (1992) Characterization of the ethylene-forming enzyme partially purified from melon. *Phytochemistry* **31:** 1485-1494.

Solano R, Stepanova AN, Chao QM, Ecker JR (1998) Nuclear events in ethylene signaling: a transcriptional cascade mediated by *ETHYLENE-INSENSITIVE3* and *ETHYLENE-RESPONSE-FACTOR1. Genes and Development* **12:** 3703-3714.

Somers DE (1999) The physiology and molecular bases of the plant circadian clock. *Plant Physiology* **121:** 9-20.

Soskic V, Godovac-Zimmermann J (2001) Improvement of an in-gel tryptic digestion method for matrix-assisted laser desorption/ionization-time of flight mass spectrometry peptide mapping by use of volatile solubilizing agents. *Proteomics* **1:** 1364-1367.

Spanu P, Grosskopf DG, Felix G, Boller T (1994) The apparent turnover of 1-aminocyclopropane-1-carboxylate synthase in tomato cells is regulated by protein-phosphorylation and dephosphorylation. *Plant Physiology* **106:** 529-535.

Ståhlberg J, Jonsson B, Horvath C (1992) Combined effect of coulombic and van der Waals interactions in the chromatography of proteins. *Analytical Chemistry* **64:** 3118-3124.

Stepanova AN, Ecker JR (2000) Ethylene signaling: from mutants to molecules. *Current Opinion in Plant Biology* **3:** 353-360.

Stock AM, Robinson VL, Goudreau PN (2000) Two-component signal transduction. *Annual Review of Biochemistry* **69:** 183-215.

Strayer CA, Kay SA (1999) The ins and outs of circadian regulated gene expression. *Current Opinion in Plant Biology* **2:** 114-120.

Strommer J, Gregerson R, Vayda M (1993) Isolation and characterization of plant mRNA. *In* Methods in plant molecular biology and biotechnology, Ed Glick, B.R., Thompson, J.E. CRC Press, Boca Raton, USA. pp 49-65.

Sugano S, Andronis C, Green RM, Wang ZY, Tobin EM (1998) Protein kinase CK2 interacts with and phosphorylates the *Arabidopsis circadian clock-associated 1* protein. *Proceedings of the National Academy of Sciences, USA* **95:** 11020-11025.

Sugano S, Andronis C, Ong MS, Green RM, Tobin EM (1999) The protein kinase CK2 is involved in regulation of circadian rhythms in *Arabidopsis. Proceedings of the National Academy of Sciences, USA* **96:** 12362-12366.

Swain M, Ross NW (1995) A silver stain protocol for proteins yielding high resolution and transparent background in sodium dodecyl sulfate-polyacrylamide gels. *Electrophoresis* **16:** 948-951.

Tabor CW, Tabor H (1984) Methionineadenosyltransferase (S-adenosylmethionine synthetase) and S-adenosylmethionine decarboxylase. *Advances in Enzymology* **56:** 251-282.

Tang X, Woodson WR (1996) Temporal and spatial expression of 1-aminocyclopropane-1-carboxylate oxidase mRNA following pollination of immature and mature *Petunia* flowers. *Plant Physiology* **112:** 503-511.

Tang X, Wang H, Brandt AS, Woodson WR (1993) Organization and structure of the 1-aminocyclopropane-1-carboxylate oxidase gene family from *Petunia hybrida. Plant Molecular Biology* **23:** 1151-1164.

Tang X, Gomes AMTR, Bhatia A, Woodson WR (1994) Pistil-specific and ethylene-regulated expression of 1-aminocyclopropane-1-carboxylate oxidase genes in *Petunia* flowers. *The Pant Cell* **6:** 1227-1239.

Tarun AS, Lee JS, Theologis A (1998) Random mutagenesis of 1-aminocyclopropane-1-carboxylate synthase: A key enzyme in ethylene biosynthesis. *Proceedings of the National Academy of Sciences, USA* **95:** 9796-9801.

Tatsuki M, Mori H (2001) Phosphorylation of tomato 1-aminocyclopropane-1-carboxylic acid synthase, LE-ACS2, at the C-terminal region. *Journal of Biological Chemistry* **276:** 28051-28057.

Ten Have A, Woltering EJ (1997) Ethylene biosynthetic genes are differentially expressed during carnation (*Dianthus caryophyllus* L.) flower senescence. *Plant Molecular Biology* **34:** 89-97.

Theologis A (1992) One rotten apple spoils the whole bushel: The role of ethylene in fruit ripening. *Cell* **70:** 181-184.

Theologis A, Oeller PW, Wong LM, Rottmann WH, Gantz DM (1993) Use of a tomato mutant constructed with reverse genetics to study fruit ripening, a complex developmental process. *Developmental Genetics* **14:** 282-295.

Thomas H (1997) Chlorophyll: a symptom and a regulator of plastid development. *New Phytologist* **136:** 163-181.

Thomas RG (1987) Vegetative growth and development. *In* White Clover, Ed Baker, M.J., William, W.M. CAB International, Oxon, UK. pp 31-62.

Thomason P, Kay R (2000) Eukaryotic signal transduction *via* histidine-aspartate phosphorelay. *Journal of Cell Science* **113:** 3141-3150.

Thompson JD, Higgins DG, Gibson TJ (1994) Clustal W: improving the sensitivity of progressive multiple sequence alignment through sequence weighting, positions-specific gap penalties and weight matrix choice. *Nucleic Acids Research* **22:** 4673-4680.

Tieman DM, Klee HJ (1999) Differential expression of two novel members of the tomato ethylene-receptor family. *Plant Physiology* **120:** 165-172.

Tieman DM, Taylor MG, Ciardi JA, Klee HJ (2000) The tomato ethylene receptors NR and LeETR4 are negative regulators of ethylene response and exhibit functional compensation within a multigene family. *Proceedings of the National Academy of Sciences, USA* **97:** 5663-5668.

Towbin H, Staehelin T, Gordon J (1979) Electrophoretic transfer from polyacrylamide gels to nitrocellulose sheets: procedures and some applications. *Proceedings of the National Academy of Sciences, USA* **76:** 4350-4354.

Tsai DS, Arteca RN, Bachman JM, Phillips AT (1988) Purification and characterization of 1-aminocyclopropane-1-carboxylate synthase from etiolated mungbean hypocotyls. *Archives of Biochemistry and Biophysics* **264:** 632-640.

Tsai DS, Arteca RN, Arteca JM, Phillips AT (1991) Characterization of 1-aminocyclopropane-1-carboxylate synthase from etiolated mungbean hypocotyls. *Journal of Plant Physiology* **137:** 301-306.

Tucker DE, Allen DJ, Ort DR (2004) Control of nitrate reductase by circadian and diurnal rhythms in tomato. *Planta* **219:** 277-285.

Van Der Straeten D, Van Wiemeersch L, Van Damme J, Goodman HM, Van Montagu M (1989) Purification and amino acid sequence analysis of characterization of 1-aminocyclopropane-1-carboxylate synthase from tomato pericarp. *In* Biochemical and Physiological Aspects of Ethylene Production in Lower and Higher Plants, Ed Clijsters, H. De Proft, M. Marcelle, R. Van Poucke, M. Kluwer Academic Publishers, Dordrecht, The Netherlands. pp 93-100.

Van Der Straeten D, Van Wiemeersch L, Goodman HM, Van Montagu M (1990) Cloning and sequence of two different cDNAs encoding 1-aminocyclopropane-1-carboxylate synthase in tomato. *Proceedings of the National Academy of Sciences, USA* **87:** 4859-4863.

Van Der Straeten D, Rodrigues-pousada RA, Villarroel R, Hanley S, Goodman HM, Van Montagu M (1992) Cloning, genetic mapping, and expression analysis of an *Arabidopsis thaliana* gene that encodes 1-aminocyclopropane-1-carboxylate synthase. *Proceedings of the National Academy of Sciences, USA* **89:** 9969-9973.

Ververidis P, John P (1991) Complete recovery *in vitro* of ethylene-forming enzyme activity. *Phytochemistry* **30:** 725-727.

Vioque B, Castellano JM (1994) Extraction and biochemical characterization of 1-aminocyclopropane-1-carboxylate oxidase from pear. *Physiologia Plantarum* **90:** 334-338.

Vogel JP, Woeste KE, Theologis A, Kieber JJ (1998) Recessive and dominant mutations in the ethylene biosynthetic gene ACS5 of *Arabidopsis* confers cytokinin insensitivity and ethylene overproduction respectively. *Proceedings of the National Academy of Sciences, USA* **95:** 4766-4771.

Wang KLC, Li H, Ecker JR (2002) Ethylene biosynthesis and signaling networks. *Plant Cell* **14:** S131-S151.

Wang KLC, Yoshida H, Lurin C, Ecker JR (2004a) Regulation of ethylene gas biosynthesis by the *Arabidopsis* ETO1 protein. *Nature* **428:** 945-950.

Wang SJ, Yeh KW, Tsai CY (2004b) Circadian control of sweet potato *granule-bound starch synthase I* gene in *Arabidopsis* plants. *Plant Growth Regulation* **42:** 161-168.

White MF, Vasquez J, Yang SF, Kirsch JF (1994) Expression of apple 1-aminocyclopropane-1-carboxylate synthase in *Escherichia coli.* kinetic characterization of wild-type and active-site mutant forms. *Proceedings of the National Academy of Sciences, USA* **91:** 12428-12432.

Whittaker DJ, Smith GS, Gardner RC (1997) Expression of ethylene biosynthetic genes in *Actinidia chinensis* fruit. *Plant Molecular Biology* **34:** 45-55.

Williams WM (1987) White clover taxonomy and biosystematics. *In* White clover, Ed Baker, M.J., Williams, M.W. CAB International, Oxon, UK. pp 323-342.

Williams OJ, Golden KD (2002) Purification and characterization of ACC oxidase from *Artocarpus altilis. Plant Physiology & Biochemistry* **40:** 273-279.

Wilson KA (2000) Protein changes during senescence in white clover leaves. PhD. Thesis. Victoria University, Wellington, New Zealand.

Woeste KE, Ye C, Kieber JJ (1999) Two *Arabidopsis* mutants that overproduce ethylene are affected in the posttranscriptional regulation of 1-aminocyclopropane-1-carboxylic acid synthase. *Plant Physiology* **119:** 521-529.

Woltering EJ, De Vrije T (1995) Ethylene: a tiny molecule with great potential. *BioEssays* **17(4):** 287-290.

Woodson WR, Park KY, Drory A, Larsen PB, Wang H (1992) Expression of ethylene biosynthetic pathway transcripts in senescing carnation flowers. *Plant Physiology* **99:** 526-532.

Wurgler-Murphy SM, Saito H (1997) Two-component signal transducers and MAPK cascades. *Trends Biochemical Science* **22:** 172-176.

Yang SF, Dong JG (1993) Recent progress in research of ethylene biosynthesis. *Botanical Bulletin of Academia Sinica* **34:** 89-101.

Yang SF, Hoffman NE (1984) Ethylene biosynthesis and its regulation in higher plants. *Annual Review in Plant Physiology* **35:** 155-189.

Yang SF, Oetiker JH (1998) Molecular biology of ethylene biosynthesis and its application in horticulture. *Journal of Japanese Society of Horticultural Science* **67:** 1209-1214.

Yang Y, Cheng P, Liu Y (2002) Regulation of the *Neurospora* circadian clock by casein kinase II. *Genes & Development* **16:** 994-1006.

Yi HC, Joo S, Nam KH Lee JS, Kang BG, Kim WT (1999) Auxin and brassinosteroid differentially regulate the expression of three members of the 1-aminocyclopropane-1-carboxylate synthase gene family in mung bean (*Vigna radiata* L.). *Plant Molecular Biology* **41:** 443-454.

Yip WK, Dong JG, Yang SF (1991) Purification and characterization of 1-aminocyclopropane-1-carboxylate synthase from apple fruits. *Plant Physiology* **95:** 251-257.

Yip WK, Moore T, Yang SF (1992) Differential accumulation of transcripts for four tomato 1-aminocyclopropane-1-carboxylate synthase homologs under various conditions. *Proceedings of the National Academy of Sciences, USA* **89:** 2475-2479.

Yoneyama T (1995) Nitrogen metabolism and fractionation of nitrogen isotopes in plants. *In* Stable isotopes in the biosphere, Ed Wada, E. Yoneyama, T. Minagawa, M. Ando, T. Fry, B.D. Kyoto University Press, Kyoto. pp 92-102.

Yoo SD (1999) Molecular characterization of ethylene biosynthesis during leaf ontogeny in white clover (*Trifolium repens* L.). PhD. Thesis. Institute of Molecular BioSciences, Massey University, Palmerston North, New Zealand.

Yoo SD, Greer DH, Laing WA, McManus MT (2003) Changes in photosynthetic efficiency and carotenoid composition in leaves of white clover at different developmental stages. *Plant Physiology and Biochemistry* **41:** 887-893.

Yoshida S (2003) Molecular regulation of leaf senescence. *Current Opinion in Plant Biology* **6:** 79-84.

Young AJ, Wellings R, Britton G (1991) The fate of chloroplast pigments during senescence of primary leaves of *Hordeum vulgare* and *Avena sativum. Journal of Plant Physiology* **137:** 701-705.

Young MW, Kay SA (2001) Time zones: a comparative genetics of circadian clocks. *Nature Reviews. Genetics* **2:** 702-715.

Yu SJ, Kim S, Lee JS, Lee DH (1998) Differential accumulation of transcripts for ACC synthase and ACC oxidase homologs in etiolated mung bean hypocotyls in response to various stimuli. *Molecular and Cells* **8:** 350-358.

Yu YB, Yang SF (1979) Auxin-induced ethylene production and its inhibition by aminoethoxy vinylglycine and cobalt ion. *Plant Physiology* **64:** 1074-1077.

Zacarias L, Reid MS (1992) Inhibition of ethylene action prevents root penetration through compressed media in tomato (*Lycopersicon esculentum*) seedlings. *Physiologia Plantarum* **86:** 301-307.

Zanetti ME, Terrile MC, Arce D, Godoy AV, Segundo BS, Casalongué C (2002) Isolation and characterization of a potato cDNA corresponding to a 1-aminocyclopropane-1-carboxylate (ACC) oxidase gene differentially activated by stress. *Journal of Experimental Botany* **53:** 2455-2457.

Zarembinski TI, Theologis A (1994) Ethylene biosynthesis and action: A case of conservation. *Plant Molecular Biology* **26:** 1579-1597.

Zegzouti H, Jones B, Frasse P, Marty C, Maitre B, Latché A, Pech JC, Bouzayen M (1999) Ethylene-regulated gene expression in tomato fruit: characterization of novel ethylene-responsive and ripening-related genes isolated by differential display. *The Plant Journal* **18:** 589-600.

Zhang ZH, Schofield CJ, Baldwin JE, Thomas P, John P (1995) Expression, purification and characterization of 1-aminocyclopropane-1-carboxylate oxidase from tomato in *Escherichia coli. Biochemical Journal* **307:** 77-85.

Zheng CC, Porat R, Lu PZ, O'Neill SD (1998) *PNZIP* is a novel mesophyll-specific cDNA that is regulated by phytochrome and a circadian rhythm and encodes a protein with a leucine zipper motif. *Plant physiology* **116:** 27-35.

Zhou DB, Mattoo AK, Tucker ML (1996) Molecular cloning of a tomato cDNA encoding an ethylene receptor. *Plant Physiology* **110:** 1435-1436.

Zor T, Selinger Z (1996) Linerization of the Bradford protein assay increases its sensitivity: theoretical and experimental studies. *Analytical Biochemistry* **236:** 302-308.

Appendix I: The Monoisotopic Peak List from MALDI-TOF Mass Spectrometry

Spot	Masses (M) of Fragments (Da)
G_1	1114.669; 1121.665; 1188.601; 1275.775; 1284.708; 1320.755; 1475.743; 1552.697; 1592.662; 1638.845; 1717.791; 1755.911; 1846.852; 1857.966
G_2	1056.572; 1098.693; 1114.749; 1121.663; 1275.861; 1320.828; 1461.897; 1531.786; 1552.774; 1592.753; 1638.925; 1791.868; 1846.979; 2384.039
G_3	1121.615; 1137.553; 1177.646; 1343.636; 1429.783; 1446.805; 1475.716; 1552.689; 1570.674; 1592.685; 1598.661; 1642.876; 1658.829; 1681.775; 1799.982; 1852.966; 1883.941; 1946.936; 2139.941; 2174.057; 2383.949; 2494.117; 2979.117
G_4	1120.539; 1137.509; 1177.609; 1299.411; 1343.597; 1359.592; 1430.708; 1450.716; 1472.603; 1535.594; 1552.624; 1592.668; 1612.653; 1637.664; 1658.766; 1681.721; 1697.642; 1708.684; 1883.846; 1946.871; 1968.975; 2173.942; 2239.933; 2493.980; 2704.923; 2968.216; 2979.013
G_5	1113.967; 1121.594; 1177.662; 1328.663; 1347.782; 1428.767; 1436.635; 1446.702; 1450.656; 1475.695; 1520.708; 1547.787; 1553.676; 1561.859; 1566.742; 1592.709; 1627.736; 1700.887; 1714.875; 1908.874; 1931.012; 1994.021; 2073.932; 2090.003; 2114.019; 2192.146; 2241.118; 2402.095; 2448.139; 2807.282
G_6	1137.447; 1177.571; 1302.942; 1359.526; 1407.183; 1429.705; 1472.558; 1536.478; 1552.574; 1594.771; 1626.697; 1633.629; 1674.772; 1681.657; 1698.624; 1883.785; 1946.811; 1968.914; 1977.802; 2082.543; 2138.963; 2173.901; 2194.972; 2383.857; 2427.916; 2450.014; 2493.969; 2509.868; 2525.897; 2921.991
S_1	1132.595; 1179.562; 1189.633; 1309.668; 1428.675; 1475.726; 1552.654; 1584.699; 1599.777; 1637.788; 1706.774; 1993.971; 2275.053; 2297.131; 2382.942; 2675.236; 2704.921; 2766.128; 3025.196; 3047.167
S_2	993.6764; 1114.679; 1179.719; 1277.836; 1307.809; 1320.765; 1383.802; 1429.797; 1475.875; 1493.868; 1523.899; 1536.790; 1570.842; 1584.801; 1592.829; 1627.894; 1657.893; 1707.927; 1716.999; 1758.028; 1791.889; 1852.083; 1910.166; 1924.092; 1942.113; 1993.971; 2184.265; 2286.212; 2312.291; 2399.167
S_3	1165.602; 1179.572; 1213.631; 1277.695; 1365.591; 1400.638; 1428.641; 1475.673; 1552.634; 1570.631; 1599.694; 1637.736; 1657.676; 1707.701; 1716.743; 1791.705; 1796.904; 1818.792; 1889.842; 1908.769; 1920.815; 1934.824; 1946.817; 1993.823; 2027.623; 2073.935; 2241.063; 2274.748; 2284.944; 2383.773
S_4	857.5460; 864.3818; 877.1140; 1056.526; 1137.525; 1159.541; 1177.615; 1446.752; 1553.636; 1570.651; 1592.598; 1642.826; 1658.721; 1681.754; 2494.047
S_5	1111.490; 1121.548; 1189.520; 1310.558; 1428.554; 1450.541; 1552.553; 1570.536; 1592.476; 1599.645; 1608.442; 1637.648; 1729.682; 2050.648; 2274.849; 2296.869
S_6	1067.511; 1089.510; 1105.477; 1129.441; 1256.648; 1278.648; 1294.610; 1316.562; 1552.521; 1570.558; 1647.748; 1669.731; 1685.722; 2037.778; 2239.806; 2552.862

Appendix II: The Full Name for Each Entry of the Twenty-Two ACC oxidases in the Phylogenetic Analysis

Short name	Full name	Accession number
TRACO2	*Trifolium repens TR-ACO2*	AF115262
MTACO	*Medicago truncatula* ACO mRNA	AY062251
PLACO	*Phaseolus lunatus* ACO mRNA	AB062359
PVACO	*Phaseolus vulgaris* ACO mRNA	AF053354
TRACO3	*Trifolium repens TR-ACO3*	AF115263
PPACO	*Prunus persica* PAO1 mRNA	X77232
MxDACO	*Malus x domestica* ACO mRNA	AB086888
FSACO	*Fagus sylvatica partial* ACO mRNA	AJ420189
NTACO	*Nicotiana tabacum* ACO mRNA	X83229
ACACO	*Actinidia chinensis* ACO	P31237
pxHACO	*Pelargonium hortorum* ACO mRNA	U07953
PHACO3	*Petunia hybrida* ACO3	Q08507
PHACO4	*Petunia hybrida* ACO4	Q08508
NTACO1	*Nicotiana tabacum* ACO1 mRNA	X98493
TRACO1	*Trifolium repens TR-ACO1*	AF115261
VRACO1	*Vigna radiate* ACO1 mRNA	U06046
MDACO	*Malus domestica* ACO	X98627
MDACO1	*Malus x domestica* ACO1	Q00985
PCACO	*Pyrus communis* ACO mRNA	X87097
CSACO2	*Cucumis sativus* ACO2	AF033582
CMACO	*Cucumis melo* (muskmelon) ACO	P54847
VRACO2	*Vigna radiate* ACO2 mRNA	U06047

(Searched on 22nd, April 2004)